EFFECTS OF AEROSOLS TRANSPORT ON MESOSCALE CONVECTIVE SYSTEMS OVER WEST AFRICA

BY

OCHEI, MICHAEL CHUKWUEMEKA

B.Tech., M.Tech. (Meteorology)

MET/05/6090

A Thesis of the Doctoral Research Programme of the West Africa Climate Systems, under the West Africa Science Service Center on Climate Change and Adapted Land Use, in the Department of Meteorology and Climate Science submitted to the School of Postgraduate Studies in partial fulfillment of the requirements for the award of the degree of Doctor of Philosophy in Meteorology and Climate Science of the Federal University of Technology, Akure, Nigeria.

May, 2023.

DECLARATION

I hereby declare that this Thesis was written by me and is a correct record of my own research work. It has not been presented in any previous application for any degree of this or any University. All citations and sources of information are clearly acknowledged by means of references.

Candidate's Name: Ochei, Michael Chukwuemeka

Signature: Date

CERTIFICATION

We certify that this Dissertation entitled "Effects of Aerosols Transport on Mesoscale Convective Systems over West Africa" is the outcome of the research carried out by Michael Chukwuemeka Ochei under the WASCAL DRP-WACS in the Department of Meteorology and Climate Science of the Federal University of Technology, Akure.

Prof. Ayodeji Oluleye ……..……..

(Major Supervisor) Signature and Date
Department of Meteorology
Federal University of Technology,
Akure, Nigeria.

Dr. Ralf Wolke ……..…….

(Co-Supervisor/Advisor) Signature and Date
Department of Modeling of Atmospheric Processes
Leibniz Institute for Tropospheric Research (TROPOS),
04318 Leipzig, Germany.

Prof. Zachariah Debo Adeyewa ……..…….

(Director) Signature and Date
Doctoral Research Program – West African Climate Systems
West African Science Service Center on Climate Change and
Adapted Land Use (DRP-WACS, WASCAL),
Federal University of Technology,
Akure, Nigeria.

ABSTRACT

Aerosols' presence in the atmosphere is known to influence health and weather-related matters. It is believed that these pollutants are available in the atmosphere all year round but are more prevalent at certain seasons of the year. Some source points can be close or far from the locations where the aerosols are prevalent, but their transportation from a long distance is mostly aided through meteorological means. Although, it is a known fact that the resultant aerosol particles from human activities (anthropogenic) such as biomass burning, carbonaceous, etc., have contributed substantially to the global mean aerosol burden since the pre-industrial era, the aerosol particles can be said to affect climate systems via different mechanisms. Aerosols' influence on Earth's climate can occur during clear sky which allows it to reflect incoming sunlight to outer space – the direct effect, or the ability to act as condensation nuclei – the indirect effect. Aside from these stated ways of aerosols' influence on Earth's climate, it is also known to absorb radiation which leads to hindering cloud formation. The fact remains that the aerosol can be said to influence meteorological variables, thus leading to climate influence. This can be a kind of feedback mechanism between these atmospheric phenomena. In determining the effect of aerosols' transport on convective systems, there is a need to determine the variability of aerosols and their relationship with climatic parameters, evaluate the capability of the COSMO-MUSCAT coupling model to simulate past episodes, assess the impact of aerosols on convection initiation and propagation, and the impact of non-local plumes on simulated cloud properties, relative humidity and temperature. This study covers the whole of West Africa, with some ten (10) selected stations for detailed analyses, namely: Abidjan, Accra, Agoufou, Banizoumbou, Dakar, Freetown, Ikeja, Kano, Ouagadougou and Praia. The work made use of concentration/aerosol (biomass burning, carbonaceous, dust and $PM_{2.5}$) and meteorological (convective precipitation, wind speed and water

vapor) data for a period of 30 years. Other data used were the initial data for some selected episodes for both concentration and meteorology. The selected episodes were; Dust and smoke episode of December 24 -27, 2015 over West Africa. The dust layer extended from the ground up to 2000m while the smoke layer occurred from 2000m – 4000m range, Dust pollution outbreak of March 20 – 29, 2010 over West Africa and spread up to the coastal cities of Lagos and southwestern Nigeria, and Convective activities of 30th August – 2nd September 2009 over Ouagadougou and other West African countries. The statistical analyses employed in achieving one of the objectives were Pearson's correlation method and the probability value (*p-value*). The graphical analyses were done with python and ferret. The result showed that most aerosols are predominant in the dry months of December, January and February, but dust was found to be present all throughout the months of the year around Bodélé depression, over Chad. The monthly trend of dust and PM2.5 exhibited same pattern. Putting the p-value into consideration, there exists a 60% - 90% statistically significant relationship between the selected climatic parameters and aerosols used in the study. In the validation of the COSMO-MUSCAT coupling model output, the EUMETSAT images showed a similar pattern of dust mobilization and southward dispersion of the aerosol (dust) from the Bodélé depression. The inability of the model to capture the aerosols around the Gulf of Guinea area of Freetown up to Dakar showed that there was an influx of moisture as observed from EUMETSAT images, leading to precipitation which may have suppressed the aerosols. The wind profiles over each of the locations exhibited continuous vertical wind shear which has showed to be responsible for increasing intensity of convective systems. The non-local plumes showed that the radiative feedback mechanism had more impacts on the climatic parameters (cloud properties, relative humidity, and temperature) especially around the surface than the non-feedback mechanism.

DEDICATION

This Ph.D. thesis is dedicated to God Almighty who in His infinite mercy and grace guided me throughout the period of the study. I say, glory and honour be to His holy name.

ACKNOWLEDGEMENT

My profound gratitude and appreciation go to my parent, Mr. and Mrs. Joseph Ochei, and the entire family for their support in all aspects of my life and for making this research come to reality. I am indebted to them for their advice and assistance. To my newfound family in The Gambia, Mr. and Mrs. George Pratt, thank you for your trust, support, and words of encouragement.

To my supervisor, Professor Ayodeji Oluleye, thank you for all the roles you have played in getting me to this point and everything you have done from the first day of our encounter till this very moment. I will always be indebted to you, sir. To my co-Supervisor and German advisor, Dr. Ralf Wolke, words cannot express how grateful I am. You took interest in my work even before we had our first conversation, welcomed me warmly in Germany, made my settling down seamless, and kicked off the supervisory role immediately; not to mention every effort you made to provide all the computing facilities I needed for the research. *Vielen Danke Dr. Ralf* (as I normally refer to him).

Special appreciation to the sponsor of the doctoral program, the German Ministry of Education and Research (BMBF) for the financial provision throughout the period of the research, the West African Science Service Centre on Climate Change and Adapted Land Use (WASCAL) Headquarters, Accra Ghana under the headship of Professor Kone, and the academic management of the Doctoral Research Program, West African Climate Systems (DRP-WACS) under the Directorship of Professor Z.D. Adeyewa for your coordination and efforts to the successful completion of the program.

I sincerely appreciate the staff of the Department of Meteorology and Climate Science, Federal University of Technology, Akure, Nigeria under the headship of Dr. A. Akinbobola, for their

various contributions to the success of the program. Specially mentioned are Drs. V.O. Ajayi, B.M. Dada, and I.E. Gbode for your ever-reliable presence when called upon for advice. To the Professors in the Department (both active and non-active), I appreciate your encouragement and guidance.

I also want to extend my sincere appreciation to the staff of the Modelling of Atmospheric Processes Department of the Leibniz Institute for Tropospheric Research, (TROPOS) Leipzig, Germany, under the headship of Prof. Dr. Ina Tegen. Appreciation to Kerstin Muller for giving me access to almost everywhere and everything I needed academically, *Danke* Dr. Sabine Reutgen for making available all the initial data for the model simulation, Dr. Bernd Heinold for his assistance in the course of using the model, Dr. Fabian for the python maneuverings, and the IT guy (Andreas Menge) for all the assistance rendered especially during the use of the cluster. To Dr. Wadinga Momba, thank you for your assistance in linking me up with my German advisor.

My heartfelt gratitude to my lovely and indefatigable wife, Mrs. Dawn Oredola Ochei, for her support, care, and concern in the course of this program. The only song I heard from her voice was "Finish up this program". She has been there from day one of this program till this moment and played a key role in the process of getting my German advisor within a short time. It is safe to say this is our degree.

Words cannot express my sincere gratitude to my colleagues in ***DRP-WACS*** (Teeda Njie, Nimon Pouwèréou, Modou Pouye, Peace Awoleye, and Peter Odoom) and ***TROPOS*** (Hanna Wiedenhaus, Sebastian Halle, Anisbel León, Sophia Gómez Maqueo Anaya, and Jason Müller) for their contribution during the research in various ways.

Table of Contents

LIST OF FIGURES

LIST OF TABLES

CHAPTER ONE

1.0 INTRODUCTION

This chapter gives a detailed introduction to what the work is all about. In this section, the background to study will enumerate some critical details of the work. The statement of the problem is to give a concise description of what is to be addressed or what to be improved upon. It identifies the gap between the current state and the proposed or desired finding in order to improve on previous works. Aim and objectives can be simply said to be what the work hopes to achieve and the actions to be taken in order to achieve the aim respectively. The justification is the purpose or major reason for carrying out the work. It can also be referred to as the answer to the questions posed in the problems of the statement. This section equally discussed the interaction between aerosols and other meteorological variables such as convective precipitation, wind, temperature, relative humidity, etc. While the scope of the study gives summary details of what the work covers which ranges from aim to data and method and what to expect as finding.

1.1 BACKGROUND TO THE STUDY

Aerosols and convective systems are two (2) major systems over Africa, especially the western part of the continent. These two major systems are associated with the two major seasons, namely: the dry and wet seasons. While the intensity of most aerosol types is found to be in existence during the dry season, the convective system is a determining factor of the rainy season. Though extraterrestrial-induced precipitation has resulted in rainfall during the dry months in time past, it does not change the climatological pattern of these systems to the seasons. Generally, aerosols are believed to be ever present in the atmosphere all year round. For example, mineral dust was ubiquitously found in the troposphere over West Africa all throughout the year. However, a typical

seasonal dust cycle is observed with maximum surface concentrations in winter due to Saharan dust transport, although extremely high daily concentrations (>4000 μg m^{-3}) are recorded during both dry and wet seasons (Marticorena *et al.*, 2010). The pulses of high dust concentrations recorded in the wet season are due to local emissions by Mesoscale Convective Systems (MCSs) (Marticorena *et al.*, 2010). These MCSs also bring precipitation to the Sahel and wet deposition acts extremely efficiently to remove dust from the atmosphere (Flamant *et al.*, 2008). The Sahel is therefore a region of Saharan dust deposition during the dry season (Rajot *et al.*, 2008), but also an intense source of local dust emission at the beginning of the wet season. Aerosols are natural and anthropogenic solid and/or liquid particles of different compositions, sizes, shapes, and optical properties suspended in the air. Examples of natural aerosols include desert or soil dust, wildfire smoke, sea salt, biogenic particles, and volcanic ash. Anthropogenic (or manmade) aerosols, which mostly originate from highly populated industrialized and agricultural areas of intense fossil fuel and biomass burning include smoke from a domestic fire and other combustion products, smoke from agricultural burning, soil dust created by overgrazing and deforestation, and draining of inland water bodies. Atmospheric aerosols are quantified by their mass concentration or an optical measure called aerosol optical depth (AOD) (also called aerosol optical thickness, AOT). It is pertinent to state that most of the aerosols over West Africa are not domain-source based, i.e. they are not *in-situ.* This means that aerosols can be transported from a long range. Long-range transport (LRT) also contributes to particles over both continents (land) and maritime (ocean). For instance, Simpson *et al.*, (2014) found long-range transport (that is, free troposphere entrainment) supplied two-thirds of the Marine Boundary Layer (MBL) non-sea-salt sulfate (nssSO4), while Dimethyl Sulfide (DMS) or methylthio methane $(CH_3)_2S$ provided only one-third over the pacific. Continental emissions including mineral dust, anthropogenic aerosols, and biomass-burning

plumes are often transported by winds from one source to another and even to the marine atmosphere. Due to longer transport times, the aerosols are mostly aged, showing increasingly oxygenated organics (Capes *et al.*, 2008). Also because particles can be transported over thousands of kilometers, they can reach the remote regions of the ocean, affecting the chemical composition of MBL aerosol particles (Fomba *et al.*, 2014). Just as particles are transported into the West Africa region, it is important to state those aerosols also advected out of the region to other continents and maritime. For example, the long-range transport of aerosol specifically, the Saharan dust, from Africa to America shows a pronounced seasonal dependence which is strongly related to the movement of the inter-tropical convergence zone (ITCZ). During summer, dust is transported by the easterlies within a warm, dry, and well-separated Saharan air layer (SAL) (Prospero and Carlson, 1972, 1980). Up to 4-6km deep aerosol layers are transported to the Caribbean Sea, the Gulf of Mexico, and the southern United States (Schepanski *et al.*, 2009; Huang *et al.*, 2010). During winter, when the ITCZ retreats southward, dust layers are restricted to a height of 1.2km (Chiapello *et al.*, 1995). Now, Saharan dust is transported to South America or deposited into the ocean (Kaufman *et al.*, 2005; Ben-Ami *et al.*, 2009). Furthermore, the dust layer is topped by biomass-burning aerosol from fires in southern West Africa (Kalu, 1979; Barbosa *et al.*, 1999; Schepanski *et al.*, 2009). These lofted layers can also contain significant amounts of mineral dust (Johnson *et al.*, 2008b; Tesche *et al.*, 2009b).

Mesoscale weather systems is a phenomenon that includes thunderstorm, squall line, tornado, mountain wave, land, and sea breeze, clear air turbulence, and hurricane but not limited to these. Using the characteristic time/space scale, mesoscale was classified into the following by (Houze *et al.*; 1990 and Marwitz; 1972a, b, c).

Table 1.1: Mesoscale convective systems classification characteristics using time/space scale (Houze *et al.*; 1990)

CLASSIFICATIONS	TIME	LENGTH	EXAMPLES
Meso-α	1day	200 – 2000km	Fronts, Hurricanes, etc.
Meso-β	1hr – 1day	20 – 200km	Squall lines, low-level jets, land & sea breeze, etc.
Meso-ɤ	30mins – 1hr	2 – 20km	Thunderstorms, flooding, etc.

Houze (1993); defined mesoscale convective systems (MCSs) as cloud system that occurs in connection with an ensemble of thunderstorms and produces a contiguous precipitation area of ~100km in horizontal scale in at least one direction. The mechanism for the daily, monthly, and inter-annual variability of the moisture transport associated with the meridional oscillation of the West African monsoon flow is not yet fully understood (Omotosho, *et al.*, 2000; Grist and Nicholson, 2001). This is critical for the onset, temporal and spatial distribution of rainfall as the variability of this moisture strongly determines the timing, type, intensity, and precipitation delivery of the mesoscale convective weather systems which produce over 75% of the rainfall over the region.

In the tropics and mid-latitudes, heavy precipitation is closely related to convective activity accounting for a large proportion of the rainfall. Most recently, these systems, known as mesoscale convective systems (MCSs), are defined as an ensemble of strong convective cells accompanied by a stratiform region evolving into organized clusters and forming a single mesoscale cloud. Line squalls and thunderstorms are regular phenomena within the tropics and are often accompanied by

rain, destructive violent winds, lightning, thunders, and hail, thereby posing serious hazardous problems to man and his socio-economic activities.

Over West Africa, line squalls have been responsible for the largest percentage of the annual deposition of precipitation

1.2 STATEMENT OF PROBLEMS

Aerosol and Convective systems, are two major atmospheric phenomena, which have contrasting impacts on man and the environment. While aerosols' presence can either be through natural sources or anthropogenic activities, convective systems are mostly natural. These atmospheric phenomena are associated with two major seasons, the dry and wet seasons. It has been ascertained that aerosols are present in the atmosphere almost throughout the year which may be due to long-range transport from outside the domain of study, but more prevalent during the drier months of the year. The high presence of some of these aerosols, e.g. dust, smoke, haze, etc., in the atmosphere can result in health-related illness, as well as cause disruption of scheduled flight activities (e.g. delay or total cancellation of flights). This can lead to huge economic losses for airline operators.

The annual rainfall supply over West Africa has convective systems as its major contributor, with over 70%. West African regions depend mostly on this rainfall for most of their socio-economic activities e.g. agriculture is rain-fed, energy is hydro-powered, etc. Persistent and slow-moving convective systems are major causes of flooding as a result of continuous precipitation which may lead to a low rate of infiltration. Flooding on its own part also leads to erosion in some cases based on the terrain and topography of the area. Flooding also has a serious negative effect on economic, social, and environmental implications in West Africa.

The interaction between aerosols and convective systems has been well documented. These were categorized under direct and indirect effects. These interactions between the two phenomena has been said to either suppress drizzle formation, reduce cloud droplets or enhance cloud formation. This impact of aerosols on the convective systems either enhancement or suppression of the latter. Hence, the extent of the impacts or effects of the aerosols presence in the atmosphere on some climatic parameters and convective systems over West African region need to be investigated.

1.3 AIM AND OBJECTIVES

The aim of this study is to determine the effect of aerosols' transport on mesoscale convective systems (MCSs) over West Africa.

The specific objectives of this study are to:

1.) determine the variability of aerosol over West Africa and their relationship with climatic parameters;

2.) evaluate the capability of the model in simulating past episodes of aerosols and heavy precipitation;

3.) assess the impact of aerosols on convection initiation and propagation; and

4.) assess the impacts of these non-local plumes on the COSMO-MUSCAT simulated cloud properties, relative humidity, and temperature.

1.4 JUSTIFICATION

Precipitation and unexpected dust episode leading to air pollution have been of major concern to climatologists, pedologists, agriculturists, hydrologists, environmental scientists, and even to the ordinary man in the street. Some of the problems arising from these phenomena include but are not

limited to, airborne-related disease, reduced visibility (for aerosols), and flooding, run-off which eventually leads to the destruction of crops as the topsoil is washed away. Mesoscale convective systems (MCSs) deliver about 75% of the total rainfall requirements for socio-economic activities. But recent studies have shown that the percentage contribution of the convective systems to total annual rainfall has reduced (Orisakwe, 2015), while its rate (frequency) of occurrence in the phase of changing climate is on the decrease (Ochei *et al.*, 2015; Ochei & Oluleye, 2017). In a rain-dependent economy setting that exists in most parts of West Africa, impacts of changes in the forms, patterns, and severity of weather components like rainfall remain a problem of great concern and the presence of aerosol in the atmosphere can be seen as one of the causes since MCSs act as a major sink for suspended particulate matter (aerosols) which are major of Sahara origin. Primarily, the aerosol impacts climate globally by reducing the amount of solar radiation that reaches the ground; knowing-fully well that the solar radiation supplies the energy that drives most if not all the systems. Presumably, low precipitation may result from suppression by aerosol while its (aerosol) impact on the hydrological cycle can be seen through its radiative forcing and microphysical effects. These impacts are potentially severe for Nigeria where energy generation is hydro-powered, agricultural activities are rain-fed, and most familiar extreme weather events (e.g. flooding and drought) depend majorly on the abundance and/or absence of MCSs over the region.

Studies have shown that dust aerosols affect the earth's energy cycle (Kaufman *et al.*, 2002) and hydrological cycle (Gunn and Philips, 1957; Ramanathan *et al.*, 2001) through their radiative forcing and microphysical effects. Despite several studies carried out on MCSs and aerosols, the effects of long-range transport of aerosols on regional Mesoscale Convective Systems (MCSs) are poorly understood especially over West Africa where convective activities are not fully explored. It has become imperative to understand the interaction of these weather phenomena, vis-à-vis, how

this interaction will benefit man and its environment since convective systems have been documented as a dominant rainfall-producing system over West Africa; and such scientific mission cannot be accomplished without the comprehensive climatology and dynamic study of these phenomena. The role aerosols plays in the convective systems of West African has led to studies that have shown several severe dust events (Flamant *et al.*, 2007; Slingo *et al.,* 2008) provide well-documented case studies for testing and improving mesoscale dust models (Menut, 2008; Tulet *et al.*, 2008).

Several of these works have only shown interaction of these systems (dust and convective system) but yet to show how the dust and other aerosols impact or have effects on the convective systems as well as other climatic factors/variables responsible for convection initiation.

1.5 INTERACTION OF AEROSOLS AND CONVECTIVE SYSTEMS

The anthropogenic process has been found to be one of the major contributors to aerosol in the atmosphere. Anthropogenic land-cover changes resulting from the increase in agricultural and other human activities provide significant changes to various land surface physical properties (e.g. surface roughness, surface albedo, etc.). This landscape heterogeneity caused by land-cover changes is a major forcing for the development of local convective cumulus clouds that could potentially trigger the development of mesoscale convective systems (MCS) (Pielke *et al.*, 2007; Brunsell *et al.*, 2011). Most atmospheric thunderstorms and cloud-to-ground lightning strikes occur over the land. The preference for deep convection over land is due to the sufficiently large convective available potential energy (CAPE) over land. Large-scale variability in land-surface characteristics significantly affects global climate despite that land covers only about 29% of the earth's surface. Land-atmosphere interactions determine how changes in surface boundary layer

conditions affect atmospheric circulations and climate patterns. The major land-atmosphere interaction mechanism is the influence of surface albedo on moisture flux convergence.

Aerosol particles can be said to affect climate systems via different mechanisms. At the top of the list is the direct effect which is a result of solar radiation reflected back to space; absorption of solar radiation by mineral dust to warm the atmospheric aerosol layer, thereby hindering cloud formation or causing cloud droplets to evaporate – semi-direct effect; and the ability to act as condensation nuclei for cloud – indirect effects. Several attributes and characteristics have been adduced to the sub-Saharan aerosols, most importantly as its serving as cloud condensation nuclei (CCNs) which reduces cloud droplet effective radius, suppresses drizzle formation, and changes cloud lifetime – highly referred to as aerosol indirect effects (AIEs) (Twomey, 1977; Seinfeld *et al.*, 2016). The aerosol may affect precipitation through both direct (scattering and absorbing of solar radiation) and indirect radiative (ability to influence the cloud optical properties) effects. Aerosols affect cloud hydrometers by acting as Cloud Condensation Nuclei (CCN) or Ice-Nucleating Particles (INP). While the CCN can lead to new droplet formation and also increase the number of cloud droplets and cloud albedo (Twomey, 1974), the INP on the other hand, a more rare type of aerosol, can trigger droplet freezing. After droplets freeze, the resulting ice particles tend to grow at the expense of existing cloud droplets, eventually leading to precipitation (Wegener, 1911; Bergeron, 1935; Findeisen *et al.,* 2015).

Of meteorological interest in the atmosphere are particles as small as molecules and up in size through clouds and precipitation elements to giant hailstones. The phase equilibrium of a droplet of the radius is an unstable one. If the droplet were to evaporate by a small fraction, its radius would decrease and the saturation vapor pressure would increase, allowing for more evaporation. Conversely, if its radius were to increase slightly, the saturation vapor pressure would decrease and

the environment would be supersaturated with respect to the droplet. Thus, to create a water droplet or ice crystal in a given environment, it is necessary to form a droplet of at least the critical radius by setting the actual vapor pressure equal to the saturation value in Kelvin's law.

Were there no aerosols (small solid or liquid particles) in the atmosphere, the only means of creating a small particle of the critical radius would be by random clumping of water molecules that occurs in a gas? This is called homogenous nucleation and in practice would require supersaturations of up to several hundred percent. In nature, however, there is a large number of aerosols consisting of combustion products, dust, and products of photochemical reactions involving sulfides, ash, and sea salt. Those particles that are wettable, and particularly those that are water-soluble, serve as nuclei on which water may condense. These are called cloud condensation nuclei (CCN) and their presence allows heterogeneous nucleation to occur. The distribution of CCN varies greatly in space and time, with the largest concentrations in urban areas and near the earth's surface, and the smallest concentration over the oceans and away from the surface. The presence of a water-soluble CC reduces the supersaturation needed for nucleation since some of the surface energy of a droplet is provided by the molecules of the solute.

1.6 SCOPE OF STUDY

This work is to investigate the effects of aerosols transport (either long-range transport or within the domain of study) on Mesoscale convective systems over West Africa. Ten (10) stations, selected to represent all climatic zones of West Africa, were chosen. The data used were sourced from NASA Earthdata *Giovanni,* covering meteorological parameters such as convective precipitation, water vapor, and wind speed as well as the aerosols' types (biomass-burning, carbonaceous, dust, and $PM_{2.5}$) used. Initial data for some selected pollution and heavy precipitation episodes were also used in the running of the COSMO-MUSCAT coupling model.

The work is to assess the effect of aerosols' transport on mesoscale convective systems over West Africa. The study will show the correlation between aerosol types and convective systems as well as the shows the spatial distribution of the selected aerosol types over West Africa.

CHAPTER TWO

2.0 LITERATURE REVIEW

This chapter is divided into two (2) sections. These sections gave detailed reviews of existing literature. Section 2.1 is about aerosol; section 2.2 is about the convective systems (heavy precipitation) while section 2.3 is about the COSMO-MUSCAT coupling model. The chapter covered varying degrees for all sections ranging from types, favorable atmospheric conditions, and classifications of convective systems to distribution, impacts, and the interaction of aerosols to the weather systems especially as it concerns West Africa; as well as model documentation.

Section 2.1: AEROSOLS

2.1 AEROSOL

Aerosols are suspensions of fine solid or liquid droplets in air or another gas. They are found over oceans, deserts, mountains, forests, ice sheets, etc. Aerosols can be natural (e.g. fog, sea spray, forest exudates, volcanoes, etc.) or anthropogenic such as particulate air pollutants, the mist from the discharge at hydroelectric dams or irrigation mist, perfume from atomizers or smoke, steam from a kettle, sprayed pesticides, and medical treatments for respiratory illnesses. One interesting area of aerosol research involves how aerosols impact clouds. Without aerosols, clouds could not exist.

Table 2.1.1: Terminology used to describe common aerosol systems.

Bio-aerosol	An aerosol of biological origin, including airborne suspension of viruses, bacteria, and fungal spores, and their fragments
Cloud	A very dense or concentrated suspension of particles in the air, often with a well-defined boundary at a macroscopic length scale.

Dust	Solid particles are formed by crushing or other mechanical action resulting in the physical disintegration of the parent material. These particles generally have irregular shapes and are larger than about 0.5μm.
Fog or Mist	Suspension of liquid droplets. These can be formed by condensation of supersaturated vapors or by nebulization, spraying, or bubbling.
Fume	Particles resulting from condensed vapor with subsequent agglomeration. Solid fume particles typically consist of complex chains of sub-micrometer-sized particles (usually <0.05μm) of similar dimensions. Fumes are often the result of combustion and other high-temperature processes. Note that the common usage of "fume" also refers to noxious vapor components.
Haze	Visibility-reducing aerosol.
Nanoparticle	A particle in the size range of 1-100nm.
Particle	A small, discrete object.
Particulate	An adjective indicating that the material in question has particle-like properties (e.g., particulate matter). Sometimes used incorrectly as a noun to represent particles.
Smog	An aerosol consisting of solid and liquid particles is created, at least in part, by the action of sunlight on vapors. The term smog is a combination of the words "smoke" and "fog" and often refers to the entire range of such pollutants, including the gaseous constituents.
Smoke	A solid or liquid aerosol is the result of incomplete combustion or condensation of

	supersaturated vapor. Most smoke particles are sub-micrometer in size.
Spray	Droplet aerosol is formed by the mechanical or electrostatic breakup of a liquid.

The above-mentioned aerosols and any other aerosols either occur individually or as a result of the combination of more than one aerosol type. The liquid or solid particles in an aerosol have diameters typically less than 1 μm (larger particles with a significant settling speed make the mixture a suspension, but the distinction is not clear-cut).

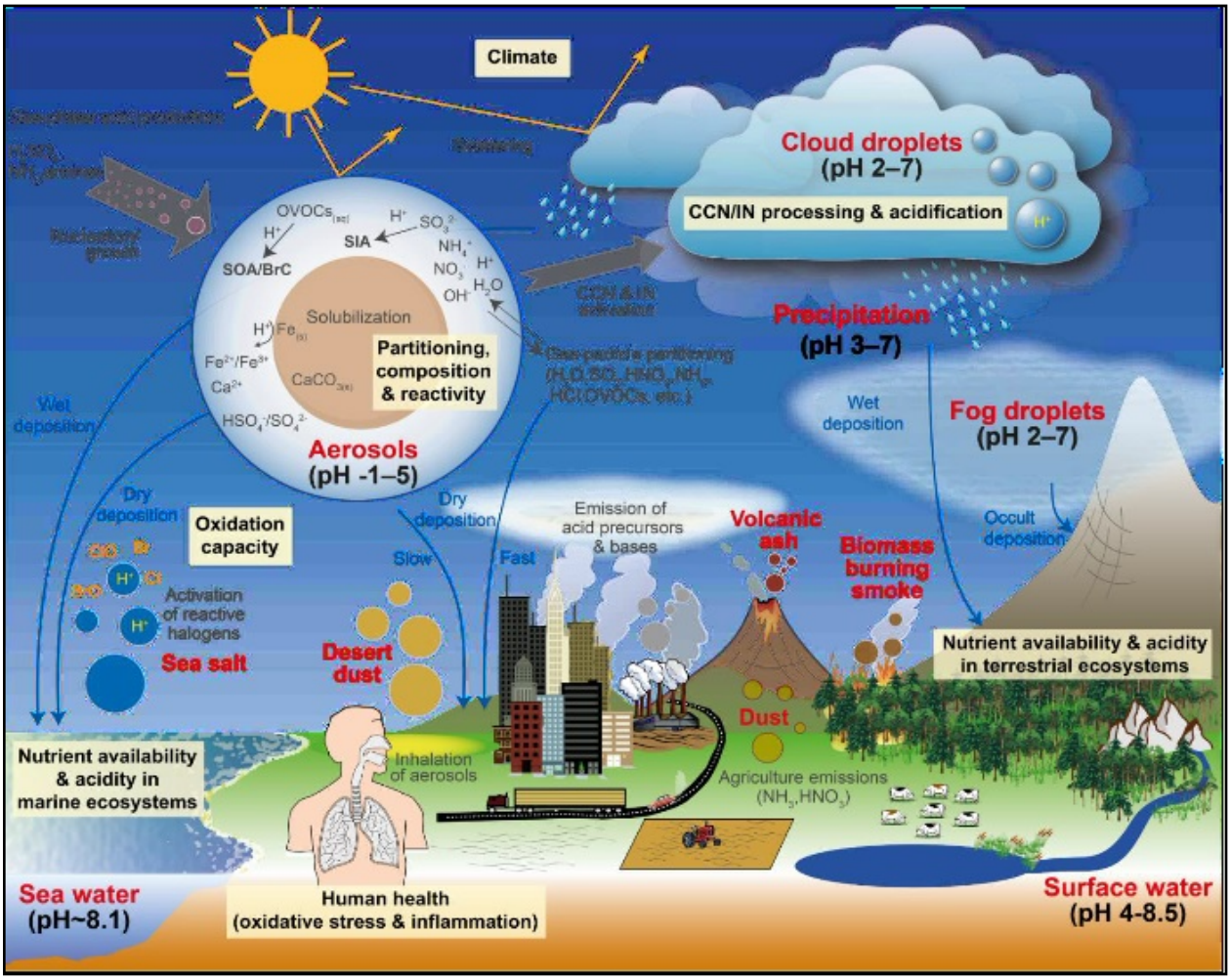

Figure 2.1: General representation of aerosol particles in the troposphere (Tilgner *et al.*, 2021).

2.1.1 PRIMARY AND SECONDARY AEROSOLS

Primary Atmospheric Aerosols are particulates that are emitted directly into the atmosphere (for instance, sea salt, mineral aerosols [or dust], volcanic dust, smoke, and soot, some organics). While secondary atmospheric aerosols are particulates that are formed in the atmosphere by gas-to-particle conversion processes (for instance, sulfates, nitrates, and some organics). Inorganic primary aerosols are relatively large (often larger than 1 μm) and originate from sea spray, mineral dust, and volcanoes. These coarse aerosols have short atmospheric lifetimes, typically only a few days. Combustion processes, biomass burning, and plant/microbial materials are sources of carbonaceous aerosols, including both organic carbon (OC) and solid black carbon (BC). Black carbon is the main anthropogenic light-absorbing constituent present in aerosols. Its main sources are the combustion of fossil fuels (such as gasoline, oil, and coal), wood, and other biomass. Primary BC and OC containing aerosols are generally smaller than 1 μm.

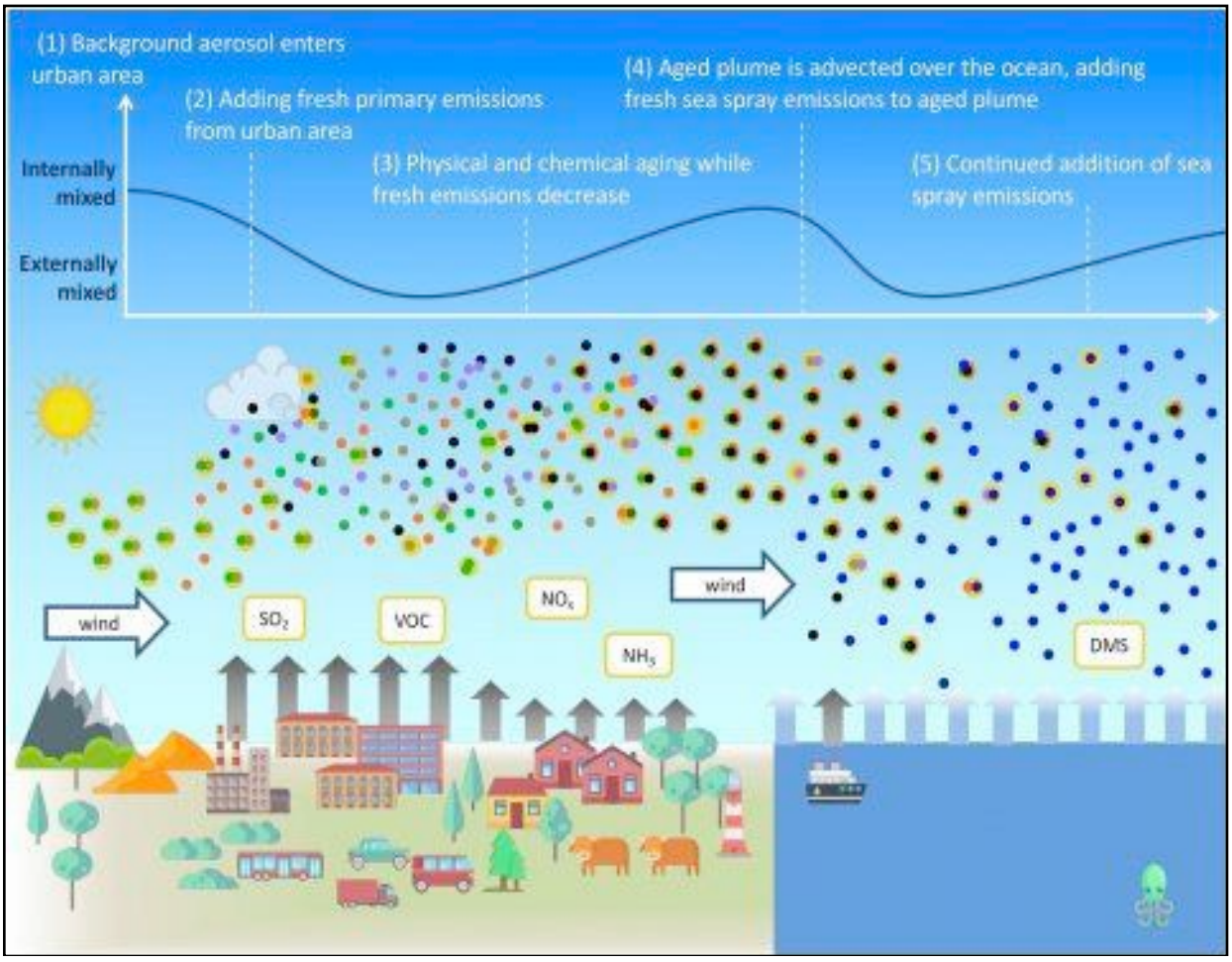

Figure 2.2: Composition of primary and secondary atmospheric aerosols (Riemer *et al.,* 2019)

Secondary aerosol particles are produced in the atmosphere from precursor gases by condensation of vapors on pre-existing particles or by nucleation of new particles. A considerable fraction of the mass of secondary aerosols is formed through cloud processing (Ervens *et al.,* 2011). Secondary aerosols are small; they range in size from a few nanometers up to 1 μm and have lifetimes of days to weeks. Secondary aerosols consist of mixtures of compounds; the main components are sulfate, nitrate, and OC. The main precursor gases are emitted from fossil fuel combustion, but fires and biogenic emissions of volatile organic compounds (VOCs) are also important. Occasionally volcanic eruptions result in huge amounts of primary and secondary aerosols both at the ground and in the stratosphere (Boulon *et al.,* 2011).

The size and chemical composition of the particles evolves with time through coagulations, condensation, and chemical reactions. Particles may grow by the uptake of water, a process that depends on chemical composition, particle size, and ambient relative humidity. The different particles have varying impacts in the atmosphere depending on composition, and the numerous sources and large range in size distributions further complicate a quantification of their effects. Both particle growth and the mixing of different particle types influence the climate effect of aerosols.

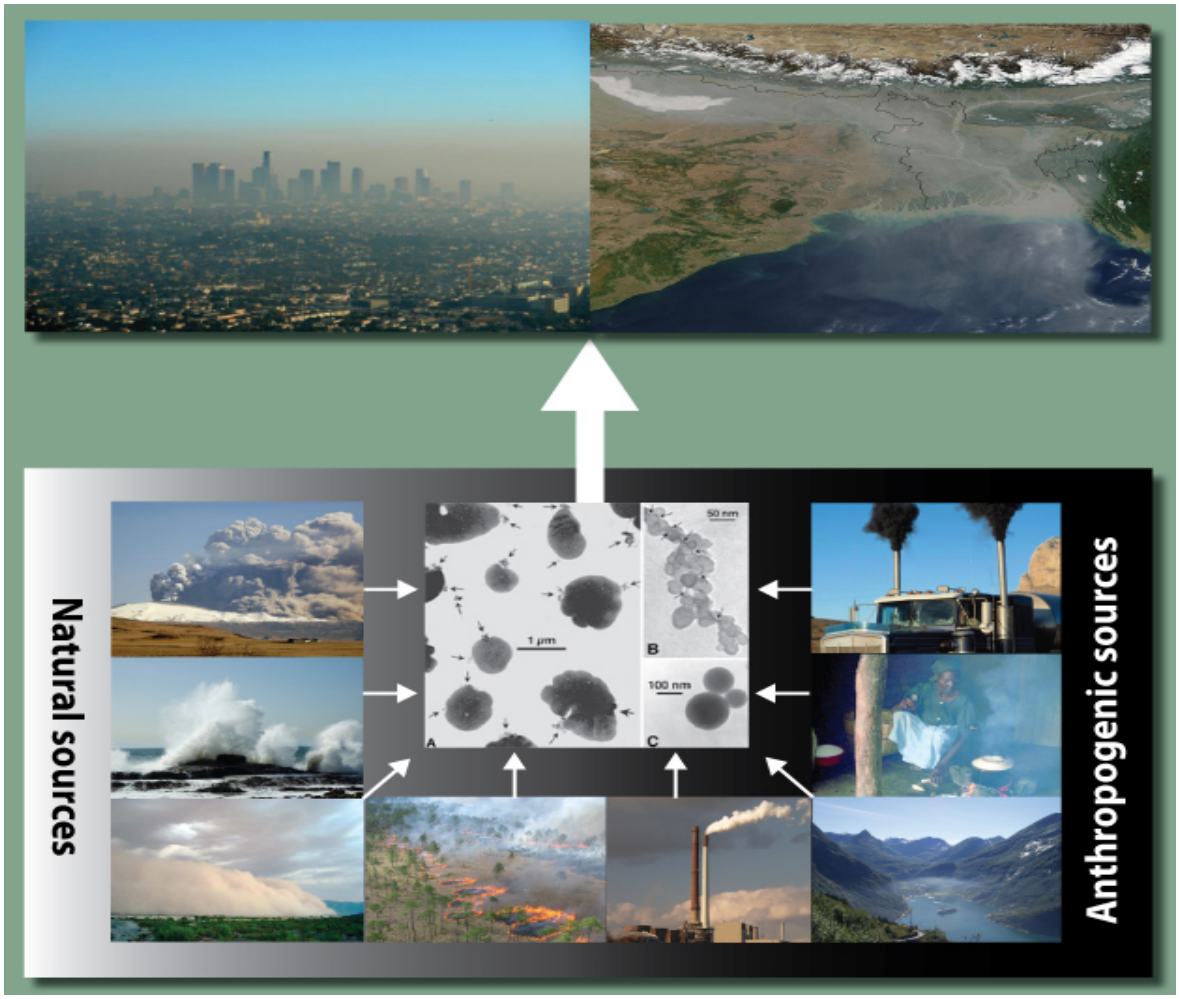

Figure 2.3: Sources and appearance of atmospheric aerosols (Posfai *et al.,* 1999).

The top images are the local and large-scale air pollution. The sources include (bottom, anticlockwise) volcanic eruptions (producing volcanic ash and sulfate), sea spray (sea salt and sulfate aerosols), desert storms (mineral dust), savannah biomass burning (BC and OC), coal power plants (fossil fuel BC and OC, sulfate, nitrate), ships (BC, OC, sulfate nitrate), cooking (domestic BC and OC), road transport (sulfate, BC, VOCs yielding OC). The center image denotes the electron microscopic images of (A) sulfate, (B) soot, and (C) fly ash, a product of coal combustion.

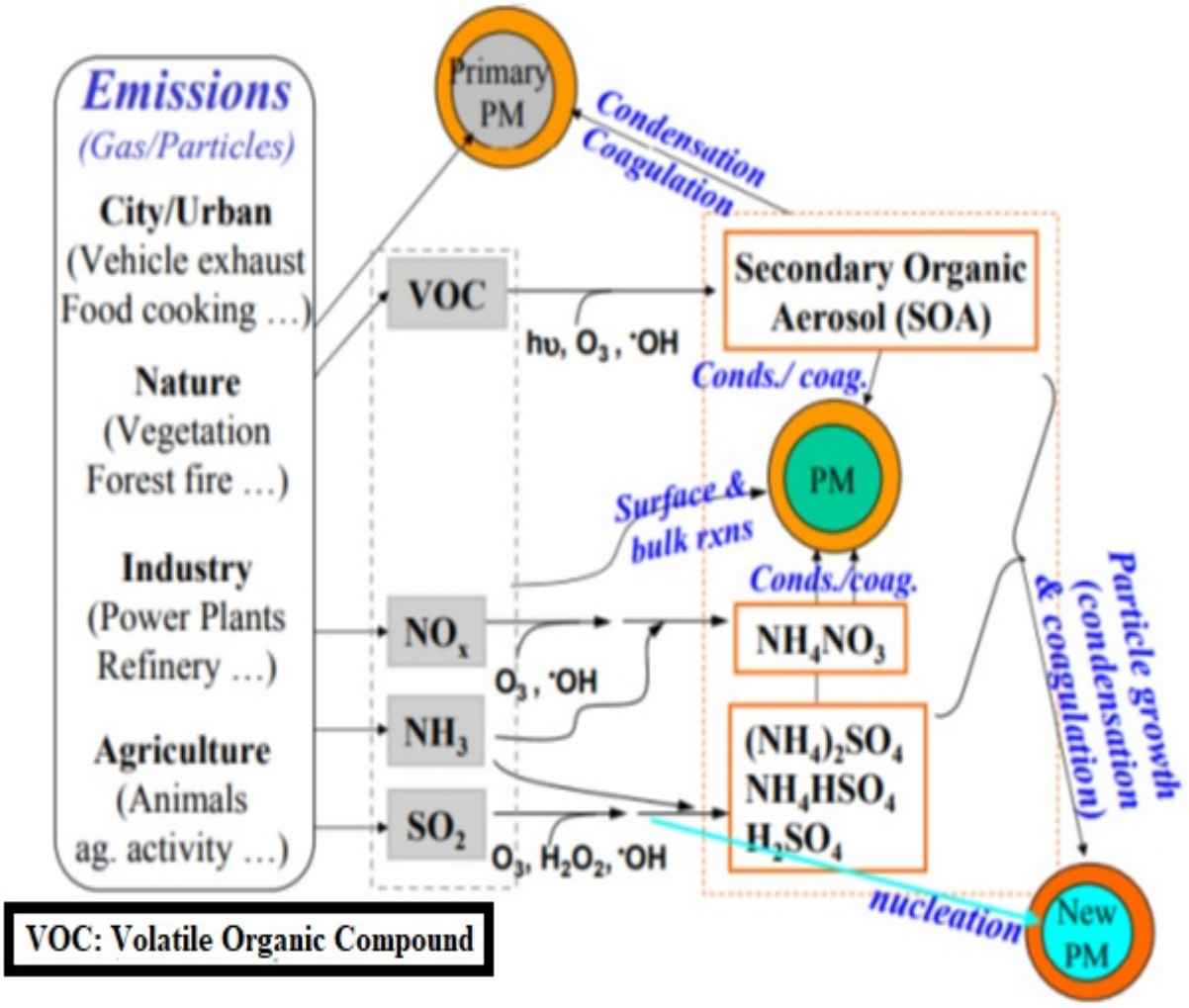

Figure 2.4: Secondary Aerosol Formation (i.e., Gas → PM Conversion)

Although coagulation modifies the size distribution of an aerosol, it causes no change in mass concentration. The other important internal process within a gas that shapes the size distribution, gas-to-particle conversion, results in an increase in the aerosol mass concentration. In studying this process, the interest is in the mechanisms by which gases are converted to particles, the rate at which conversion takes place, and the distributions of the condensed matter concerning particle size. Gas-to-particle conversion may result from homogenous gas-phase processes, or it may be controlled by processes in the particulate phase. Gas-phase processes, either physical or chemical, can produce a supersaturated state which then collapses by aerosol formation. Physical processes producing supersaturation include an adiabatic expansion or mixing with cool air or radiative or conductive cooling. Gas-phase chemical reactions such as the oxidation of SO_2 to sulfuric acid in the atmosphere or the oxidation of $SiCl_4$ to SiO_2 in the industry also generate condensable products.

Once a condensable species has been formed in the gas phase, the system is in a non-equilibrium state. It may pass toward equilibrium by the generation of new particles (homogenous nucleation) or by condensation on existing particles (heterogeneous condensation). If all collisions among condensable molecules are effective, the process resembles aerosol coagulation. It should be noted that the prediction of aerosol coagulation rates is a two-step process. The first is the derivation of a mathematical expression that keeps count of particle collisions as a function of particle size; it incorporates a general expression for the collision frequency function. An expression for the collision frequency based on the physical model is then introduced into the equation that keeps count of collisions. However, in certain important cases, small molecular clusters are unstable, and an energy barrier must be surmounted before stable nuclei can form.

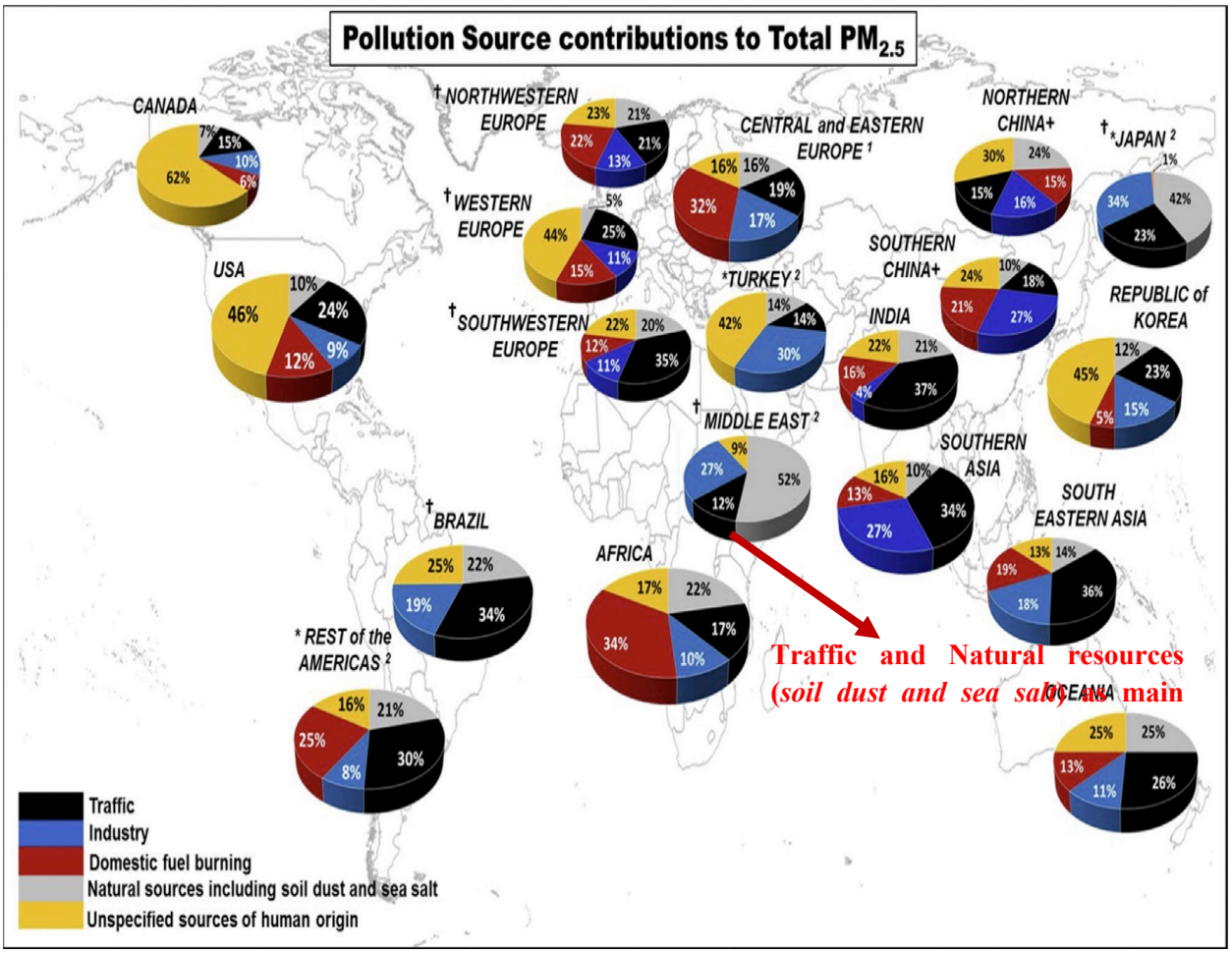

Figure 2.5: Population-weighted averages for relative source contributions to total $PM_{2.5}$ in Urban sites (Karagulian *et al.,* 2015).

Understanding the concept of Source Apportionment (SA) involves the concept of deriving information about pollution sources and the amount they contribute to ambient air pollution. The task can be accomplished using three (3) main approaches namely; emission inventories, source-oriented models, and receptor-oriented models. The analysis of source apportionment studies as highlighted in (Karagulian *et al.,* 2015) showed the complexity of mapping source categories. Many of the source apportionment studies used different source categories that were mainly determined by the available techniques for the chemical analyses. In most of the studies, a large portion of the particulate matter remains unexplained, and this often includes secondary particles (herein referred to as "unspecified sources of human origin"). The figure above made use of 419 source apportionment (Karagulian *et al.,* 2015), and the output suggests that traffic contributed 25% of urban ambient particulate matter ($PM_{2.5}$) from global averages of source contributions, 15% by industrial activities, 22% from unspecified sources of human origin, 20% from domestic fuel and 18% from natural dust and sea salt. With regards to Africa, domestic fuel burning emerged as the main contribution in Africa with about 34%, natural sources including soil dust and sea salt recorded at 22%, while the unspecified sources of human origin and traffic recorded the same contribution of 17% each. It should be noted that atmospheric modeling studies indicated a large contribution from solid fuel combustion in households, this category was not distinguished in many source apportionment studies or lumped together with traffic emissions.

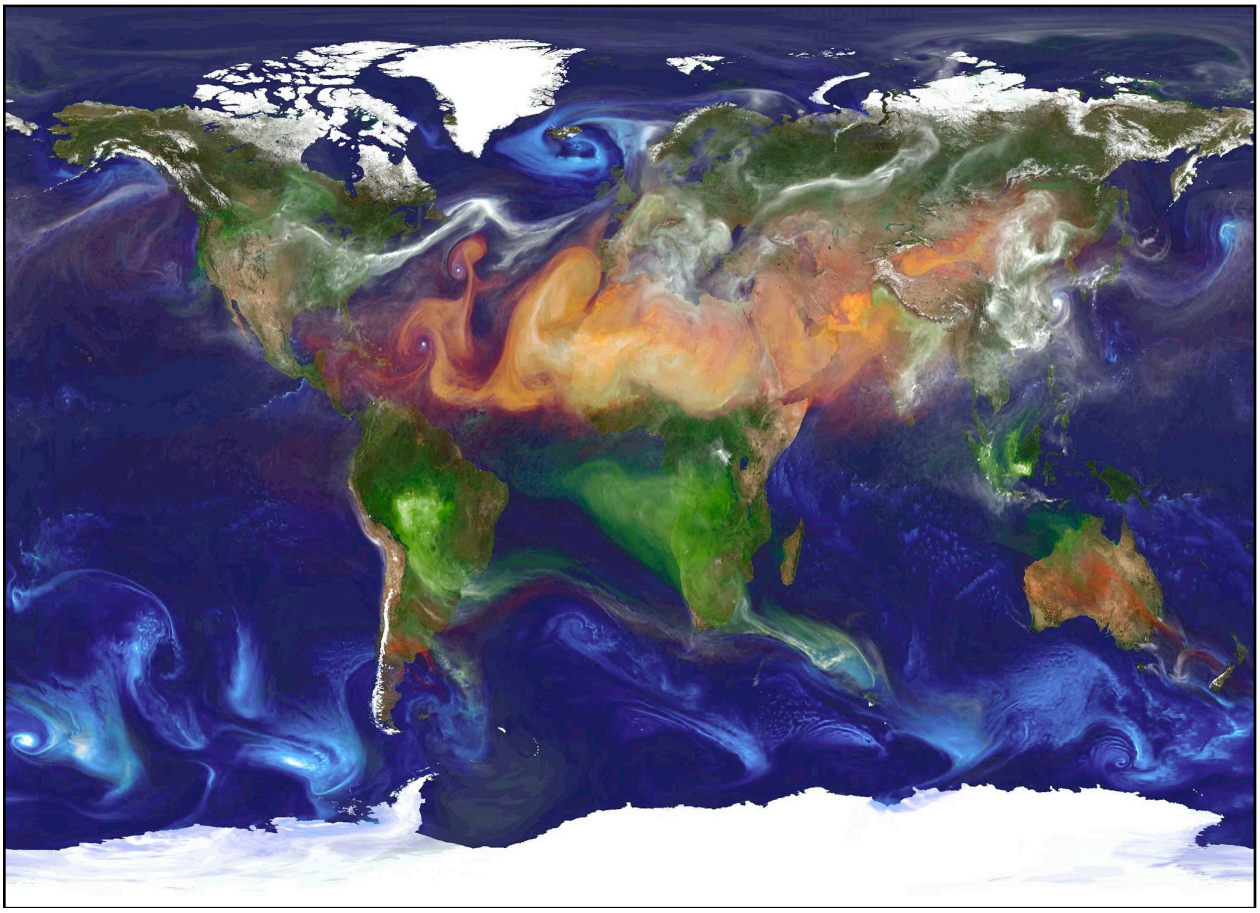

Figure 2.6: Overview of large clouds of aerosols around Earth (Green: Smoke; Blue: Salt; Yellowish brown: Dust; White: Sulfate (*Source: William Putman, NASA/Goddard*)

Several types of atmospheric aerosol have significant effects on Earth's climate: volcanic, desert dust, and sea salt, which originate from biogenic sources and are human-made. Volcanic aerosol forms in the stratosphere after an eruption as droplets of sulfuric acid that can prevail for up to two years, and reflect sunlight, lowering the temperature. Desert dust and mineral particles are blown to high altitudes, absorb heat, and may be responsible for NASA, inhibiting storm cloud formation. Human-made sulfate aerosols, primarily from burning oil and coal, affect the behavior of clouds (NASA, 2014). Although all hydrometeors, solid and liquid, can be described as aerosols, a distinction is commonly made between such dispersions (i.e. clouds) containing activated drops and crystals, and aerosol particles.

2.1.2 EFFECTS OF AEROSOLS

Several attributes and characteristics have been adduced to the sub-Saharan aerosols, and these are not limited to their long-range transport of nutrients (Duce *et al.* 1991), bacteria (e.g Bovallius *et al.* 1978; Maki *et al.*, 2019) and pollutants (e.g. Lyons *et al.* 1978; Lindqvist *et al.*, 1991), to its serving as cloud condensation nuclei (CCNs) which reduces cloud droplet effective radius, suppresses drizzle formation, and change cloud lifetime – highly referred to as aerosol indirect effects (AIEs) (Twomey 1977; Seinfeld *et al.*, 2016). Aerosols interact with the Earth's energy budget in two (2) ways; *directly* and *indirectly*. For example, a direct effect of aerosols is the scattering and absorption of solar radiation (Dong, 2019). This will mainly lead to the cooling of the surface (solar radiation is scattered back to space) but may also contribute to the warming of the surface (caused by the absorption of the incoming solar radiation) (IPCC, 2018). This can lead to additional elements to the greenhouse effect and therefore contribute to global climate change (Kommalapati & Valsaraj, 2009). The *indirect* effects refer to the aerosols interfering with

formations that interact directly with radiation. For example, aerosols can modify the size of the cloud particles in the lower atmosphere, thereby changing the way clouds reflect and absorb light and therefore modifying the Earth's energy budget (Allen, 2014). This is evidence to suggest that anthropogenic aerosols offset the effects of greenhouse gases in some areas, which is why the Northern Hemisphere shows slower surface warming than the Southern Hemisphere, although that just means that the Northern Hemisphere will absorb the heat later through ocean currents bringing warmer waters from the South (Irving *et al.*, 2019). On a global scale, aerosol cooling decreases greenhouse-gases-induced heating without offsetting it completely (IPCC, 2021). When aerosols absorb pollutants, it facilitates the deposition of pollutants to the surface of the earth as well as to bodies of water (Kommalapati & Valsaraj, 2009). This has the potential to be damaging to both the environment and human health. Aerosol particles with an effective diameter smaller than 10 μm can enter the bronchi, while the ones with an effective diameter smaller than 2.5 μm can enter as far as the gas exchange region in the lungs (Grainger, 2014), which can be hazardous to human health. Volcanic eruptions release large amounts of sulphuric acid, hydrogen sulfide, and hydrochloric acid into the atmosphere. These gases represent aerosols and eventually return to Earth as acid rain, having several adverse effects on the environment and human life (Allen, 2014). Aerosols in the 20 μm range show a particularly long persistence time in air-conditioned rooms due to their jet rider behavior (move with air jets gravitationally fall out in slowly moving air) (Hunziker, 2020), as this aerosol size is most effectively absorbed in the human nose (Kesavanathan & Swift, 1998), the primordial infection site in COVID-19, such aerosols may contribute to the pandemic.

2.1.3 PREVIOUS WORKS ON AEROSOL OVER WEST AFRICA

Several campaigns over West African aerosols (mainly the mineral dust) dynamics, chemistry, interaction with clouds, etc. have been done over the years to achieve different findings. For example, the Dynamics-Aerosol-Chemistry-Cloud Interactions in West Africa (DACCIWA) program comprises about sixteen (16) partners of higher institutions from Germany, the United Kingdom, France, Switzerland, and Nigeria. AMMA (African Monsoon Multi-Disciplinary Analysis) program (Polcher *et al.*, 2011) made an integrated observational and modeling study, using ground-based and airborne and satellite measurements, to characterize the aerosol loads over continental West Africa. The program described aerosol processes from emission through atmospheric transport, to deposition or advection outside the African domain and the physico-chemical properties that control their impacts, and in particular their direct radiative effect. The West African Multi-disciplinary Monsoon Analysis (AMMA) field campaign according to (Redelsperger *et al.*, 2006) has provided an excellent opportunity to improve the understanding of the life cycle of desert dust and its feedback with atmospheric dynamics. The first Special Observing Period (SOP0) of the program was devoted to the improvement in the current understanding of the desert dust particle atmospheric processes, especially in terms of their emission and transport from their source areas to their redistribution and sedimentation (Schepanski *et al.*, 2009), and their impacts on the atmospheric radiative budget. The long-range transport of aerosols can influence the air quality of the world. For instance, aerosols that had their source in Asia can be transported to locations as far as North America, and substantially contribute to the local levels of air pollutants (Lin *et al.* 2012; Cooper *et al.* 2015; Verstraeten *et al.* 2015). S
Dust episodes over Nigeria and indeed over West Africa are a well-known characteristic of the dry season between November and January extending sometimes (but on rare occasions) to the end of

February over the south coast of Nigeria. Dust is usually mobilized and transported, from the source region of the Bodélé depression (Herrmann *et al.* 1999), and other neighboring source regions, southward during the boreal dry season. Dust aerosol is one of the atmospheric constituents that have been well studied because of its radiative property (Kaufman *et al.* 2002). A well-known effect of dust on radiation is the scattering of rays of light to produce cooling or reduce horizontal visibility (Tegen and Lacis, 1996; Levin *et al.* 1996; Han *et al.* 1998; Haywood and Boucher 2000; Harrison *et al.* 2001).

2.1.4 AEROSOL SOURCES: TYPICAL SPATIAL AND SEASONAL PATTERNS

Specific inventories of carbonaceous aerosols have been developed for the 2000–2007 period over the African continent (Liousse *et al.*, 2010). Aerosol emissions from biomass burning are estimated based on satellite observations of burned areas and types of combustion (Liousse *et al.*, 2010). In the northern hemisphere, they are maximum in December and are mainly located in Central Africa, with a few hot spots in Western Africa and a year-to-year variability as high as 50%. Regional inventories of anthropogenic emissions due to fossil fuel and biofuel (gasoline, diesel, wood, crop residues, etc.) consumption, include regional specificities, such as traffic from two-wheel vehicles (Assamoi and Liousse, 2010). These inventories highlight the local contribution of large African cities (e.g. Lagos, Cotonou), in agreement with observations (Reeves *et al.*, 2010). Regional and global simulations using these new inventories better agree with observations (Liousse *et al.*, 2010; Tummon *et al.*, 2010). The anthropogenic emissions (fuel/biofuel/traffic/industry) of carbonaceous aerosols are comparable to those from open biomass burning, with emission scenarios suggesting a likely future increase.

2.1.5 CHEMICAL AND PHYSICAL PROPERTIES AND PROCESSING OF SOME AEROSOLS.

Physico-chemical properties of mineral dust, and in particular those controlling their radiative effect, have been extensively investigated. For the first time, size-resolved mineral dust emission fluxes have been measured *in situ*, confirming the change in the emitted dust size distribution with dynamical conditions (Sow *et al.*, 2009). Significantly different size distributions are recorded between locally produced and advected dust (Rajot *et al.*, 2008). While the non-sphericity of mineral dust particles has been clearly stated, their aspect ratio (1.7) was found almost constant on the whole size spectrum (Chou *et al.*, 2008). Regional signatures in iron oxides have been distinguished according to dust origin (Formenti *et al.*, 2008). Despite their low contribution to the dust mass (2.4 – 4.5%, i.e. 46% and 59% of total iron), iron oxides strongly influence dust absorption characteristics (McConnell *et al.*, 2010) and may thus impact the sign of the dust's direct radiative effect. Evidence of the internal mixing of mineral dust with biomass-burning particles was given during the dry season (Hand *et al.*, 2010). Dust chemical properties are also modified during the wet season by their incorporation into cloud droplets, becoming internally mixed with sulfate, chloride, and nitrate (Crumeyrolle *et al.*, 2008; Matsuki *et al.*, 2010). Mineral dust radiative and CCN properties may thus be significantly impacted by interactions with biomass-burning aerosols in the dry season and with soluble organic and inorganic components brought by the monsoon flow in the wet season.

During the dry season, biomass burning is the overwhelming source of submicron organic aerosol, with size evolving by coagulation from 0.08 μm close to the sources to 0.1–0.2 μm for aged biomass burning aerosol (Johnson *et al.*, 2008; Capes *et al.*, 2009). A constant ratio between organic mass and carbon monoxide has been observed in biomass-burning plumes, close to and far downwind fire sources, while the oxygen-to-carbon ratio increases. This implies a loss of carbon

within the plume, as highlighted in some, though not all, field and chamber studies (Grieshop *et al.*, 2009). The observed organic mass is grossly underestimated by the production yields derived from simulation chamber studies (Capes *et al.*, 2009). This highlights very large gaps in our understanding of the evolution of organic aerosol in West Africa.

For the atmospheric particulate matter (PM) as of today, the regional modeling of this aerosol is of major importance for air quality studies (Dreher and Costa, 2002) as well as climate considerations. As models are important tools for air quality management and the evaluation of emission control policies, it is necessary to assess their ability in simulating air quality. However, the modeling of PM concentrations is a difficult task because PM is a conglomerate of many particles with different physical and chemical properties. These particles are both emitted directly from a large variety of anthropogenic, biogenic, and natural sources and formed in the atmosphere by chemical and physical processes from gas-phase precursors

2.1.6 AEROSOL SPATIAL DISTRIBUTION OVER WEST AFRICA

The spatial redistribution of aerosols in the atmosphere is linked to large-scale dynamical patterns. For instance, the field observations from AMMA show that various small-scale and mesoscale processes are also involved in the generation of mineral dust, aerosol mixing in the boundary layer, and vertical transport to upper atmospheric layers.

During the dry season, two main anti-cyclonic regions are located close to the Azores and Saint Helena islands, with low pressure over central Africa linked to large-scale heating. The Inter-Tropical Discontinuity (ITD) is located slightly north of the Equator and a reduced monsoon inflow prevails south of the Sahel. The so-called ‘Harmattan Front’ separates the dusty air to the north from the biomass-burning-laden air to the south although significant mixing occurs at the boundary (Haywood *et al.*, 2008). The stronger heating to the South causes the relatively unstable,

moist, warm, and biomass-burning-laden air to be undercut by drier cooler dust-laden air. This leads to a two-layer structure: the lower (elevated) layer is dominated by dust (biomass-burning aerosol). Ground-based and airborne (Cloud-Aerosol Lidar and Infrared Pathfinder Satellite Observations, CALIPSO) lidar systems offered the unique capability to monitor the aerosol vertical distribution and demonstrate the persistency of this two-layer structure at the regional and multi-annual scale (Léon *et al.*, 2009; Cavalieri *et al.*, 2010).

In the wet season, the energy budget of the system is modified. A strong heat low develops over Sahara, reinforcing the pressure gradient with the Gulf of Guinea. The ITD moves north, and the monsoon inflow reaches the North Sahel (Lafore *et al.*, 2011), depending on the month of the wet season, with the northernmost position of the ITD said to be at 22°N (Ilesanmi, 1971; Adefolalu, 1984; Omotosho, 1985; Nymphas *et al.,* 2004). Meanwhile, the anticyclone in the southern hemisphere extends over land and into central Africa. These dynamic patterns and the development of boundary layer height over northern Africa by solar heating (Milton *et al.*, 2008) favor dust transport over the Atlantic and the Caribbean Sea by the trade winds in the Saharan Air Layer (SAL). The vertical structure of this dust-laden SAL has been documented from the central Sahara (Cuesta *et al.*, 2009) to the Atlantic coast, where the maximum summer aerosol optical depth (AOD) is associated with a maximum in the SAL elevation (up to 6 km) (Léon *et al.*, 2009).

The systematic formation of nocturnal gusts, evidenced locally by several lidar observations (Haywood *et al.*, 2008) and from satellite (MODIS Deep Blue; SEVIRI/MSG; GIOVANNI) is one of the possible processes leading to increased dust content in the lower Saharan boundary layer. During this same wet season, ‘density currents’ linked to convective clouds are responsible for additional dust emissions in the Sahara (Marsham *et al.*, 2008). It has also been shown that the dynamics of the Inter-Tropical frontal (ITF) disturbance cause significant dust vertical transport

from the boundary layer aloft, both for the dust in the wet season (Bou Karam *et al.*, 2008) and for the biomass particles in the dry season (Pelon *et al.*, 2008).

Biomass-burning aerosol events, mainly driven by deforestation and agricultural practices (Echalar *et al.* 1998; Reddington *et al.* 2015), prevail in the Amazon Basin (Setzer and Pereira, 1991) during the dry season, typically between July and October (Gan *et al.* 2004), injecting large amounts of aerosols into the atmosphere. Long-range transport of biomass-burning aerosols from southern Africa further increases aerosol loadings during this period (Holanda *et al.* 2020). Biomass burning as the main source of fine particles can influence weather and climate through complex feedbacks with radiation and clouds on regional and global scales (Ramanathan *et al.* 2001; Kaufman and Koren 2006; Rosenfeld *et al.* 2008; Shrivastava *et al.* 2017; Ditas *et al.* 2018). Aerosols emitted from biomass burning contain black carbon (BC) and brown carbon, which enable them to scatter and absorb solar radiation directly, the so-called "direct radiative effect" (Charlson *et al.* 1992; Ackerman *et al.* 2000). Biomass burning aerosol makes up a majority of primary combustion aerosol emissions (Bond *et al.* 2013; Andreae 2019), with the main sources of global BB mass being Africa (~52%), South America (~15%), Equatorial Asia (~10%), Boreal forests (~9%), and Australia (~7%) (van der Werf *et al.* 2010). The composition, size, and mixing state of BB aerosols determine the optical properties of smoke plumes in the atmosphere, which in turn is a major factor in dictating how they perturb the energy balance in the earth system.

Dust emission and source activation are generally associated with strong surface winds like the Harmattan, the dry northeasterly winds that dominate over most of the Sahara and Sahel during the northern hemispheric dry season (December to March). Engelstaedter and Washington (2007) noted that the annual cycle of the activity of the dust sources in western Africa is controlled by dry convection which comes along with an increase in the occurrence of small–scale high–wind

events. Furthermore, dust is often mobilized in the morning hours, when the nocturnal low–level jet breaks down with the beginning evolution of the planetary boundary layer and momentum is mixed to the surface (Knippertz 2008, Schepanski *et al.* 2009). Other likely meteorological effects that cause the strong winds necessary to trigger dust mobilization are squall lines and density currents which are associated with moist convection (Knippertz 2008, Knippertz *et al.* 2009, Schepanski *et al.* 2007, 2009).

2.1.7 AEROSOL OPTICAL PROPERTIES AND RADIATIVE IMPACT

The single scattering albedo (SSA), i.e. the ratio of scattering to total light extinction (absorption plus scattering) is a critical parameter to determine the sign of the aerosol forcing. Single Scattering Albedo and local direct radiative forcing were estimated at several locations in West Africa with different aerosol conditions.

The year 2006 dry season in Niamey experienced the mineral dust surface layer and the upper biomass burning aerosol layer contributing almost equally to a daytime solar direct radiative effect at the surface, ΔF_{SURF}, estimated at −56 W m^{-2} (Haywood *et al.*, 2008; Milton *et al.*, 2008). During the same period, in Djougou, the daily average ΔF_{SURF} was estimated to be −45 W m^{-2} (Mallet *et al.*, 2008). The daily forcing efficiency at the surface (ΔF_{SURF}/AOD) has been estimated as −31 W m^{-2} AOD^{-1} for heavy dust events and −62 W m^{-2} AOD^{-1} for mixtures of biomass burning and dust aerosol (Derimian *et al.*, 2008). Independent estimates consistently show that mineral dust is mainly scattering radiation in the visible range. The SSA of the submicron dust has been estimated to be ∼0.99 ± 0.01 (at 0.55 μm) (Osborne *et al.*, 2008), and ∼0.90 with the addition of the coarse mode (McConnell *et al.*, 2008). The dust SSA is lower in the wet season than in the dry season, possibly due to sources with different mineralogies. This range of SSA is consistent with previous estimations from the literature derived from ground-based, aircraft, or satellite measurements in

this region. Likewise, F_{SURF} is strongly influenced by the total AOD, while the radiative effect at the top of the atmosphere, F_{TOA}, is mainly controlled by the relative proportions of dust and biomass burning aerosols and the surface reflectance (Raut and Chazette, 2008). But the dusty layer possibly enhances the absorption of the upper biomass burning layer. These results underline the large direct radiative effect of mineral dust and biomass burning layers and highlight the importance of aerosol layering on this forcing. The optical properties of biomass-burning aerosol exhibit a much higher variability, likely due to different ages, sources, and combustion characteristics. From airborne observations, the SSA of biomass burning aerosol over West Africa is 0.81 on average (Johnson *et al.*, 2008), i.e. comparable to estimates in Brazilian fires but significantly more absorbing than in South African or boreal fires. Regions affected both by mineral dust and biomass burning particles display a large variability in the SSA (0.81–0.98 at 0.52 μm, i.e. Mallet *et al.*, 2008) depending on the relative contributions of each aerosol, the lower (higher) value representing higher contributions from biomass burning (mineral dust).

Finally, the solar atmospheric forcing (i.e. the amount of energy absorbed by the atmospheric layer), $\Delta F_{ATM,}$ is higher for biomass-burning aerosols than for mineral dust. But a significant terrestrial ΔF_{ATM} is caused by the absorption and re-emission of terrestrial radiation by mineral dust (Mallet *et al.*, 2009).

2.1.8 AEROSOL PROCESSES IN COSMO-MUSCAT COUPLING MODEL

For the description of the particle size distribution and aerosol dynamical processes, the modal aerosol model M7 (Vignati *et al.*, 2004) is used. In this approach, the total particle population is aggregated from seven lognormal modes with different compositions. The modes represent a dry diameter size range and can be water-soluble or water-insoluble. The soluble particles are assumed to be in equilibrium with water vapor and other gas-phase precursors. Particle size distribution

changes owing to various mechanisms, which are divided into external processes like particle transport by internal processes like condensation and coagulation. Currently, only coagulation due to particle Brownian motion, which is the dominating coagulation mechanism for sub-micron particles, is considered in the M7 approach (Stier *et al.*, 2005). The prognostic aerosol variables that are transported in COSMO-MUSCAT are the total number of aerosol particles as well as all primary and secondary species (organic and inorganic) within each mode. The original version, which considers the components sulfate, sea salt, dust, black and organic carbon, has been extended by nitrate and ammonium. The species within the four soluble modes are assumed to be internally mixed, which means, all particles of a mode have the same composition. The insoluble aerosols are represented by three modes: an Aitken mode of internally mixed black and organic carbon, and accumulation and coarse modes containing dust. The thermodynamic equilibrium model ISORROPIA (Nenes *et al.*, 1998) is used to determine the particle/gas partitioning of semi-volatile inorganic species. The model calculates the thermo-dynamical equilibrium of the system: sulfate-nitrate-ammonium-sodium-chloride-water at a given temperature and relative humidity.

Especially for long-term simulations (e.g. annual runs), a more simplified mass-based particle model can be applied, which is computationally less expensive. The used approach is quite similar to that of the EMEP Eulerian model (Simpson *et al.*, 2003).

The resolution of the COSMO-MUSCAT is 14 km x 14 km. Though there are other models with higher resolution, several studies have examined the effects of higher grid resolution on the accuracy of meteorological model simulations (Salvador *et al.*, 1999). In most cases, increasing resolution produces more realistic structures. But a higher resolution does not necessarily imply improvements in prediction skills (Mass *et al.*, 2002).

Section 2.2: MESOSCALE CONVECTIVE SYSTEMS (MCSs)

The western equatorial sector of Africa is, meteorologically speaking, one of the world's most interesting but also most poorly understood regions. Some of the world's highest rainfall totals are reported over Mt. Cameroon, at its western edge, where mean annual rainfall exceeds 10 meters. The coastal sector experiences inter-annual fluctuations in association with Atlantic warming that rival those produced by El Nino along the South American desert coast (Nicholson and Entekhabi, 1987). This region also experiences the world's most intense thunderstorms and the highest frequency of lightning flashes (Zipser *et al.* 2006, Toracinta and Zipser 2001, Petersen and Rutledge 2001).

The greatest proportion of the annual rainfall of West African countries is from convective systems. (Hamilton and Archbold, 1945) were the first to note the occurrence of the squall line and thunderstorm as a mesoscale disturbance. Adefolalu (1974) also showed the interaction of the moist southwest flow of the lower layer of the African atmosphere with the mid-tropospheric easterly wave that indicates the type, intensity, and horizontal coverage of the resulting thundershowers. While Nymphas *et al.*, (2004) showed that the seasonal weather variation in West Africa can be classified into two: the wet season and the dry season. The south-westerlies supply about 90% of rainfall in West Africa via squall line activities. The peak rainfall period depends on the location – two peaks in the southern region (July and October), and one peak in the northern region (July/August).

Even within the tropics, western equatorial Africa is a convective anomaly. The only regions with comparable storm intensity, the United States, Argentina, and parts of the Indian sub-continent, are in the mid-latitudes (Mohr and Zipser 1996a, b). Despite the intensity of storms, rainfall in the region is only moderate compared with equatorial regions of the Amazon and Indonesia (Petersen

and Rutledge 2001, Zipser *et al.*, 2006). Western equatorial Africa is also the only tropical region with intense convection in all seasons. Storms are anomalously large, with the mean size of all precipitation features exceeding 500 km^2 in some parts of the region (Nesbitt *et al.*, 2006). The diurnal cycle of rainfall also differs from that of most other tropical and subtropical land areas; rainfall from mesoscale convective systems (MCSs) has a broad minimum during the afternoon and early evening hours and a maximum during the night and early morning (Nesbitt and Zipser, 2003).

2.2.1 THUNDERSTORMS

Thunderstorms are a fundamental component of the nation's climate, serving as a key element in the water cycle and the global atmospheric electric circuit. As a result, numerous in-depth studies have assessed the physical nature of thunderstorms, their predictions, and their climatology. Balogun (1984) studied the distribution of thunderstorms in Nigeria which showed that though both rainfall and thunderstorm distribution exhibit a double maximum over coastal areas, the first and primary peak in rainfall lags that of thunderstorms by about two months. However, the storm peak in October is preceded by a secondary rainfall maximum. The single maximum in each distribution for inland areas north of 8^oN however correlates well with thunderstorm occurrence. But here again, no distinction was made between the various weather components to the rainfall and their separate contribution. It is rare to have high-intensity rainfall without thunderstorms in West Africa.

Omotosho (1984) corroborated an earlier finding that over 70% or more of annual rainfall is associated with a moving belt of thunderstorms. The relative importance of line squalls, thunderstorms, and monsoon precipitation to the rainfall on both the monthly and annual time scales and the variation of each component of rainfall latitude have been studied. These studies

have shown that the mean line squall contributes the greatest proportion of the total precipitation. These propagating mesoscale systems are responsible for over 70% of the precipitation north of 10^{o}N. There is a double maximum in the line squall rainfall as far as 12^{o}N but thunderstorm precipitation shows only one peak north of 8°N (Bello, 1989).

Omotosho *et al.*, (2000) used the anomalies of these parameters (θ_e and θ_{es}) to develop prediction methods for not only the onset but also the cessation as well as the annual total amount of rainfall for Nigeria and West African countries. It was also found that total thunderstorm rainfall decreases linearly with latitude whereas line squall precipitation shows a maximum of around 9°N and rainfall from the monsoon decreases exponentially with increasing latitude. Finally, the month-month rainfall latitude relationship appears to be a reliable technique for forecasting the onset/cessation of rain for a particular location. The rate of decrease of total rainfall with latitude is twice as fast towards the end as against the onset of the rains.

Thunderstorms and the phenomenon they produce e.g. lightning, tornadoes, hail, strong winds, and heavy rainfall; have received great attention because of the significant damage they produce. For example, thunderstorms during the 1949–1998 period caused $87 billion in damages to property in the United States; Changnon (2001a). Thunderstorms damages rank just behind floods and hurricanes as the nation‘s most damaging weather condition; Changnon (2001b). Surprisingly, very little attention has been given to the amount of precipitation produced by thunderstorms and to measuring the environmental impacts of precipitation. The benefits are likely to be very large but not well-defined. For example, thunderstorm rainfall contributes to all the annual run-off measured on small river basins in Arizona and New Mexico (Osborn and Reynolds, 1963), and represents 75% - 80% of the average growing season rainfall in Illinois; Changnon (1957). A thunderstorm is characterized by strong winds in the form of squalls, heavy precipitation, and low-

level wind shear. The formation, intensification, and propagation of thunderstorms are mostly governed by the synoptic and thermodynamic conditions of the atmosphere; their microphysical and electrical characteristics are known to affect significantly the formation and the intensity of precipitation (Rycroft *et al.*, 2007; Yair, 2008; Sanders, 2008). Various research programs such as the Thunderstorm Research International Programme (TRIP), the Down Under Doppler, and Electricity Experiment (DUNDEE). Rutledge *et al.*, (1992), the Severe Thunderstorm Electrification and Precipitation Study (STEPS) Lang *et al.*, (2004) have been launched involving both ground and airborne measurements to study the electrical properties of thunderstorms and related phenomena. Thunderstorms are the deepest convective clouds caused by buoyancy forces set up initially by the solar heating of the earth's surface. Thunderstorm forms when moist, unstable air is lifted vertically into the atmosphere. Hence, the lifting of this air results in condensation and the release of latent heat. Numerous unorganized and frequent thunderstorms may be caused by any or combination of:

- Strong diurnal heating results in a super-adiabatic lapse rate near the surface.
- Orographically forced ascent, particularly during early and late monsoon season.
- Dynamic lifting because of the presence of a frontal zone.

Immediately after lifting begins, the rising parcel of warm moist air begins to cool because of adiabatic expansion. At a certain elevation, the dew point is reached resulting in condensation and the formation of a cumulus cloud. For the cumulus cloud to form into a thunderstorm, continued uplift must occur in an unstable atmosphere. With the vertical extension of the air parcel, the cumulus cloud grows into a cumulonimbus cloud. Cumulonimbus clouds can reach heights of 20 km above the earth's surface. Severe weather associated with some of these clouds includes hail, strong winds, thunder, lightning, intense rain, and tornadoes.

2.2.1.1 TYPES OF THUNDERSTORMS

Generally, two types of thunderstorms are common:

- Single-cell (or air mass) thunderstorms occur in the mid-latitudes in summer and at the equator all year long.
- Multi-cell or thunderstorms associated with mid-latitude cyclone cold fronts or dry lines.
- Super-cell.

Although the natural environment does not fall into three distinct categories, we break them down to help illustrate significant differences. The differences arise because of varying atmospheric profiles, especially those concerned with vertical shear, defined as the change in wind velocity (speed or direction) with height, or dv/dz.

The air mass thunderstorm is a common and usually non-severe phenomenon that forms away from frontal systems or other synoptic-scale disturbances. They form where moist and unstable conditions exist in the atmosphere. Air mass thunderstorms are usually produced in areas of very little vertical shear. As a result, the threat of severe thunderstorms is small. When they do reach severe limits, the thunderstorms may produce brief high winds or hail which develop because of high instability. These storms are known as ***pulse-severe storms.*** Although several storm cells can develop, each cell lasts about 30-60 minutes and has three stages. They include;

1.) Convective/Cumulus Stage

i. Starts with a warm plume of rising air.

ii. The updraft velocity increases with height.

iii. Entrainment pulls outside air into the cloud.

iv. Super-cooled water droplets are carried far above freezing level.

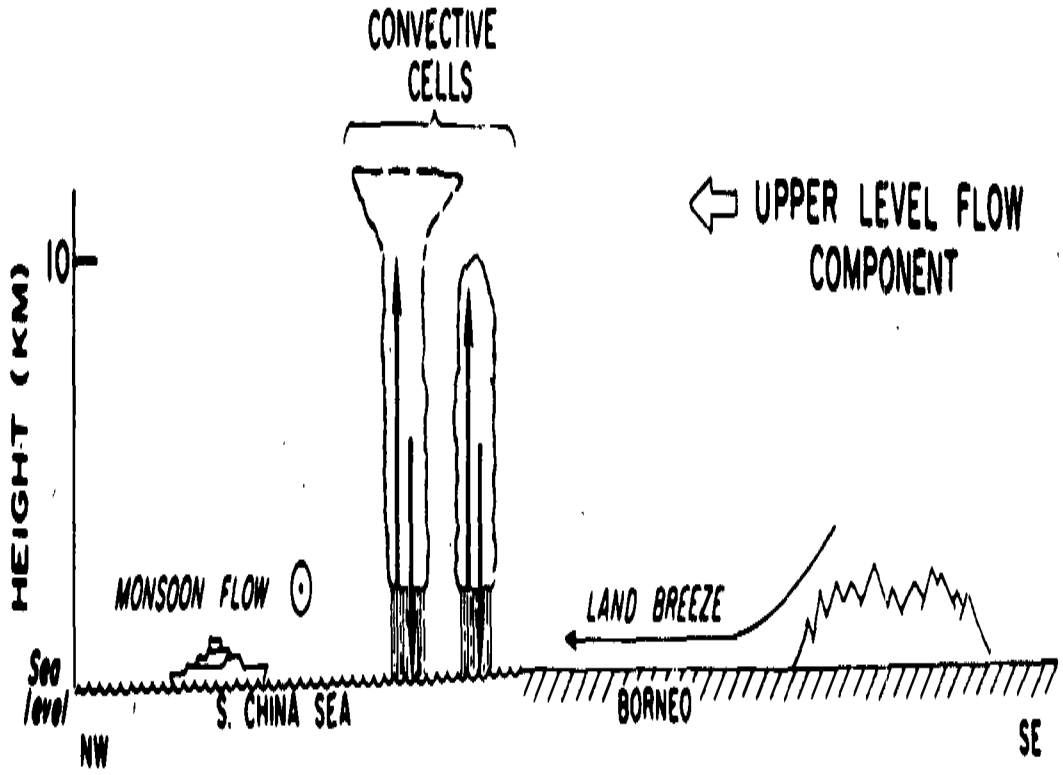

Fig. 2.7: Schematic depiction of the development of a diurnal generated non-squall tropical cloud cluster off the coast of Borneo at a convective stage. (Houze et al; 1981)

2.) Mature Stage

i. The heaviest rains occur.

ii. The downdraft is initiated by the frictional drag of the raindrops.

iii. Evaporative cooling leads to negative buoyancy.

iv. The top of the cloud approaches tropopause and forms an anvil top.

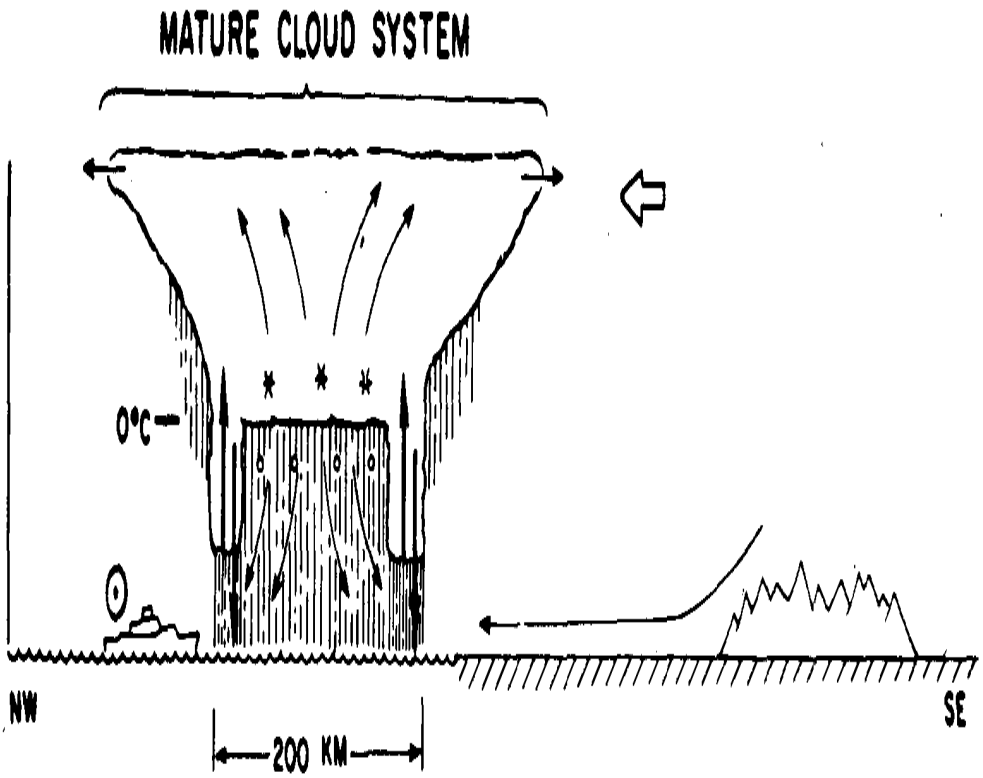

Fig. 2.8: Schematic depiction of the development of a diurnal generated non-squall tropical cloud cluster off the coast of Borneo at a mature stage. (Houze et al; 1981)

3.) Dissipating Stage

i. The downdraft takes over the entire cloud.

ii. The storm deprives itself of super-saturated updraft air.

iii. Precipitation decreases.

iv. The cloud evaporates.

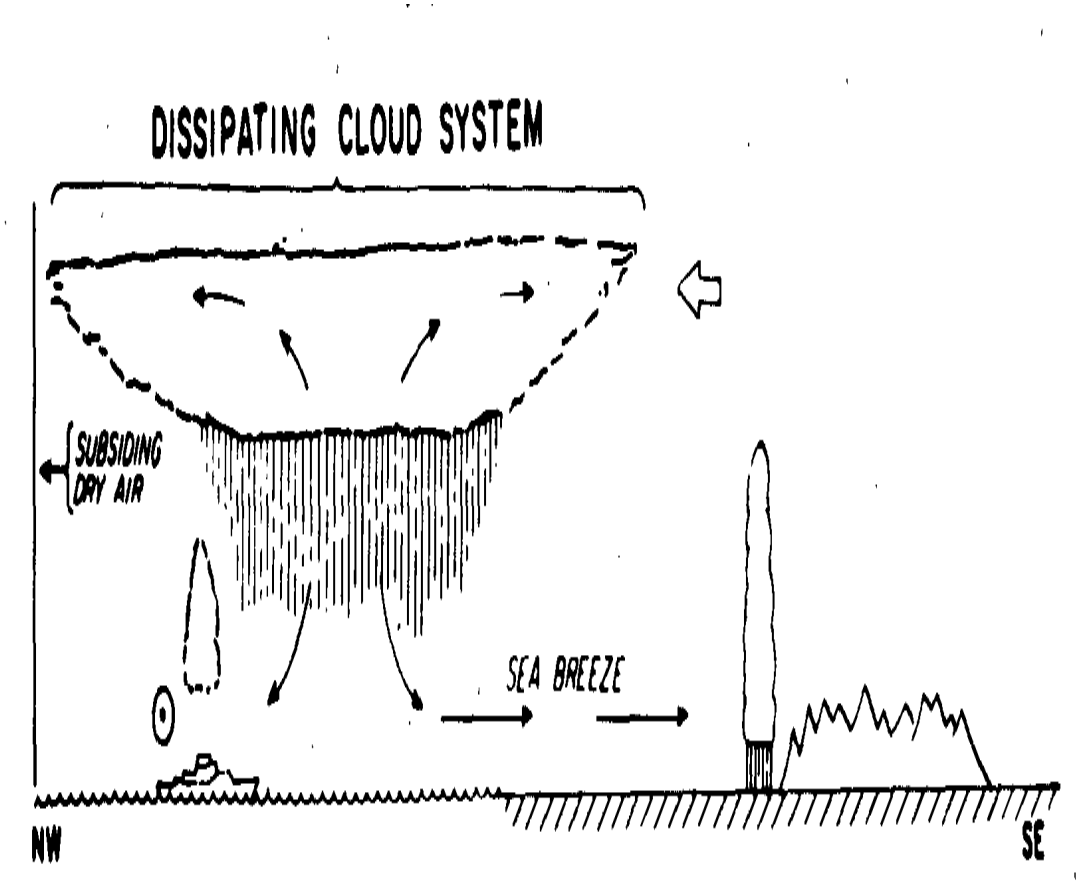

Fig. 2.9: Schematic depiction of the development of a diurnal generated non-squall tropical cloud cluster off the coast of Borneo at a dissipating stage. (Houze et al; 1981)

As wind shear organizes the convection, new thunderstorms form as a result of parent thunderstorm outflows converging with warm, moist inflow creating new updrafts. Multi-cell storms can form in a line known as a **squall line**, where continuous updrafts form along the leading edge of the outflow, or gust front. Multi-cell clusters indicate new updrafts are forming where the low-level convergence is strongest, usually at the right, or right-rear flank of existing cells.

Thunderstorms that organize in response to synoptic-scale forcing usually need:

i. Warm, moist air at a low level.
ii. Cool, dry air at upper levels.
iii. Upper-level divergence (above 500 mb).
iv. A synoptic-scale disturbance

In these conditions, thunderstorm formation is probable. Synoptic scale vertical motions tend to create favorable conditions for thunderstorms, but thunderstorm initiation is usually a result of mesoscale forcing. Increasingly favorable vertical wind profiles may lead to a greater possibility of super-cell development rather than multi-cell storms. The development of squall lines, or more commonly storm clusters, when thunderstorms do develop is virtually guaranteed in association with strong linear synoptic-scale forcing.

2.2.2 SQUALL LINES.

According to Balogun (1974), a squall line was defined as a line of disturbed weather about 300-1000km long oriented roughly North-South, moves from east to west with a speed between 15-20ms^{-1}. While Omotosho *et al.*, (2000) defined the Squall line as a bound of a very active

convective cloud about 50km wide (eastwards direction) and 100km long (northwards direction), moving from east to west at a speed of $12.5ms^{-1}$ Ξ 25knots.

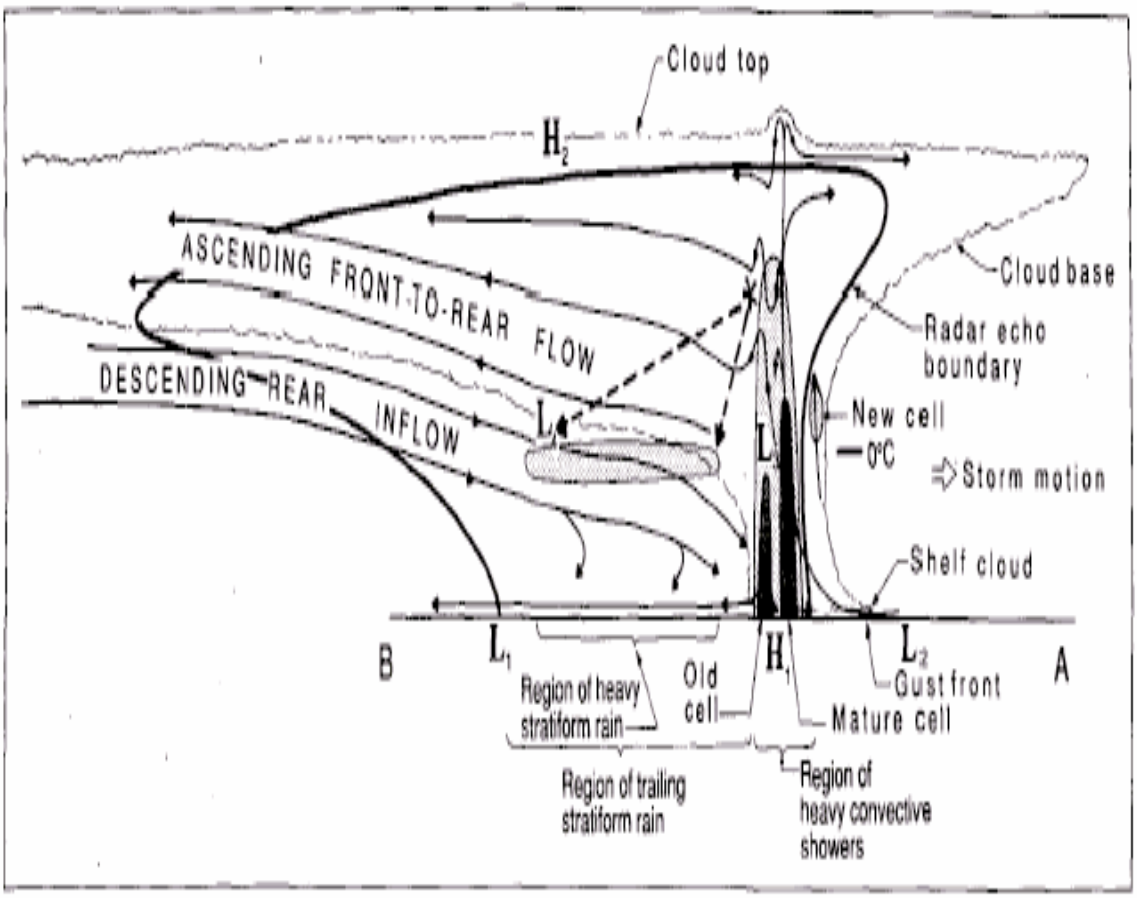

Fig. 2.10: The structure of a well-formed squall line (Houze, 1989).

Large ice clouds spread by winds aloft dominate the view of earth from space. These cirri-form cloud tops emanate from cyclones, both tropical and extra-tropical and large convective storms. Mesoscale Convective Systems (MCSs) are the largest of the convective storms. They form when clouds occurring in response to convective instability amalgamate and organize upscale into a single cloud system with a very large upper cirri-form cloud structure and rainfall covering large contiguous rain areas. They account for a large proportion of precipitation in both the tropics and warmer mid-latitudes. Long-lasting, slow-moving MCSs are a major cause of flooding, and these systems often contain hail, strong winds, and even tornadoes. MCSs over the ocean sometimes evolve into tropical cyclones. In producing all these effects, MCSs take on a variety of forms. A broad descriptive definition of MCSs that includes most, if not all, of its forms is a cumulonimbus cloud system that produces a contiguous precipitation area of ~100 km or more in at least one direction. Houze (1993) suggested a similar definition and further noted that the dynamics of MCSs are often more complex than those of individual cumulonimbus clouds or lines of cumulonimbus. And Maddox (1980) further defined Mesoscale convective complex [MCC], which is a special case of MCSs as long-lasting, quasi-circular, extremely cold-topped MCSs.

MCSs are an important link between atmospheric convection and large-scale atmospheric circulation. For example, they are associated in various ways with larger-scale wave motions (e.g., Payne and McGarry, 1977; Hodges and Thorncroft, 1997; Houze *et al.*, 2000; Carbone *et al.*, 2002), and some of the largest MCSs occur over the Pacific Ocean warm pool as a fundamental ingredient of intra-seasonal and inter-annual climate variations (Nakazawa, 1988; Chen *et al.*, 1996)

2.2.3 ATMOSPHERIC CONDITIONS FAVOURABLE TO THE FORMATION OF MESOSCALE CONVECTIVE SYSTEMS/ TRIGGER MECHANISMS

West Africa Mesoscale Convective Systems are the combination of complex interactions between different weather features as shown in (Fig.2.11) and these are all features in which the West African Mesoscale systems form;

i.) Subtropical High-pressure Systems.

ii.) The Subtropical Easterly jet.

iii.) Inter-tropical Discontinuity [ITD].

iv.) The Mid Tropical jet.

v.) The Monsoon Trough [MT].

vi.) Northeast and Southwest Trades

vii.) Boundary-Layer

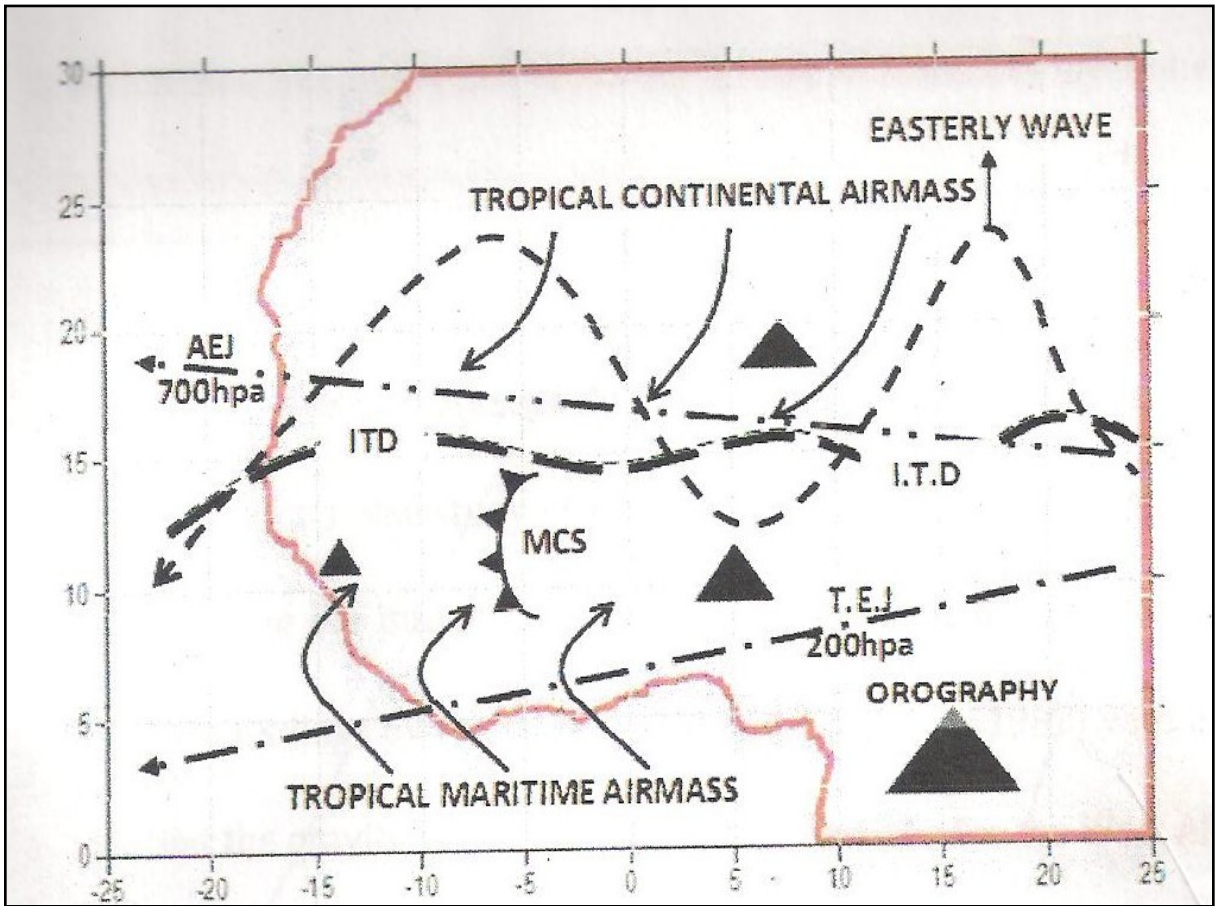

Fig. 2.11: Coupling of weather features in a mesoscale environment (Adapted from Bounoua, 1980).

Granted that, there is evidence of some relationships between rainfall and each of these features stated above, it must be realized that the implication is that they somehow reveal the fundamental structure of the basic flow. After all, they do not exist or evolve in a vacuum. All these thus pave the way for an in-depth investigation of the basic flow and Adefolalu (1974) documented a third – and perhaps the most important – synoptic-scale aspect of the monsoon circulation. The 4-6 day oscillation of its monsoon trough (MT) in West Africa (MT is a nomenclature for the air mass confluence in the lower troposphere other than at the surface where the surface discontinuity is the ITD) is not restricted to West Africa.

Fortune (1977) also noted that although the settings of the West Africa mesoscale systems are very different from what was obtained in the temperate region, most of the atmospheric conditions found favorable for deep convective systems in the temperate region are also found within the settings of the West Africa systems. Other features which have been considered for typical West African conditions favorable for the formation of Mesoscale systems include:

a.) AEJ and TEJ;

b.) ITD, ITCZ, and Monsoon Trough;

c.) Orography – forced ascent;

d.) Conditional Instability of the Second Kind (CISK);

e.) Asymptotes of convergence;

f.) Barotropic and Baroclinic Instabilities;

g.) Short gravity waves (Barefores, 1964)

Deep convective systems and storms over West Africa are consequences of one or a combination of the following:

1.) Differential surface heating: Convection is essentially an isolation phenomenon.

2.) Destabilization due to upper-level or cloud-top radiative cooling leads to convective overturning (Omotosho, 1981).

3.) The availability of abundant moisture supply at low levels, with a relatively drier middle troposphere.

4.) The inherent conditional or convective instability is present in the basic flow up to 800mb (which is true for the entire tropical atmosphere).

5.) The presence of the so-called African Easterly Jet (AEJ), and the associated vertical wind shear (Moncrieff & Miller (1976), Omotosho (1987)).

However, despite all the above, the instability has to be released, thus;

- A release mechanism for (4) above in the form of low-level convergence is associated with vortices and asymptotes of convergence (Okulaja (1970), Obasi (1974)).
- Another release mechanism is the Richardson number which indicates the role of boundary layer energy in storm development Omotosho (1987).

2.2.3.1 AEJ, TEJ, AND MESOSCALE CONVECTIVE SYSTEMS

The TEJ is part of the Indian summer monsoon system and it extends from India over Africa in the Northern Hemisphere summer months, generally at a height of around 12-15 km. The west-east axis of the TEJ is located between 4-10^{o}N. On the southern side of the axis, conditions are conducive to the ascent of air and consequently rainfall occurrence whilst the northern side is marked by subsidence. The TEJ, therefore, reinforces aridity over the extreme northern part of the country but causes a belt of above-average rainfall in the central part.

Omotosho (1987) mapped the vertical wind shear, the depth of the moist layers, and the zone of the Africa Easterly Jet to investigate the causes of the initiation and development of the deep

convective system (fig. 2.12). They found that scattered thunderstorms occur over the area with mostly positive boundary layer shear (both *u* and *v* components), a moist layer of one-kilometer depth, and distinct AEJ. But the lack of availability of either radiosonde or pilot balloon data over Nigeria has rendered the use of this method impossible.

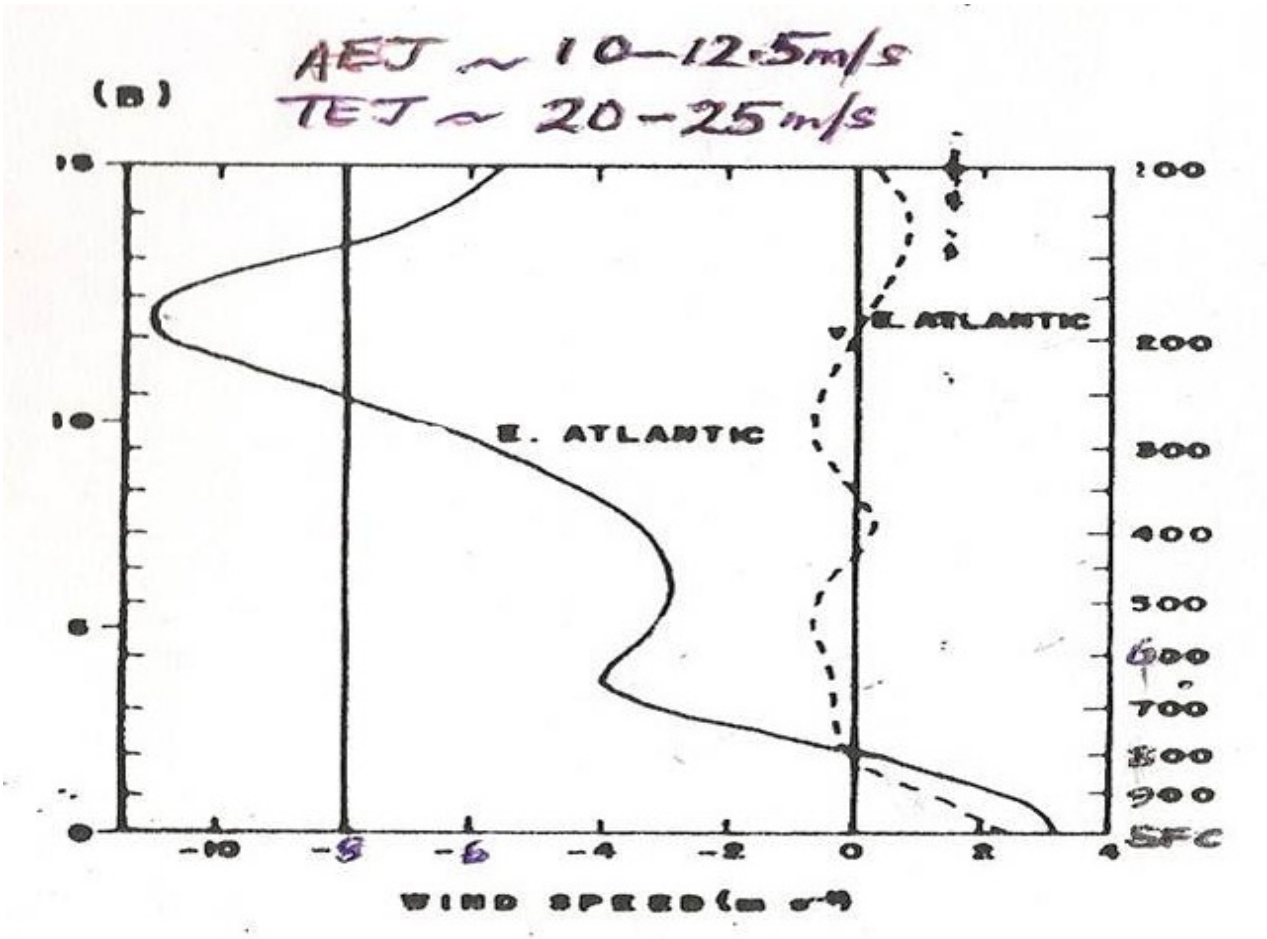

Fig. 2.12: Wind component profile for West Africa (Adapted from Omotosho 1987).

Adefolalu (1983) had shown that scale interaction exists between the three aspects of global monsoon manifested in the variable nature of the patterns of precipitation in West Africa. Among these main circulation features are the two currents – the Tropical Easterly Jet (TEJ) in the upper troposphere and the African easterly jet (AEJ) in the mid-troposphere, which are found in the easterly flow overlying the monsoon circulation. While Omotosho (1990) further demonstrated the following – the onset of the rainy season is determined by the early or late occurrence of these storms. In other words, how early the prescribed shear limit is met and the amount of seasonal rainfall to be expected depends on the time and strength of moisture build-up within the boundary layer and the relative dryness of the 700-600mb layer where the AEJ is embedded.

AEJ and TEJ play major roles in the differences between the wet and dry composite. The TEJ reaches its maximum intensity in July and August in both composites and the location of its core, which is generally at 5^{o}–8^{o}N from June to September, is relatively stable. The jet is markedly stronger in the wet composite, with core speeds exceeding 20 ms^{-1} from June through September, compared to 8–16 ms^{-1} in the dry composite. In contrast to the TEJ, the AEJ is generally weaker and situated farther north during the wet years. Monthly mean core speeds generally reach 10ms^{-1} during the wet years but 12ms^{-1} in the dry years. The core is slightly lower in the dry years, lying near 600mb, compared to about 500mb during the wet years. During the dry year composite, the jet core migrates from about 7^{o}N in June to 12^{o}N in August and September.

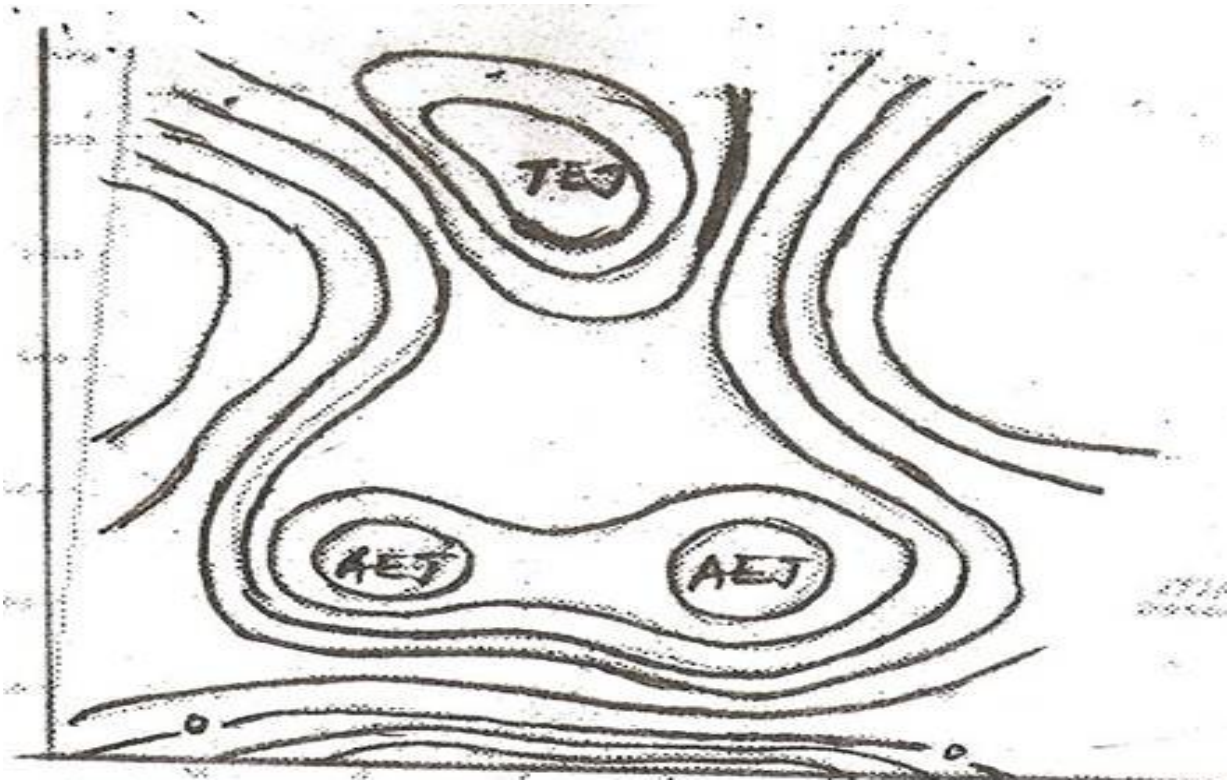

Fig. 2.13: Vertical-time distribution of the zonal component of the wind over Niamey (Adapted from Bounoua, 1980)

During the wet year composite, it migrates from 13°N in June to 17°N in August, retreating to 15°N in September. In August and September, a second mid-tropospheric jet core is also apparent in the Southern Hemisphere at roughly 5°–10°S in the dry composite. Its core lies near 5°S in August and speeds are about 6 ms^{-1}. In September its core lies near 7°S and speeds exceed 10ms^{-1}. In the wet composite, this second jet is apparent in June and September and it is roughly 4° farther north than in the dry composite. In June its core lies near the equator and is quite weak, but in September, when the core is near 6°S, speeds are more than 8ms^{-1}.

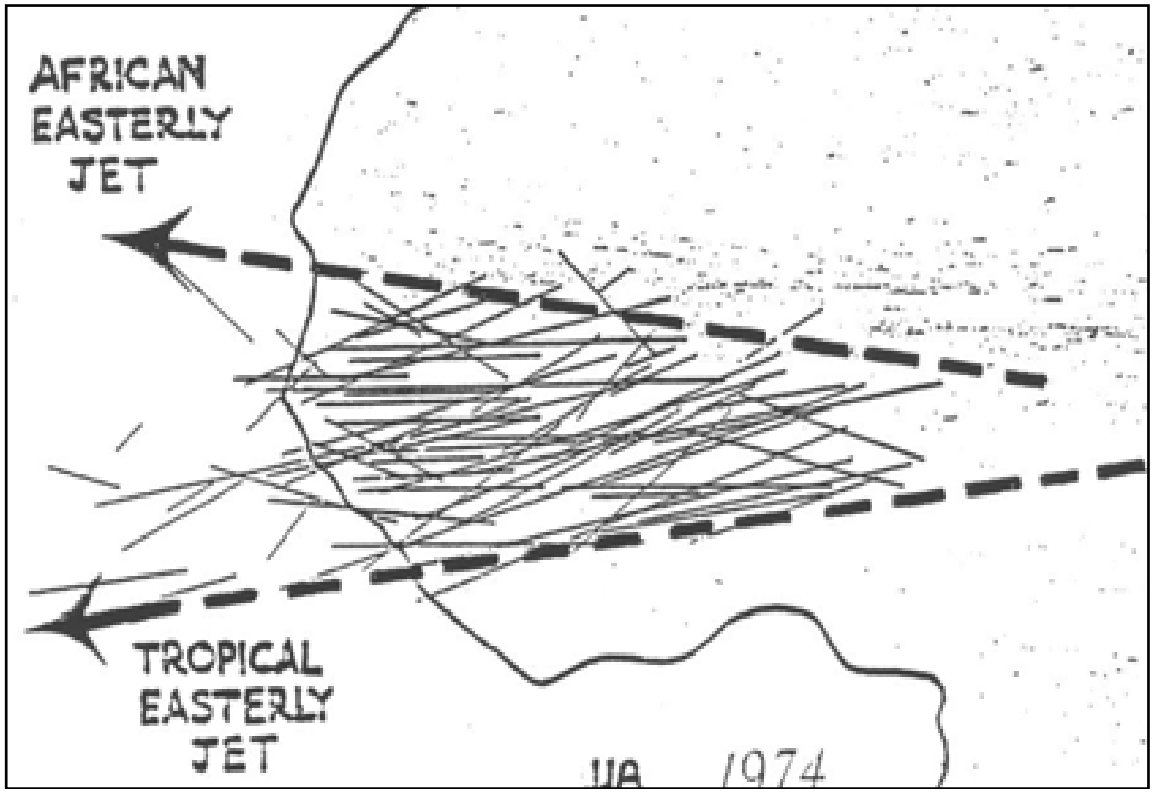

Fig. 2.14: Composite of 96 squall line trajectories and jet axes in summer of 1974 (Bounoua, 1980)

The above diagram shows the relative position of the region of MCSs/squall lines to the AEJ and TEJ. It also indicates that MCSs are highly dependent on the two jets, particularly AEJ because it is a more crucial and strong factor for MCSs' development, sustenance, and movement over West Africa. Bounoua (1980) stated that all convective activities resulting in precipitation during the summer monsoon are restricted to the areas bounded by the TEJ to the north and AEJ to the south over West Africa (fig. 2.14), and also showed the contribution of the two jets by stating that a normal rainy season corresponds to an early but weak AEJ and a strong TEJ, while the absence of rain during the season is as a result of strong but late AEJ and a weak TEJ. Jet strength, associated vertical wind shear, and level of available moisture essentially determine the occurrence, size, intensity, and rainfall delivery effectiveness of MCSs.

2.2.3.2 ITD, ITCZ, AND MESOSCALE CONVECTIVE SYSTEM

From Adefolalu (1984), the transition zone between southerlies and northerlies (the monsoon) is known as the inter-tropical Discontinuity (ITD) and is defined as the surface position of the northern limits of the southwest monsoon. Rainfall occurrence and distributions are however dependent on the two air masses that prevail over the country.

The differences in the percentage contribution of the mesoscale weather systems to total precipitation in a different part of the country largely depend on the latitudinal position of each station and most importantly, the position of Inter-Tropical Discontinuity (ITD).

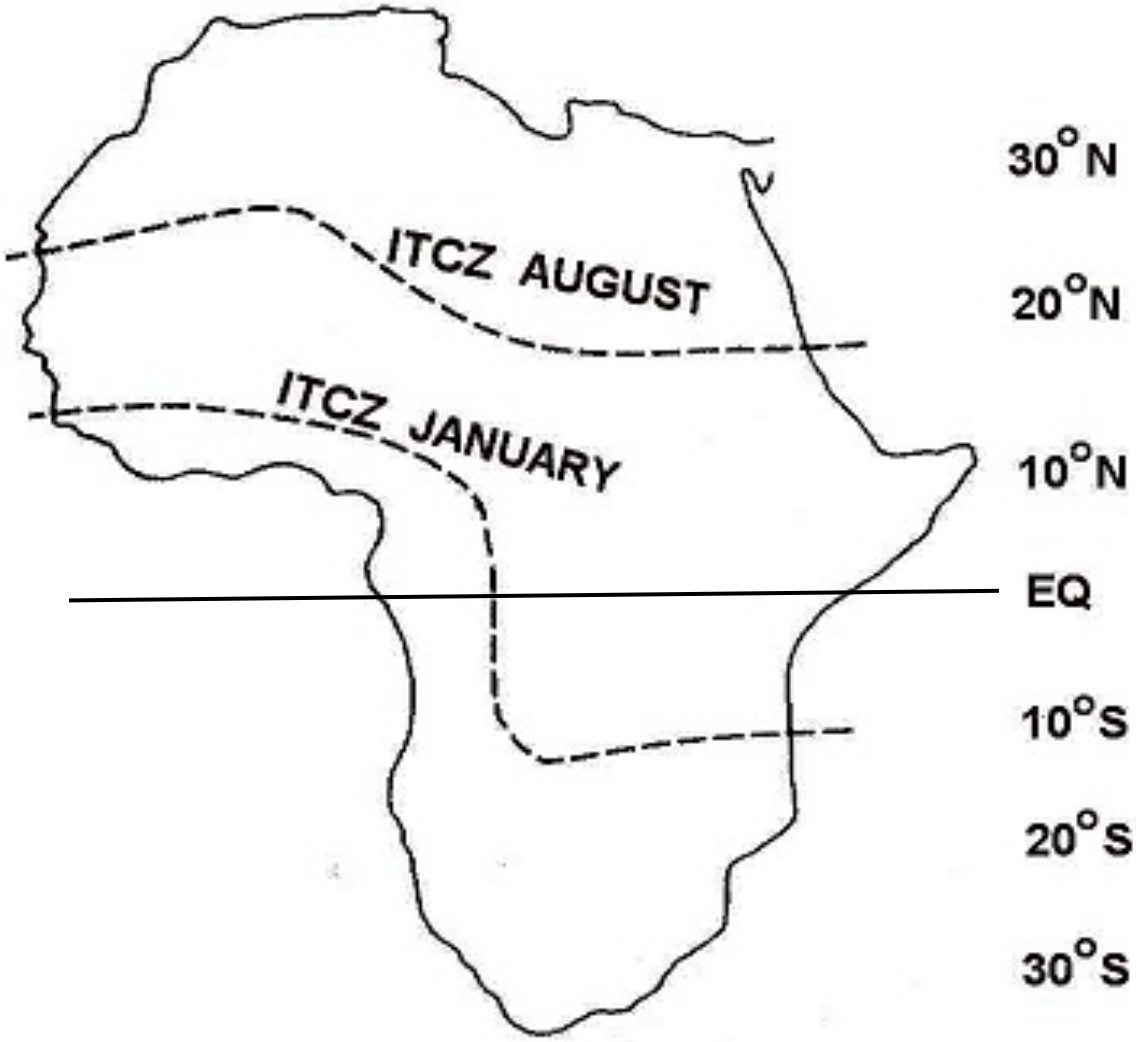

Fig. 2.15: Map of the mean position of ITCZ over Africa in January and August (Based on Goudie, 1996; and Rasmusson, 1988).

This relationship between the position of the ITD and rainfall was apparent in the findings of Ilesanmi (1968 & 1969) which showed rainfall increased at Nigerian stations coinciding with a persistent northerly location of the ITD relative to the stations and a decrease of rainfall with a rapid southward movement of the discontinuity. While also suggests that the area of maximum rainfall lies 500-600 miles south of the discontinuity at which point the dry northern air is considerably above the surface.

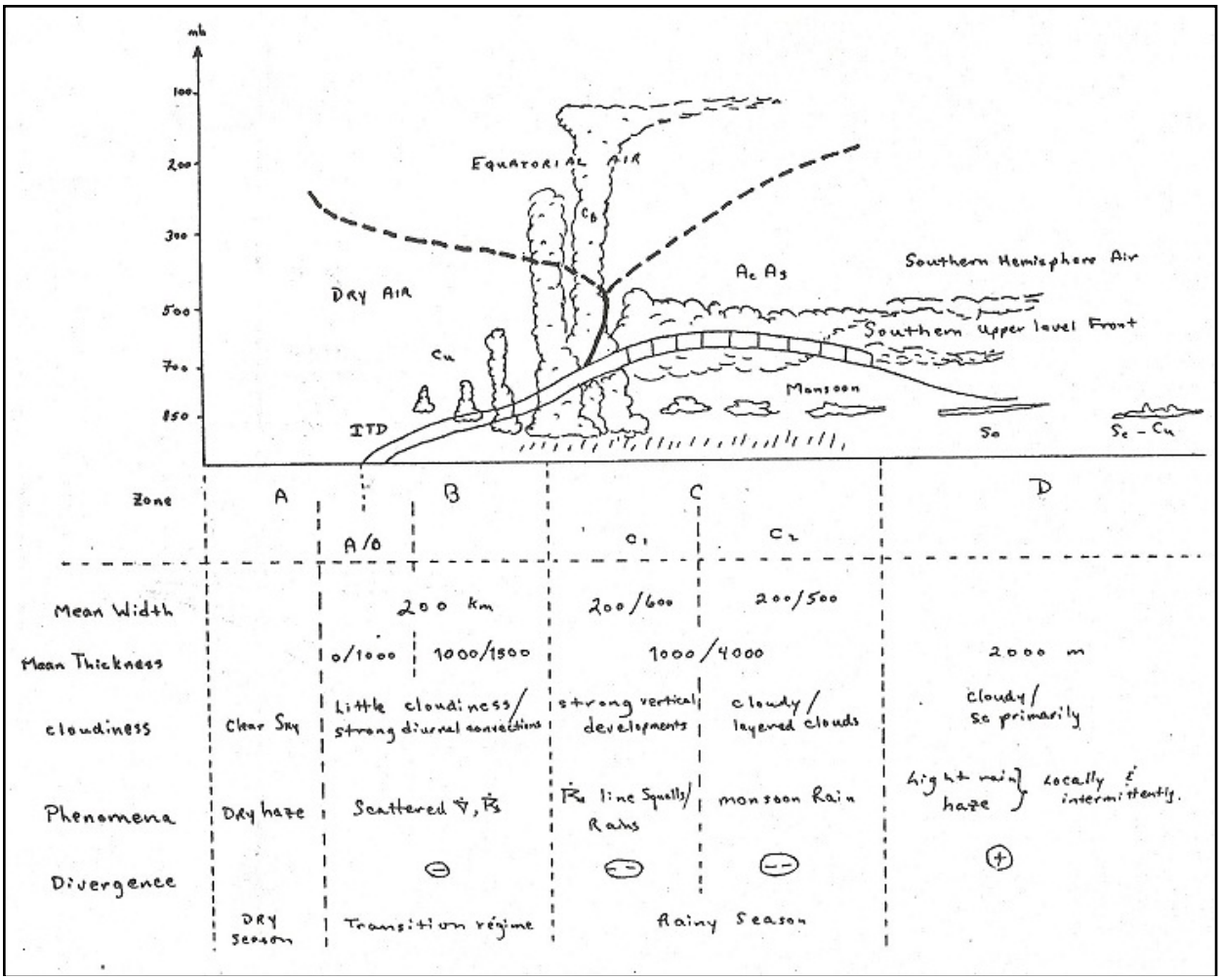

Fig. 2.16: Schematic longitude cross-section representation of the ITD showing zones of weather types relative to the surface ITD and predominant cloud types for each zone (Dhonneur, 1970).

2.2.4 CLASSIFICATION OF MESOSCALE CONVECTIVE SYSTEMS

Mesoscale Convective System (MCS) is the general name for the forms of cumuli-formed and well-developed cloud or cloud clusters. Their classification was before now, made over the ocean based on their speed and divided into three classes (Barnes and Sieckman 1984) using rawinsonde data from the GATE experiment, and deep convections were classified into: the fast-moving MCSs named squall line, and the slow-moving MCSs, which was also called MCSs. Although there have been many detailed observational case studies about the structure of intense, mature squall lines in the mid-latitude and tropics (e.g. Newton, 1950; Sanders and Emanuel, 1977; Houze, 1977; Zipser, 1977; Ogura and Liou, 1980; Elmore, 1982; Kessinger, 1983), there has been no systematic investigation of how the "building blocks" that form the mature squall line system initially become organized into a line.

Over the Sahel, where atmosphere and surface conditions facilitate the maintenance of organized big systems, Mathon *et al.*, (2002) have found that only 12% of the MCS explain 78% of the nebulosity (at the temperature of 233K) and 83% of the rainfalls. Those systems are the largest and last the longest. They are prevalent from June to September. Their cloud cover is modified by their size, which is emphasized in August. They propagate quickly (faster than 10m/s) towards the west. In a more general way, classifications of different forms of MCSs have been done by so many authors and these include:

a.) Mesoscale Convective Complexes of circular type (MCC were first defined by Maddox (1980);

b.) Squall lines are linear type (Lafore and Moncrieff, 1989);

c.) Super-clusters of (Mapes and Houze, 1993) which last for more than two days; and

d.) Organized Complex Systems (OCSs) (Mathon and Laurent, 2001) give more precipitations over the Sahelian band.

2.2.4.1 CLASSIFICATION BASED ON MCSs COLD-CLOUD SHIELD CHARACTERISTICS

It's easiest to identify and subsequently classify MCSs by their cold cloud shield characteristics (i.e. size, shape, and duration). An objective non-overlapping MCS classification scheme based on an infrared (IR) satellite might be useful in this type of classification (Jirak *et al.*, 2003). They are;

a.) MCC (from Maddox 1980).

b.) Persistent Elongated Convective System (PECS), with eccentricity < 0.7 (from Anderson and Arritt, 1998).

c.) Meso-β Circular Convective System (MβCCS): with cold cloud shield, area of 30,000km^2, and life cycle > 3hrs.

d.) Meso-β Elongated Convective System (MβECS): with cold cloud shield, area of 30,000km^2, and life cycle < 0.7

2.2.4.2 CLASSIFICATION BASED ON MCSs ORGANIZATION

This type of classification has been done subjectively based on the radar characteristics of MCSs. The two common approaches of classification arrived at based on the systems are;

i.) Organization.

ii.) Development.

These approaches have focused on squall lines but only about half of MCSs have organized convective lines Jirak (2002).

With the classification based on 'Organization', Houze *et al.* (1990) identified the leading-line trailing stratiform (TS) structure as the most common organization of mature MCSs. And (Parker

and Johnson, 2000) also recognized leading stratiform (LS) and parallel stratiform (PS) as common arrangements.

2.2.4.3 CLASSIFICATION BASED ON MCSs DEVELOPMENT

(Bluestein and Jain, 1985) identified common patterns of severe squall line formation

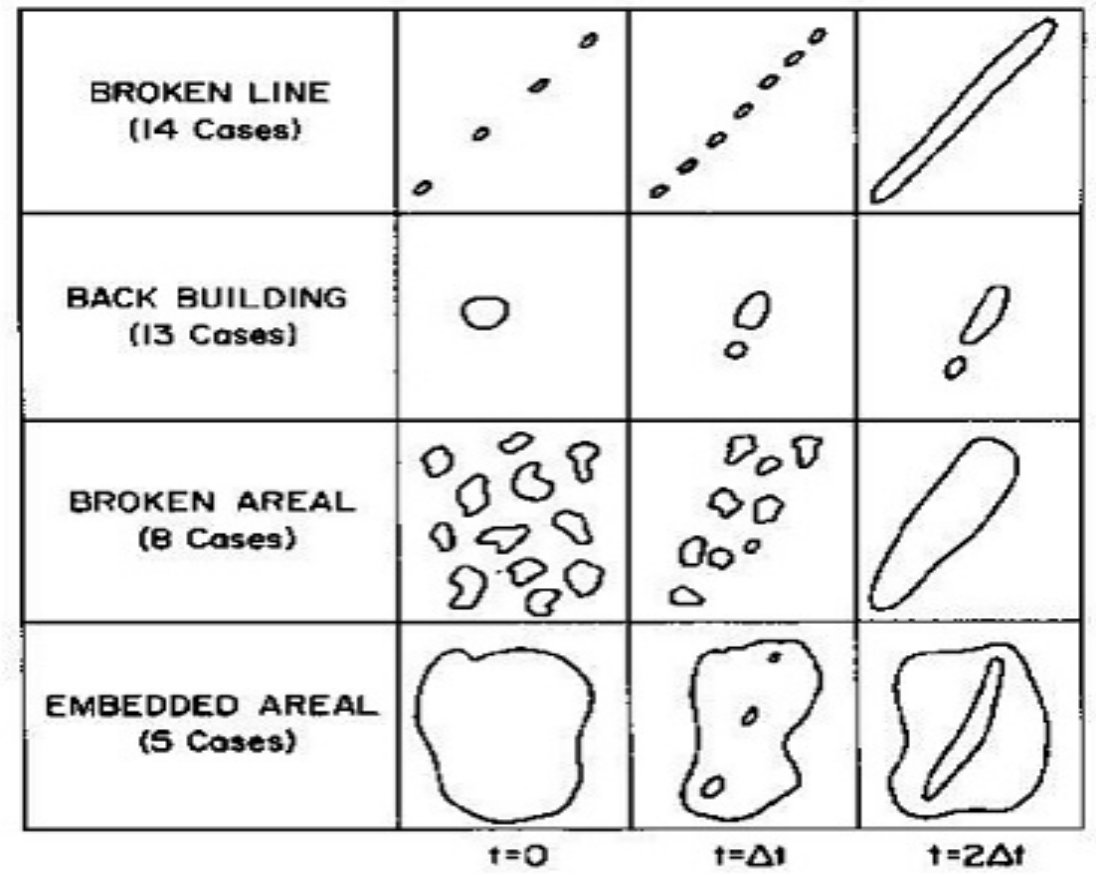

Fig. 2.17: Classification of squall line development [Bluestein and Jain (1985)]

Expanding on the above scheme (i.e. development of squall line), Jirak *et al.*, (2003) classifies all MCSs by their development and thus produce the structure below.

2.2.5 MECHANISM FOR MAINTENANCE, PROPAGATION, AND TRANSLATION OF MESOSCALE CONVECTIVE SYSTEMS

One of the most exciting discoveries in meso-meteorology is that some mesoscale convective systems (MCSs) develop a warm-core vortical circulation within their stratiform region (Houze 1977; Ogura and Liou 1980; Smull and Houze 1985; Leary and Rappaport 1987). Hereafter, these weather systems are referred to as *rotating MCSs*. These rotating cloud systems can become inertially stable and sometimes persist for several days until their vorticity is absorbed by the larger-scale flow (Johnston 1981; Wetzel *et al.* 1983; Kuo *et al.* 1986; Menard *et al.,* 1986).

Attempting to find answers to numerous questions concerning the possible identification of the mechanisms responsible for the propagation and persistence of MCSs, Chancellor (1946) asserted that winds between 2000m and 4000m give the best indication of the movement of the squall lines which travels westward over West Africa. Meanwhile, Balogun (1974) through the analysis of several upper-level charts showed that the West African squall line often moves faster than the winds at any level. In some cases, the inertially stable vortices appear to be responsible for multiple MCS development; Johnston (1981), and in the appropriate larger-scale environment, are observed to be a precursor to tropical cyclogenesis (Velasco and Fritsch 1987). There is increasing observational evidence that the rotating MCSs, termed by Maddox (1980) the mesoscale convective complex (MCC) (Johnston 1981; Johnson 1986; Velasco and Fritsch 1987). But LeRoux (1976) hypothesized that the AEJ at 700mb propel the squall lines. Barefors (1964) suggested that the system propagates as gravity waves; Okulaja (1970) also

concluded that the 700mb trough acted as a conveyor belt that carried the squall line system westward. Adefolalu (1974), Obasi (1974), and Fasheun (1979) also identified the system with the motion of trains of vortices that move from east to west over West Africa. Omotosho (1983) also concluded that the downdraft that originates from AEJ at 700 mb (Low θ_e– Very dry & cold) blows towards the cloud which produces precipitation. The precipitation resulted in drag with the horizontal air and leads to friction which converts the air to vertical movement. This dry air evaporates some of the precipitation and becomes cold and thereby falling to the surface at a very high speed. On getting to the surface, the cold air spreads at the surface thereby making the warm air lift from the surface as shown in (Fig. 2.18). The ascent air which is warm and moist (High θ_e) replenishes the cloud and produces latent heat, thereby maintaining the convective activities, especially in West Africa e.g squall line. This is regarded as the propagation and maintenance of the squall line.

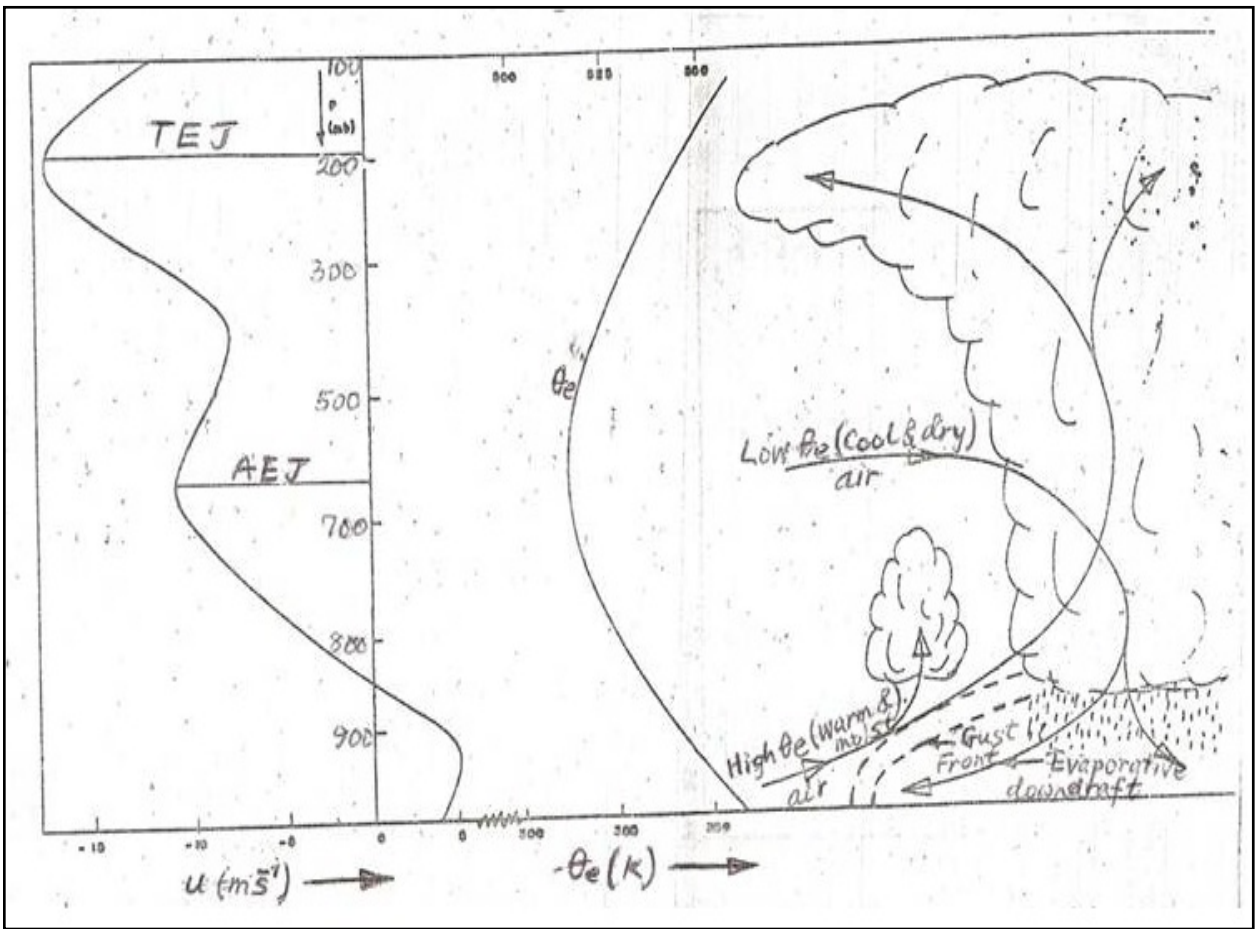

Fig. 2.18: The AEJ and θ_e interaction with storm updraft/downdraft to thunderstorm/squall line sustenance (Adapted from Omotosho 1983)

Also, when the TEJ is very strong and AEJ is weak, then a thunderstorm is expected. This agrees with the observation of Dhonneur (1971) that a rupture of the AEJ is a required condition for CB – cluster development. Once the clusters have developed, the AEJ will re-establish and the shear between AEJ and TEJ decreases. And when the gust front moves too far from the parent CB cloud, it will be cut off. The warm air that is been supplied into the parent cloud, therefore, moves up to form another cloud. The parent cloud decays (dies) thereby leaving the newly growing cloud to continue; this phenomenon is regarded as ***Translation.***

Although, several possible cooperative mechanisms may be involved in the discrete initiation of convection; First, (Mapes and Houze, 1995) pointed out that latent heating by a storm can excite a low-frequency gravity wave environmental response which can accomplish lower tropospheric lifting away from any cold pool. In numerical studies of organized mid-latitude storms, Fovell (2002) found this response to make the storm's near-field inflow environment more convectively favorable, and its role in discrete propagation of a nocturnal squall line was discussed by Fovell *et al.*, (2006). Second, Tompkins (2001) showed that moist, high CAPE bands of boundary layer air form at the cold pool boundary of a precipitating storm and remain after the pool decays. Convection can be re-triggered from this air after surface fluxes remove the convective inhibition (CIN), a process that takes time. Third, cold pools present obstacles to the flow and can cause convergent ascent in their wakes, away from the cold pool itself. The Tompkins mechanism implies air in newly developed convection may be directly traceable to older storms but, due to the time needed for CIN removal, the new cloud will not necessarily appear near already established ones.

2.3 COSMO-MUSCAT: AN OVERVIEW

The forecast model COSMO is based on the primitive hydro-thermo-dynamical equations describing compressible non-hydrostatic flow in a moist atmosphere (Steppeler *et al.*, 2003; Schättler *et al.*, 2009). It uses a staggered Arakawa C-grid on a rotated geographical coordinate system and a hybrid terrain-following vertical coordinate. The model includes the dynamic kernel for the atmosphere as well as the necessary parameterization schemes for various meteorological processes, boundary conditions, and surface exchange relations.

COSMO can describe the atmospheric flow and phenomena between the meso- and micro-scale (i.e. grid resolutions from 50 km to 50 km), in particular near-surface properties, convection, clouds, precipitation, and orographic and thermal wind systems. The model is capable of self-nesting and four-dimensional data assimilation.

COSMO offers the possibility to use different meteorological parameterizations' independence on the spatial model resolution.

2.3.1 The online-coupled Chemistry-Transport model MUSCAT

In MUSCAT, different horizontal resolutions can be used for individual sub-domains in the multi-block approach (Wolke *et al.*, 2004). The structure originates from dividing an equidistant horizontal grid (usually the meteorological grid) into rectangular blocks of different sizes. Employing doubling or halving the refinement level, each block can be coarsened or refined separately. This technique allows finer resolutions in selected regions of interest (e.g. urban areas or around large point sources).

An implicit-explicit (IMEX) time integration scheme was implemented (Wolke and Knoth, 2000) to efficiently combine the slow process of horizontal advection and the fast processes of vertical exchange and chemical transformations. Whereas the slow processes are integrated by explicit

Runge-Kutta methods any suitable solver can be applied to the fast processes. A change of the solution values as in conventional operator splitting is avoided in this approach. Within the implicit integration in the chemistry transport code MUSCAT, the stiff chemistry, and all vertical transport processes are integrated in a coupled manner by the second-order BDF (Backward Differential Formula) method. The size of the "large" explicit time step depends on the CFL (Courant Friedrichs Lewy) number.

COSMO and MUSCAT work widely independently on different grid structures and have their time step control. The coupling procedure is adapted to the applied IMEX schemes in the chemistry-transport code (Lieber and Wolke, 2008). Coupling between meteorology and chemistry-transport takes place at each horizontal advection time step only. All meteorological fields are given concerning the uniform horizontal meteorological grid.

They have to be averaged or interpolated from the base grid into the block-structured chemistry-transport grid with different resolutions. The coupling scheme provides time-interpolated meteorological fields (vertical exchange coefficient, temperature, humidity, density) and time-averaged mass fluxes. Since COSMO solves a compressible version of the model equations, with pressure as a prognostic variable, mass conservation is not ensured. Therefore, an additional adjustment is necessary for the coupler routine. The velocity components are projected such that a discrete version of the continuity equation is satisfied. The coupling scheme allows not only the forcing of the chemistry-transport calculations by the meteorological model. Furthermore, the feedback of changes in the atmospheric composition on the radiative fluxes and, consequently, on the dynamics in the meteorological model can be realized (Heinold *et al.*, 2011).

CHAPTER THREE

3.0 METHODOLOGY

This chapter discusses the research methodology which is divided into data, study area, and the methods of analysis. The data were obtained from different sources and different periods. While one part of the data was obtained from a satellite source, the others were obtained as the initial data for running the model.

3.1 DATA

To determine the variation of convective precipitation and some selected aerosol over West Africa for this research work, some selected meteorological and chemistry data were gotten from NASA Earthdata *Giovanni* source. The selected aerosols were dust, carbonaceous, $PM_{2.5,}$ and biomass burning; while the convective precipitation types were extracted from the (TRMM 3B42 and 3B43) source. The details supplied by the data source were employed in distinguishing between carbonaceous and biomass-burning aerosol. Both the aerosol (concentration) and meteorological data are on a grid point of 0.625^{o} by 0.625^{o}. These data cover a period of 30 years from 1988 to 2017, for ten (10) stations namely: Abidjan, Accra, Agoufou, Banizoumbou, Dakar, Freetown, Ikeja, Kano, Ouagadougou, and Praia. Because the COSMO-MUSCAT coupling model has not been used over West Africa before now, this influences the choice of some selected episodes of aerosols (dust and/or smoke) and heavy precipitations (thunderstorms and squall lines), to validate the output with results from other sources. The selected episodes are:

1.) Dust and smoke episode of December 24 -27, 2015 over West Africa. The dust layer extended from the ground up to 2000m while the smoke layer occurred from the 2000m – 4000m range.

2.) Dust pollution outbreak of March 20 – 29, 2010 over West Africa and spread up to the coastal cities of Lagos and southwestern Nigeria.

3.) Convective activities of 30th August – 2nd September 2009 over Ouagadougou and other West African countries.

3.2 THE STUDY AREA

The research study was majorly over West Africa, though some parts of the Central and North African countries were considered due to the possibility of observing the propagation/transport of aerosols from those regions into West Africa. The area is bounded in the south by the Gulf of Guinea, mount Cameroun or Adamawa highlands to the east, the Atlantic Ocean to the western boundary, and in the north by the Sahara and the Sahel, a belt-like semiarid transition zone between the Sahara Desert and the Sudanian Savannah. The area cover is 5,112,903 km^2 (1,974,103 sq. mi), which is about one-fifth of the total land mass of Africa, while the population is about 419 million people as of 2021 (United Nations, 2022) and is about 5 % of the world's population. The domain of study was latitude 4^oN – 30^oN and longitude 15^oE – 25^oW. West African ecological zones are divided into Guinea, Savannah, and Sahel (Abiodun and Omotosho, 2007). The selected stations considered for this research under the region are presented in figure 3.2 below.

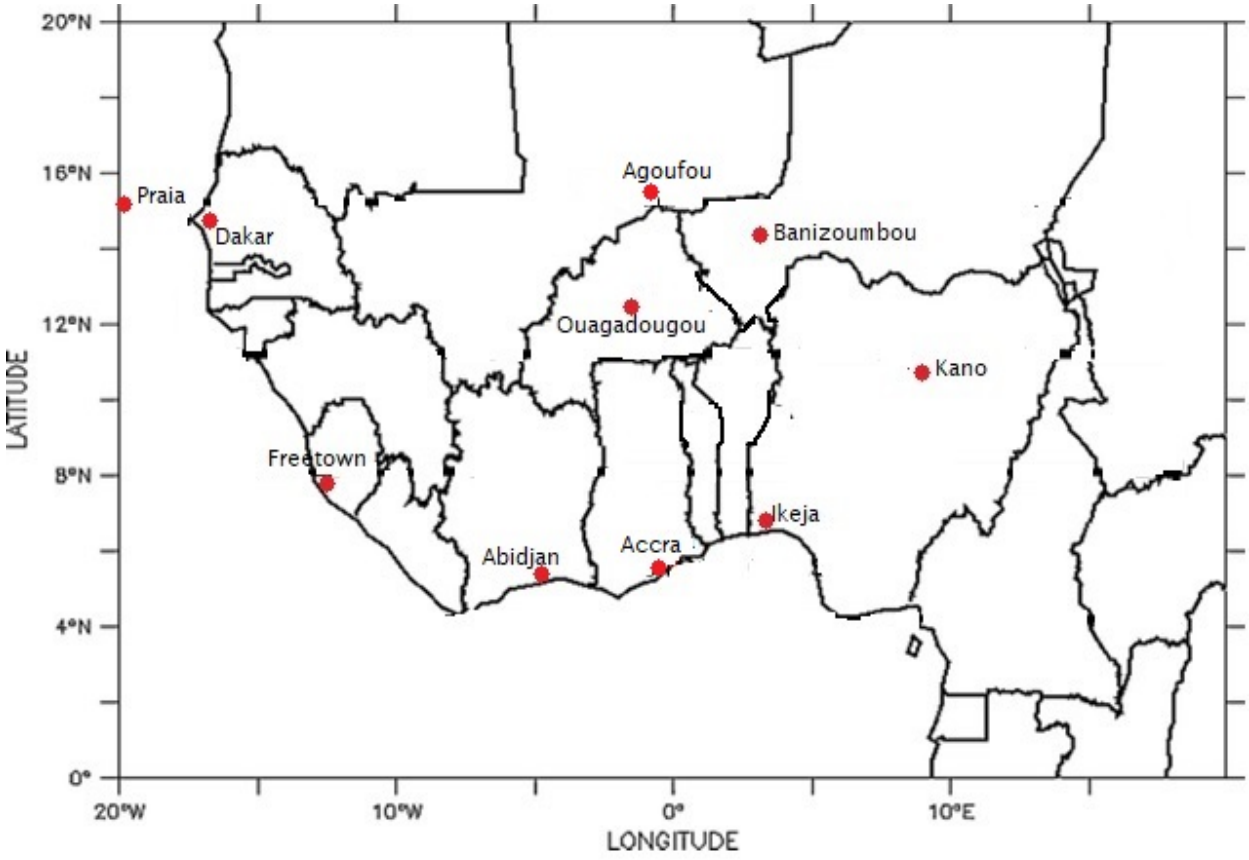

Figure 3.1: Map of West Africa showing the study locations

The distribution of these selected stations was done in a way to ensure that all the zones as defined by Abiodun and Omotosho (2007) were captured. The criteria for choosing these stations were to have a good representative of all climatic zones of the West African region. The coordinates and climatic characteristics of the selected stations were defined in table 3.1 below.

Table 3.1: Selected stations under research study, their coordinates, and climatic characteristics

Stations	Latitude	Longitude	Climatic Characteristics
Abidjan	5° 20¹ N	4° 10¹ W	Rainfall with double peaks; Average temperature is between 27.78°C – 31.67°C; Relative Humidity over the course of the year stays within 4% of 96% throughout.
Accra	5° 36¹ N	0° 12¹ W	Despite its closeness to the coast, it is hot and oppressive year-round; Temperature typically varies between 23.33°C – 32.78°C; the Rainy period lasts for 9.8 months and double peaks.
Agoufou	15° 09¹ N	0° 40¹ E	The climate is a hotbed. The average temperature is 28°C (the warmest month is May at 32°C, and the coldest is January at 22°C). The average rainfall is 488mm. Thus, exhibiting the characteristics of the Sahelian region.
Banizoumbou	13° 34¹ N	2° 09¹ E	It is remarkably hot throughout the year. Average monthly high temperatures reach 38°C in four months out of the year. Annual rainfall is expected between 500mm and 750mm.
Dakar	14° 43¹ N	17° 28¹ W	The climate is generally warm. The rainy season lasts from July to October, while the dry seasons cover 8 months. It has an ocean-influenced hot semi-arid region. It is cooled year-round because of the sea breezes.
Freetown	8° 29¹ N	13° 14¹ W	It is a tropical climate with a rainy season from May through November. The average temperature is 28°C
Ikeja	6° 36¹ N	3° 20¹ E	It is a tropical savannah climate. Mean high temperatures ranged from 28.3°C to 39°C. Rainfall is bi-modal with the month of July/August recording the Little Dry Season.
Kano	12° 00¹ N	8° 31¹ E	It has a tropical savannah climate. Annual precipitation is about 980mm. Kano is very hot for most of the year, peaking in April. The Harmattan months of DJF record

			less temperature, averaging between 14°C and 16°C, especially in the morning hours.
Ouagadougou	12° 21¹ N	1° 32¹ W	It is hot semi-arid and closely borders tropical wet and dry. Annual rainfall is 800mm. Temperature is as high as 43°C in March/April, with the least in Oct-Feb at 16°C
Praia	14° 55¹ N	23° 30¹ W	Despite being an island, it has a desert climate, with a short-wet season and a lengthy, very pronounced dry season. Annual rainfall is about 210mm. The coldest month is far above 18°C while the highest is 27°C.

3.3 METHODS

The methods of analysis for this research study are divided into the statistical approach and the modeling approach. The outputs from these two methods were graphically analyzed using python and ferret.

3.3.1 Statistical Approach

The correlation between the aerosols and some of the selected climatic parameters was done to determine the relationship between the independent (aerosols) and dependent (climatic) variables. The validity of the relationship was tested using the probability value (p-value) at a significance level of 0.05. The introduction of p-value and significance level to the correlation outcome was to either reject the NULL hypothesis in favor of the alternate or vis-à-vis. The rejection of the null hypothesis is evident that the relationship between two correlated variables is **statistically significant** but when the NULL hypothesis is not rejected, the relationship between the two correlated variables is **not statistically significant.**

The correlation and probability value from a significant level can be calculated using equations (i) and (ii) respectively as shown below;

$$r = \frac{\Sigma(xi-x)(yi-y)}{\sqrt{\Sigma(xi-x)2(yi-y)2}} \quad \ldots\ldots\ldots\ldots\ldots\ldots\ldots\ldots \quad \text{(i)}$$

$$t = \frac{r\,x\sqrt{n-2}}{\sqrt{1-r^2}} \quad \ldots\ldots\ldots\ldots\ldots\ldots\ldots\ldots \quad \text{(ii)}$$

where; r = Correlation; x = independent variable; y = dependent variable; n-2 = degree of freedom.

The probability value (*p*-value) can be derived from equation (ii) above. After deriving the value for *t*, the degree of freedom (n-2) and the number of tails were put together to give the value of *p* to be 0.05. This value aided in determining whether the relationship between two (2) variables was statistically significant or not depending on the value of the correlation. The climate Data Operator (CDO) was also employed to carry out several data manipulation and statistical computations directly from the NetCDF file. The various computations include monthly mean, annual mean, and the differences between feedback and non-feedback mechanisms from the model output. The COSMO-MUSCAT coupling model was used in the simulation of the selected episodes as detailed in section 3.1.

3.3.2 Model Simulation Process

The model is a coupling system that was used to analyze both the concentration and convective activities in the atmosphere. The COSMO is an acronym for Consortium for Small-scale Modelling, while MUSCAT stands for Multi-Scale Chemistry Transport. The model system COSMO-MUSCAT runs in a regime without data assimilation. The simulations are performed in a "forecast regime". This means that the simulations are done only by forcing via the boundaries without any data assimilation and nudging. The integration period has been subdivided into overlapping short-term cycles (Fig. 3.1). Each of these cycles consists of a one-day pre-run for

spin-up of the meteorology, followed by two days with a coupled run of meteorology and chemistry transport. The COSMO pre-run of the domain was initialized and forced by operational global forecast and reanalysis data ICON (Icosahedral Non-hydrostatic) of the DWD (German Weather Service). It should be noted that these initialization data were further processed with *int2lm*. The global data sets (ICON) were made available with a horizontal resolution of up to 0.05º (14km). To run a real case scenario of COSMO-MUSCAT, boundary files and initial files for COSMO are required.

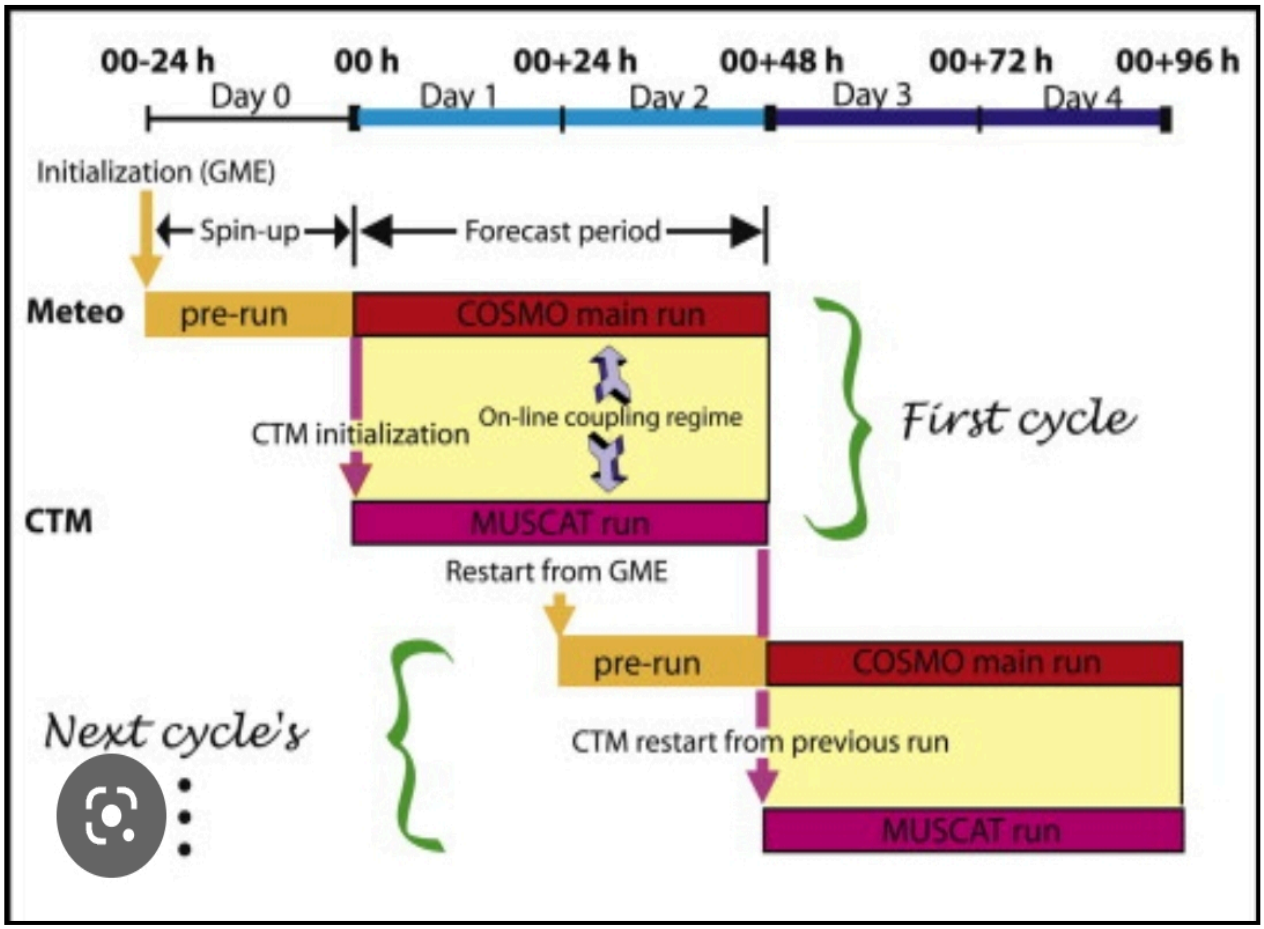

Figure 3.2: The schematic flow chart of the cyclic COSM-MUSCAT simulations (Adapted from Wolke *et al.,* 2012).

Once the data were at the TROPOS server, the data were then adapted and executed with the three (3) shell scripts named below in that given order:

1.) scripts_at_TROPOS/link_invar_ec.sh;

2.) scripts_at_TROPOS/run_ifs2cosmo_NO_0p125; and

3.) scripts_at_TROPOS/link_24h_*_cycl.sh.

The first script provides the external parameters for the second script. The second script sets up and executes the ***intl2m***. The third script links the processed boundary files for the respective cycle set-up. Hence, for a 72-hour cycle (e.g., 24hrs COSMO pre-run and 48hrs COSMO-MUSCAT simulation), the driving data for COSMO for the three (3) days needed to be linked (or copied) into one directory per cycle.

Sequel to the preparation of the model, some input and control files were modified as detailed below;

1.) **INPUT_ORG:** It contains the specification of the domain and the size of the grid. This specification is referred to as LMGRID, and the initial date of the model is set. The number of preferred processors is also set under this file.

2.) **INPUT_IO:** This is the file where the initial and boundary data directory (input data) is named.

3.) **Job_data:** It is the control file of Jobmanager (the Jobmanager is a file that contains the details of all the process that is involved in the model). It shows the kind of model to be used (COSMO or MUSCAT or the coupling system), boundary data, start and end dates, output interval (3D is usually employed, and this is why the first output is cm3d), CTM_out starting date was also modified and the project ID which must be included in the run_file amongst others.

4.) **'Project ID'_HH.run:** The run_file name was first changed to reflect the lettering used in the project ID as stated in the Job_data. The grid path was set, and the run_file at the gas phases (ctReGas I). It also contains lateral boundaries. It should be noted that when a particular data under the gas phase is not available, 'without' would be used for such data.

5.) varList: The variable list is a file that contains all the selected concentrations (aerosols) and meteorological variables needed to be simulated in the model.

It is important to note that the primary outputs of the model were only available in a binary format. But it was easily converted to NetCDF or the TROPOS' cm3d format. This was done by using the tool manipuAlone and several other control files. The output of the model converted into cm3d format with the aid of manipuAlone was further converted to rotated coordinate and later to geographical coordinate using <*cm3d_2netcdf.sh*> and <*unrot_grid.sh*> respectively.

3.4 The coupling model system COSMO–MUSCAT

COSMO-MUSCAT is a modern mesoscale chemistry transport model for process studies and air quality applications (Wolke *et al.*, 2012). The online-coupled system consists of the regional weather model COSMO (COnsortium for Small scale MOdelling) and the chemistry transport model MUSCAT (MUltiScale Chemistry Aerosol Transport). COSMO, which until 2020 was the operational forecast model of the German Weather Service (DWD), solves the atmospheric equations on the basis of a terrain-following grid (Schättler *et al.*, 2018; Baldauf *et al.*, 2011). Driven by the meteorological model, MUSCAT deals with atmospheric transport and chemical transformations for various gas-phase species and aerosol particle populations. Its core is based on mass balances, which are described by a system of time-dependent, three-dimensional advection-diffusion-reaction equations. The online coupled chemical transport model COSMO–MUSCAT is

qualified for the operation forecast of pollutant and process studies in regional and local areas (Heinold *et al.,* 2011; Renner and Wolke, 2010; Hinneburg *et al.,* 2009; Stern *et al.,* 2008).

Unlike other works done using the two nested domains, the modeled study area for this research covers every part of West Africa and North Africa due to the consideration of the transport of aerosols from that region into the West African domain. The spatial grid resolution of 14 km X 14 km. The simulation period was divided into several overlapping short periods, each of which included a 1-day spin-up followed by a 2-day run with meteorology and chemistry coupled. The main features of the model system are described in detail and well documented in Wolke *et al.,* (2004, 2012) and Baldauf *et al.,* (2011). Adequate modeling of dynamics requires an online coupling between the chemical transport model (MUSCAT) and the meteorological model (COSMO). Here, the compressible non-hydrostatic flow in a moist atmosphere is described by the primitive hydro thermo-dynamical equations (Steppeler *et al.,* 2003; Doms *et al.,* 2011a). The vertical diffusion is parameterized by a level 2.5 closure scheme, which adopts a prognostic equation for turbulent kinetic energy (Doms *et al.,* 2011b). Moist convection is parameterized according to Tiedtke (1989). A two-stream formulation (Ritter and Geleyn, 1992) is applied for radiative transfer. Radiative fluxes could be modified by aerosol clouds and tracer gases via absorption, scattering, and emission. The reanalysis data of the German Weather Service (DWD) derived from the global meteorological model GME (Majewski *et al.,* 2002) were used for initial and boundary conditions.

MUSCAT describes the transport, chemical, and removal processes of atmospheric aerosols. The gaseous chemistry was represented by RACM-MIM2, which consists of 87 species and more than 200 reactions (Karl *et al.,* 2006; Stockwell *et al.,* 1997). A simplified mass-based approach (similar to the EMEP model; Simpson *et al.,* 2003) was used to represent the aerosol processes with high

efficiency. Dry deposition is modeled by using the resistance approach following Seinfeld and Pandis (2006) and considering the kinetic viscosity, the atmospheric turbulence state, and the gravitational settling of particles. The resistances for the aerodynamic and quasi-laminar layer are taken from COSMO and analogous to the deposition of water vapor. The parameterization of the wet deposition is dependent upon size-resolved collection efficiency and scavenging (Simpson *et al.,* 2003).

The modeled dust emissions depend on surface wind friction velocities, surface roughness, soil particle size distribution, and soil moisture (Heinold *et al.,* 2011). Biogenic emissions depend on land use and meteorology in the approach of Steinbrecher *et al.,* (2009) and the Saarikoski *et al.,* (2007) scheme was applied to estimate biomass burning emissions.

Table 3.2: Chemistry emission of the model and the corresponding scheme.

S/N	Options	Model
1.	Biogenic emission	Stembrecher *et al.*, 2009 scheme
2.	Dry deposition	Seinfeld and Pandis, 2006 scheme
3.	Biomass burning emission	Saarikoski *et al.*, 2007 scheme
4.	Soil NO	Williams *et al.*, 1992; Stohl *et al.*, 1996 schemes
5.	Dust emission	Tegen *et al.*, 2002 scheme.
6.	Anthropogenic emissions	Crippa *et al.,* 2018 EDGARv5 dataset
7.	Wind-induced aerosol emissions	Heinold *et al.,* 2011; Long *et al.,* 2011 scheme
8.	Multiphase chemistry	Stockwell *et al.,* 1997; Schltz *et al.,* 2018
9.	Aerosol dynamics	Vignati *et al.,* 2014.

The numerical aspect of the MUSCAT has a static horizontal grid staggering referred to as Multi-block grid structure (Knoth and Wolke, 1998b; Wolke and Knoth, 2000). The meteorological model COSMO uses a rotated spherical grid with a hybrid vertical coordinate. To distribute the horizontal grid across all processors, it is broken down into rectangular partitions with as many grid cells as possible. The MUSCAT grid is based on that of the COSMO, but is placed in so-called blocks, which can have different horizontal resolutions.

The numerical aspect of the model makes use of some schemes which are;

Table 3.3: Chemistry emission of the model and the corresponding scheme

S/N	Options	Model
1.	Time integration scheme	Knoth and Wolke, (1998b); Wolke and Knoth, (2000, 2002).
2.	Online coupling meteorology-chemistry	Lieber and Wolke, (2008).
3.	Parallelization and dynamic load balancing	Karypis *et al.,* (2003).

CHAPTER FOUR

4.0 RESULTS AND DISCUSSION

4.1 Introduction

This section shows the results produced with some graphical tools and these graphs depend on the content of the specified objectives. Some of the results range from monthly linear variation to seasonal spatial variation. The analyzed simulated outputs also considered the impact of radiative feedback of aerosols on some meteorological variables such as temperature, relative humidity, vertical profiling of the wind components, cloud properties, etc., both at the surface and upper level.

4.2 Monthly Variations of Aerosols over the selected Stations

Biomass burning analyses showed that the areas along the coast of the Atlantic Ocean (Abidjan, Accra, Freetown, and Ikeja) followed the same trend in which there seems to be more abundance of the aerosol within the dry seasons and months preceding the rainy months of March to May depending on the longitudinal positions of the stations. Least values in biomass burning, which correspond to the low amount of aerosol in the atmosphere, were recorded between March and November for Accra, but May and November for Ikeja and Freetown. The peak value of biomass burning in Ikeja was between February and March, April in Freetown, and January in Accra. Could the climatic abnormality of Accra when compared to other West African coastal cities as detailed in several studies (Acheampong 1982; Amekudzi *et al.* 2015) and regarding its climatic classification (FAO 2005; Abass 2009; Darfour and Rosentrater, 2016) be the reason for its non-alignment in trends with other stations of the same climatic region? Other aerosol types over Accra

seem to follow the same pattern, having their peak values in the dry months of December/January/February (DJF).

4.2.1 Monthly Variations over Rainforest zone (Equator – 8°N)

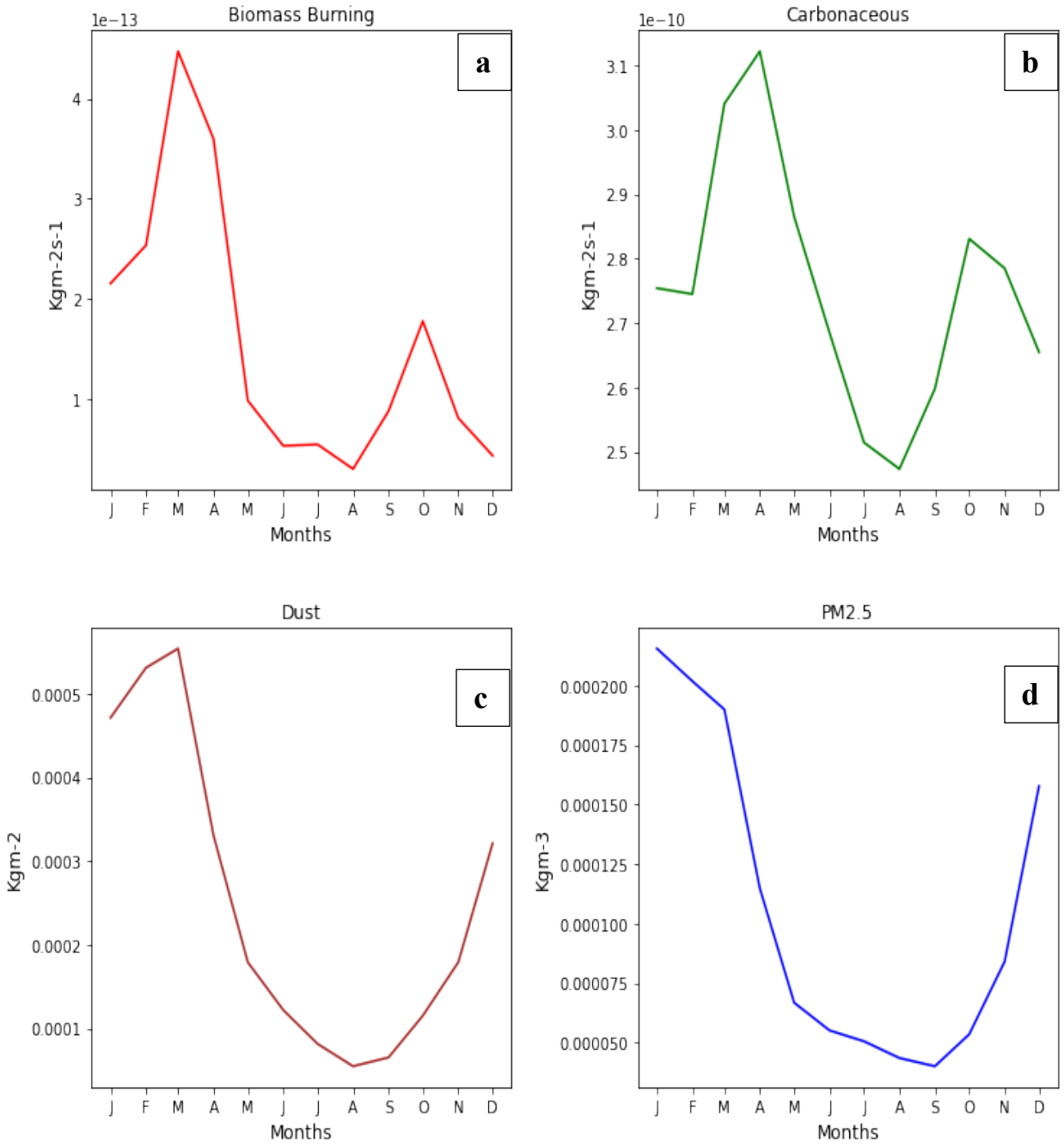

Figure 4.1: Monthly Aerosol (a) biomass burning, (b) carbonaceous, (c) dust, (d) $PM_{2.5}$ Variability over Abidjan

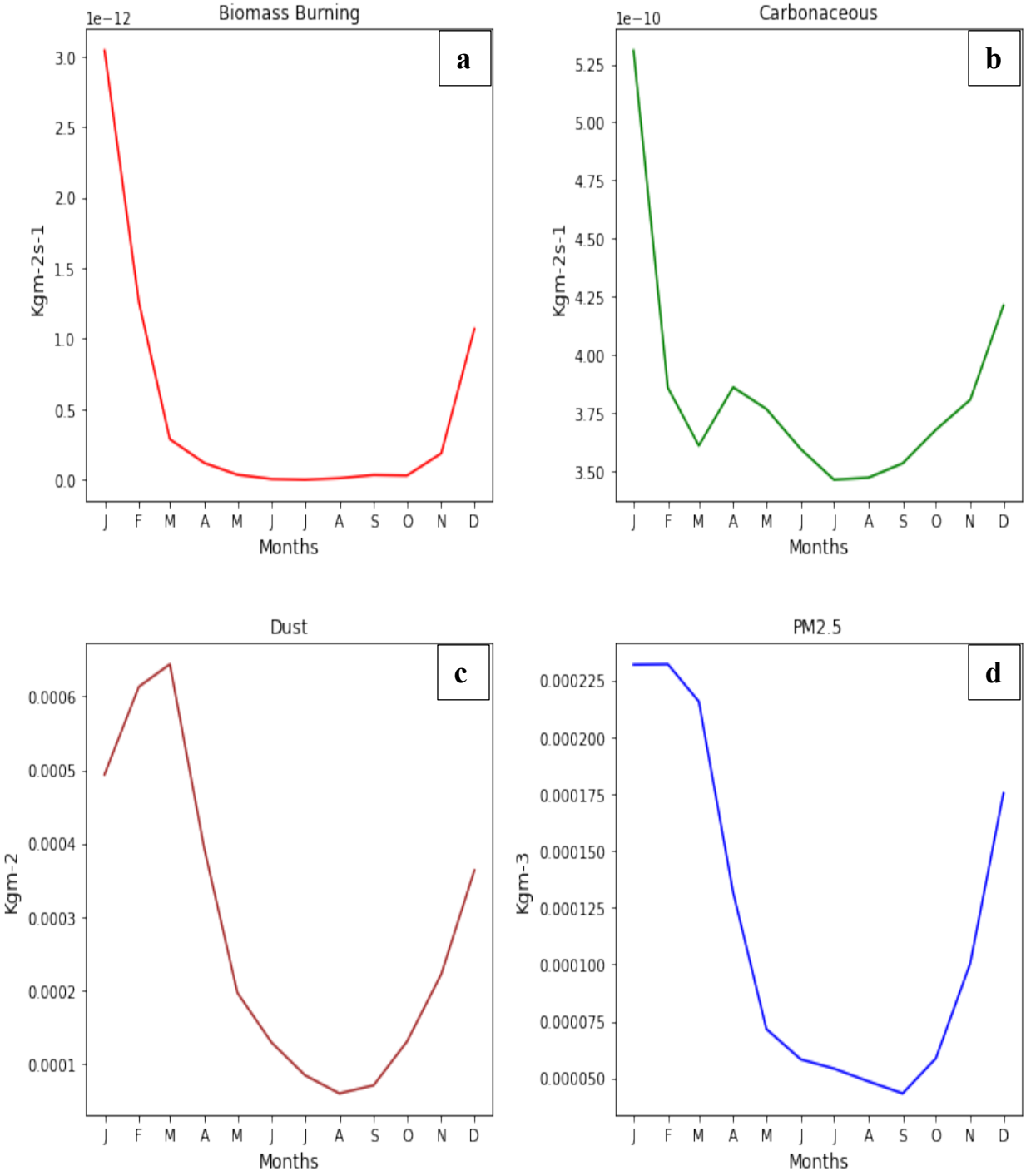

Figure 4.2: Monthly Aerosol (a) biomass burning, (b) carbonaceous, (c) dust, (d) $PM_{2.5}$ Variability over Accra

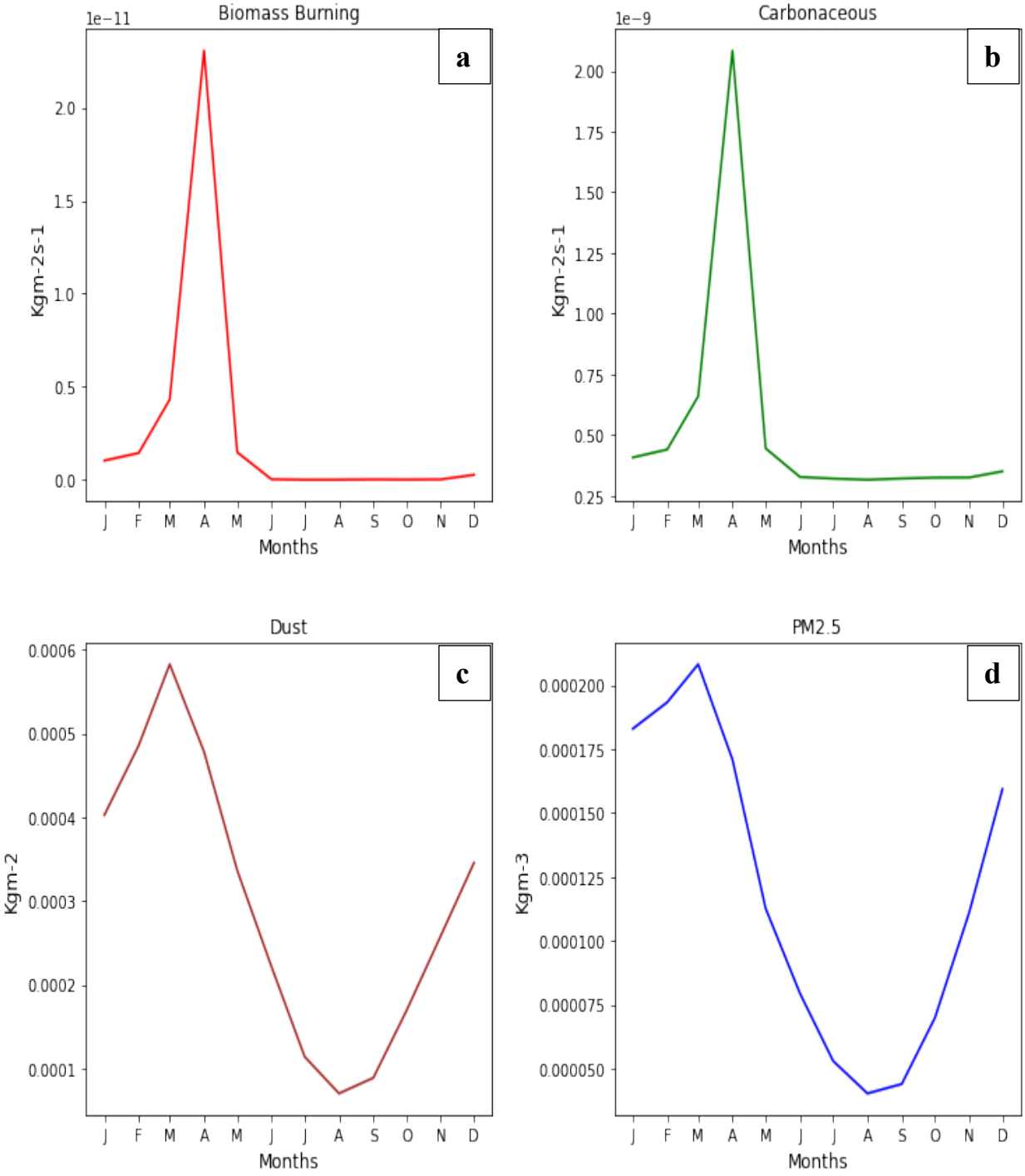

Figure 4.3: Monthly Aerosol (a) biomass burning, (b) carbonaceous, (c) dust, (d) $PM_{2.5}$ Variability over Freetown

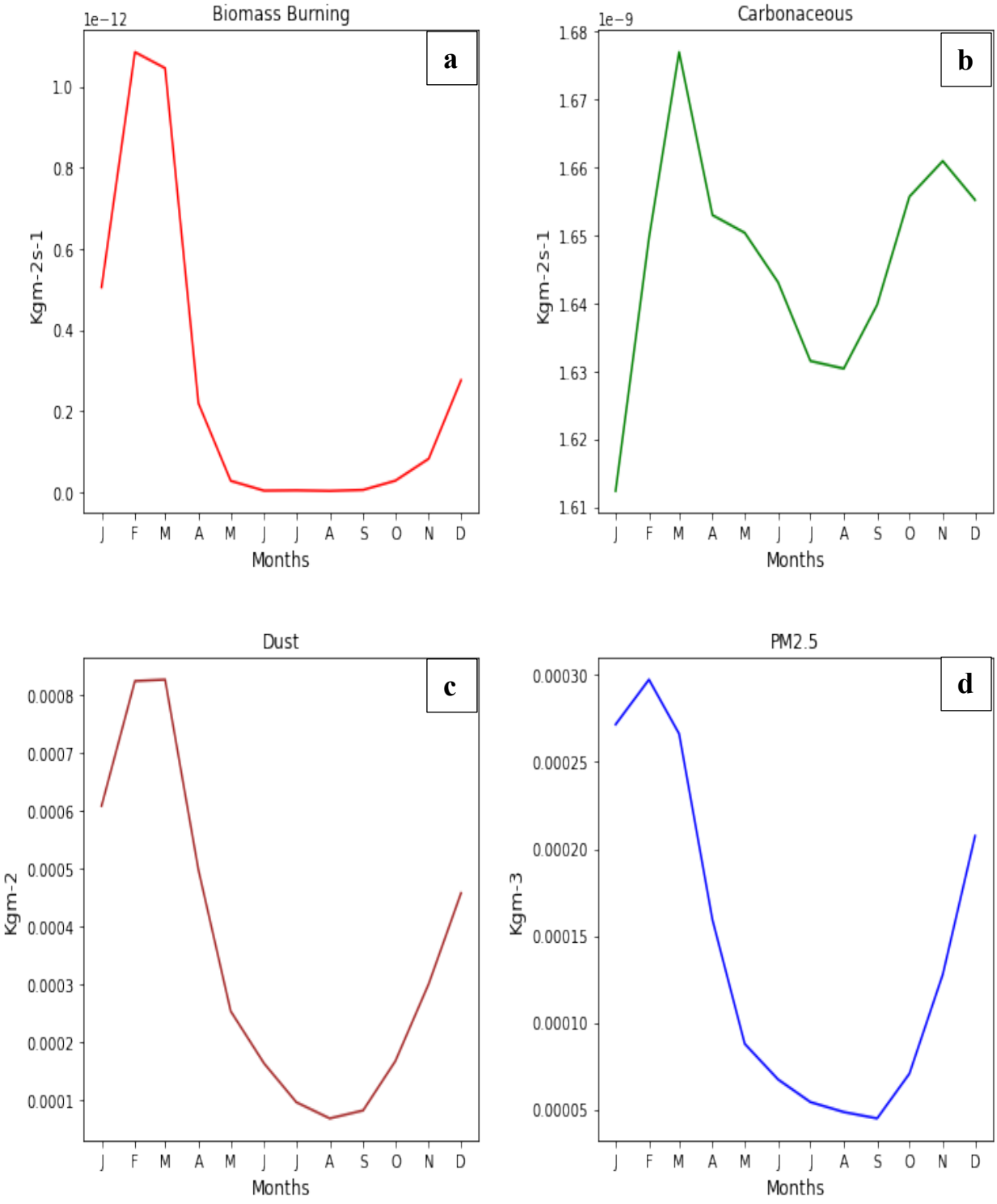

Figure 4.4: Monthly Aerosol (a) biomass burning, (b) carbonaceous, (c) dust, (d) $PM_{2.5}$ Variability over Ikeja

As stated in the data and methodology section, the idea behind the selection of the stations across West Africa is to have a balanced representation across the major climatic zones; rainforest and savannah zones. Representatives of rainforest are Abidjan, Accra, Freetown, and Ikeja.

Figures 4.1 – 4.4 show the monthly variations of the rainforest stations. It can be deduced that Accra (fig. 4.2) exhibited the almost same pattern of variation in dust and particulate matters, with the former recording the least value in August and the latter in September. However, the peak values for the aerosols were recorded in February/March for dust and January/February for particulate matter. Biomass and carbonaceous also exhibited the same pattern of variation and recorded peak values in January for the stations, but carbonaceous recorded a deviation from normal in value in April when compared to other rainy months. For Freetown (fig. 4.3), there existed an unexpectedly high value, more of a spike, in April for biomass burning and carbonaceous. The other months recorded negligible values, especially in the rainy season. The other two aerosol types (dust and $PM_{2.5}$) for this station also exhibited the same pattern but with peak and least values in March and August respectively. It can be assumed that the continuous downward trend of the aerosol types from March to August can be attributed to what is known as coagulation. That is, precipitation attracts aerosol particles in the atmosphere.

The biomass burning over Ikeja (fig. 4.4) exhibited an almost identical seasonal value to other stations within the rainforest region. That is, the dry season of February and March recorded the highest values while the rainy months of May to October recorded the least values. The dust and $PM_{2.5}$ over this station showed identical patterns, and this conforms to the study of De Longueville *et al.*, (2010) which showed that Saharan dust contributes up to 1100 Tg of particulate matter to the annual, thereby making it the most active among all source regions worldwide. The highest value

for dust was recorded in February/March while $PM_{2.5}$ recorded its highest value in February. The month of JAS corresponds to the period of moisture-laden southwesterly monsoon wind being prevalent over the country (Oluleye and Okogbue 2013; Oluleye and Adeyewa 2016) as a result of the position of Inter-Tropical Discontinuity (ITD) in its northernmost position (Omotosho 2008). Carbonaceous exhibited an undefined pattern when compared with other aerosol types within this zone, especially with double peaks. The month of March recorded the highest value of the peaks while the other peak was recorded in October/November. It can be deduced from fig. 4.4 that the carbonaceous values were low during July and August, while January had the least value.

4.2.2 Monthly Variation over Savannah zone (8°N – 13°N)

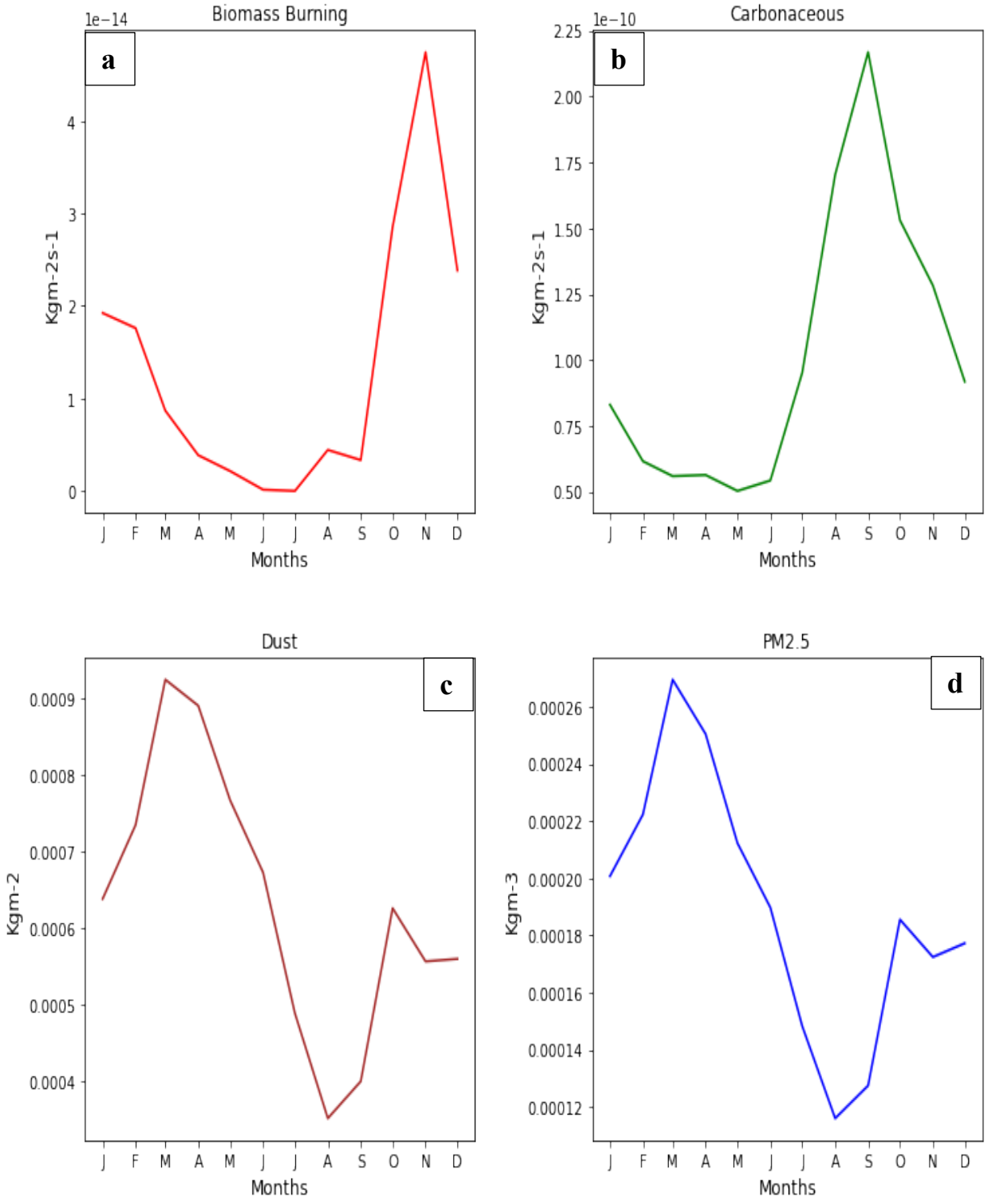

Figure 4.5: Monthly Aerosol (a) biomass burning, (b) carbonaceous, (c) dust, (d) $PM_{2.5}$ Variability over Banizoumbou

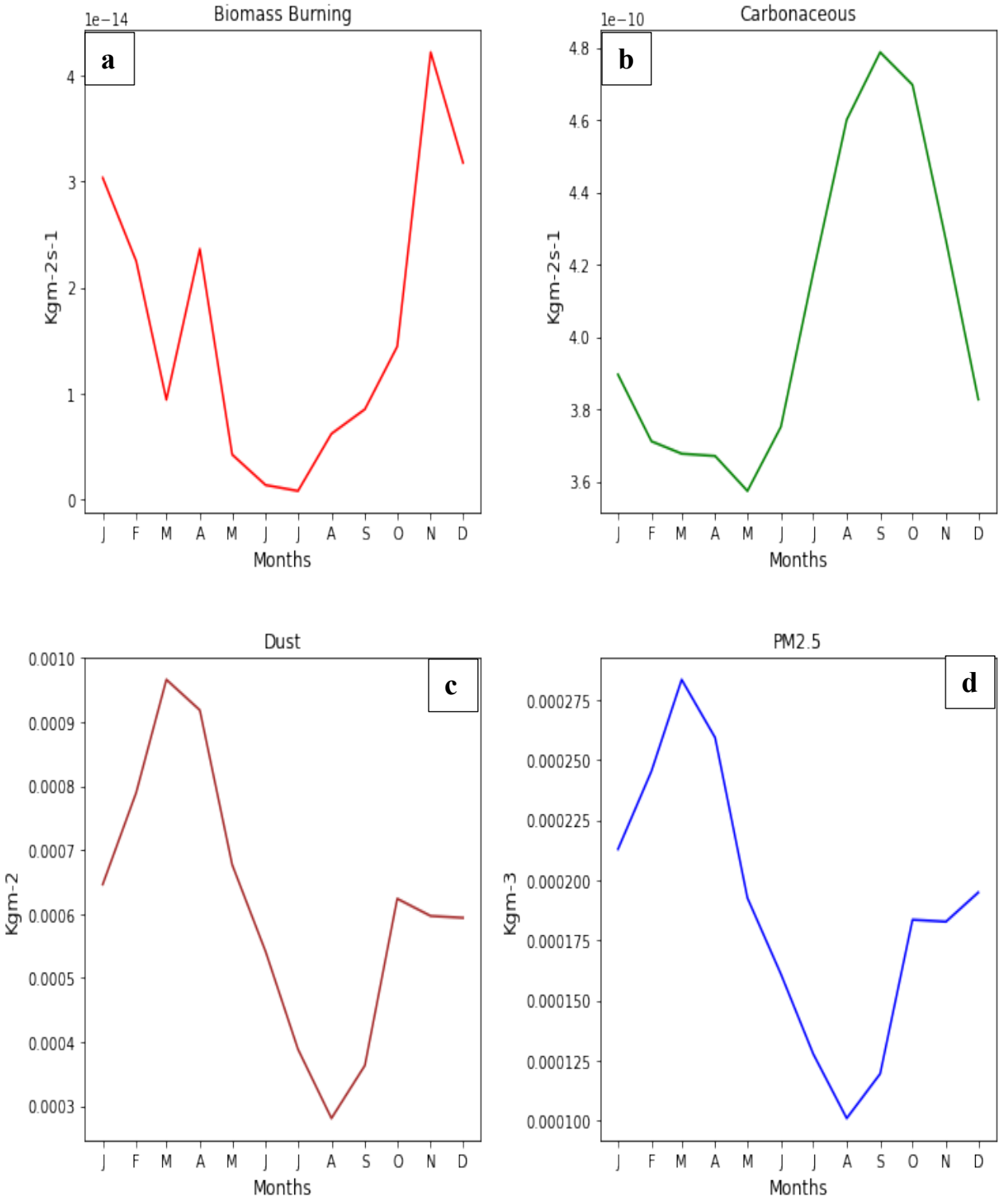

Figure 4.6: Monthly Aerosol (a) biomass burning, (b) carbonaceous, (c) dust, (d) $PM_{2.5}$ Variability over Kano

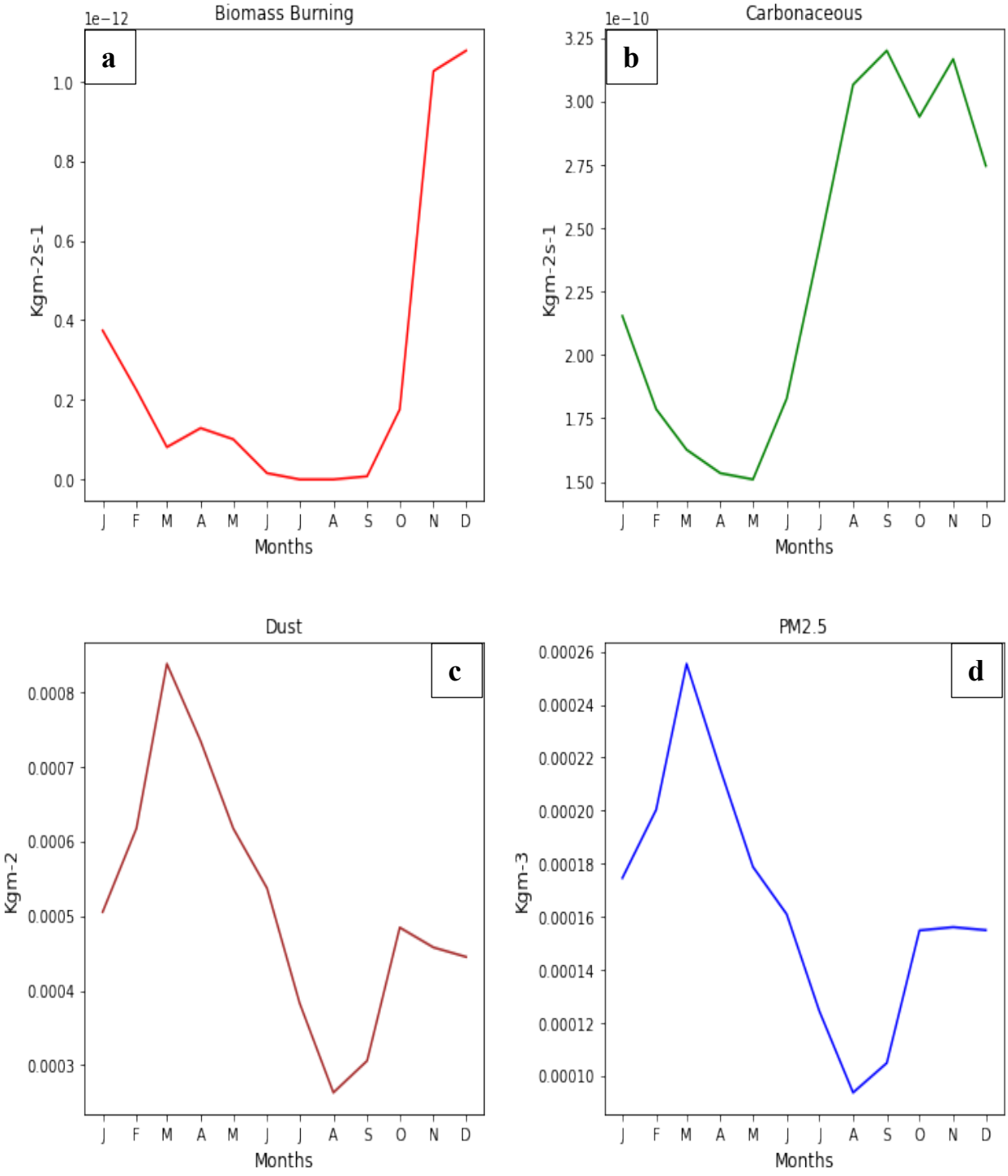

Figure 4.7: Monthly Aerosol (a) biomass burning, (b) carbonaceous, (c) dust, (d) $PM_{2.5}$ Variability over Ouagadougou

The biomass burning and carbonaceous recorded low values in the first six (6) months over Banizoumbou (fig. 4.5). While Biomass picked up around September to record its highest value in November, carbonaceous increased from June and had its highest value in September. The dust and particulate matter showed almost identical figures, with the least values in August, and the highest values recorded in March. For Kano (fig. 4.6), biomass values were recorded in the pre-and post-monsoon months of JFMA and OND respectively; and these correspond with the pre-planting and harvesting periods as related to agricultural activities as agreed with the study of (Reddington *et al.*, 2015). Carbonaceous was found to be low from January to May but started recording a rising trend to its highest value in September. The dust and particulate matter exhibited the same pattern of flow. High values were recorded between the dry months of January and April, with the peak values observed in March/April for the Sudan-Sahelian region. This is in agreement with the study of Ochei and Adenola (2018) which define the peak months of thick dust haze (TDH) and light dust haze (LDH) to be between November/December and January/February respectively. The low value experienced in this savannah region in August cannot be said to be a coincidence, rather can be associated with the farthest position of the ITD at 22^{o}N, thereby making southwest monsoon wind to be dominant and prevalent over the region (Oluleye and Okogbue 2013; Grist and Nicholson 2001), bringing in moisture and thereby washing away the aerosols from the atmosphere.

Biomass burning presence over Ouagadougou (fig. 4.7) was low between the rainy months of June and September, while January to May recorded some activities. This is to show that some activities have taken place for the preparation of the planting season in anticipation of precipitation. It started showing an increasing trend from October, with November and December recording the

highest value. The rainfall months recorded the least values of biomass burning. The carbonaceous recorded its least value in March but continues to its highest value in September and November, with a slight dip in October; thereby forming a double peak-like pattern. The dust and $PM_{2.5}$ showed quite identical patterns, with the highest and least values recorded in March and August respectively.

4.2.3 Monthly Variation over the Desert zone (13°N and above)

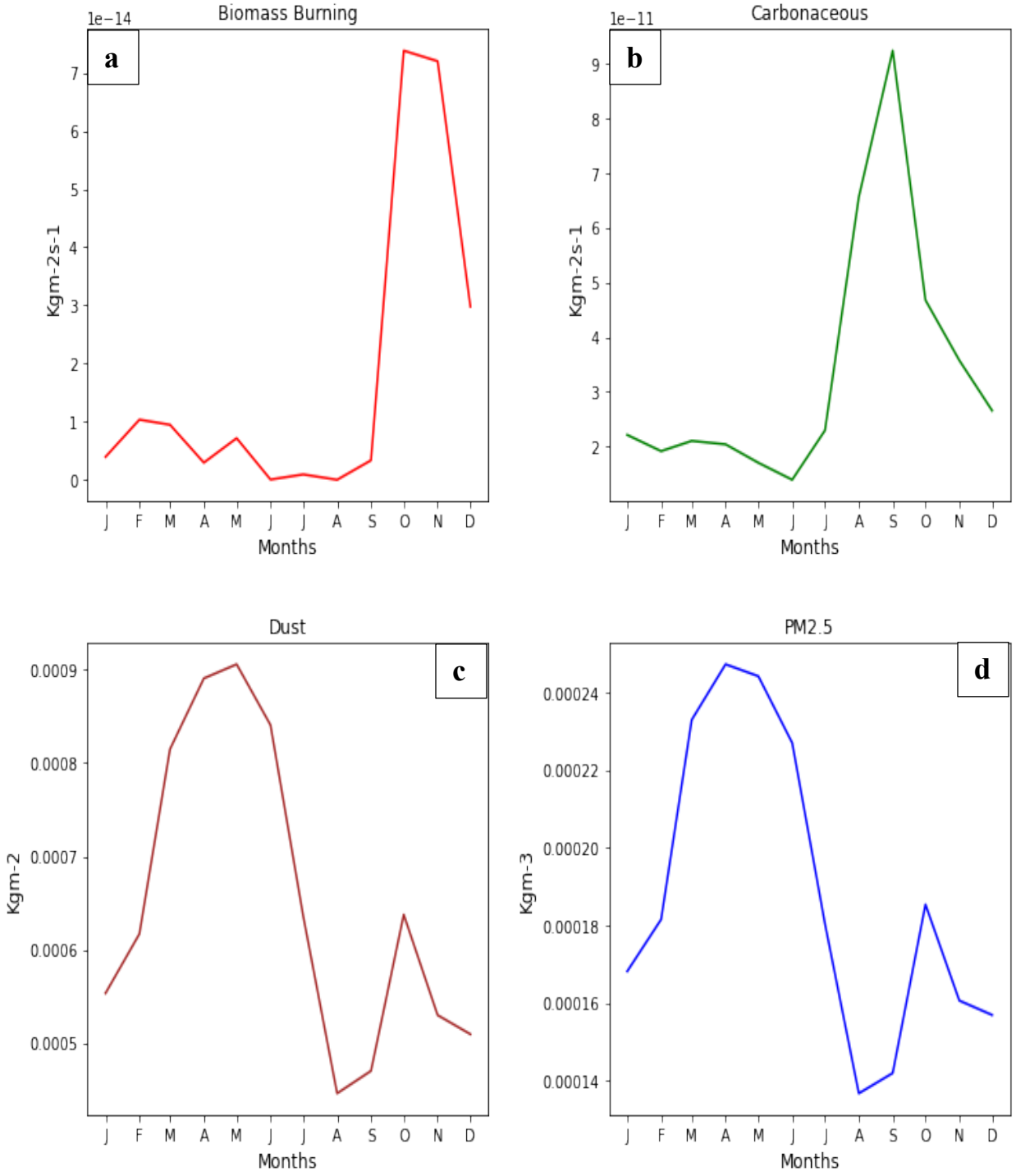

Figure 4.8: Monthly Aerosol (a) biomass burning, (b) carbonaceous, (c) dust, (d) $PM_{2.5}$ Variability over Agoufou.

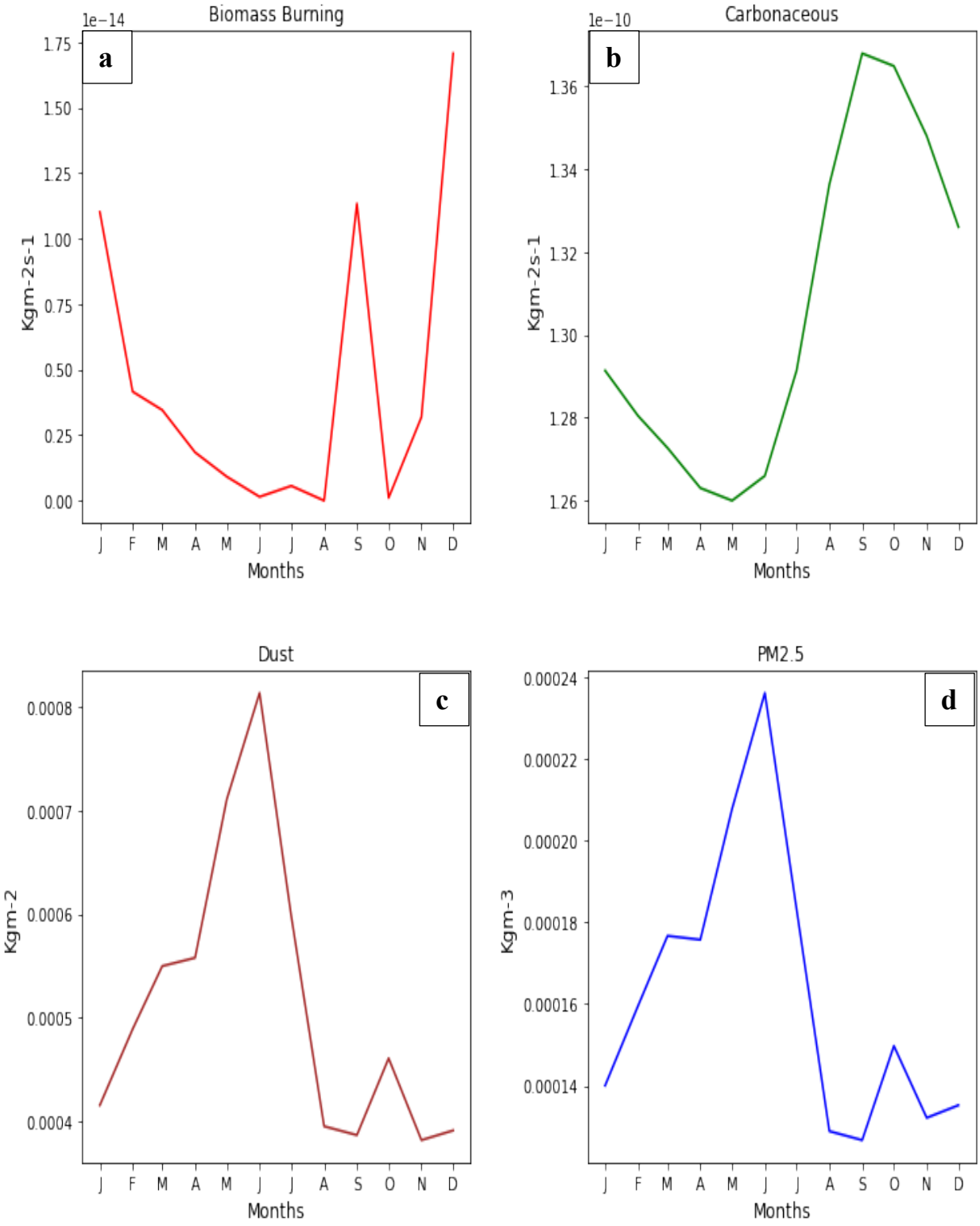

Figure 4.9: Monthly Aerosol (a) biomass burning, (b) carbonaceous, (c) dust, (d) $PM_{2.5}$ Variability over Dakar

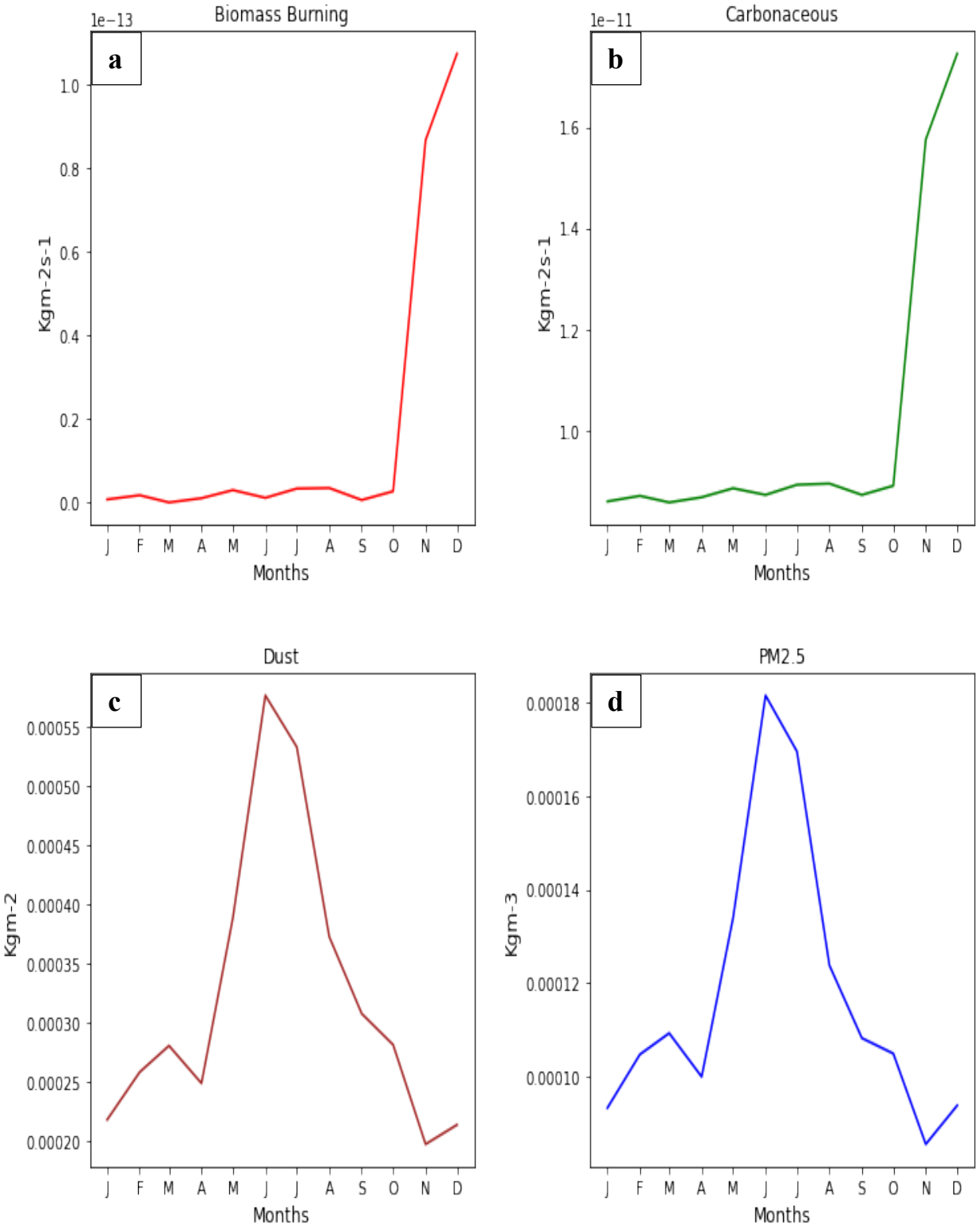

Figure 4.10: Monthly Aerosol (a) biomass burning, (b) carbonaceous, (c) dust, (d) $PM_{2.5}$ Variability over Praia

The desert with three (3) locations, designated from areas north of 13ºN, showed a very low level of biomass burning and carbonaceous across the selected locations between January and June in some cases while some extended to September. The values of the biomass burning and the carbonaceous were higher during the dry months of October, November, and December, except Dakar which recorded its highest value of biomass burning in September and December. The carbonaceous for Agoufou (fig. 4.8b) showed a low value from January to July and peaked in September. The value plummeted again around the months of November and December. Thus, it can be deduced that the carbonaceous over Agoufou was more pronounced during the peak months of the rainy season, while the dry months experience less carbonaceous in the atmosphere. The biomass burning over Dakar (fig. 4.8a) recorded a double peak in September and December/January. The activities of the biomass were less conspicuous from the dry months of February through to the rainy month of August. The carbonaceous in figure 4.8b showed the month of April, May, and June recording the least values, while September and October recorded the highest values. The monthly aerosol distribution over Praia (fig. 4.10) showed identical features for both biomass burning (fig. 4.10a) and carbonaceous (fig. 4.10b). It can be observed from the two figures that biomass burning and carbonaceous were absent from January to October, while only the months of November and December recorded some activities of aerosol over the area. These designated desert areas namely Agoufou (fig. 4.8), Dakar (fig. 4.9) and Praia (fig. 4.10) have the same thing in common, which is the fact that all the figures representing both clouds of dust and $PM_{2.5}$ showed the same pattern and trend. This is in support of the study of De Longueville *et al.*, (2010) which showed that Saharan dust contributes up to 1100 Tg of particulate matter to the annual

4.3 Seasonal and Inter-seasonal Distribution of Aerosols over West Africa.

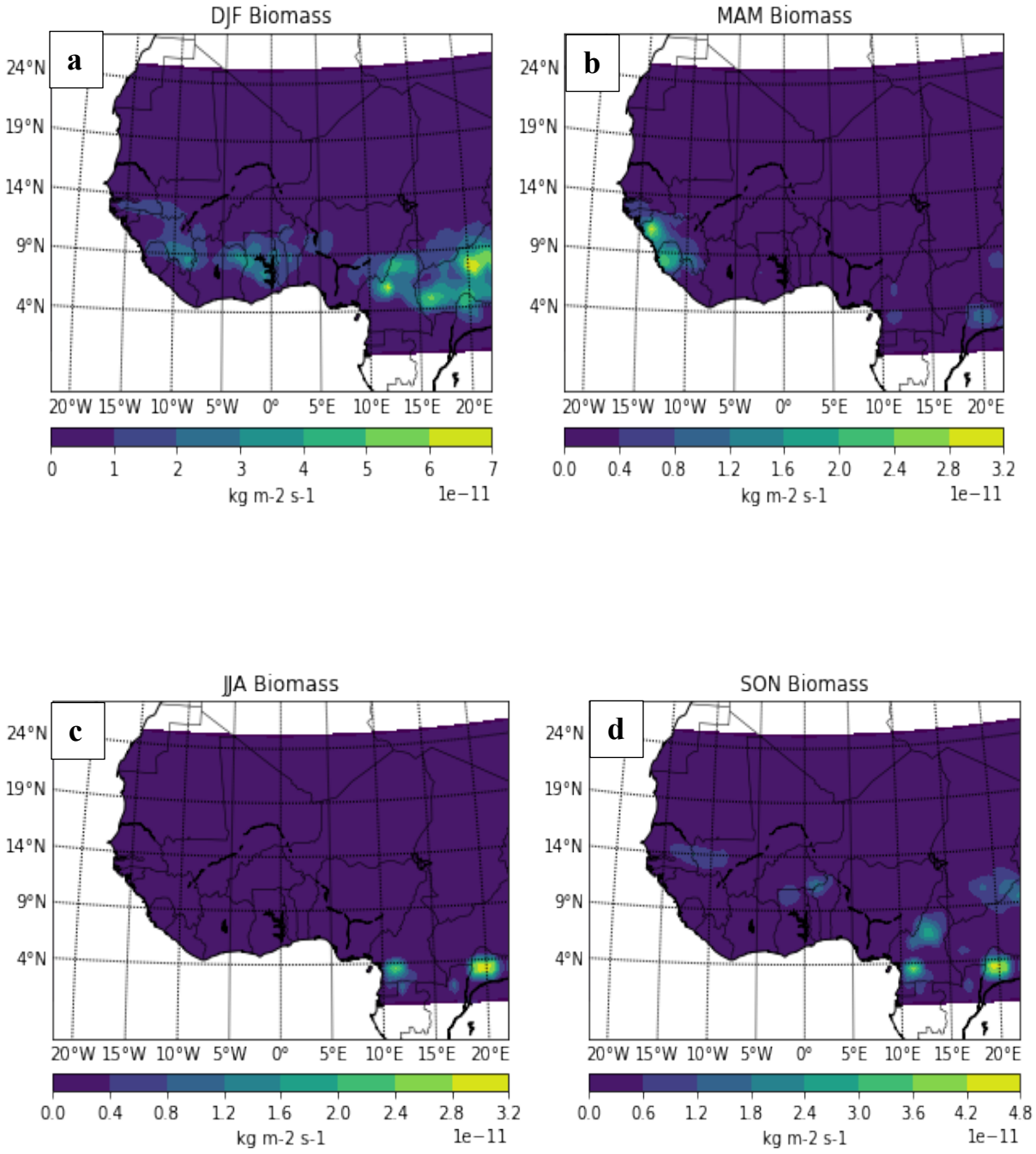

Figure 4.11: Seasonal (a) DJF – December/January/February, (b) MAM - March/April/May (c) JJA - June/July/August, (d) SON - September/October/November distribution of Biomass Burning

The availability of biomass in the seasonal months of December/January/February around the stretches of the Atlantic bounded areas can be said to be a result of two possibilities. The first result can be deduced to be the pre-planting activities in expectation of the onset of the rainy season in the region. Another possible scenario can be adduced to the role of the prevailing easterly wind which can aid the transportation of the pollutant from Central Africa to Western Africa. The large presence of biomass burning in central Africa can be attributed to the fact that the area is said to have an estimated carbon emission from deforestation in 1980 to range from 17.9 to 22.5million tonnes, accounting for about 20% of the total carbon emissions over the entire area of tropical Africa (Brown *et al.*, 1989; Hall and Uhlig, 1991). It should be noted that the prevailing wind during this period of the year is easterlies. Hence, the second theory or possibility can be said to be truer in this scenario. The months of March/April/May showed the activity of biomass spotted around Freetown. Freetown may be a coastal zone but partly share the characteristic of the savannah region in which the onset of rain has been pegged on average to be around the month of May. Hence, the presence of biomass can be adduced to pre-planting season activities as the onset of rainfall over this location is not the same as in other rainforest zones. In the consideration of June/July/August, there was no evidence of biomass activity over the study area. But patches were discovered in the transition months of September/October/November depending on the latitudinal position.

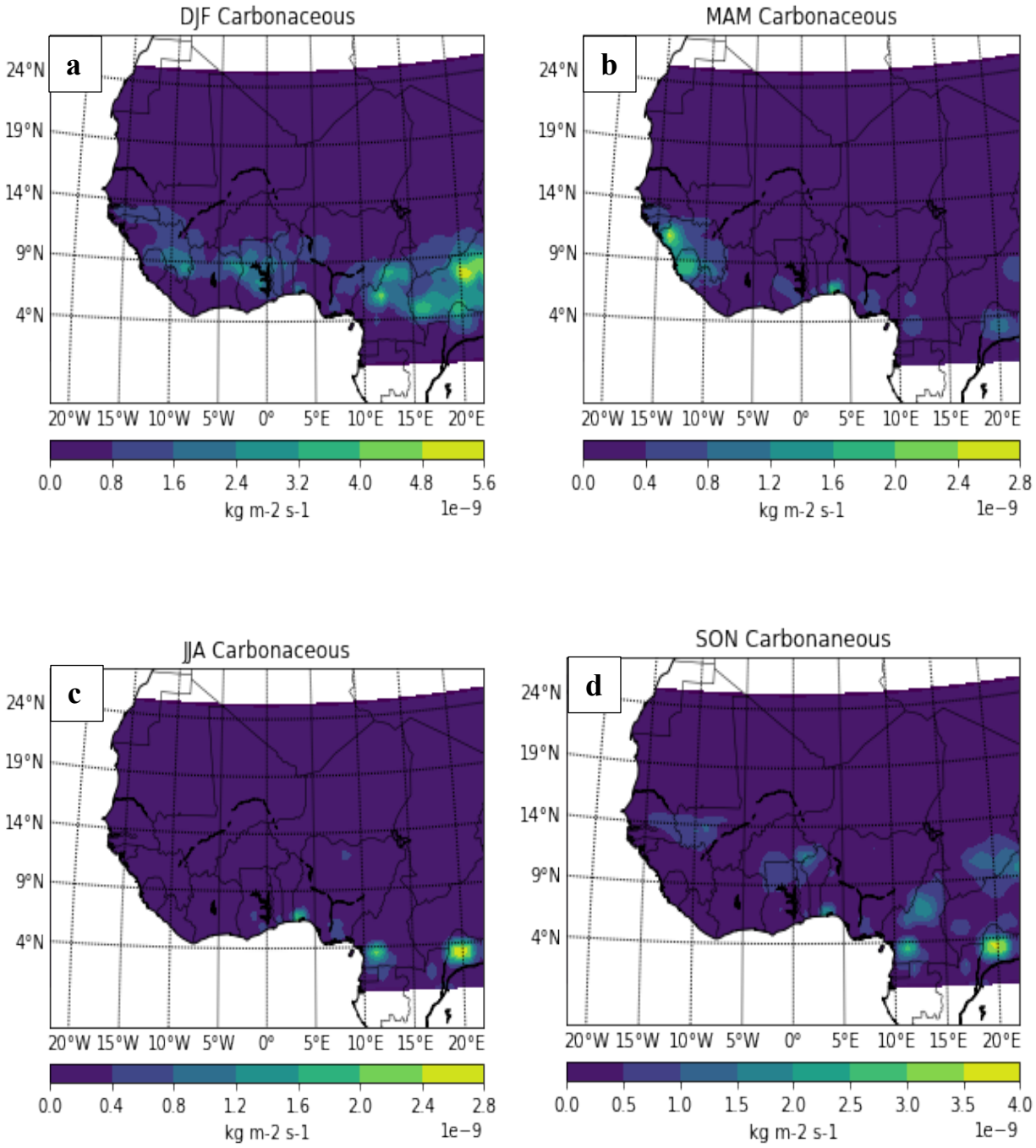

Figure 4.12: Seasonal (a) DJF – December/January/February, (b) March/April/May, (c) June/July/August, (d) September/October/November distribution of Carbonaceous

The carbonaceous aerosol used for this analysis is compounding carbon, which is a production of incomplete combustion of fossil fuels and oxidation of methane and other hydrocarbons. Carbonaceous presence in the atmosphere is well pronounced in the Harmattan months of DJF, spanning the whole length of the coastal cities. This is in a similar pattern to biomass burning, and thus supports the study of van der Werf *et al.*, (2010) which estimated around 2PgC/year of global CO_2 emissions due to about 4% of the global land area subjected to burning (Giglio *et al.*, 2013). Though studies may have shown similarities in biomass and carbon but comparing the results of both pollutants in the months of March/April/May (MAM), it can be observed that carbon seems pronounced around Ikeja which is not available in biomass burning during the said period. Also, Freetown seems to record an expanded area under carbon prevalence when compared to biomass. The reason for the high concentration of the pollutant at Ikeja and Freetown only within the coastal areas during this period can be attributed to anthropogenic effects. The wet months of June/July/August still showed Ikeja having a concentration of pollutants while Freetown is clear. The continuous presence of carbonaceous in Ikeja all through the year can be attributed to the fact that it is the commercial hub of West Africa with engrossed vehicular and human activities (industrial emissions).

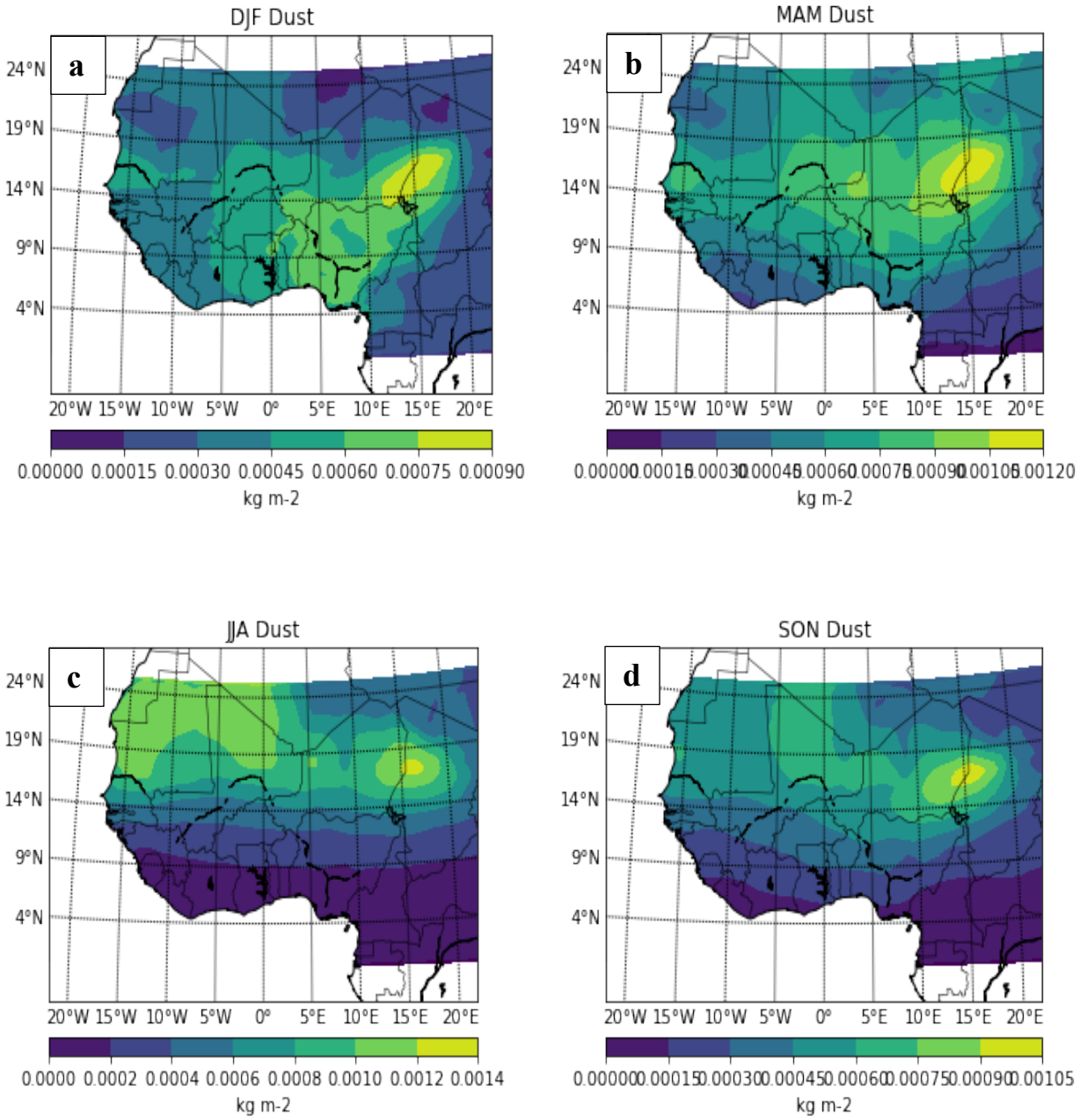

Figure 4.13: Seasonal (a) DJF – December/January/February, (b) MAM - March/April/May (c) JJA - June/July/August, (d) SON - September/October/November distribution of Dust

The analysed dust particle is a combination of both fine mode as a suspended atmospheric particles and coarse mode due to the accumulation as sediment on the surface of the earth. Most importantly, the considered dust particles here is in the range of about 1 – 100 μm. During the harmattan months of DJF, it was observed that the dust spread to the southernmost part of the study area, covering the whole of Nigeria and spreading up to 5^{o}W, and also a significant patch of it around Dakar at 15^{o}N. Due to the depth of this pollutant southward, it is often regarded as a thick dust haze (TDH) and reduces visibility (Ochei and Adenola, 2018). The source point showed a well-laden dust event, with a significant amount spreading across Sudan and some parts of the Guinea savannah. The potential 'early' onset of the rainforest part in the months of MAM seems to have pushed back the dust further north, and this can be attributed to the northward migration of the ITD, thereby making south of the ITD to be under the influence of moist southwest monsoon (Oluleye and Okogbue, 2013). The month of JJA exhibited characteristics that showed that the whole rainforest and Guinea savannah were under the influence of convective activities due to the northernmost position of ITD. Though, some areas north of 15^{o}N (Sahel) and most especially the point source are mostly under the influence of dust activities. The dust seems to be intensifying again and thereby pushing further down the south towards the Atlantic Ocean in the transition month of SON.

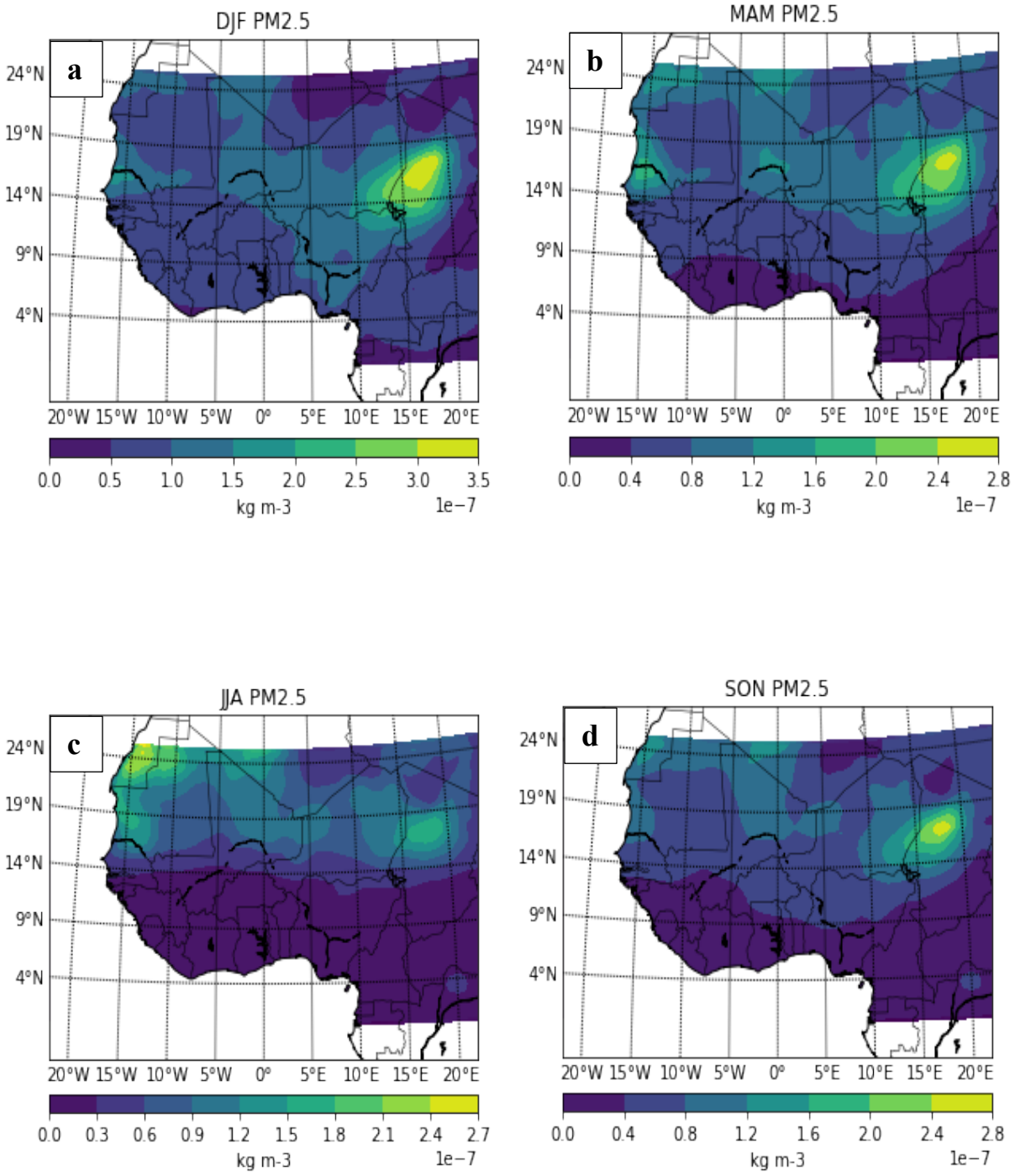

Figure 4.14: Seasonal (a) DJF – December/January/February, (b) MAM - March/April/May (c) JJA - June/July/August, (d) September/October/November distribution of Particulate Matters ($PM_{2.5}$).

Particulate Matters ($PM_{2.5}$) showed similar features in Harmattan months of DJF and onset months of MAM. Though the coastal axes did not have a record of the pollutant in the onset months, further inland to the north showed a similar pattern with DJF over the Sahel and desert areas. For the wet months of JJA, the pollutant is completely negligible from the equator up to 15^{o}N, but some traces can be seen over the Sahel. The cessation months of SON witnessed the spread of the pollutant towards the southern part. Though, areas south of 9^{o}N - 10^{o}N are not under the influence of the pollutant. The point source of dust in Bodélé depression exhibited a similar pattern with $PM_{2.5}$ and this is in support of De Longueville *et al.*, 2010 study which showed that Saharan dust contributes up to 1100 Tg of particulate matter to the annual, thereby making it the most active among all source regions worldwide.

4.4 Annual Variability of Aerosols over West Africa.

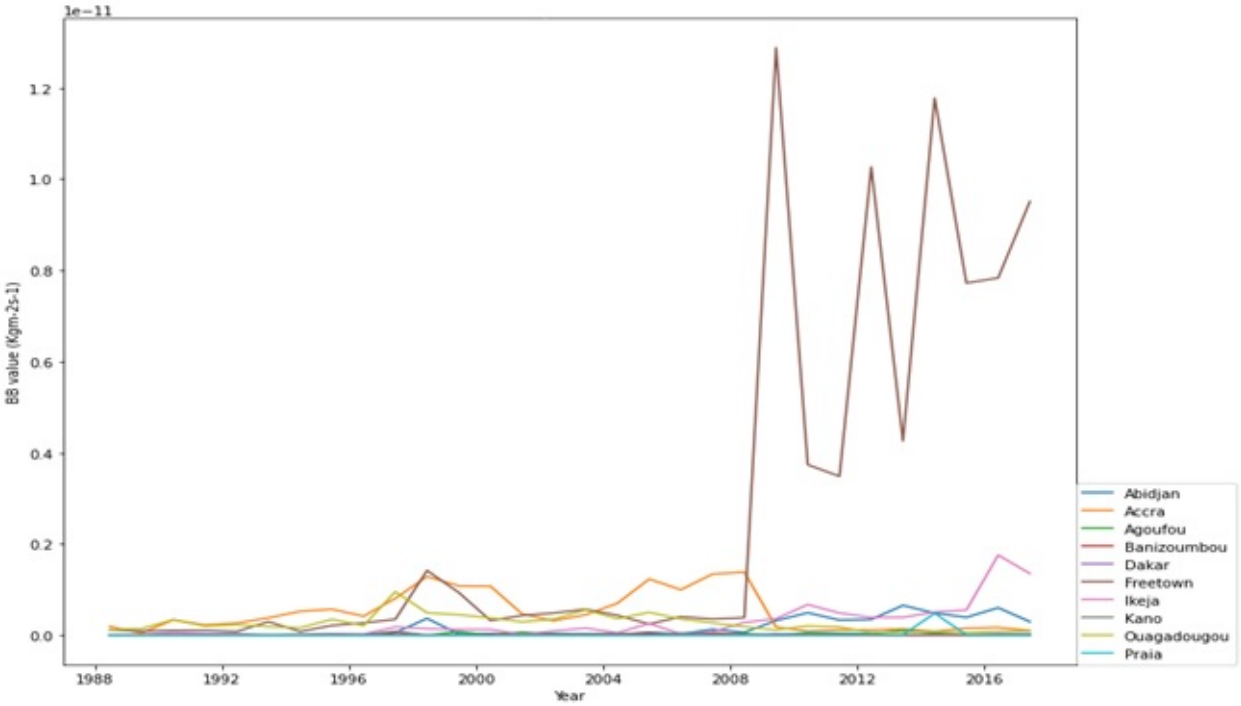

Figure 4.15: Annual Variability of Biomass burning Aerosol over the study locations.

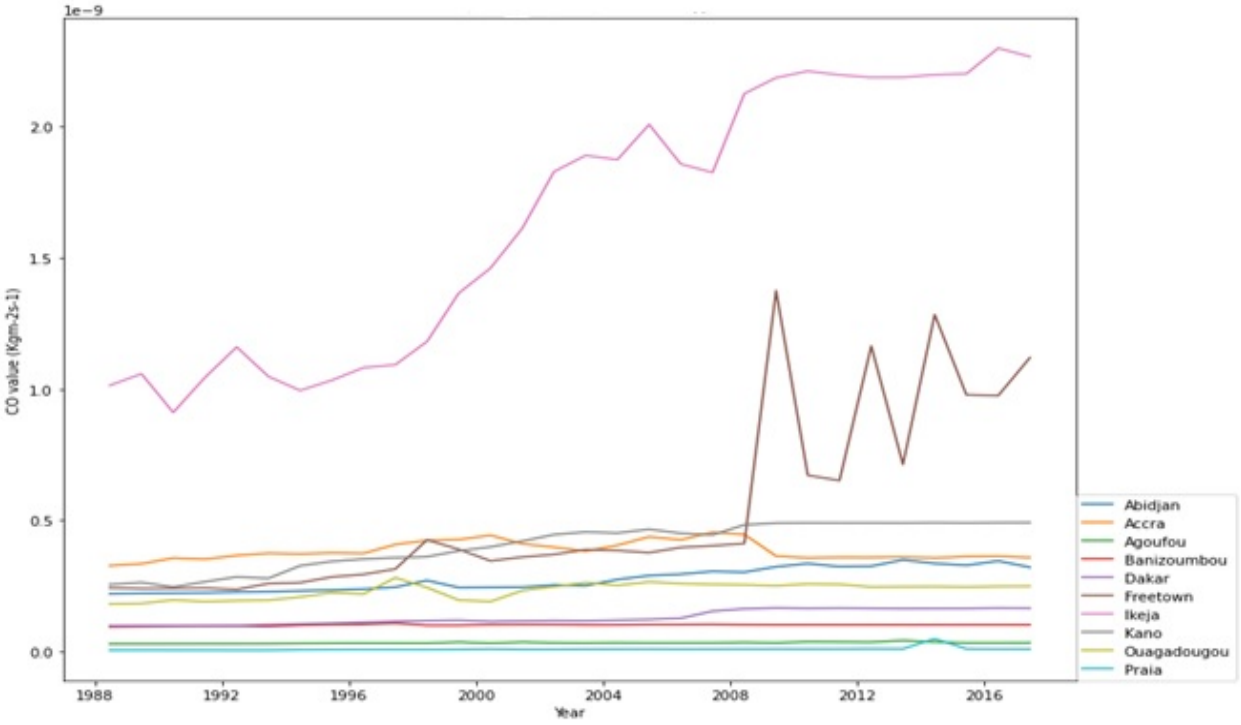

Figure 4.16: Annual Variability of Carbonaceous over the study locations.

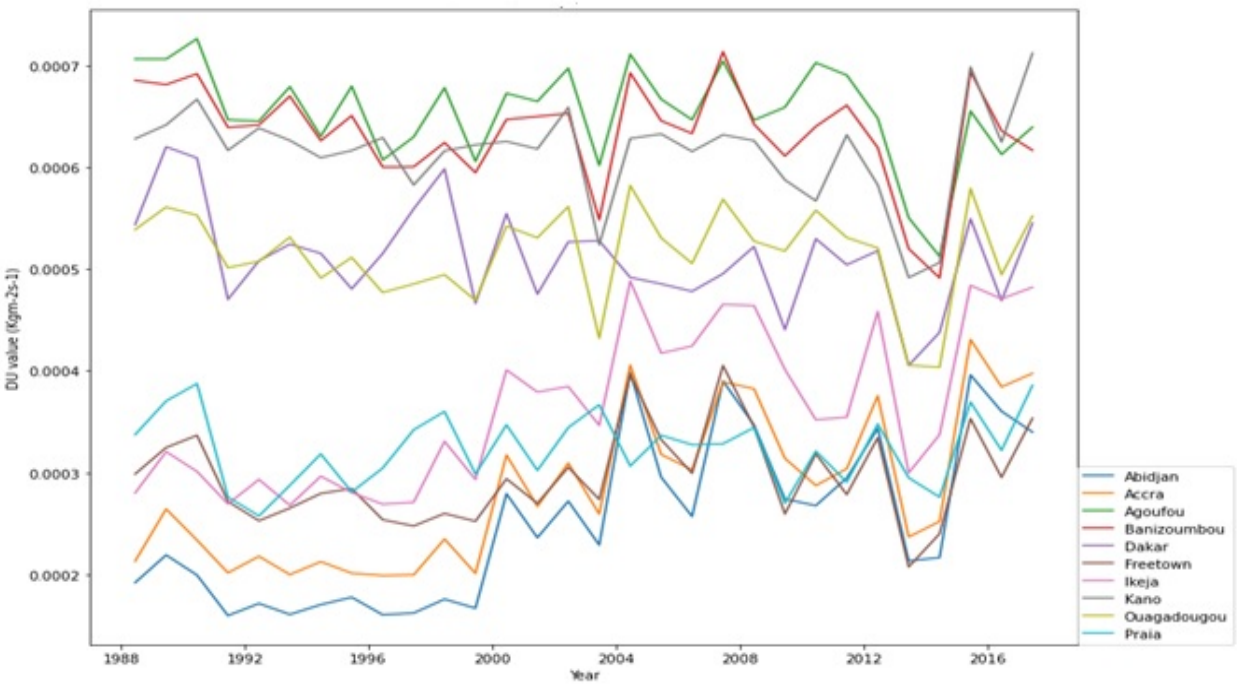

Figure 4.17: Annual Variability of Dust Aerosols over the study locations.

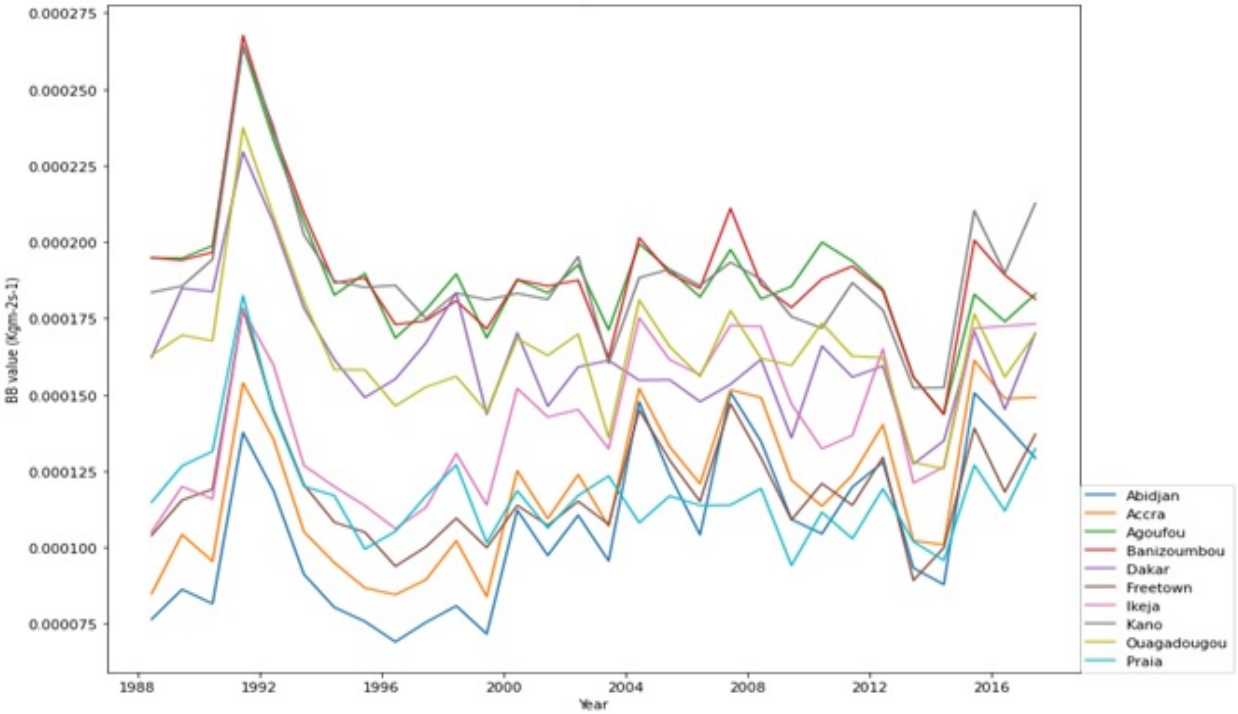

Figure 4.18: Annual Variability of Particulate Matters ($PM_{2.5}$) over the study locations.

The annual variation of aerosol types over a period of 30 years sheds light on some dominating types of pollutants and also the locations. The dust and $PM_{2.5}$, which can be termed natural pollutants, seem to be evenly distributed over the stations. This is not taking the fact away that Banizoumbou had more dust prevalence than other locations, and this can be attributed to its closeness to the source location, Bodélé depression (Herrmann *et al.*, 1999). The distribution and variability of $PM_{2.5}$ can also be said to be even as dust. But BB and CO cannot be said to be like the previous pollutants discussed. Freetown seems to record extreme event of BB, and this is in support of the report from Arevalo *et al.* (2016) study that 78% of 20,000 sampled households in Sierra Leone relies on wood fuel. Ikeja seems to be the more dominating location when it comes to CO, and this can be attributed to its status as the industrial hub of West Africa, its busiest ports, heavy traffic, and the city with the largest population (Kamer 2022). This result conforms with Assamoi and Liousse, (2010) study and agrees with observations (Reeves *et al.,* 2010) which spotted Lagos as one of the African largest cities with regional inventories of anthropogenic emissions due to high fossil fuel and biofuel consumption, including regional specificities, such as traffic from two-wheel vehicles And closely followed in the figure is Freetown as it is a well-known fact that wood fuel also contains some carbon.

4.5 Correlation Graphs of Aerosols and Climatic Parameters.

This section assesses and discusses the relationship between the selected aerosols (biomass burning, carbonaceous, dust, and $PM_{2.5}$) against each of the climatic parameters used (convective precipitation, wind speed, and water vapor). The analyses contain daily aerosols and climatic parameter variables for 30 years. To determine if there exists a relationship between the correlated variables, probability value (*p*-value) analysis was employed at a significance level of 0.05. If the *P*-value is smaller than the significance level ($\alpha = 0.05$), the null hypothesis is rejected in favor of the alternative. It can be concluded that the correlation is **statically significant** or in simple words "it can be said that there is a linear relationship between an independent variable - x (aerosol type) and the dependent variable – y (climatic parameter) in the population at the α level." If the *P*-value is bigger than the significance level ($\alpha = 0.05$), the null hypothesis is not rejected. It can then be concluded that the correlation is **not statically significant**. Or in other words "we conclude that there is not a significant linear correlation between an independent variable - x (aerosol type) and the dependent variable – y (climatic parameter) in the population at α level."

4.5.1 Convective Precipitation Correlated with Aerosols

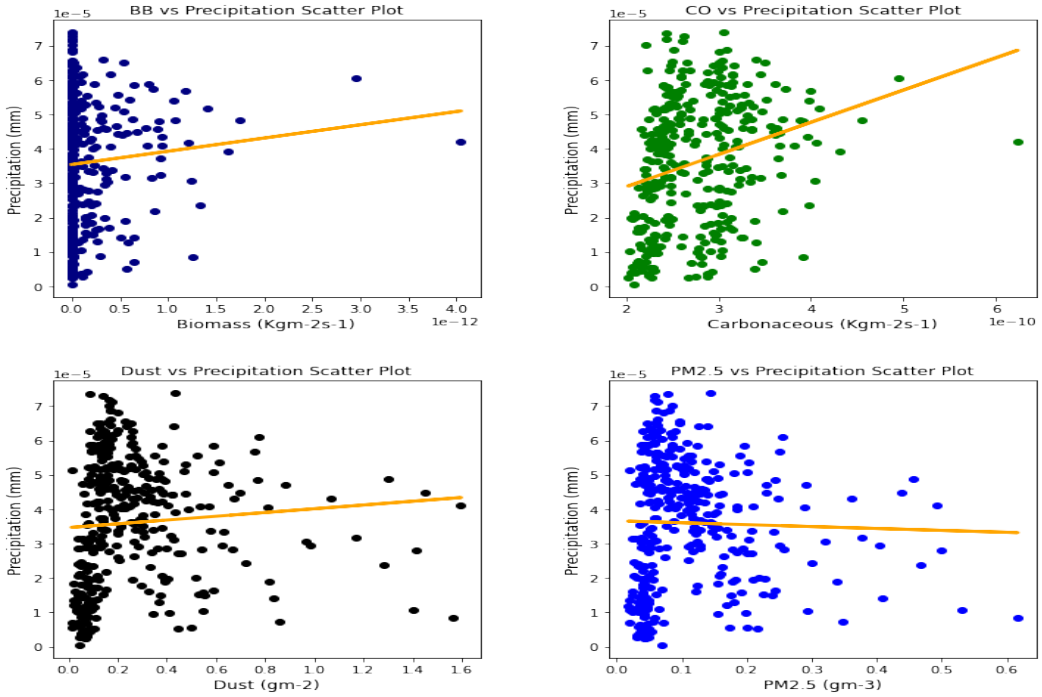

Figure 4.19: Correlation graphs of convective precipitation and aerosol types over Abidjan

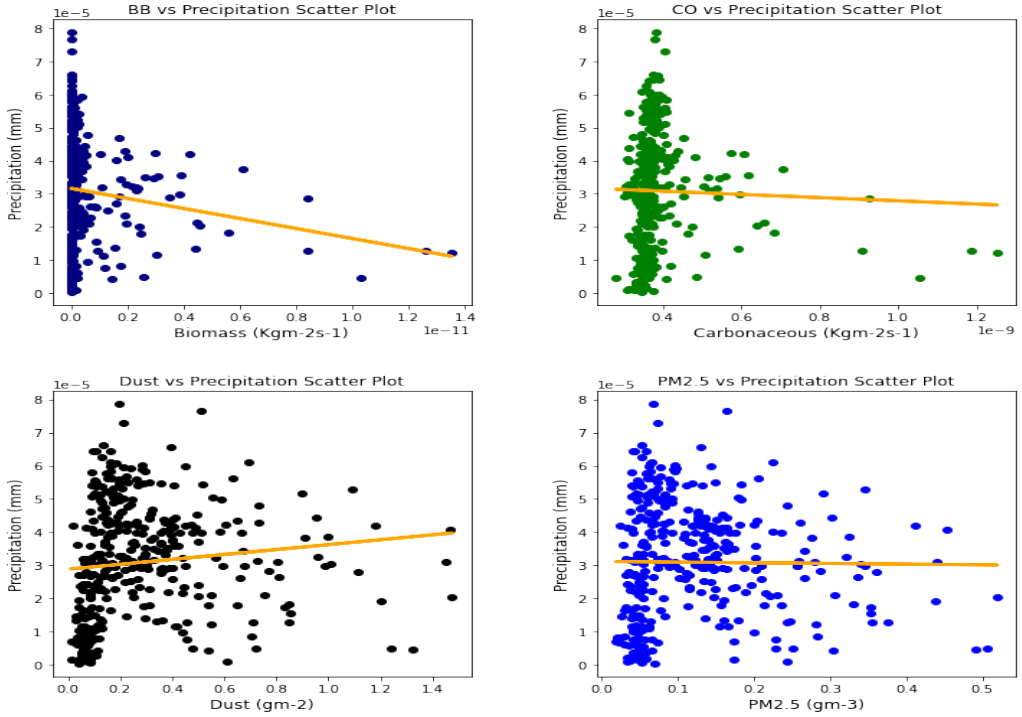

Figure 4.20: Correlation graphs of convective precipitation and aerosol types over Accra

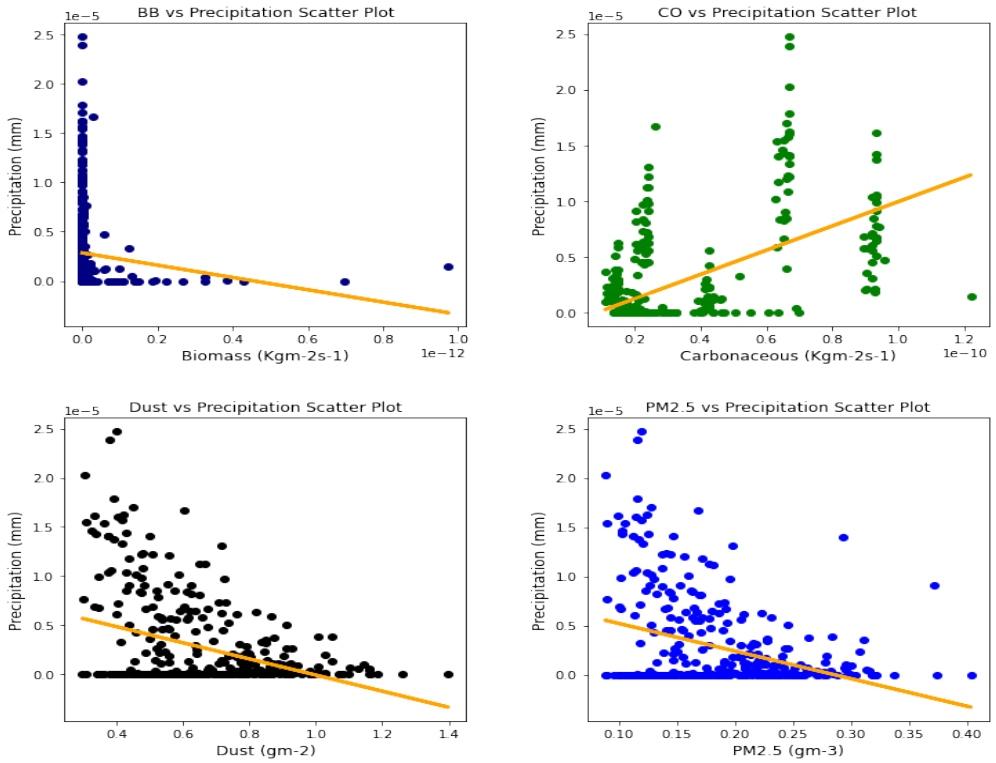

Figure 4.21: Correlation graphs of convective precipitation and aerosol types over Agoufou

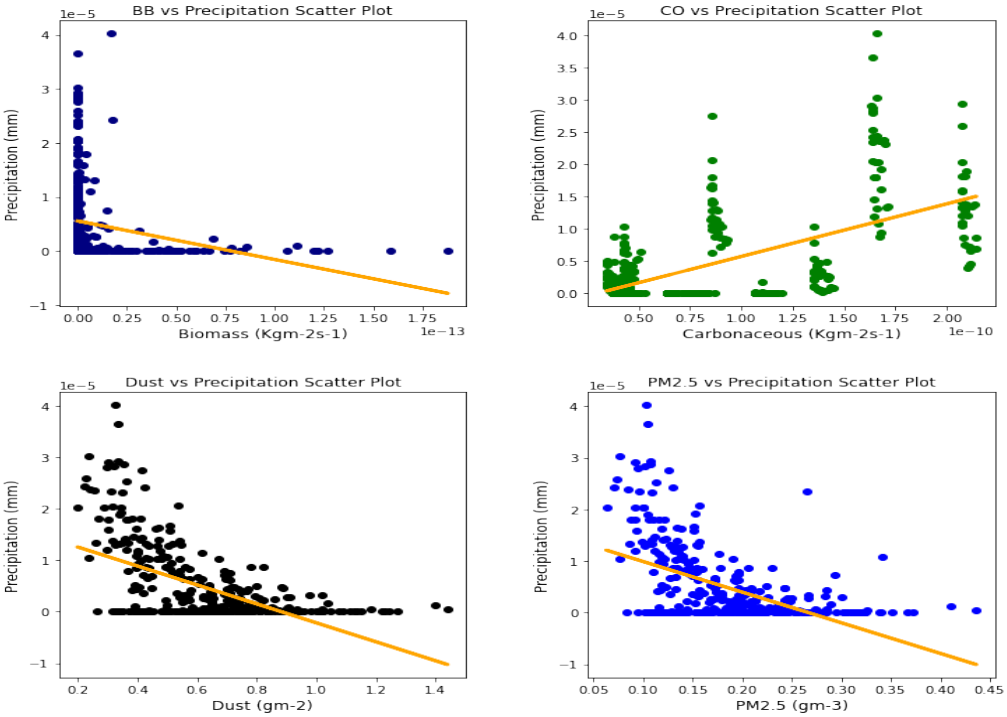

Figure 4.22: Correlation graphs of convective precipitation and aerosol types over Banizoumbou

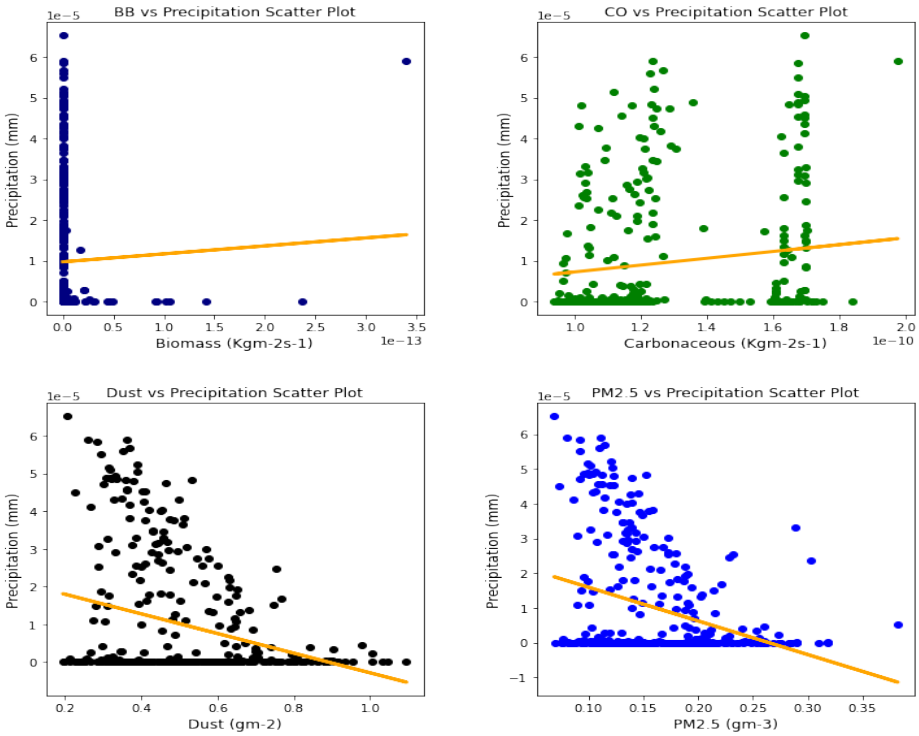

Figure 4.23: Correlation graphs of convective precipitation and aerosol types over Dakar

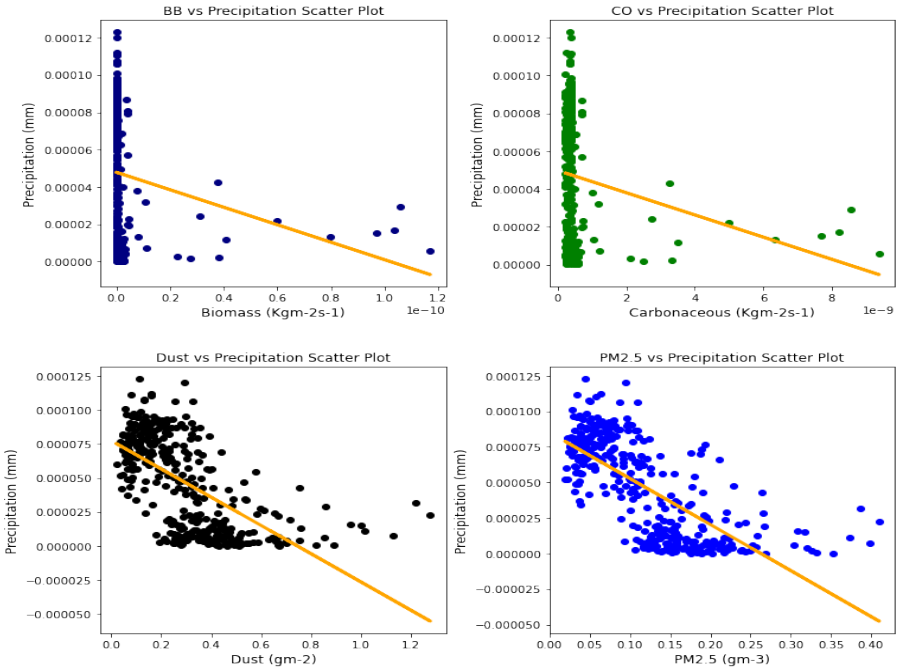

Figure 4.24: Correlation graphs of convective precipitation and aerosol types over Freetown

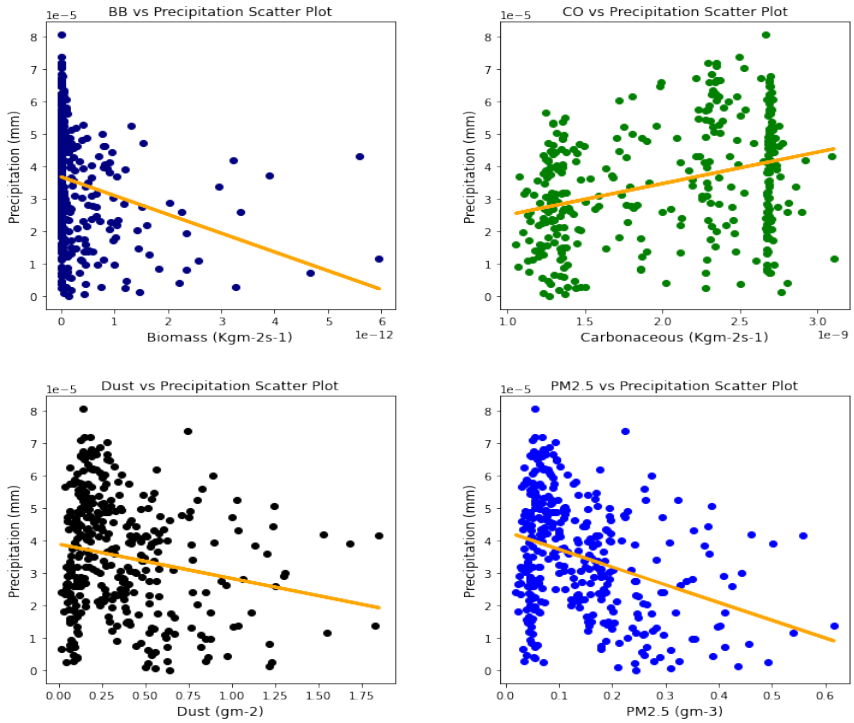

Figure 4.25: Correlation graphs of convective precipitation and aerosol types over Ikeja

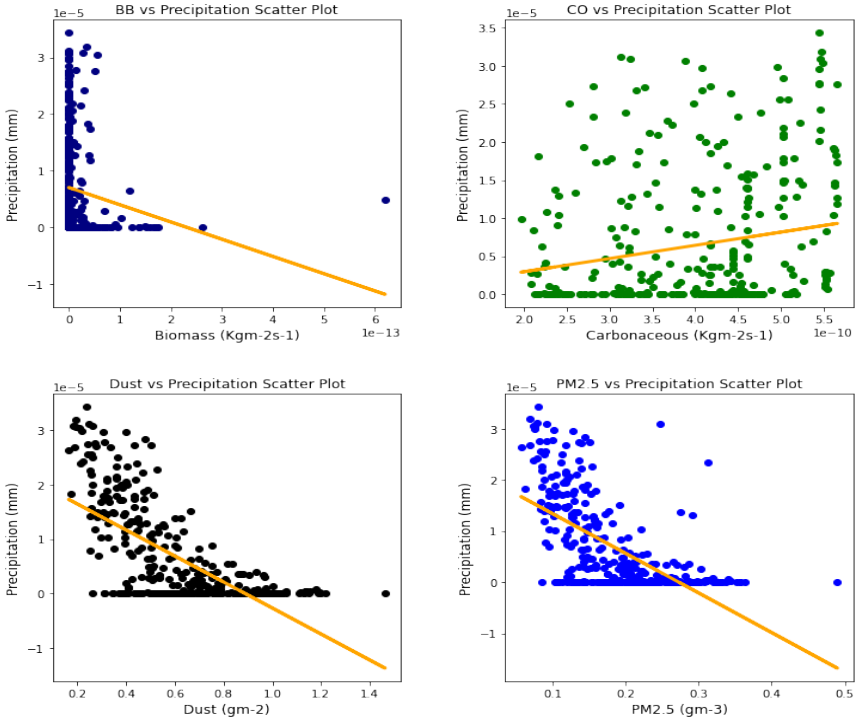

Figure 4.26: Correlation graphs of convective precipitation and aerosol types over Kano

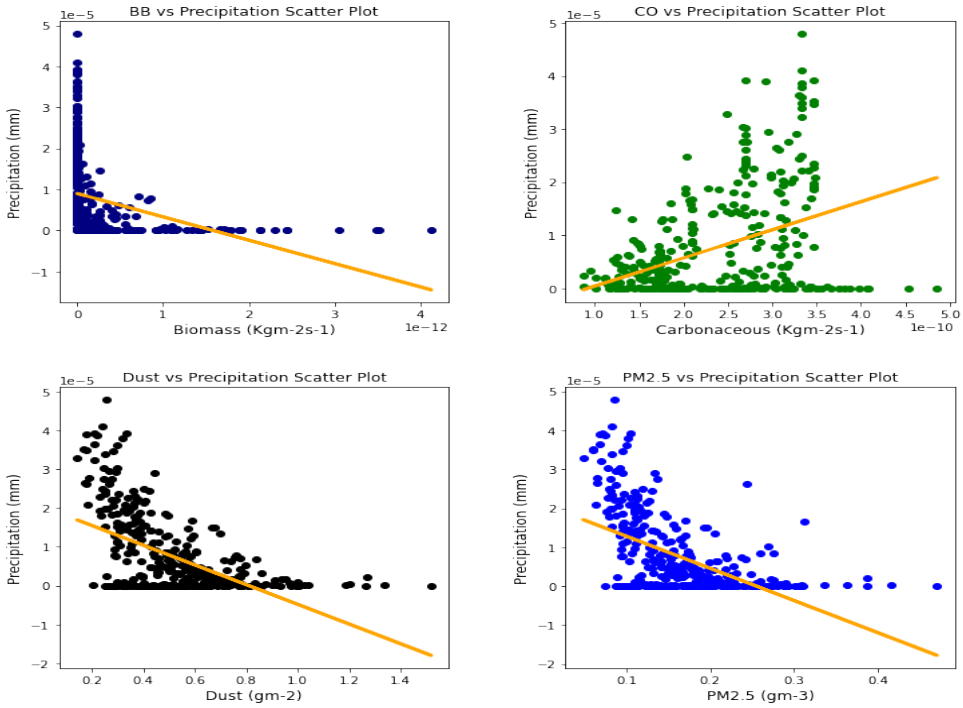

Figure 4.27: Correlation graphs of convective precipitation and aerosol types over Ouagadougou

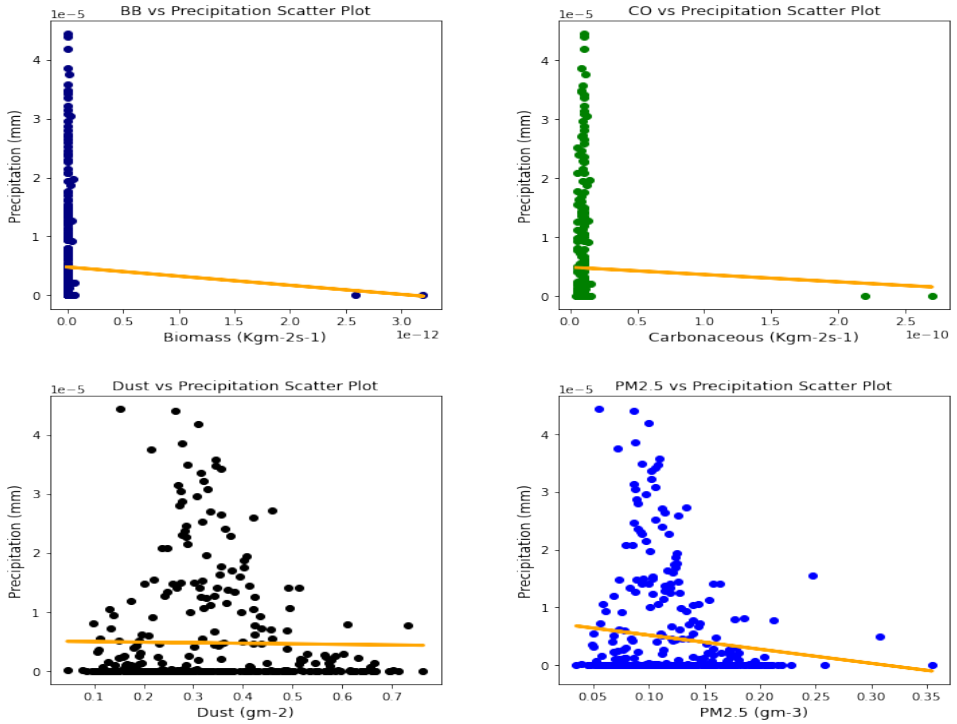

Figure 4.28: Correlation graphs of convective precipitation and aerosol types over Praia

S/N	Stations	Biomass Burning (BB)			Carbonaceous (CO)			Dust (Du)			Particulate Matters ($PM_{2.5}$)		
		R	***p-value***	**Status**	**R**	***p-value***	**Status**	**R**	***p-value***	**Status**	**R**	***p-value***	**Status**
1.	Abidjan	0.08	*0.13*	Accepted	0.27	*2.11e-7*	**Rejected**	0.08	*0.15*	Accepted	-0.03	*0.61*	Accepted
2.	Accra	-0.13	*0.01*	**Rejected**	-0.03	*0.60*	Accepted	0.11	*0.03*	**Rejected**	-0.01	*0.84*	Accepted
3.	Agoufou	-0.11	*0.04*	**Rejected**	0.56	*1.11e-30*	**Rejected**	-0.37	*4.54e-13*	**Rejected**	-0.35	*6.12e-12*	**Rejected**
4.	Banizoumbou	-0.25	*3.23e-06*	**Rejected**	0.60	*9.24e-37*	**Rejected**	-0.55	*6.81e-30*	**Rejected**	-0.52	*3.62e-26*	**Rejected**
5.	Dakar	0.03	*0.56*	Accepted	0.14	*0.00*	**Rejected**	-0.30	*7.26e-09*	**Rejected**	-0.32	*2.82e-10*	**Rejected**
6.	Freetown	-0.18	*0.00*	**Rejected**	-0.17	*0.00*	**Rejected**	-0.63	4.24e-41	**Rejected**	-0.71	*7.59e-56*	**Rejected**
7.	Ikeja	-0.24	*3.46e-06*	**Rejected**	0.33	*6.27e-11*	**Rejected**	-0.19	*0.00*	**Rejected**	-0.34	5.13e-11	**Rejected**
8.	Kano	-0.15	*0.00*	**Rejected**	0.19	*0.00*	**Rejected**	-0.66	*8.18e-47*	**Rejected**	-0.62	*9.12e-40*	**Rejected**
9.	Ouagadougou	-0.32	*6.92e-10*	**Rejected**	0.40	*6.17e-15*	**Rejected**	-0.53	*4.85e-28*	**Rejected**	-0.53	*8.15e-28*	**Rejected**
10.	Praia	-0.04	*0.49*	Accepted	-0.02	*0.65*	Accepted	-0.02	*0.77*	Accepted	-0.12	*0.02*	**Rejected**

Table 4.1: Table showing the correlation (R) between convective precipitation and aerosols, with the corresponding *p-values* at $\alpha = 0.05$

Summary

Biomass Burning = 7 Rejected, 3 Accepted**;**

Carbonaceous = 8 Rejected, 2 Accepted**;**

Dust and $PM_{2.5}$ = 8 Rejected, 2 Accepted

Several studies have been done to unravel the relationships vis-à-vis the effect of aerosol on meteorological variables or the other way around. One such study showed that squall lines and density currents which are associated with moist convection are meteorological effects that cause strong winds necessary to trigger dust mobilization (Knippertz, 2008; Knippertz *et al.*, 2009; Schepanski *et al.*, 2009).

For the relationships between aerosol types and convective precipitation in table 4.1, it showed that all locations recorded a negative correlation in biomass, dust, and $PM_{2.5.}$ This shows that the presence of aerosols can lead to reduced precipitations presence in the atmosphere. This is in support of Wu *et al.*, (2011) study which established that investigation of regional modeling has shown that the radiative effect of aerosol could cause an overall reduction in precipitation but may increase nighttime precipitation; and also intensify extremely high precipitation rates (Kolusu *et al.*, 2015). The strongest relationships between convective precipitations and aerosol types can be observed in Banizoumbou (for Carbonaceous) at 0.60, Kano (for dust) at -0.66, and Freetown (for $PM_{2.5}$) at -0.71. The strong correlation between dust and convective precipitation over Kano can be supported by studies of Knippertz, (2008) and Schepanski *et al.*, (2009) which showed that associated moist convection of squall lines triggers dust mobilization. Biomass burning recorded low or no correlation with convective precipitation in all the locations, with the highest value being -0.32 at Ouagadougou. Relating the probability value of the correlation values of each of the climatic variables with aerosol types to the significance test of 0.05, it can be deduced under biomass burning that all locations except Abidjan, Dakar, and Praia, had a statistically significant relationship with convective precipitation. For carbonaceous, Accra and Praia were the only two (2) stations that do not have a relationship that is statistically significant with convective precipitation. The correlation under dust also showed Abidjan and Praia not

having a statistically significant relationship with convective precipitation with values higher than 0.05; while Abidjan and Accra values also accepted the null hypothesis which showed that these are the two (2) locations where there exist no statistically significant relation between the $PM_{2.5}$ and convective precipitation.

In summary, all the correlated aerosols over Praia with convective precipitation, except $PM_{2.5}$, do not exhibit a statistically significant relationship between the aerosol and the climatic parameters; while Accra, as the only coastal location, also recorded no statistically significant relationship under carbonaceous and $PM_{2.5}$. This anomaly in Accra as compared to other locations, especially regions within the same climatic borders, cannot be said to be unrelated to the anomaly in weather situations as detailed by Acheampong (1982).

4.5.2 Wind Speed Correlated with Aerosols

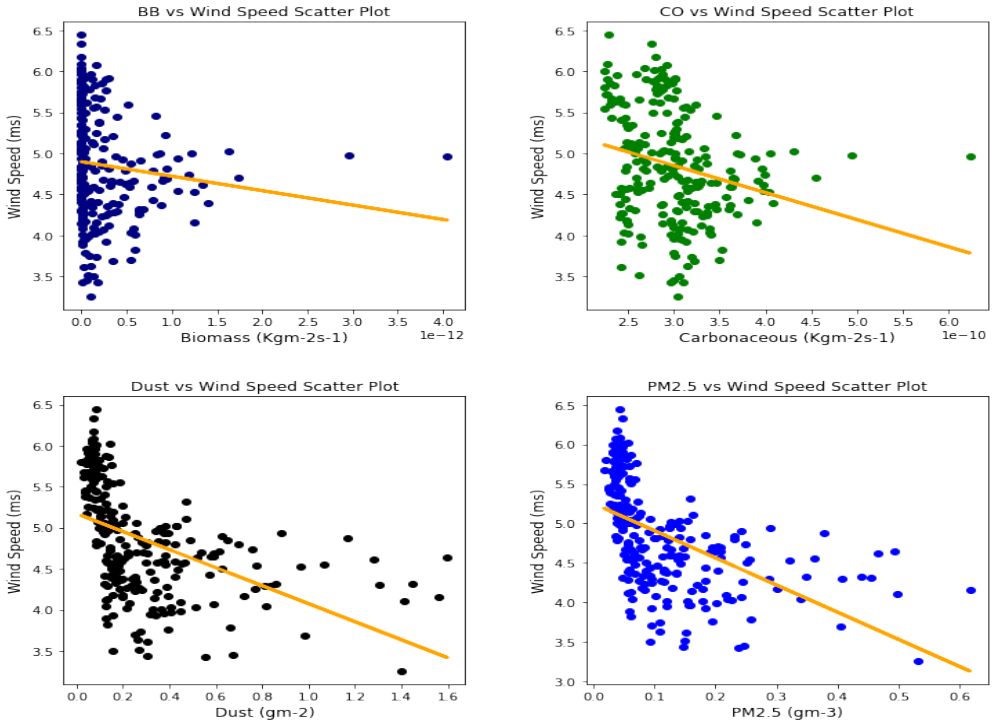

Figure 4.29: Correlation graphs of wind speed and aerosol types over Abidjan

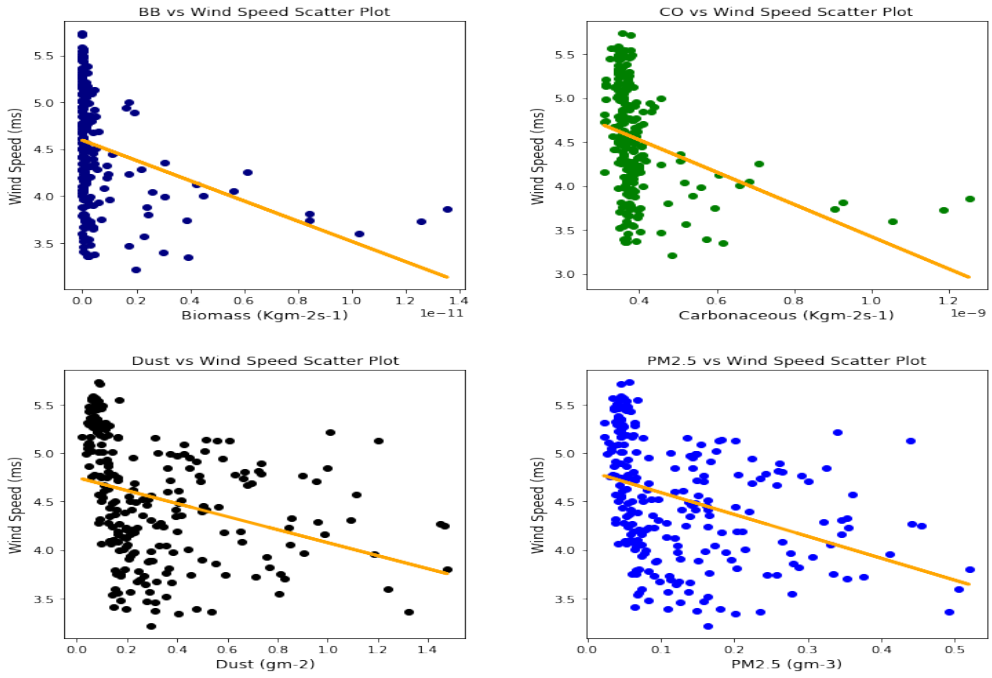

Figure 4.30: Correlation graphs of wind speed and aerosol types over Accra

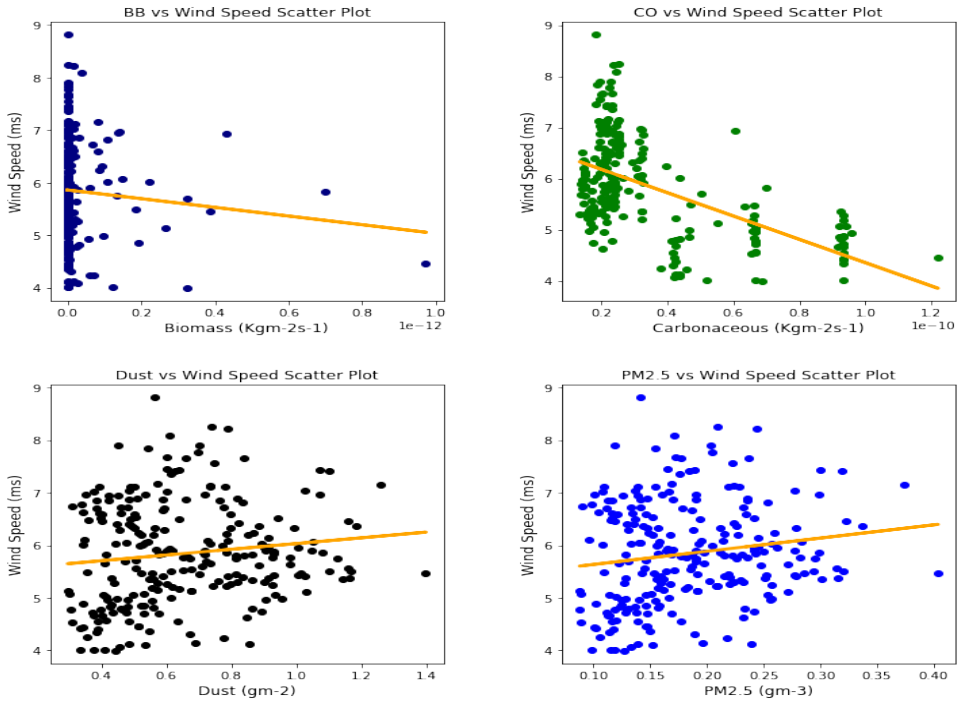

Figure 4.31: Correlation graphs of wind speed and aerosol types over Agoufou

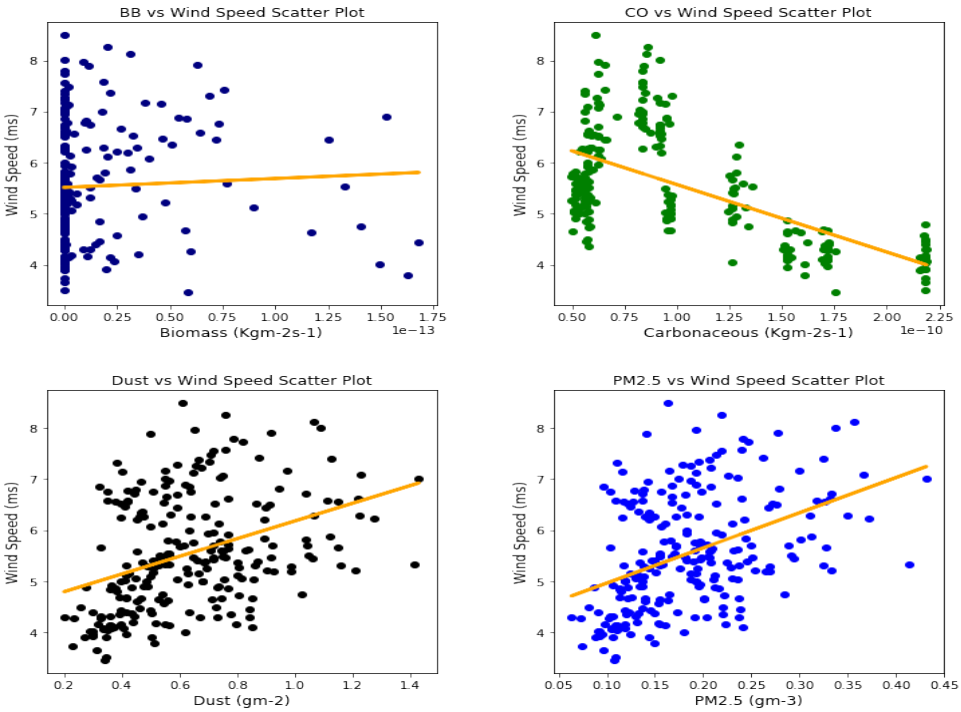

Figure 4.32: Correlation graphs of wind speed and aerosol types over Banizoumbou

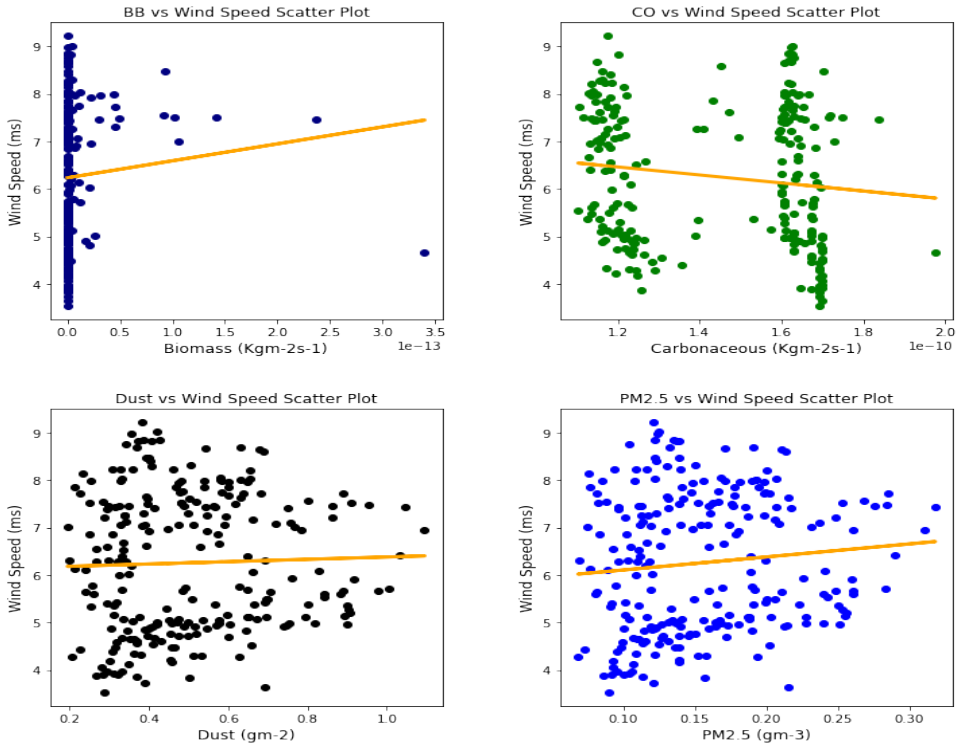

Figure 4.33: Correlation graphs of wind speed and aerosol types over Dakar

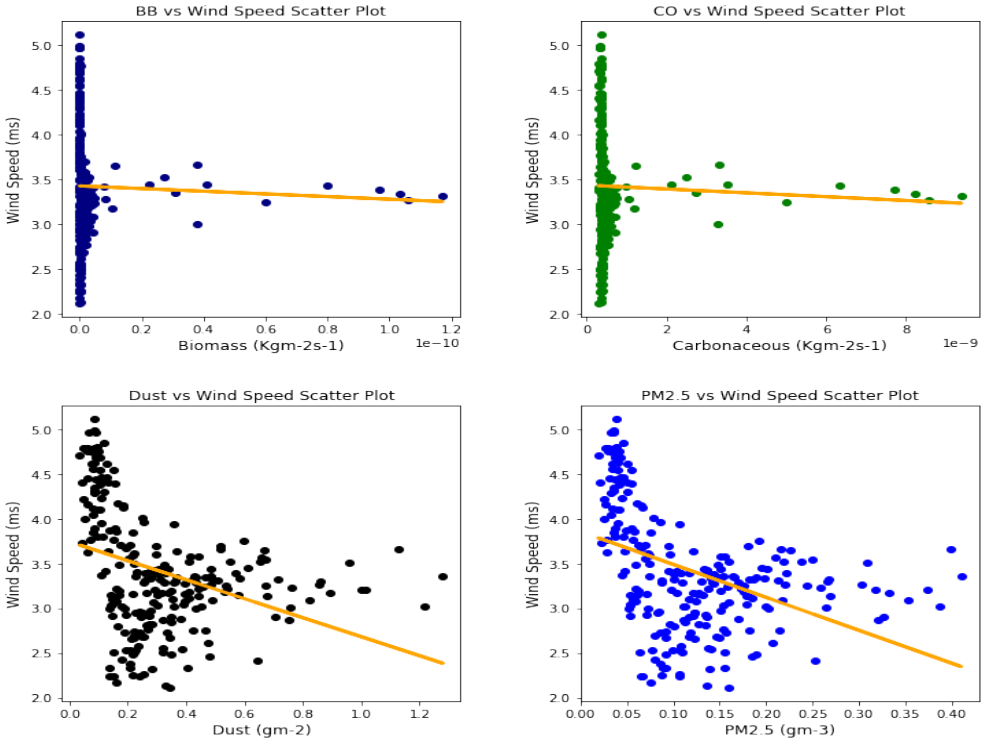

Figure 4.34: Correlation graphs of wind speed and aerosol types over Freetown

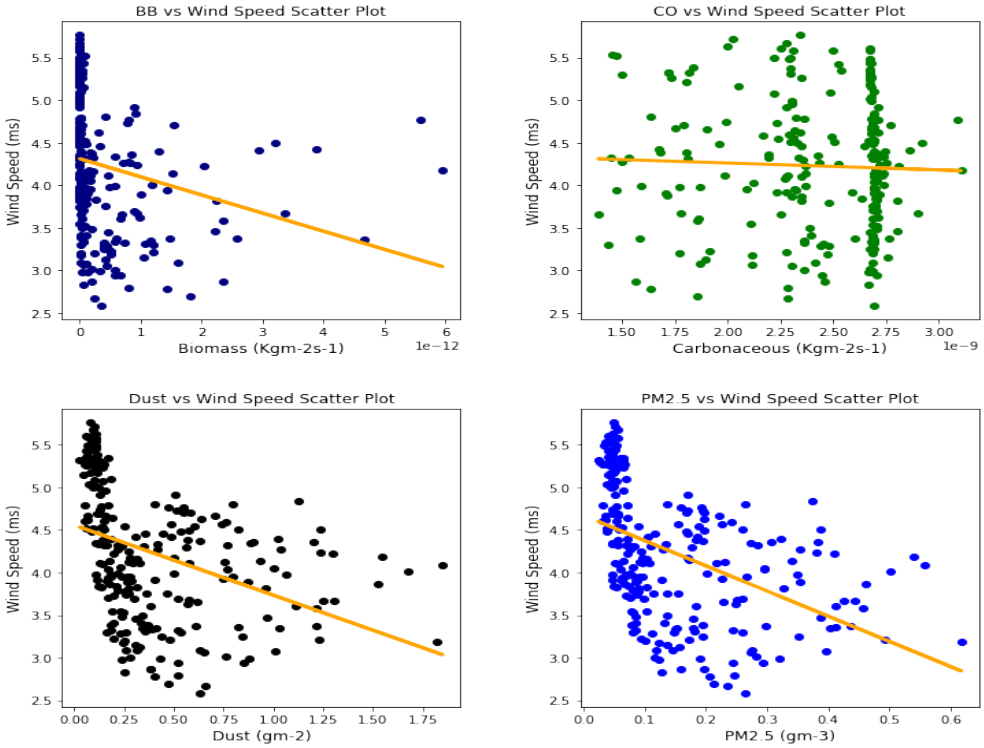

Figure 4.35: Correlation graphs of wind speed and aerosol types over Ikeja

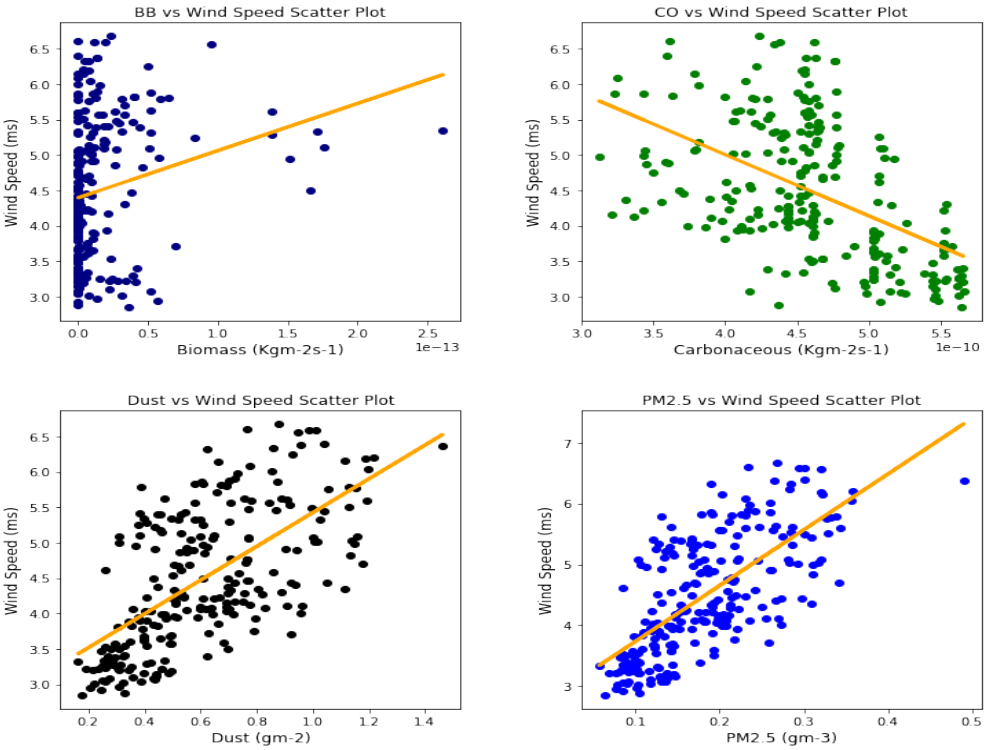

Figure 4.36: Correlation graphs of wind speed and aerosol types over Kano

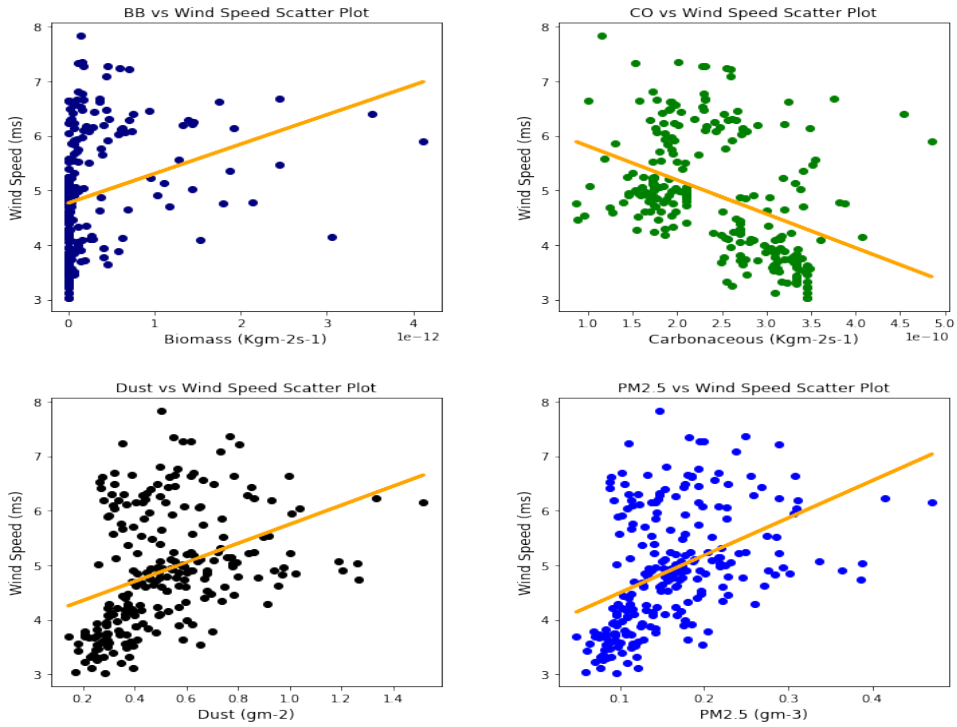

Figure 4.37: Correlation graphs of wind speed and aerosol types over Ouagadougou

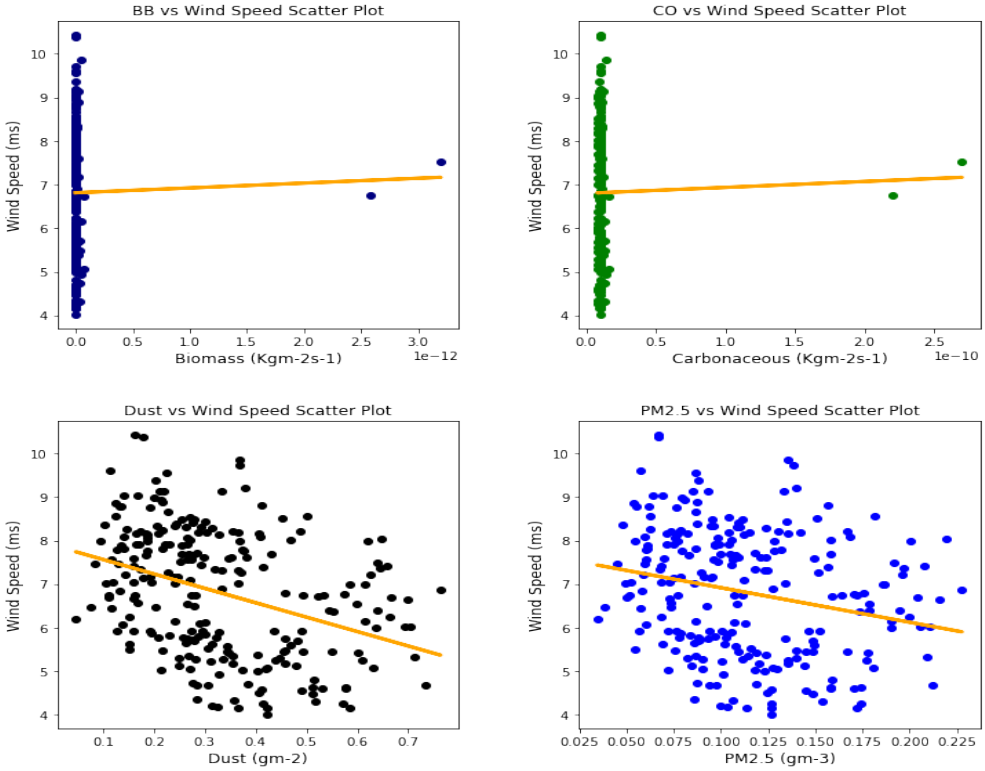

Figure 4.38: Correlation graphs of wind speed and aerosol types over Praia

S/N	Stations	Biomass Burning (BB)			Carbonaceous (CO)			Dust (Du)			Particulate Matters ($PM_{2.5}$)		
		R	***p-value***	**Status**	**R**	***p-value***	**Status**	**R**	***p-value***	**Status**	**R**	***p-value***	**Status**
1.	Abidjan	-0.12	*0.07*	Accepted	-0.25	*0.00*	**Rejected**	-0.48	*4.82e-15*	**Rejected**	-0.53	*1.95e-18*	**Rejected**
2.	Accra	-0.30	*1.72e-06*	**Rejected**	-0.34	*7.55e-08*	**Rejected**	-0.32	*2.87e-07*	**Rejected**	-0.38	*1.74e-09*	**Rejected**
3.	Agoufou	-0.08	*0.21*	Accepted	-0.56	*7.45e-21*	**Rejected**	0.13	*0.05*	**Rejected**	0.16	*0.02*	**Rejected**
4.	Banizoumbou	0.05	*0.47*	Accepted	-0.62	*1.04e-26*	**Rejected**	0.38	*1.05e-09*	**Rejected**	0.43	*5.17e-12*	**Rejected**
5.	Dakar	0.08	*0.24*	Accepted	-0.13	*0.04*	**Rejected**	0.03	*0.61*	Accepted	0.10	*0.12*	Accepted
6.	Freetown	-0.03	*0.60*	Accepted	-0.04	*0.56*	Accepted	-0.34	4.44e-08	**Rejected**	-0.43	*5.68e-12*	**Rejected**
7.	Ikeja	-0.23	*0.00*	**Rejected**	-0.04	*0.55*	Accepted	-0.38	*7.22e-10*	**Rejected**	-0.46	3.81e-14	**Rejected**
8.	Kano	0.22	*0.00*	**Rejected**	-0.51	*3.98e-17*	**Rejected**	0.63	*2.05e-28*	**Rejected**	0.69	*4.74e-35*	**Rejected**
9.	Ouagadougou	0.29	*5.21e-06*	**Rejected**	-0.42	*1.15e-11*	**Rejected**	0.38	*1.11e-09*	**Rejected**	0.44	*1.17e-12*	**Rejected**
10.	Praia	0.02	*0.75*	Accepted	0.02	*0.75*	Accepted	-0.36	*5.88e-09*	**Rejected**	-0.23	*0.00*	**Rejected**

Table 4.2: Table showing the correlation (R) between wind speed and aerosols, with the corresponding *p-values* at $\alpha = 0.05$

Summary

Biomass Burning = 4 Rejected, 6 Accepted**;**

Carbonaceous = 7 Rejected, 3 Accepted**;**

Dust and $PM_{2.5}$ = 9 Rejected, 1 Accepted

The correlation values between aerosol types and wind speed (table 4.2) show strong and low relationships across the aerosol types and also location dependence. It can be deduced that the stronger the wind speed, the less the presence of these aerosol types. This is so because the wind is responsible for the dispersion of aerosols in the atmosphere. The aerosol can be said to have been transported from one location to another, thus resulting in a low and sometimes negative relationship. This is in support of the Danjuma *et al.*, (2020) study which showed the transportation of aerosol from central Africa to West Africa over maritime. Dust and $PM_{2.5}$ showed a strong relationship with wind speed over Kano with correlation values of 0.63 and 0.69 respectively. But it was a moderate relationship between $PM_{2.5}$ and wind speed over Abidjan. For the correlation between wind speed and carbonaceous, Banizoumbou recorded a strong correlation value of -0.62, while Kano and Agoufou recorded a moderate correlation of -0.51 and -0.56 respectively. The same cannot be said for the relationship of biomass burning with wind speed which showed low correlation values over all the locations for this study. The *p-value* also corroborated the statistical significance of the result of the correlation values. As regards biomass burning and wind speed, Accra, Ikeja, Kano, and Ouagadougou are the only locations that showed the relationship between the two aforementioned variables are statistically significant. The null hypothesis (H_o) is accepted for the other six (6) locations under the biomass burning correlation with wind speed, which showed no statistically significant relationship between the variables as evident in their p-values which are greater than the significant value of 0.05. For the carbonaceous, the null hypothesis was accepted in Freetown, Ikeja, and Praia, thus translating that there is no statistical significance in the relationship between wind speed and carbonaceous. Only Dakar showed no statistically significant relationship between wind speed and the other two variables (Dust and $PM_{2.5}$). Hence, 90% of the locations showed that there exists statistical

significance in the relationship between dust and wind speed. The dust results are in support of studies by Knippertz (2008) and Schepanski *et al.* (2009) in which strong wind from line squalls can trigger dust mobilization.

4.5.3 Water Vapor Correlated with Aerosols

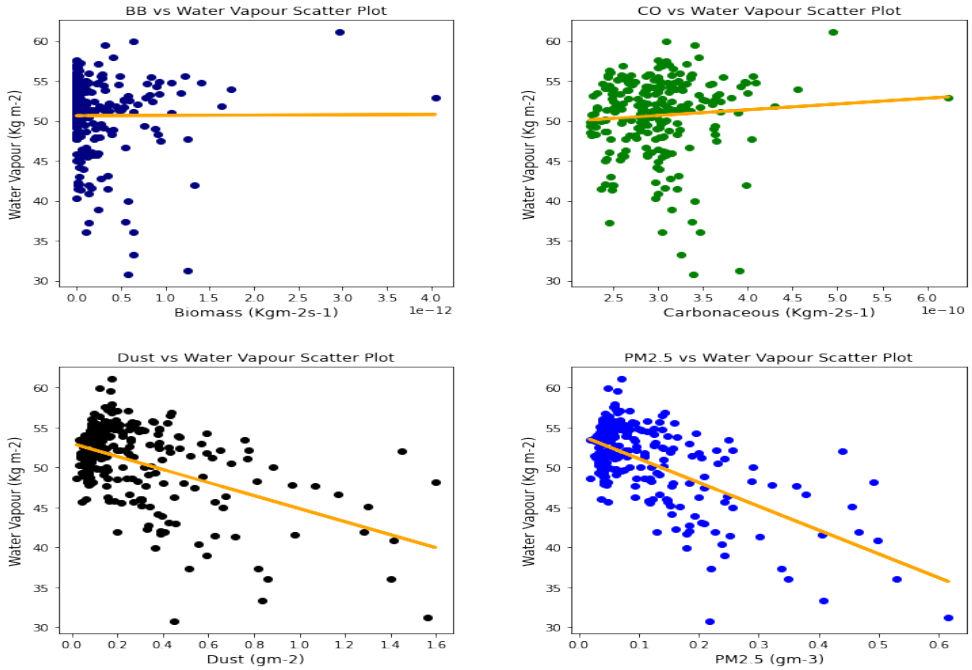

Figure 4.39: Correlation graphs of water vapor and aerosol types over Abidjan

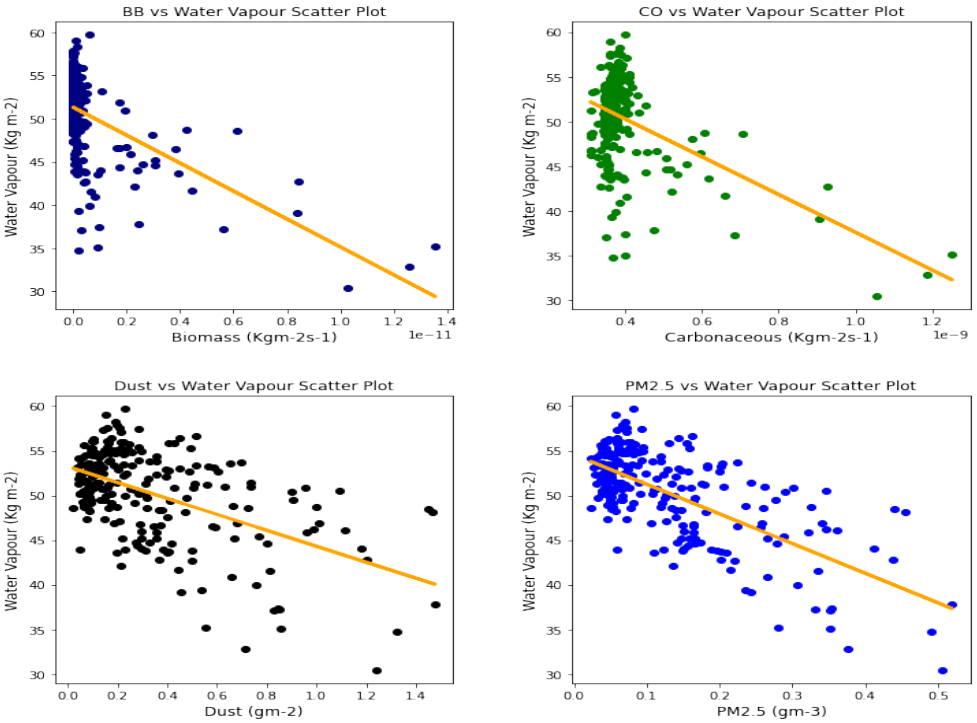

Figure 4.40: Correlation graphs of water vapor and aerosol types over Accra

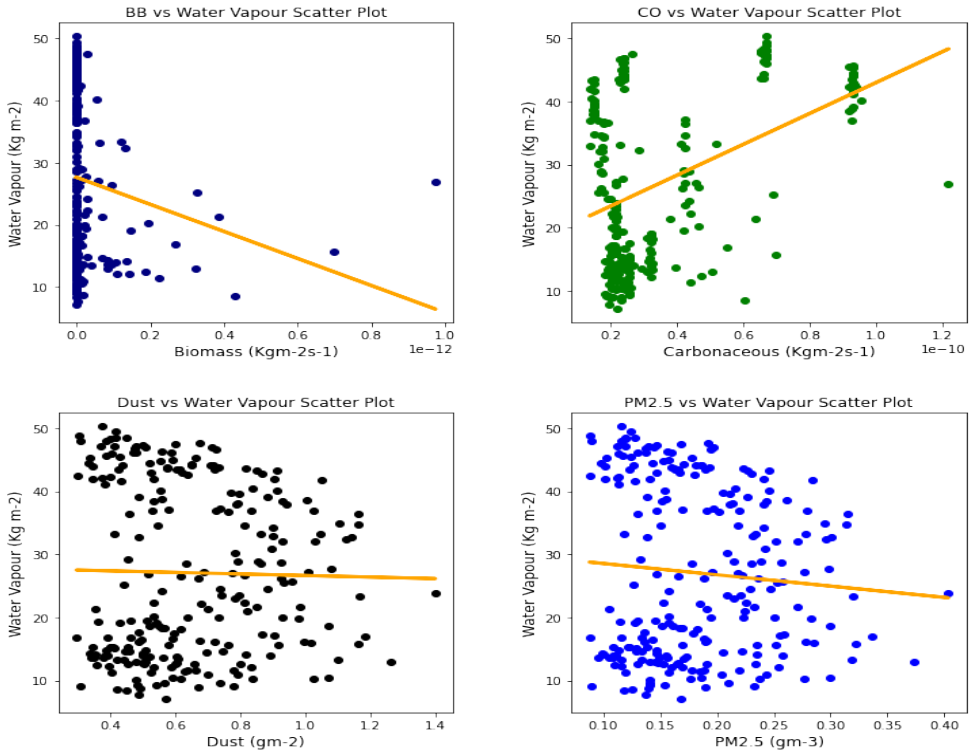

Figure 4.41: Correlation graphs of water vapor and aerosol types over Agoufou

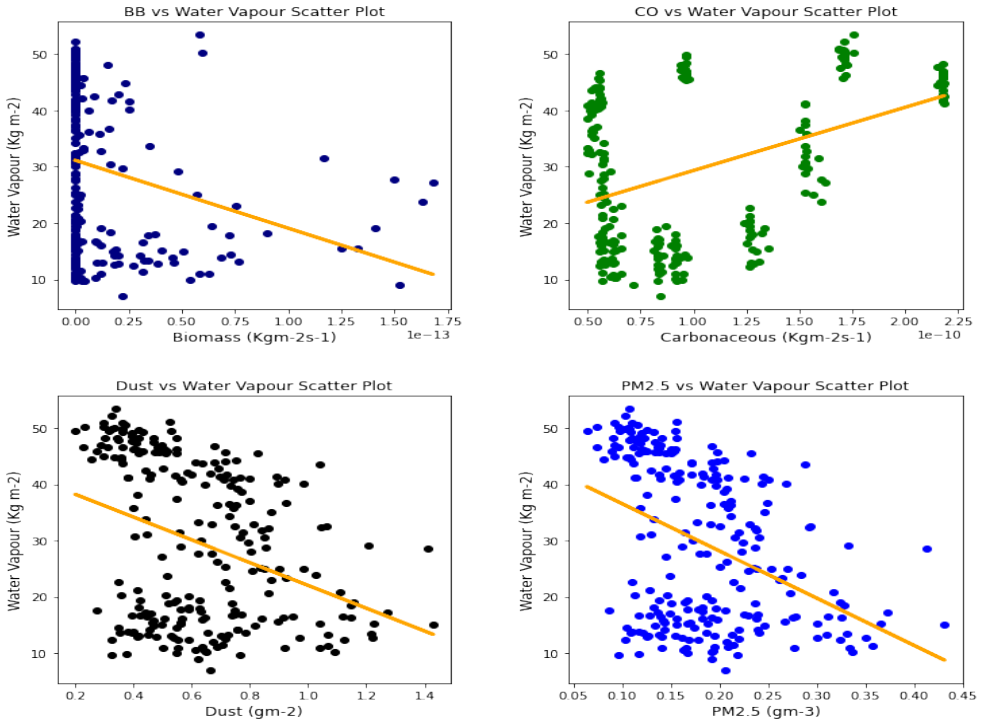

Figure 4.42: Correlation graphs of water vapor and aerosol types over Banizoumbou

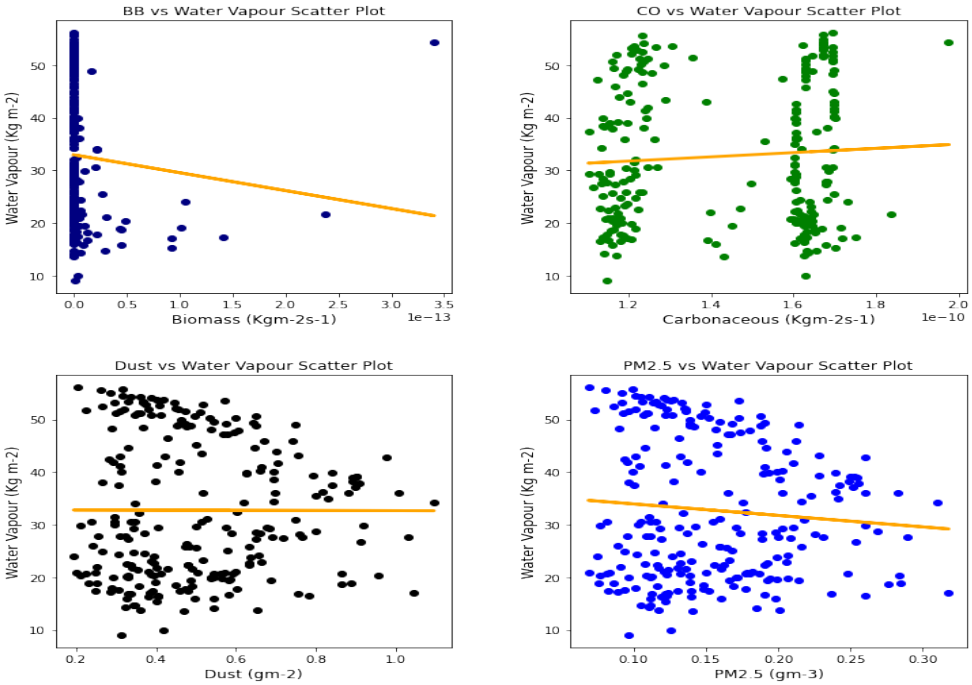

Figure 4.43: Correlation graphs of water vapor and aerosol types over Dakar

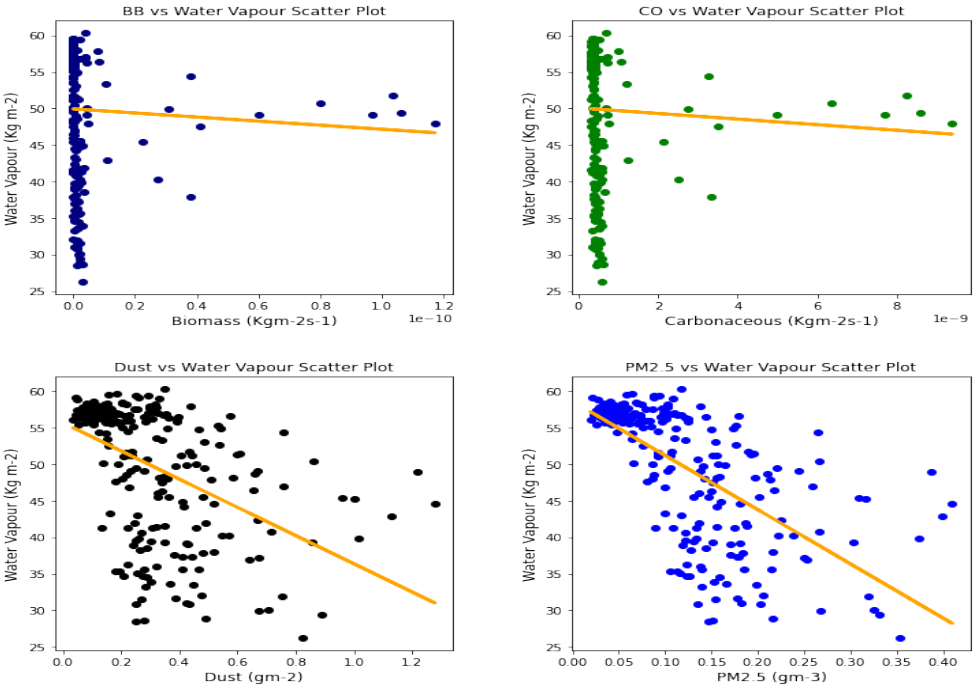

Figure 4.44: Correlation graphs of water vapor and aerosol types over Freetown

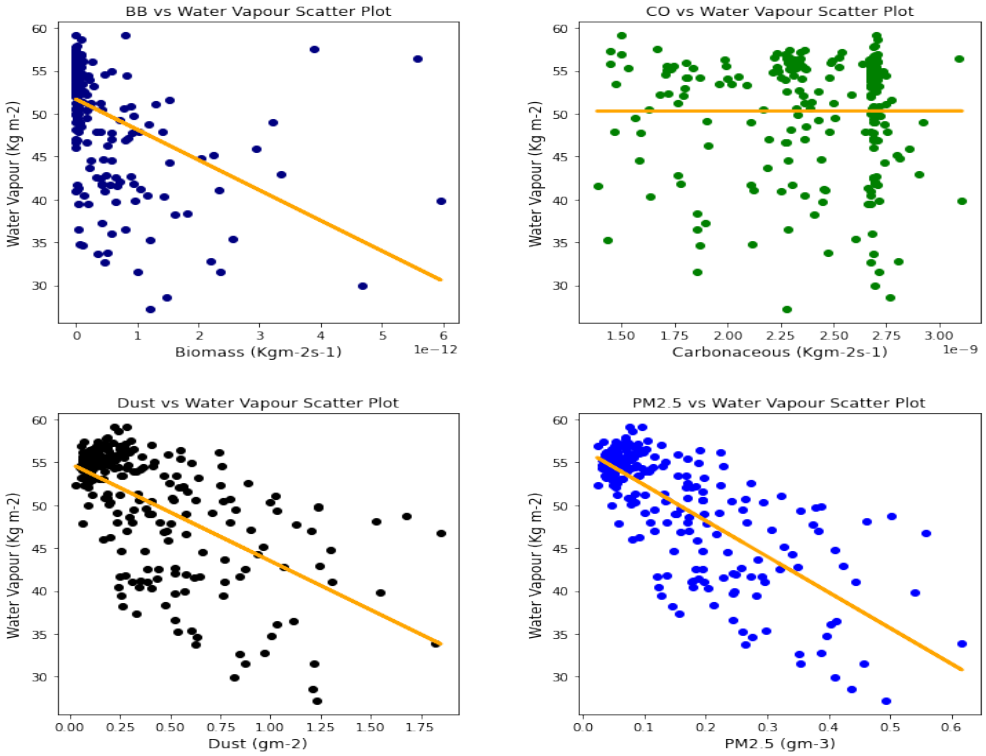

Figure 4.45: Correlation graphs of water vapor and aerosol types over Ikeja

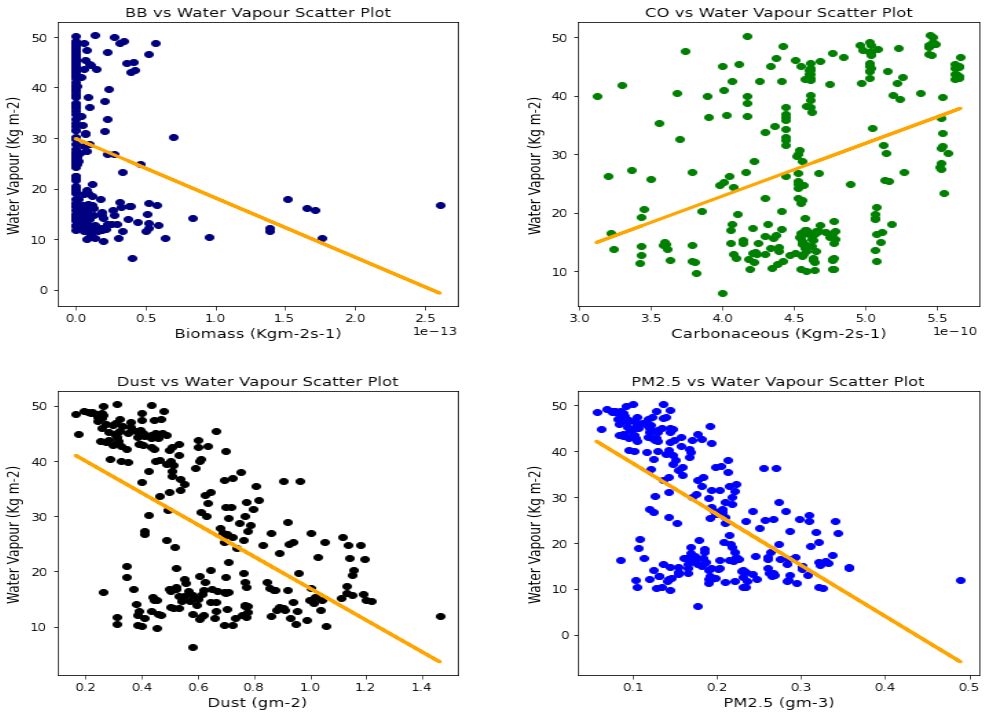

Figure 4.46: Correlation graphs of water vapor and aerosol types over Kano

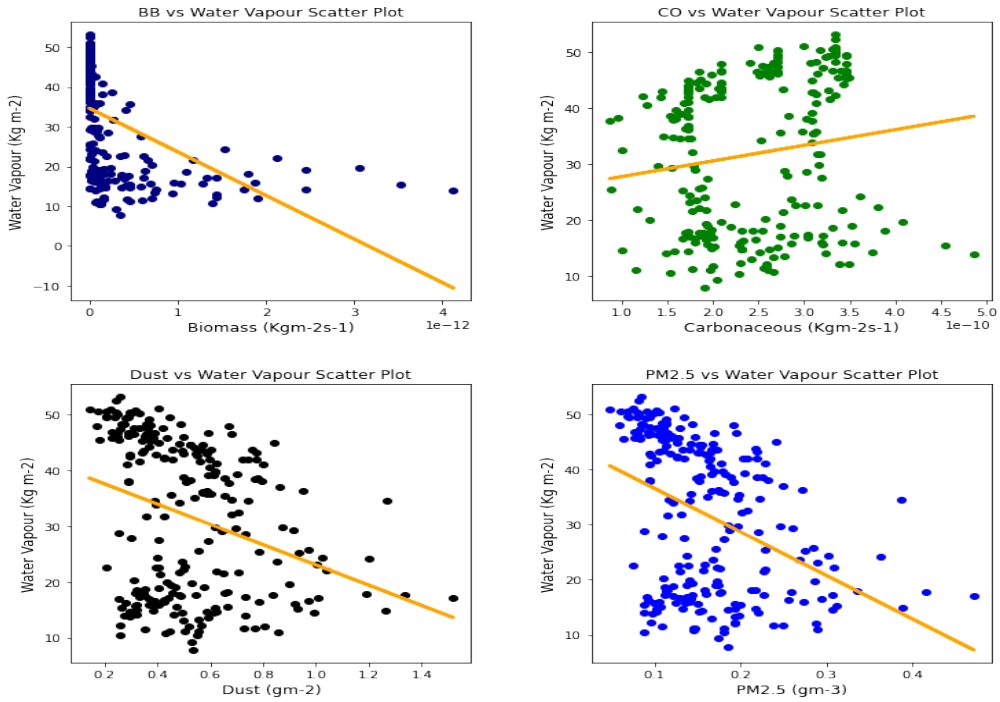

Figure 4.47: Correlation graphs of water vapor and aerosol types over Ouagadougou

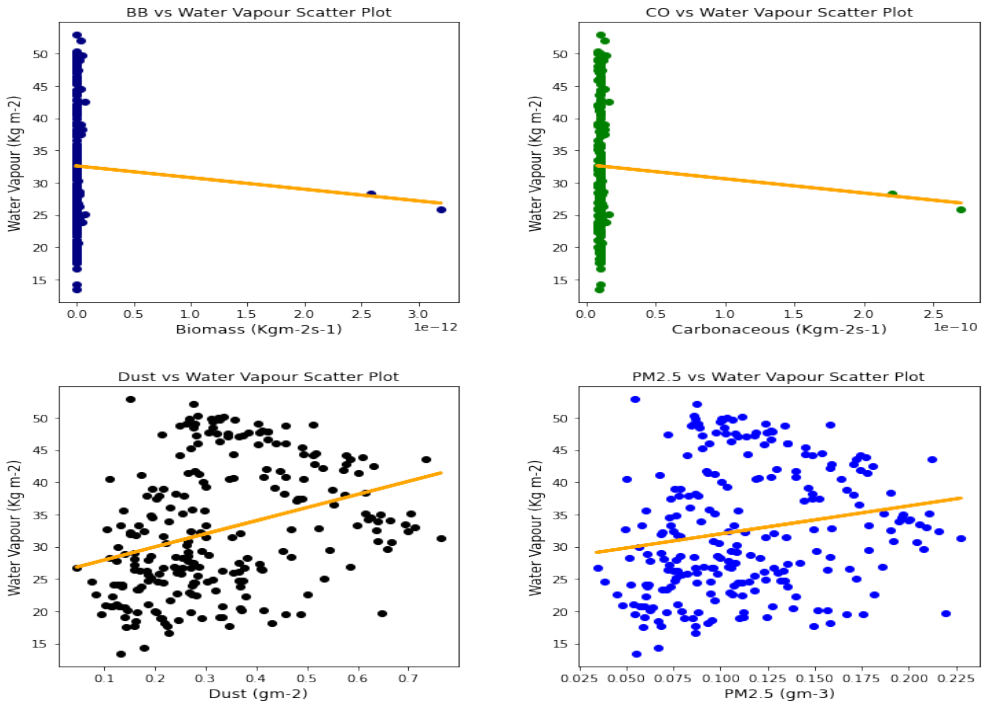

Figure 4.48: Correlation graphs of water vapor and aerosol types over Praia

S/N	Stations	Biomass Burning (BB)			Carbonaceous (CO)			Dust (Du)			Particulate Matters ($PM_{2.5}$)		
		R	***p-value***	**Status**	**R**	***p-value***	**Status**	**R**	***p-value***	**Status**	**R**	***p-value***	**Status**
1.	Abidjan	0.00	*0.96*	Accepted	0.07	*0.25*	Accepted	-0.48	*1.73e-15*	**Rejected**	-0.62	*6.91e-27*	**Rejected**
2.	Accra	-0.56	*1.56e-21*	**Rejected**	-0.48	*1.59e-15*	**Rejected**	-0.53	*4.94e-19*	**Rejected**	-0.69	*1.03e-34*	**Rejected**
3.	Agoufou	-0.16	*0.02*	**Rejected**	0.43	*2.22e-12*	**Rejected**	-0.02	*0.75*	Accepted	-0.08	0.21	Accepted
4.	Banizoumbou	-0.26	*5.23e-05*	**Rejected**	0.41	*2.20e-11*	**Rejected**	-0.35	*2.28e-08*	**Rejected**	-0.41	*4.12e-11*	**Rejected**
5.	Dakar	-0.08	*0.21*	Accepted	0.07	*0.28*	Accepted	0.00	*0.97*	Accepted	-0.09	*0.17*	Accepted
6.	Freetown	-0.05	*0.45*	Accepted	-0.05	*0.43*	Accepted	-0.48	2.25e-15	**Rejected**	-0.66	*1.97e-31*	**Rejected**
7.	Ikeja	-0.44	*1.32e-12*	**Rejected**	0.00	*0.99*	Accepted	-0.60	*4.84e-25*	**Rejected**	-0.74	7.39e-43	**Rejected**
8.	Kano	-0.28	*7.90e-06*	**Rejected**	0.39	*6.45e-10*	**Rejected**	-0.56	*7.48e-21*	**Rejected**	-0.61	*2.36e-25*	**Rejected**
9.	Ouagadougou	-0.49	*1.76e-14*	**Rejected**	0.15	*0.02*	**Rejected**	-0.32	*6.29e-07*	**Rejected**	-0.40	*9.63e-11*	**Rejected**
10.	Praia	-0.05	*0.46*	Accepted	-0.05	*0.46*	Accepted	0.33	*2.15e-07*	**Rejected**	0.12	*0.00*	**Rejected**

Table 4.3: Table showing the correlation (R) between water vapor and aerosols, with the corresponding *p-values* at $\alpha = 0.05$

Summary

Biomass Burning = 6 Rejected, 4 Accepted**;**

Carbonaceous = 5 Rejected, 5 Accepted**;**

Dust and $PM_{2.5}$ = 8 Rejected, 2 Accepted

The relationship between the aerosol types and water vapor as seen in Table 4.3 showed that $PM_{2.5}$ had strong correlation values with water vapor in five locations namely: Abidjan, Accra, Freetown, Ikeja, and Kano; while Banzioumbou and Ouagadougou recorded moderate correlation values of -0.41 and -0.40 respectively. But Agoufou and Praia recorded low correlation values between water vapor and $PM_{2.5}$. In summary, all the rainforest-categorized stations of Accra, Ikeja, and Freetown recorded correlation values of -0.69, -0.66, and -0.71 respectively. Kano was the only station with a strong correlation value of -0.61 among the savannah stations. Dust occurrence and water vapor correlation showed Kano, Ikeja, and Accra recording strong but negative relationships. There was low and moderate correlation existence between carbonaceous and water vapor for all stations under study. But only Accra had a moderate correlation between water vapor and biomass burning with a value of -0.56. It is important to state that all values between water vapor and three aerosol types (biomass burning, dust, and $PM_{2.5}$) were negatively correlated. Under carbonaceous, only Accra, Freetown, and Praia recorded negative correlation values of -0.48, -0.05, and -0.05 respectively. The p-value showed that there exists a relationship between all the aerosol types and water vapor except in Freetown (for Biomass burning and carbonaceous) and Ikeja (for carbonaceous only). The outcome also suggests that all savannah locations (Banizoumbou, Kano, and Ouagadougou) showed that there is statistical significance in the existing relationship between water vapor and all pollutants.

4.6 Simulation from the COSMO-MUSCAT coupling model

This section is to validate the coupling model of COSMO-MUSCAT on two (2) distinct activities of West Africa seasons: dry and wet seasons. Some selected episodes were used to validate the model. The two (2) selected events were: (i) dust and smoke episodes of 24th – 27th December 2015 over West Africa, having a dust layer that extended from the ground to 200m, and smoke layer; and (ii) the convective precipitation of 30th August – 2nd September 2009 over Ouagadougou and Mali. The simulated results of these events were validated with observation/satellite data from Giovanni and EUMETSAT Imagery Gallery Animations (https://eumetview.eumetsat.int/) of the said dates. Literature on previous works done on the same date of the event was also considered in validating the result.

The simulation started on the 21st of December as seen in the figure above. The model output was on a 48-hours result. In analyzing this result, the cooler and hotter hours of each day (represented with Day 1, Morning and Day 1, Afternoon respectively) at the surface and upper level were considered. The choice of the hours of the day was in consideration of the atmospheric dynamics the emphasis on radiation and turbulence (i.e. mixing of air from the earth's surface to the atmosphere) was considered (Holtslag, 2003).

4.6.1 Dust episode of 21st – 30th December 2015 at the surface, Upper level, and Average of all the layers/levels.

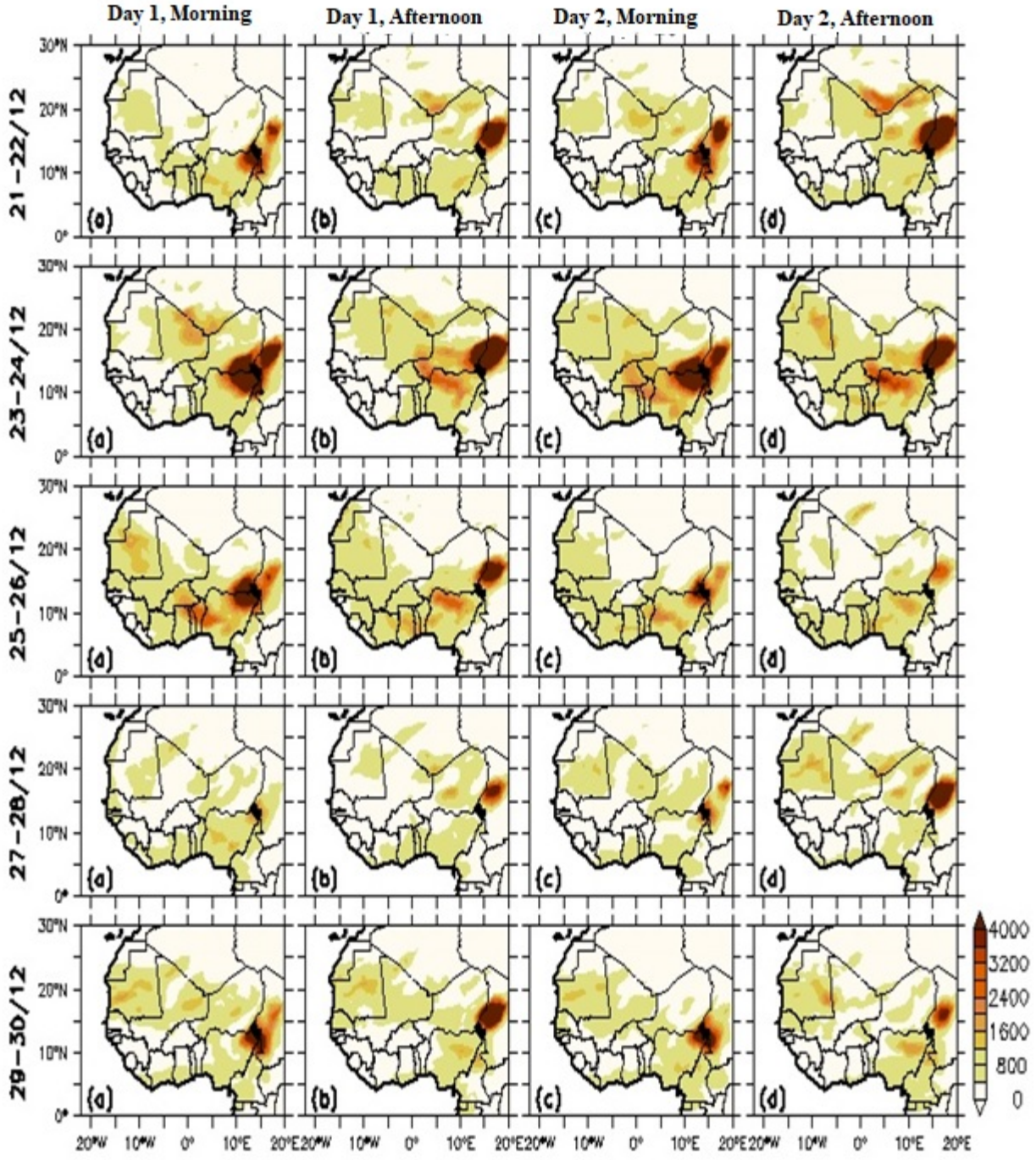

Figure 4.49: Surface analysis of dust episode of 21st – 30th December 2015 over West Africa.

The result as shown in figure (4.49) showed four (4) panels per row for analyzed results from 21st – 30th December 2009 for the surface. The rows showed results for two (2) days (48-hour output), with consideration of the cooler and hotter period of each day at the surface only. The result showed the development of the dust systems in two separated but close locations which are Bodélé depression and Chad basin areas on the 21st and 22nd of December 2015 of "Day 1, Morning & Day 2, Morning. But the dust system seems to have been clustered together during the afternoon hours of each day as seen in the same date. Despite these changes in the dust development, the observed situations could still be seen around the *spot system;* thus regarded as the hot spots or epicenter of the dust region. That is, there was no evidence of transportation of the systems to other parts of the West African region. This is more of a system developing around a source region without any available atmospheric propagating variable. The dust system became bigger in panel d, which corresponds to the afternoon hour of the 22nd of December. The activities became more noticeable as the dust started propagating toward other parts of the West African region. The aftermath of the event was still noticeable between the morning hours of 25th – 26th December, while it died off in the evening hours of 26th December. From the afternoon of the 26th to the morning of the 28th, the system was completely unavailable, but a second dust system seems to pick up in the afternoon of the 28th of December through the 30th of December, but it was not in consideration in this work.

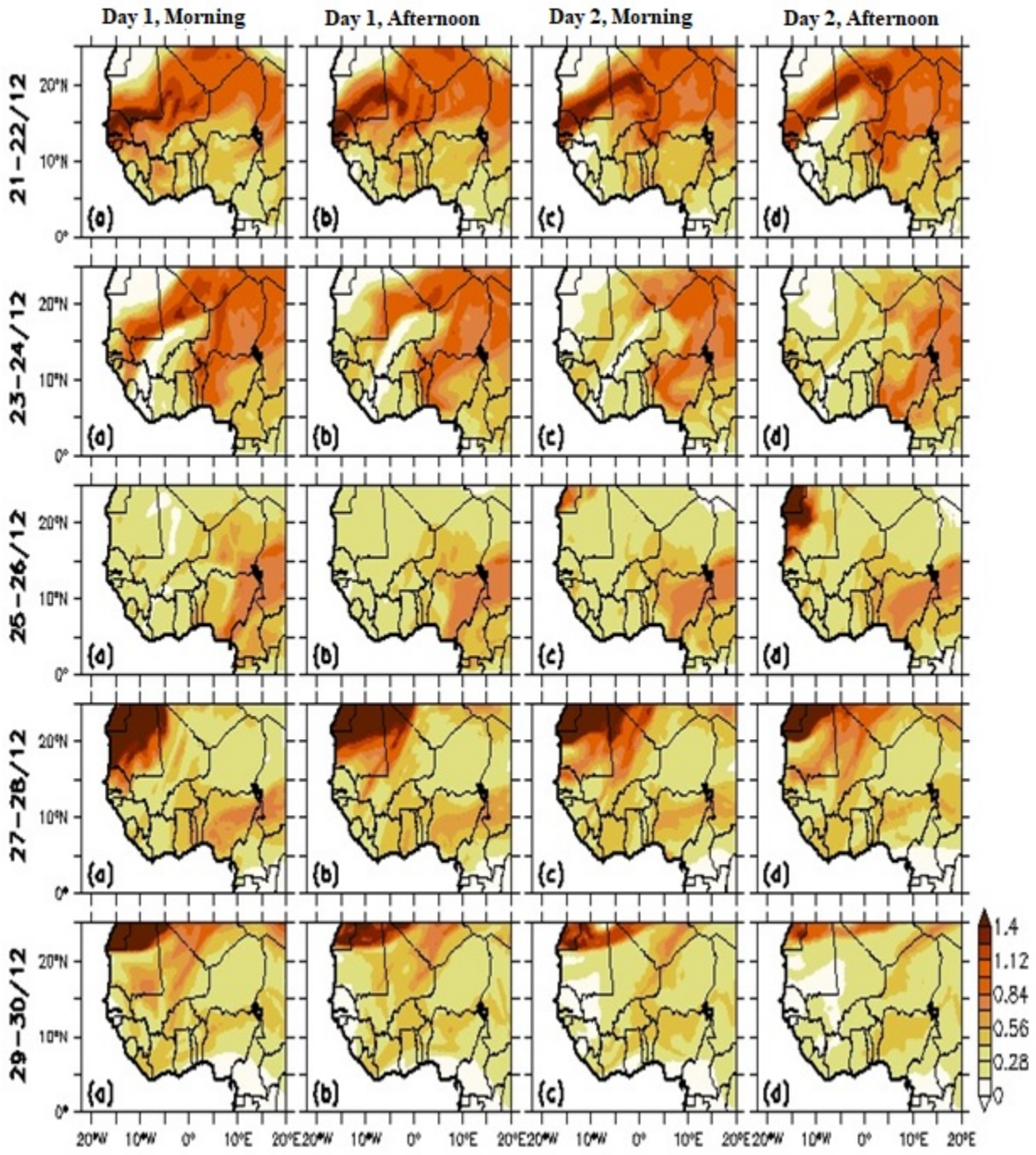

Figure 4.50: Upper-level analysis of dust episode of 21st – 30th December 2015 over West Africa

Figure (4.50) above showed the output or result of the modeled system at the upper level. Though, the dust around the surface has its health implications, dust at the upper level helps in cloud condensation nuclei (CCN) processes. The core of the dust is seen over Mauritania, Senegal, and The Gambia on the 21st of December, while the 22nd of December showed an extension of the particle north of Mali. The coastal axes were under the influence of light particles across the two (2) days when compared to the inland section. The development of the core dust particles at the upper level covered only three (3) countries namely: The Gambia, Senegal, and Mauritania; in the morning hours. But there was an extension of the systems into the north-western part of Mali in the afternoon hours. While the dust system was later transported from the north-western part of Mali further inland in an eastward direction during the morning hours of the 26th of December, the afternoon hours showed that the system has further moved into the southern part of Algeria. But the atmosphere seems to be clear of any particles around Guinea and Senegal and some parts of Mauritania during the morning hours, while the afternoon hours showed the clear parts gaining further space into Mali in addition to the parts covered in the morning hours. The 23rd day of December showed the thickness of dust being transported into the northwestern part of Nigeria, covering the whole of Burkina Faso, and the northwestern parts of the Niger Republic. The thick part of the dust has been dispersed or transported, thus leaving an almost clear atmosphere over Senegal, Gambia, Guinea, and Mauritania axes but the thick dust still occupied the northern part of Mali. The whole of Nigeria became occupied with dust in the morning hours of 24th December, leading to the clearance of the thick dust completely from Mali but still with the presence of only the light dust. The thick dust seems to be under the influence of westerlies. The afternoon hours of the same day showed light dust occupying most parts of the region. The thick dust has propagated eastwards. The light dust-laden atmosphere continues its existence over most parts of Western

Africa from 25th to 26th December, except Nigeria which has thick dust. Also, there seems to exist a new thick dust system developing over the northern axis of Mauritania in the afternoon period of the 26th day of December. The development of the dust system continues from the morning of the 27th day but started dying off in the afternoon hours of the 28th of December. As the continued clearing of the atmosphere from the dust continues, the south-south parts of Nigeria and the axes of The Gambia, Senegal, Mauritania, and Guinea are devoid of any presence of dust between the morning hour of the 29th and afternoon hour of the 30th day of December.

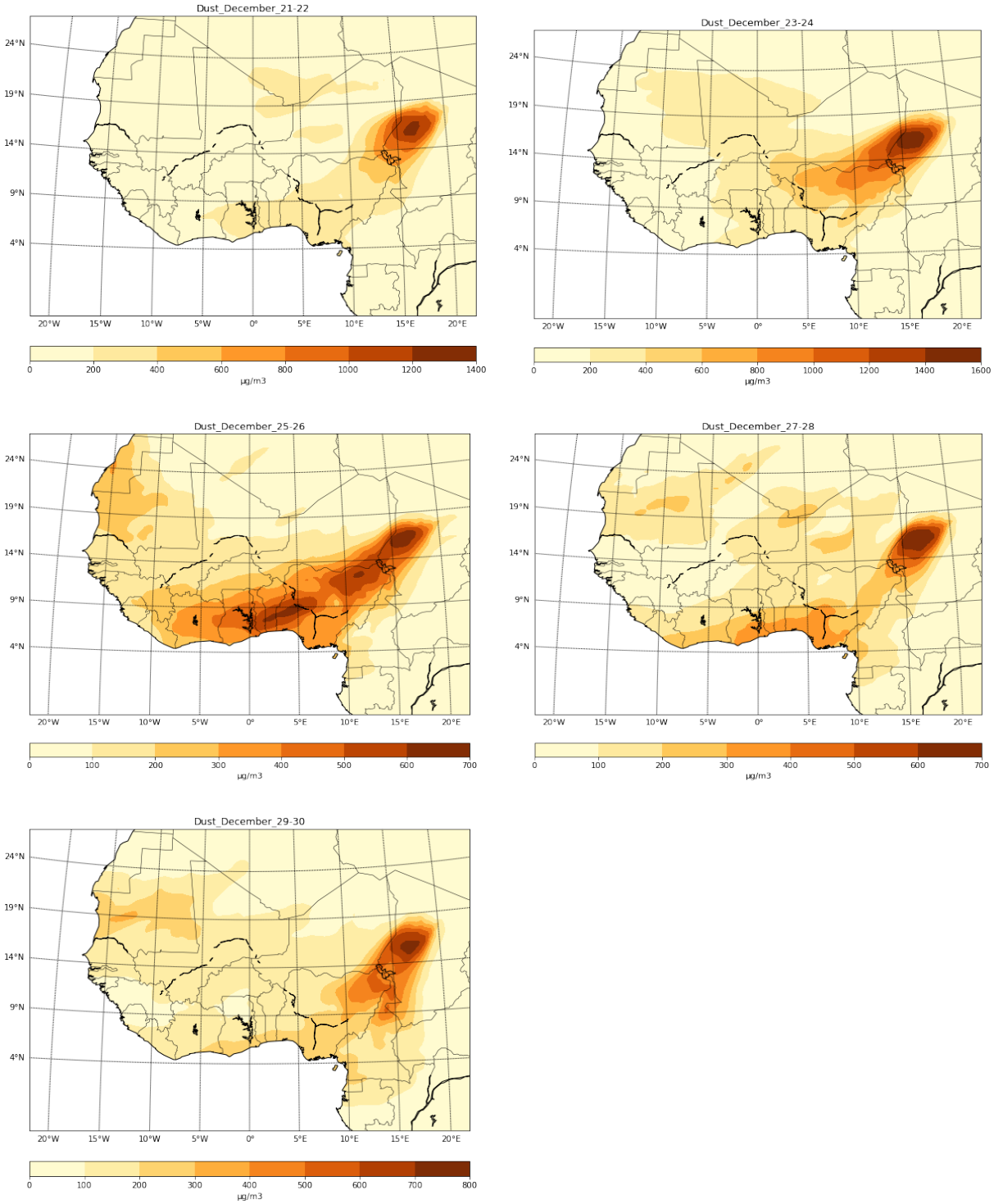

Figure 4.51: Averaged levels/layers of dust episode of 21st – 30th December 2015 over West Africa.

Figure 4.51 above is the average of all pressure levels of the simulated output. Each figure was over 48 hours (2 days). The result from the figure for the 21st and 22nd of December showed the initial development of the dust over the well-known Bode depression region (Herrmann *et al.*, 1999). The thickness of the dust was at the epicenter of the source region, spreading out down south towards the coastal areas. The thickness of the dust extended from the source region to the axis of Lake Chad. There were also some fragments of light dust over Nigeria, and some parts of Niger, Mali, and south of Algeria. The thickness of the dust continues to propagate down south from the epicenter, covering the Sahel and Sudano region of Nigeria on the 23rd and 24th of December. The light dust has extended and covered Benin, Togo, Ghana, Burkina Faso, Mali, and Mauritania. The 25th and 26th December figures showed the total propagation of the thick dust to the coastal areas of the West African region. This also led to complete coverage of some areas (Nigeria, Benin, Togo, and Ghana) with thick dust. This shows that the main long-range transport paths of dust are westward towards the North Atlantic to South or North America (Middleton and Goudie, 2001). The implications of this scenario mean the atmosphere can lead to serious air pollution-health-related issues, such as silicosis which is suspected to be playing a role in the spread of meningitis during the dry season in northern Africa (Morman and Plumlee, 2014), due to the exposure to high dust concentrations, especially during dust storms (Kelishadi and Poursafa, 2010; Manucci and Franchini, 2017). Other parts of the West African region were under light dust. The 27th and 28th December results showed the sparse distribution of the light dust over some areas of the region while the thick dust was clear over the northern part of Nigeria. The coastal axes of Nigeria, Benin, Togo, and Ghana still showed evidence of the presence of thick dust. The presence of this aerosol around the coast is a confirmation of the existing literature which attributed water bodies as a good retention of dust, as it brings nutrients to the ocean and increases phytoplankton growth (Levitus *et*

al., 2000; Shinn *et al.*, 2000), which serves as food to juvenile fish. The thicker dust can be spotted around the source region. The 29th - 30th December figure showed the presence of dust around the Chad basin and the source region. Every other part is under the influence of light or no dust.

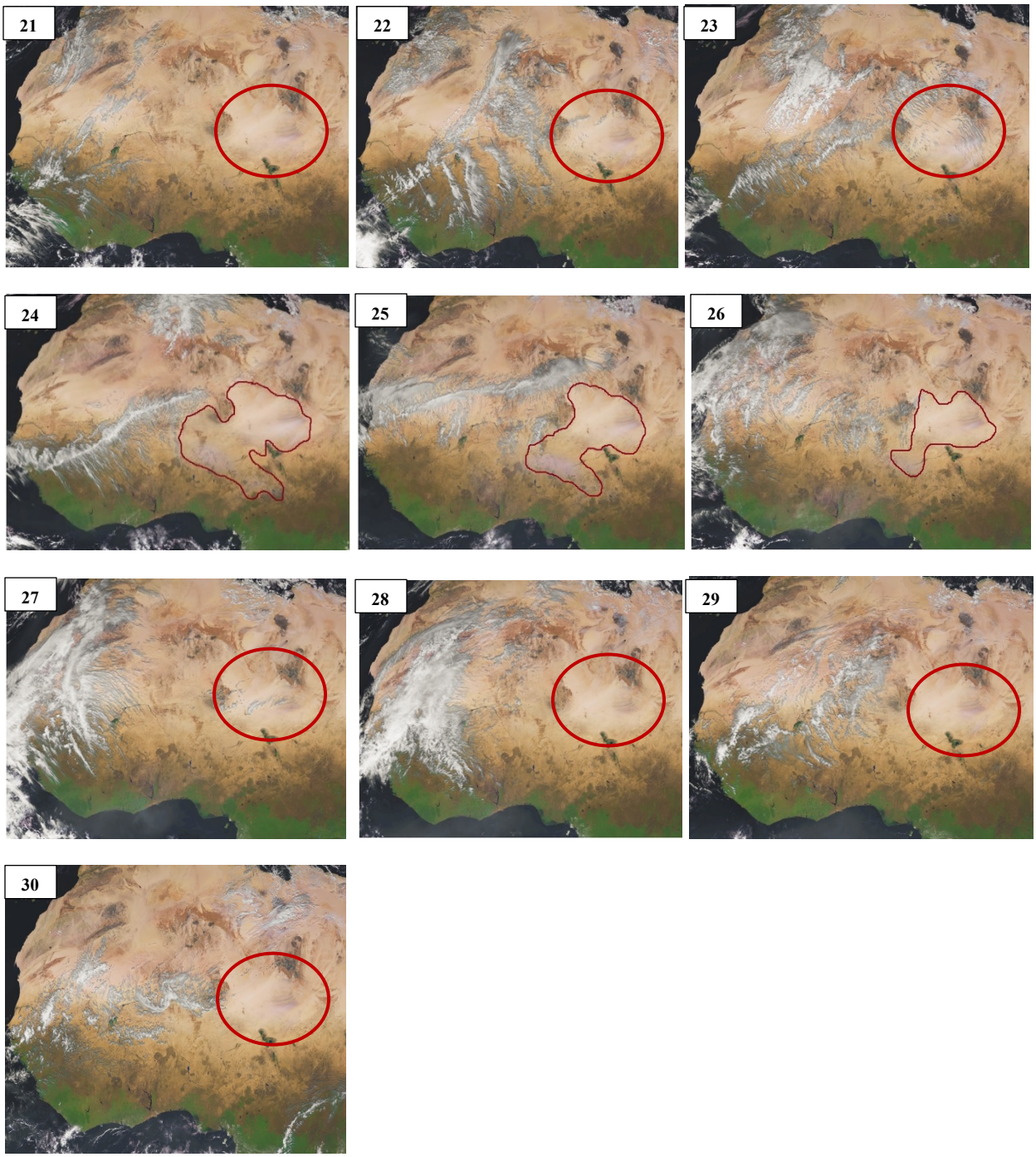

Figure 4.52: EUMETSAT images of 21st – 30th December 2015 over West Africa.

Figure 4.52 are images of dust and smoke days between the 21st and 30th of December 2015 from the European Organization for the Exploitation of Meteorological Satellites (EUMETSAT). The information from the images was for validation purposes of the COSMO-MUSCAT model output. It is imperative for such validation to be carried out since the model is been used for the first time in West Africa. As observed from Figure.52 and compared with the model output in Figure 4.51, it can be deduced that the first 3 days (21st, 22nd, and 23rd December 2015) showed evidence of dust mobilization around the Bodélé depression region. The dispersion of the dust from the point source became more pronounced from 24th – 26th December 2015. Another interesting finding from the two figures (4.51 and 4.52) showed the extreme western part of the region to Mali, Dakar and the Gulf of Guinea area did not experience the pollutant as pronounced over Nigeria. This can be attributed to an influx of moisture around those regions during these periods as seen in the EUMETSAT images. This precipitation during this dry month of the year (December) can be said to be extra-tropically induced. The moisture of the 24th day was seen flowing inland through Freetown, but the system had moved further north towards the boundary of Dakar and Mauritania. The 26th – 28th day recorded the largest amount of moisture influx, covering the whole Western axis of the Atlantic Ocean from the Gulf of Guinea axis of Freetown to the Canary axis of North Africa. Also, the dust seems to have cleared from the atmosphere of the rainforest zone, limiting the presence of the dust only over Bodélé depression.

4.6.2 Simulated Precipitation Output of 25th August – 5th September, 2009 over West Africa

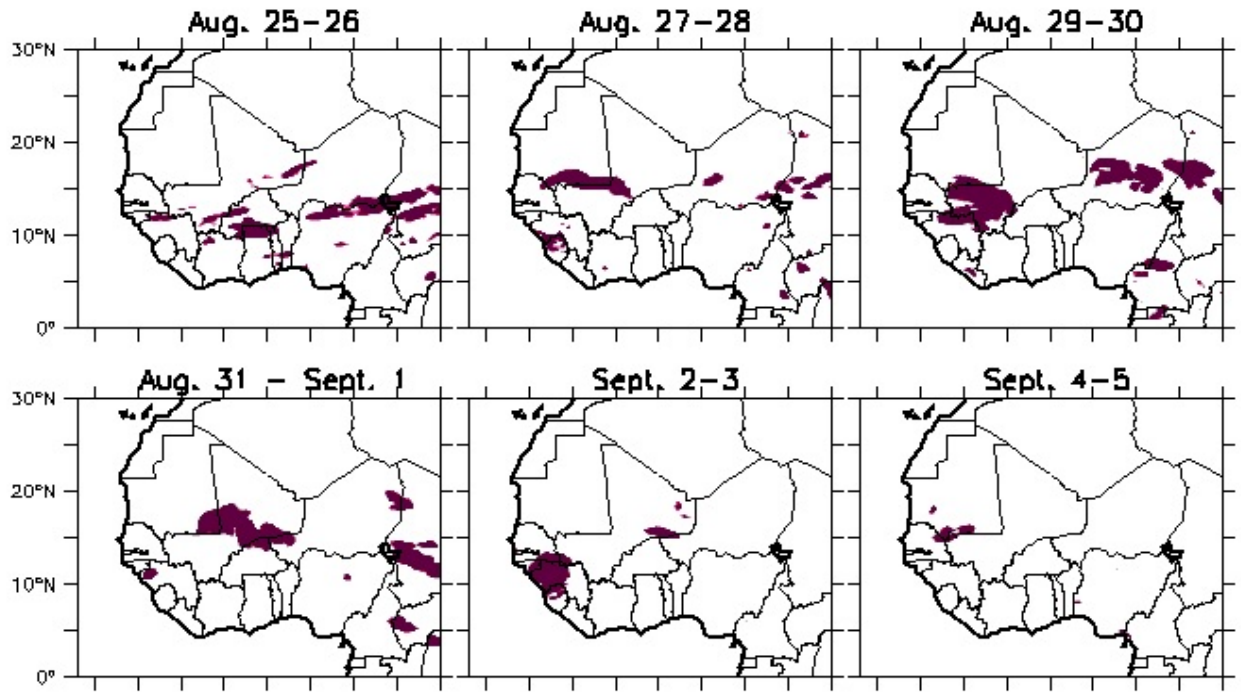

Figure 4.53: Non-Feedback precipitation episode of 25th August – 5th September 2009 over West Africa.

Upon analyzing the aerosol types in the atmosphere, herein referred to as the chemistry component of the model, the meteorology component was analyzed, that is, precipitation. Although, other meteorological variables such as wind components, relative humidity, temperature, etc. were some of the variables inputted in the simulation model. The heavy precipitation episode used for this simulation was within the period 25th August – 5th September 2009 but the event occurred between 30th August and 2nd September. The simulation was done for both feedback and non-feedback mechanism. Under the later condition or mechanism for the 25th and 26th of August, heavy precipitation was captured by the model around the boundary of Ghana and Burkina Faso. Other systems were seen developing in the Central African countries of Cameroun, Chad republic, and the Central African Republic; which confirms earlier affirmation that most convective systems over West Africa are easterlies, or simply say that they originated from the eastern part of the region. The northern part of Cote d'Ivoire and the western part of Burkina Faso also recorded some amount of heavy precipitation. Less activity of convective systems was recorded over the boundary of Burkina Faso and Ghana on the 27th - 28th of August as most of the heavy patches of precipitation (mature system) have fully dissipated, leaving evidence of developing systems across the region of West and Central Africa. Though, the boundary between Liberia and Sierra Leone showed significant activity in action. Mali and Mauritania also recorded patches of light precipitation. Going from the above explanation concerning the exact period of the precipitation activity, it can be confirmed from the figure the extent of heavy precipitations scattered over the West African region. These systems were observed significantly over Mali, Niger Republic, Cameroun, and Chad Republic. The two (2) systems over southern Mali were the strongest in terms of the space occupied; followed by the system over the Niger Republic. In all of these events, areas south of 10^{o}N are devoid of any system (Riehl, 1954; Thompson, 1965; Garnier, 1971; Oluleye and

Okogbue, 2013; Ochei *et al.*, 2015). This is in support of (Ireland, 1962; Adefolalu, 1972; Adekoya, 1979; Omotosho, 1988; Eludoyin, 2009) studies which attributed the period to little dry seas (LDS) or otherwise known as August break, as a result of the northernmost position of the Inter-Tropical Discontinuity (ITD) at 22^{o}N (Ilesanmi, 1971; Omotosho, 1985). Thus, limiting the strong activities of convective systems to areas north of 10^{o}N. It should also be noted that the limitation of the strong systems in such a position is that most systems occur about 1.5km south of the ITD (Adefolalu, 1984; Ilesanmi, 1968 & 1969). The event of 31st August – 1st September showed the systems in decaying stages when compared to the information from the preceding figure. Only central Mali and southeastern Mauritania recorded heavy precipitation presence while some scattered systems can be observed around, Freetown, Chad, and Central Africa Republic (CAR). The systems have completely cleared from areas between 10^{o}W and 10^{o}E and south of 10^{o}N. This position has been defined as the area of Little Dry Season (LDS) (Omotosho, 1988); while it is also referred to as *"anomalous August weather"* (Adefolalu, 1972). The figure for 2nd – 3rd September showed the clustering of the systems over Guinea, with some patches of the systems around the Gulf of Guinea bordering countries of Sierra Leone and Guinea Bissau. Some of these systems can also be found at the boundary of Mali and Senegal. The Gulf of Guinea has been known as an area of intense convective systems as a result of the high sea-surface temperatures (SSTs) present (Janicot *et al.*, 1998; Fontaine *et al.*, 1998), and this has made the area to be under heavy precipitation almost throughout the boreal summer period and the northward penetration of the rain band (Eltahir & Gong, 1996). Thus, not falling under the little dry season designated area of 10^{o}W - 10^{o}E and south of 10^{o}N (Omotosho, 1988). The last figure dated 4th – 5th September only has heavy precipitation presence at the border of Mali and Mauritania, and patches of the system at the border

of three (3) countries namely: Mali, Mauritania, and Senegal, while the other parts of Western Africa and the central states were cleared of the heavy precipitation presence.

Summarily, the days preceding the dates of rainfall activities were either showing the true state of events in the atmosphere or the level of the convective systems not precipitable enough to be captured by the model under non-feedback. In comparison to feedback output, the events preceding the dates of heavy precipitation were more pronounced when compared to non-feedback output, but the period of occurrence of the convective systems was not visible as seen under non-feedback. This can be attributed to the radiative interaction of the aerosol on the precipitation, thereby acting to suppress the precipitation. This is in support of earlier studies (Twomey, 1977; Seinfeld *et al.*, 2016).

Two (2) pieces of literature were employed to validate the ability of the COSMO-MUSCAT to capture the rain episode of September 1, 2009, over Ouagadougou. Though the results from Beucher *et al.,* (2019) captured the rainfall event at the boundary of Burkina Faso and Niger Republic, Lafore *et al.,* (2017) showed that convective systems a little further over Ouagadougou. Hence, it can be agreed or deduced that the model output of COSMO-MUSCAT worked well in capturing convective activities over West Africa.

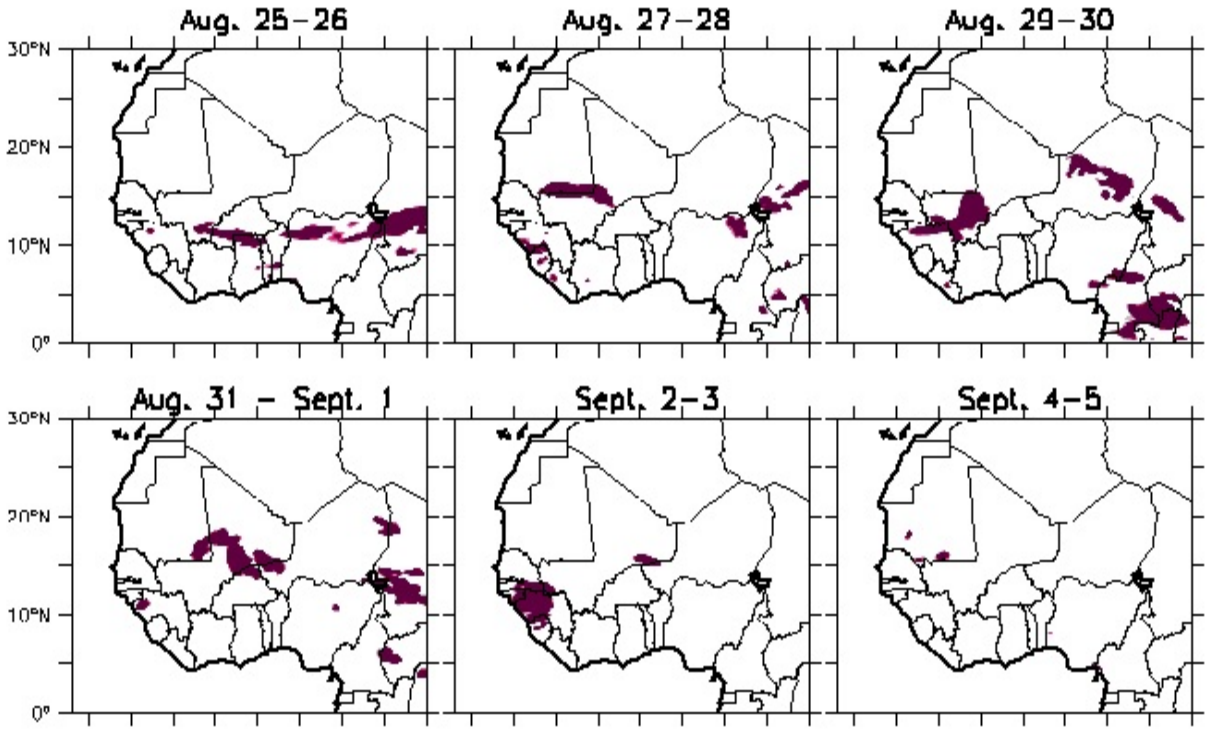

Figure 4.54: Feedback precipitation episode of 25th August – 5th September 2009 over West Africa.

The heavy precipitation simulation under the feedback mechanism was carried out to see the impact of the presence of aerosols on the amount of precipitation gotten. Unlike the non-feedback mechanism which gives what was simulated without considering the impact of any other substance in the atmosphere. Based on the results of heavy precipitation of the same months and date as specified in the non-feedback mechanism, it can be deduced from 25th – 26th August 2009 that the intensity of the systems over Chad Republic was stronger compared to the simulation result of non-feedback. The system spans the full length of the east-to-west of the country, but when compared to the non-feedback of the same date, the system was divided at the center of the country, and could only be seen in the eastern and western parts of the country. In furtherance to the impact of the aerosols on the heavy precipitation, it can be seen that a system was seen developing around the eastern part of the Central Africa Republic, which was not present in the non-feedback simulation. Over Accra Ghana, the system remains the same as the non-feedback showed it, but there was a trace of a developing system over the northwestern part of Nigeria, precisely Kebbi and Zamfara states. From 27th – 28th August 2009, the systems observed at the boundary of Mali and Mauritania had more intensity in the feedback mechanism compared to what was observed in a non-feedback mechanism. This result is in support of early studies that have shown that the aerosol particles serve as cloud condensation nuclei which aid its formation and also increase the number of cloud droplets and cloud albedo (Twoney, 1974). Other features of the systems over the Chad Republic remained the same as seen in the other mechanism. In considering the figures from 29th – 30th August and 31st August – 1st September 2009 showed an opposite result when compared to the non-feedback mechanism, especially over West Africa. The figures showed the systems in a developing or dying stage, unlike in the non-feedback mechanism where the systems seem like mature systems, which carried heavy precipitation. The Central Africa Republic, Chad Republic, and Mali recorded

evidence of heavy precipitation presence from 29th – 30th August 2009. The same can be said of the presence of heavy precipitation evidence in the figure of 31st August – 1st September 2009 but with the inclusion of Burkina Faso, Mauritania, and Guinea. The 2nd – 3rd September figure showed the heavy clustering of the system over Guinea and the border of Mali and Senegal. The remaining parts of West Africa and central Africa, where most of the systems developed, did not record the presence of any system. This is also the same feature as seen in the non-feedback mechanism for this day except there was a record of heavy precipitation systems at the border of Guinea and Guinea Bissau. The figure for 4th – 5th September only has spotted heavy precipitation in southern Mauritania. Other parts of West Africa are devoid of any heavy precipitation activities.

4.6.3 Simulated Mixing Layer Height Output of 25th August – 5th September, 2009 over West Africa

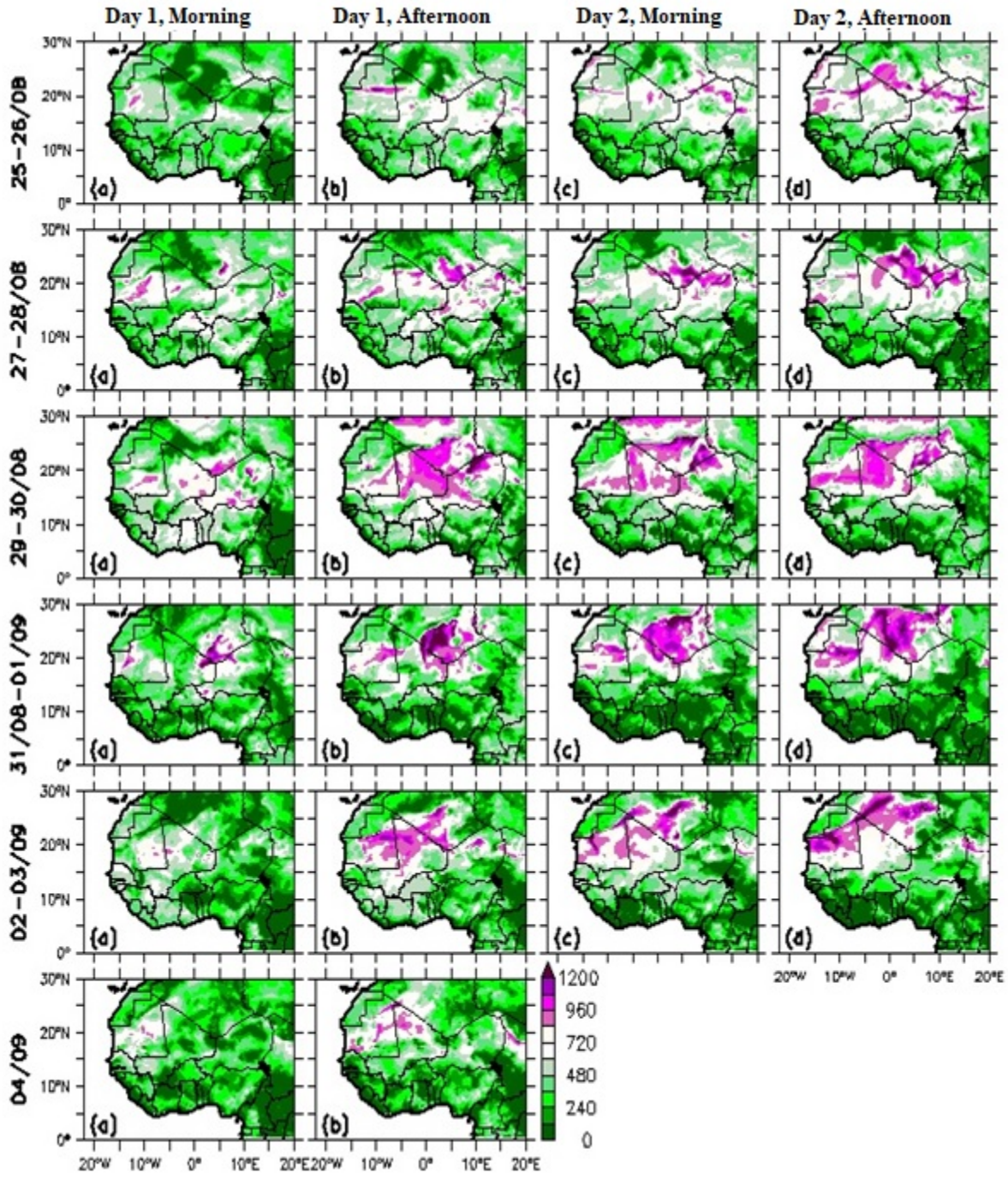

Figure 4.55: Mixing Level height of 25th August – 5th September 2009 over West Africa.

The mixing layer is formed when discontinuous turbulence exists due to discontinuities in temperature stratification between the upper and lower layers of the atmosphere. The atmospheric mixing layer height (MLH) is an important meteorological factor that affects the vertical diffusion of atmospheric pollutants and water vapor concentrations; therefore, it impacts the formation and dissipation of air pollutants (Aron, 1983; Stull, 1988). The mixing layer height (MLH) can also be said to be a measure of the vertical turbulent exchange within the boundary layer, which is one of the controlling factors for the dilution of pollutants emitted near the ground.

Relating the definition above to the details of Figure 4.55, it can be deduced that most of the morning hours are seldom calm and devoid of any turbulence, except the morning of 28th – 30th August. The mixing in the morning of the 28th – 30th August 2009 could be attributed to the turbulent activity of the previous afternoons due to the influence of abnormal conditions of the atmosphere like inversions and isotherms which may be attributed to radiative cooling of the Earth's surface and adjacent air layers, air subsidence, etc., and this is in support of (Stryhal *et al.*, 2017; Czarnecka *et al.*, 2019; Palarz *et al.*, 2018, 2020) studies. The turbulence experienced in virtually all the afternoon periods can be attributed to the variation in temperature between the surface and upper atmosphere due to the presence of radiation. But the areas mostly affected by high turbulence are desert areas of Mali and Niger, and the North African region.

Comparing the above observation from Figure 4.55 (mixing layer height) to Figures 4.69 (surface temperature) and 4.70 (upper-level temperature), it can be deduced that these three (3) figures followed almost the same pattern which means that there exists a relationship between temperature at surface and upper-level and mixing layer height (turbulent region).

4.7. Simulated Wind Component of 25th August – 5th September 2009 over selected stations in West Africa

This section assesses the impact of aerosols (both radiative feedback and non-feedback mechanisms) on the convection initiation and propagation over West Africa. In resolving this, Omotosho, 1985 analysis of propagation, maintenance, and sustainability of West African convective systems was employed. The said analysis enumerates the process in which low theta-E (Θ_e) air blows from the African Easterly Jet (AEJ) towards a convective system and thus results in an evaporative downdraft. The cool and dry cold Θ_e becomes heavy and spreads on the surface. A gust front is formed and this allows the warm and moist high Θ_e to take an upward motion, thus energizing the cloud. In summary, the above-explained process describes the AEJ and Θ_e interaction with storm updraft/downdraft to convective precipitation sustenance. Thus, explaining the impact of jets on the convective systems of West Africa.

4.7.1 Wind Profile over Coastal Areas (Equator – 8°N)

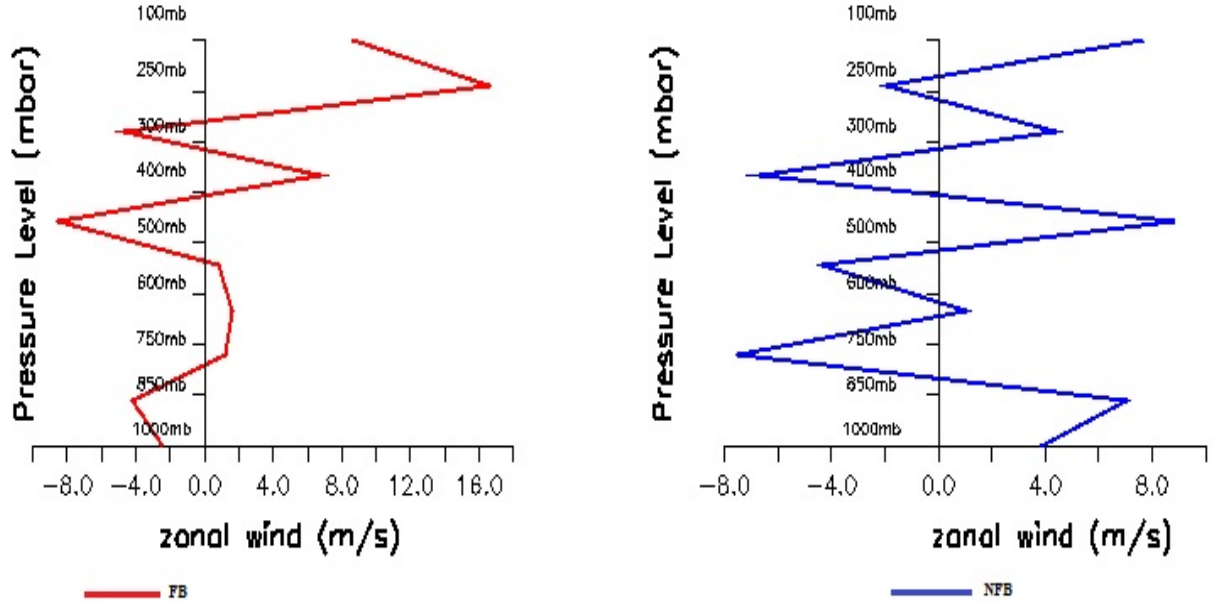

Figure 4.56: Feedback (red) and Non-Feedback (blue) wind profile of 25th August – 5th September 2009 over Abidjan.

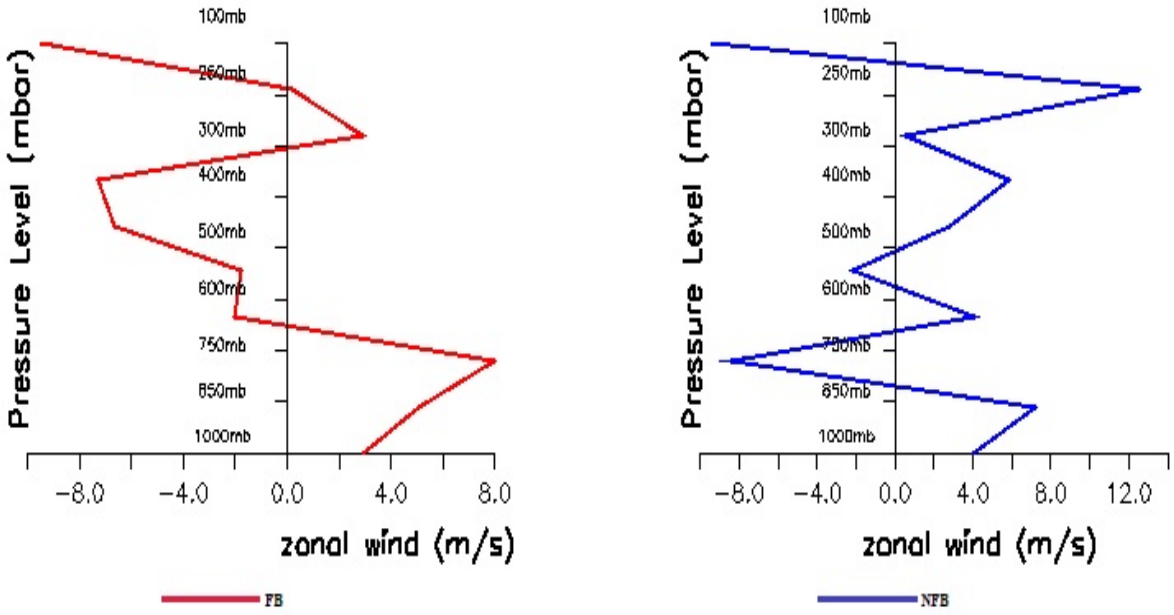

Figure 4.57: Feedback (red) and Non-Feedback (blue) wind profile of 25th August – 5th September 2009 over Accra.

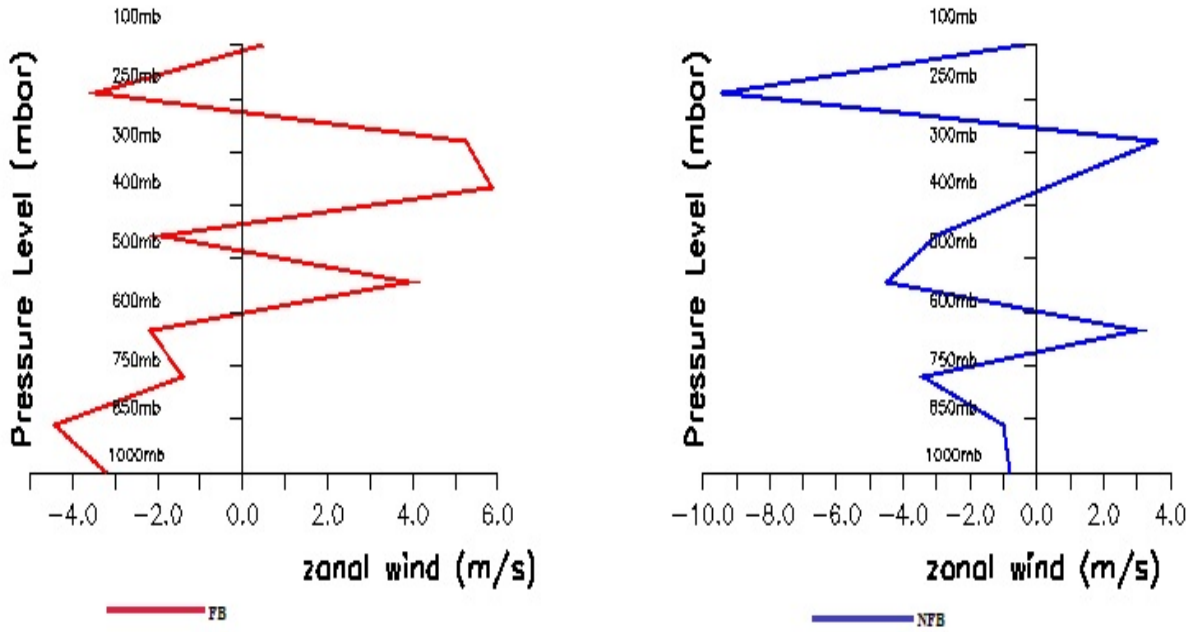

Figure 4.58: Feedback (red) and Non-Feedback (blue) wind profile of 25th August – 5th September 2009 over Freetown.

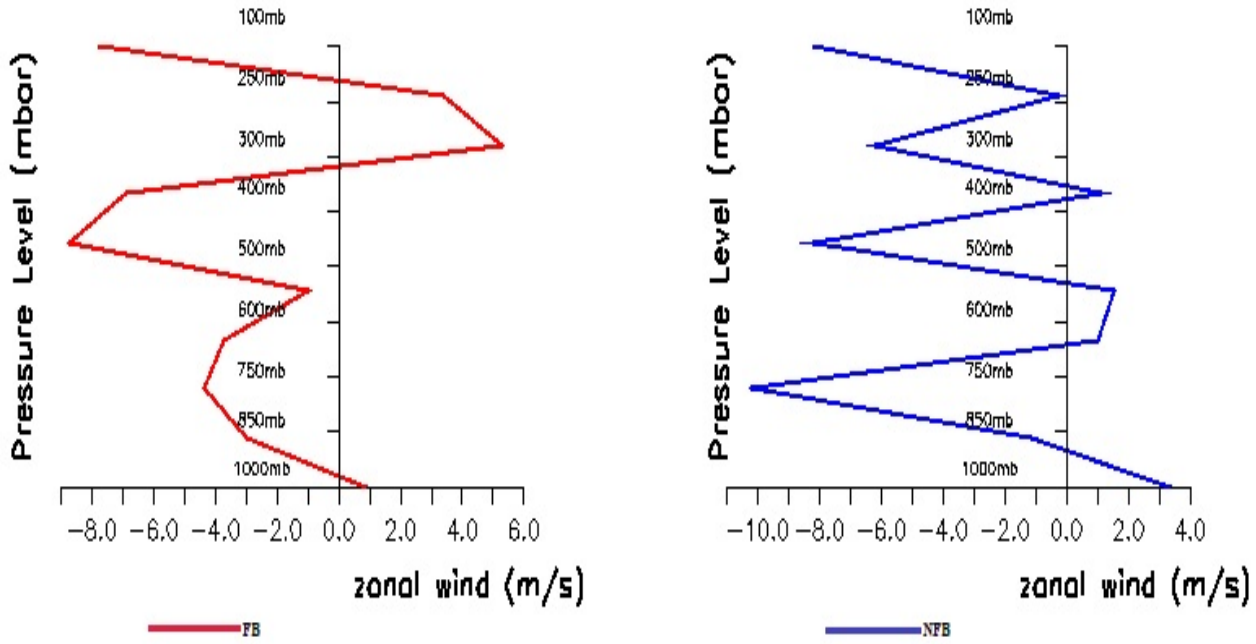

Figure 4.59: Feedback (red) and Non-Feedback (blue) wind profile of 25th August – 5th September 2009 over Ikeja.

The wind profile, especially over this period of the year, is mainly focused on African Easterly Jet (AEJ) and Tropical Easterly Jet (TEJ). The AEJ and TEJ are the two (2) most important jets responsible for the convective systems over West Africa. While the AEJ can be said to be responsible for the production and sustenance of the convective systems i.e. it determines the storm type (storm organization and movement), TEJ helps to modulate the convective systems (Adefolalu, 1976; Omotosho, 1983). Studies have also shown that shear wind (surface to 700 mb) favors fast-moving MCSs in the region of the AEJ. Also, the direction of the shear vector is crucial and indicates the propagating direction for the whole MCS.

Studies from deep convection have shown that wind shear can have several effects such as the effective organization of deep convective systems into rain bands and squall lines (e.g. Thorpe *et al.*, 1982; Rotunno *et al.*, 1988; Parker, 1996; Hildebrand, 1998; Robe and Emmanuel, 2001; Weisman and Rotunno, 2004). In the same vein, shear can also limit convection during the developing stages (Pastushkov, 1975), reduction in the updraft speeds in slanted thermals by enhancing the (downward oriented) pressure perturbations (Peter *et al.*, 2019), inhibit deep convection by blowing off cloud tops (Sathiyamoorthy *et al.*, 2004; Koren *et al.*, 2010) which is interpreted as an increase in the cloud surface area that experiences entrainment, which also plays a role in setting updraft buoyancy and updraft speeds.

Figures 4.56 – 4.59 showed the wind profiles of the selected locations regarded as rainforest or coastal areas. It is called a coastal area because all the locations shared boundaries with the Atlantic Ocean. The figures showed wind profiles from radiative feedback (in red color) and non-feedback mechanism (in blue color). All stations in this zone, except Abidjan, recorded a strong TEJ around 200 mb – 250 mb with Abidjan, Accra and Freetown (radiative feedback) recording weak jets at the AEJ level of 700 mb. This combination has a higher possibility of producing thunderstorms

(Dhnonneur, 1971), and it also supports an (Omotosho, 1983) study which showed weak AEJ during the month of August when the inter-Tropical Discontinuity (ITD) has migrated to its northernmost position of 22^{o}N. Though, the non-feedback of Abidjan, Accra and Freetown as well as both feedback and non-feedback for Ikeja recorded strong jets at the AEJ level. All the figures under the coastal stations recorded shear close to the surface, and this is an indication of possible storms. This finding is in support of Ludlam's (1980) study that pointed to strong shear as the key feature for severe storms. Abidjan station (figure 4.56) was the only location where the winds took their source at different zonal axes, with feedback on the negative zonal wind component and the non-feedback on the positive side. But the other three locations of the same classification namely: Accra (figure 4.57), Freetown (figure 4.58), and Ikeja (figure 4.59) had two (2) winds taking off from the same axis of the zonal wind component. This means that the impact of the radiative feedback on the wind is more pronounced over Abidjan at the surface when compared to the other locations, as the wind recorded weak jet.

4.7.2 Wind Profile over Tropical Savannah/Semi-Arid Area (8°N – 13°N)

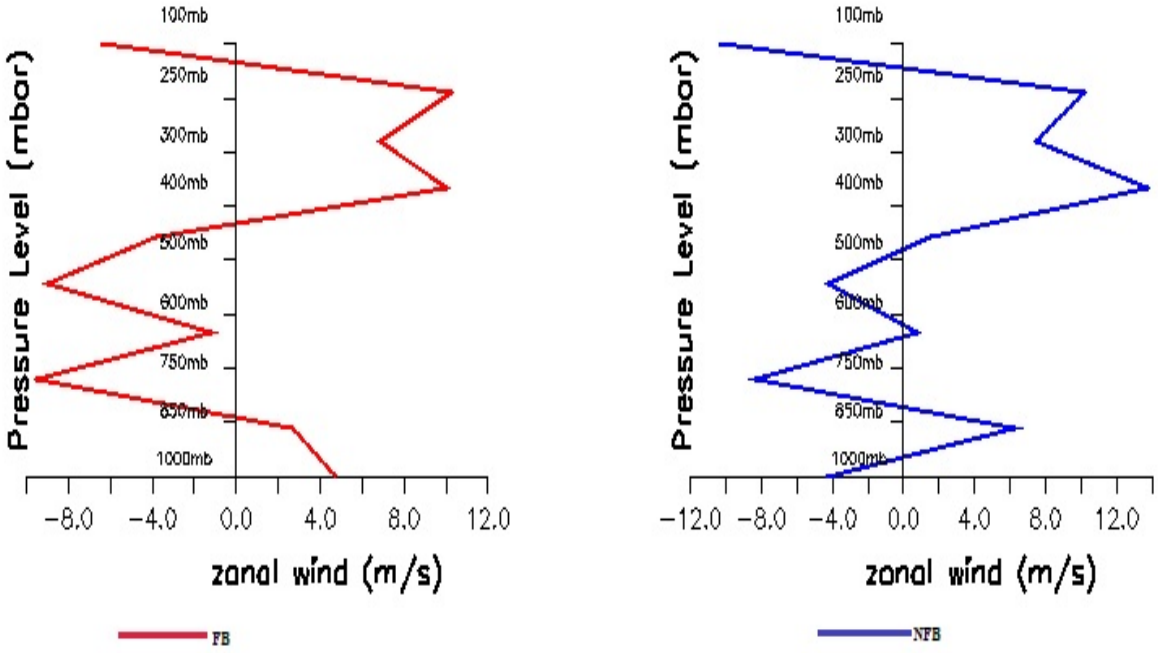

Figure 4.60: Feedback (red) and Non-Feedback (blue) wind profile of 25th August – 5th September 2009 over Banizoumbou.

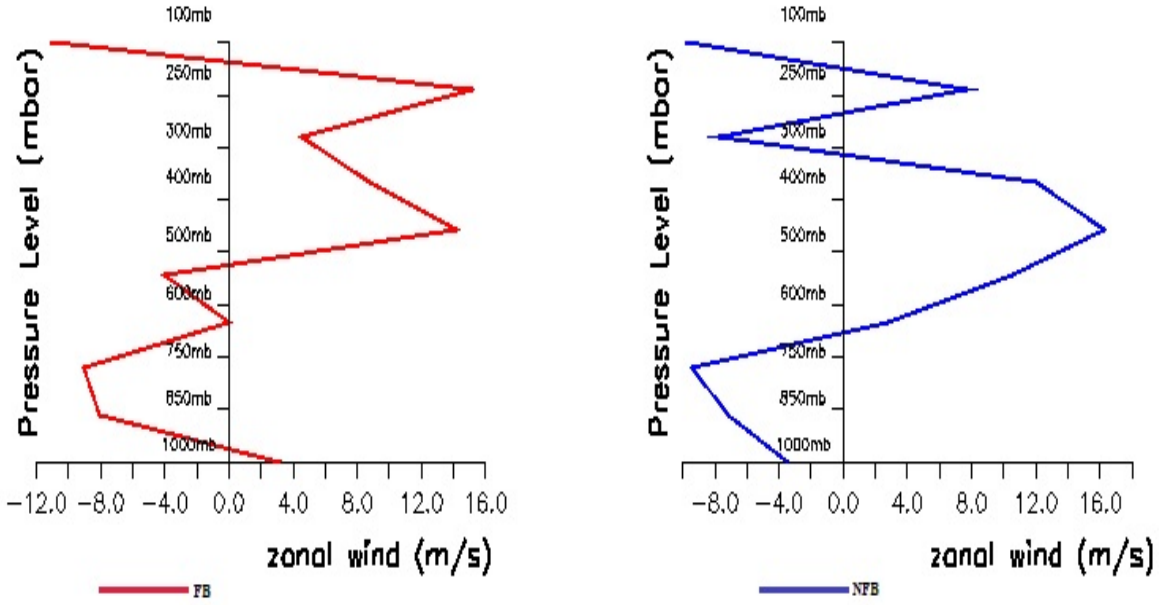

Figure 4.61: Feedback (red) and Non-Feedback (blue) wind profile of 25th August – 5th September 2009 over Kano.

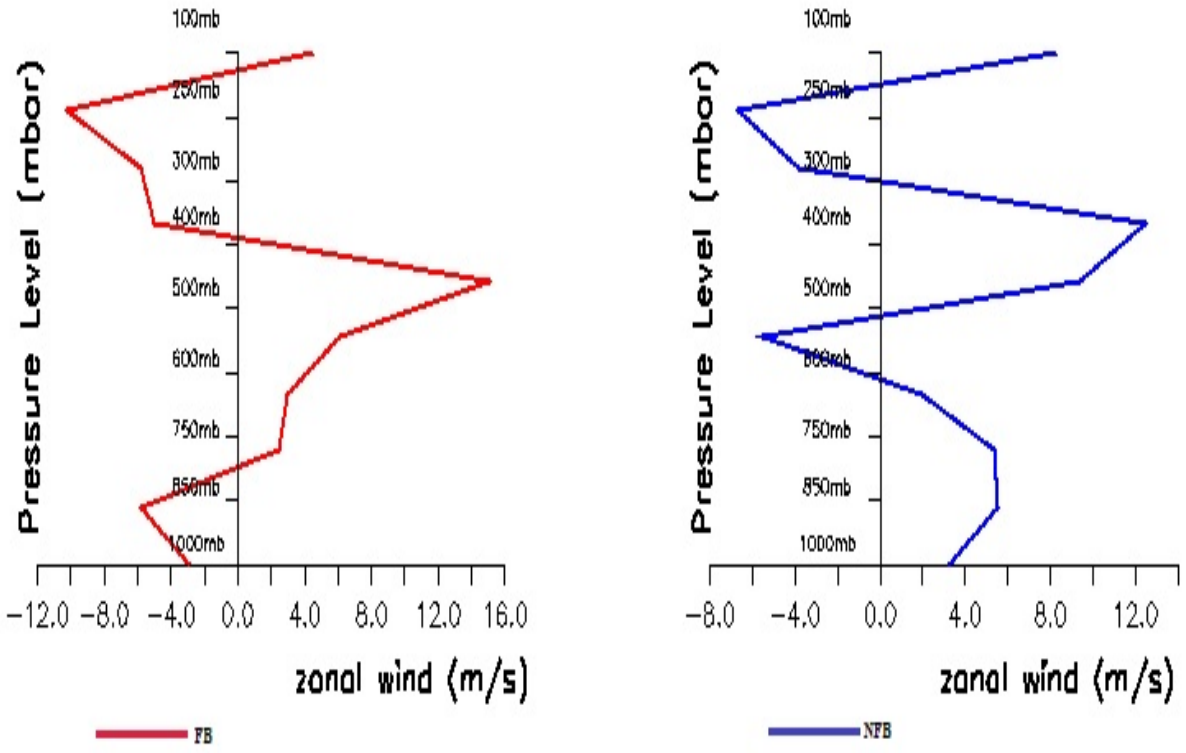

Figure 4.62: Feedback (red) and Non-Feedback (blue) wind profile of 25th August – 5th September 2009 over Ouagadougou.

Figures 4.60, 4.61, and 4.62 represents the Banizoumbou, Kano, and Ouagadougou stations respectively. They are locations classified as tropical savannah or semi-arid regions. The wind profile over Banizoumbou (figure 4.60) showed the radiative feedback wind component taking its source from the positive zonal wind axis while the non-feedback took its source from the negative zonal wind axis. Shear exists from the surface to about 700 mb, and this favors fast-moving in the region of the African Easterly Jet (AEJ). The direction of the shear vector is crucial and indicates the propagation direction for the whole convective systems because the propagating MCSs show a preference to propagate in the same direction as the lower-stratospheric shear vector (i.e., down-shear) at the expense of the convective systems propagating in opposite direction to the lower-stratospheric shear (i.e., up-shear). The strength of the wind is strongest between 700 mb and 400 mb, with radiative feedback and non-feedback recording a wind strength of $10ms^{-1}$ and $14ms^{-1}$ respectively, which is an area favorable to trigger and intensify convection.

Figure 4.61, which represents Kano, the taking off of the wind source is similar to that of Banizoumbou (Figure 4.60), that is, the non-feedback wind starting from a negative zonal wind component. The wind is strongest at 500 mb and 250 mb. There exists a strong Tropical Easterly Jet (TEJ) and African Easterly Jet (AEJ) which is important in modulating and strengthening the convective systems.

Unlike figure 4.61 (Kano) which recorded the strongest wind at 500 mb and 250 mb, figure 4.62 (Ouagadougou) showed that the wind strength was at its peak from 550 mb to 100 mb. Also, the radiative feedback-impacted wind took its source from the negative axis of the zonal wind while the non-feedback wind took its source from the positive axis. The wind source information at the surface over Ouagadougou is at variance to the other locations (Banizoumbou and Kano) within this

same climatic classified region or zone. The TEJ is also strong while the AEJ is weak as seen across all figures under this zone.

This vertical wind shear is known to play a key role in the organization and intensity of Mesoscale convective systems (MCSs) in West and Central Africa. Summarily, there exits continuous change in vertical wind shear over the stations in this classified savannah or semi-arid region, and by implication, can be responsible for the increasing intensity of MCSs over this region. This is in support of (Richardson, 1999; Weisman and Rotunno, 2004; Taylor *et al.*, 2017, 2018; Klein *et al.*, 2021) studies that linked the decadal increase in vertical wind shear to the recent decadal increase in intense MCSs over the Sahel.

4.7.3 Wind Profile over Desert Climate (13°N upward)

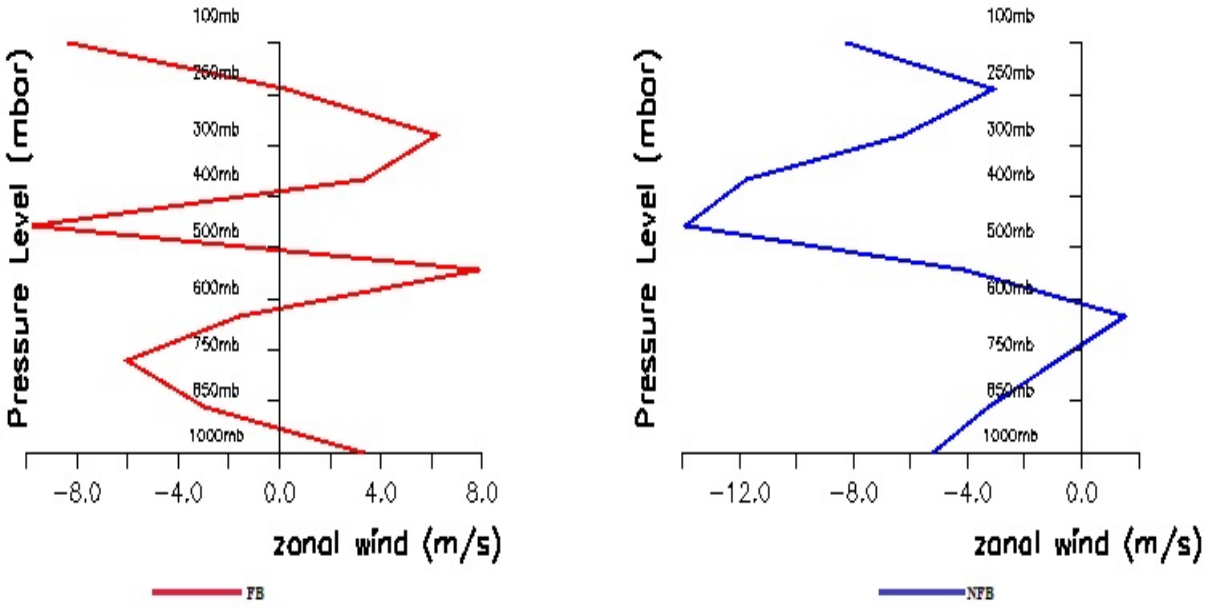

Figure 4.63: Feedback (red) and Non-Feedback (blue) wind profile of 25th August – 5th September 2009 over Agoufou.

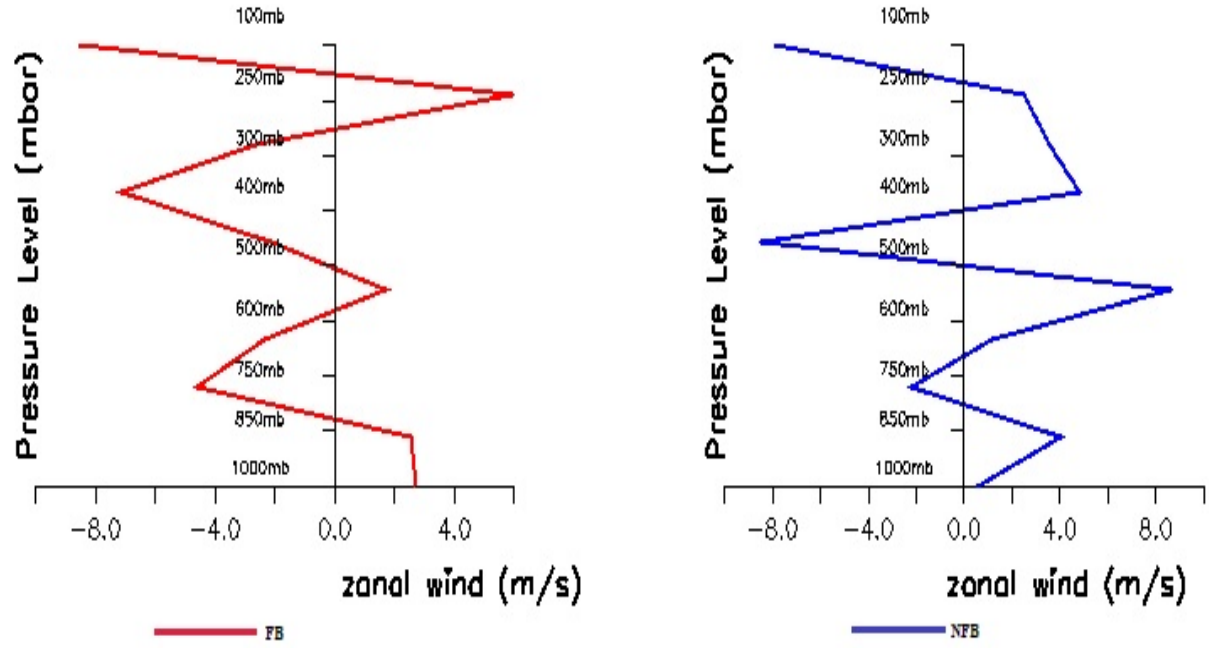

Figure 4.64: Feedback (red) and Non-Feedback (blue) wind profile of 25th August – 5th September 2009 over Dakar.

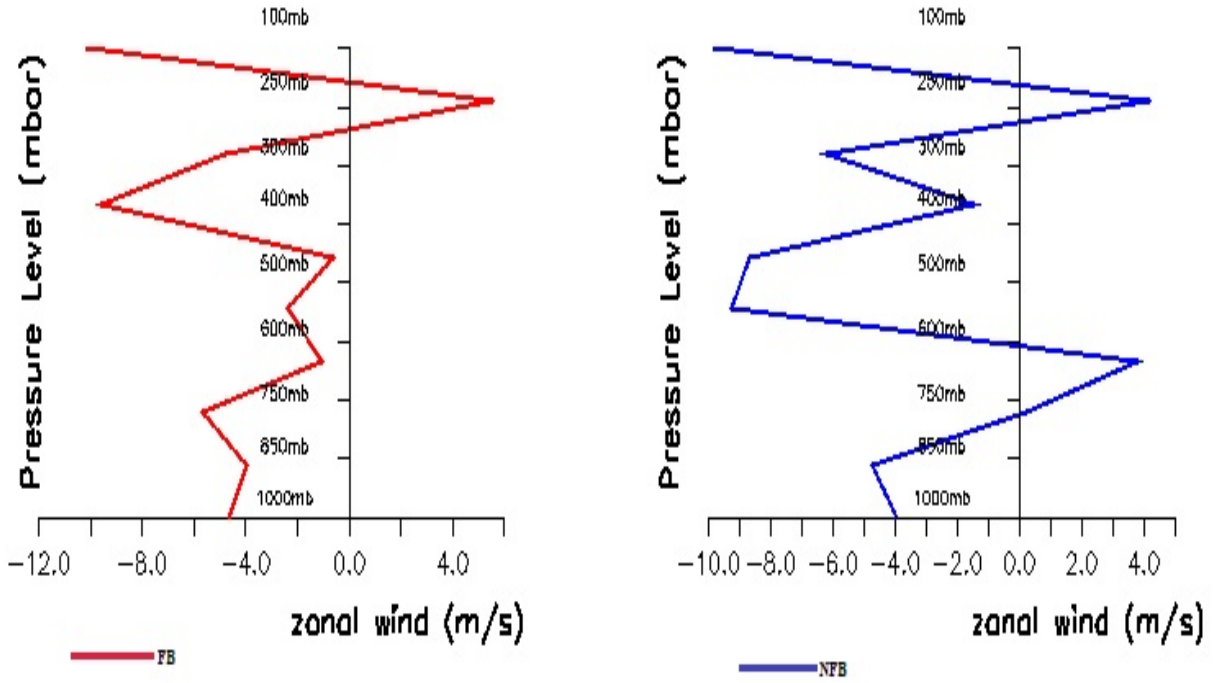

Figure 4.65: Feedback (red) and Non-Feedback (blue) wind profile of 25th August – 5th September 2009 over Praia.

Figures 4.63, 4.64, and 4.65 representing Agoufou, Dakar, and Praia respectively are classified as the desert climate for stations north of 13^{o}N in this study. It is expected that convective activities should be prevalent during this period of the year (August), with the rainforest region experiencing or just exiting the little dry season (LDS). Observational and numerical studies have shown that the combination of the horizontal wind and its corresponding vertical wind structures have important impacts on the development of convective activities. Omotosho (1987) further defined certain conditions to be met before thunderstorms can occur, with the first criterion being the low-level wind shear below AEJ (surface to 700 mb) ranging from -20 to -5ms^{-1}; and the second criterion is the mid-troposphere (700 to 400 mb) ranging from 0 to 10ms^{-1}. Based on the above definition, only Agoufou (feedback and non-feedback), Dakar (feedback only), and Praia (non-feedback only) met the criteria for thunderstorms to occur while the non-feedback for Dakar and feedback for Praia only met the second and first criterion respectively for the mid-troposphere (700 to 400 mb) ranging from 0 to 10ms^{-1}.

The non-feedback and radiative feedback impacted horizontal wind value over Agoufou (figure 4.63) was greater than -5ms^{-1} (> -5ms^{-1}) between the surface and 700mb, thus meeting the 1st criterion of thunderstorm occurrence. While the strength of the wind at the AEJ (i.e. 700 mb) is stronger and easterlies under radiative feedback, the strength is weak and westerlies under non-feedback. But at TEJ levels (i.e. 250 mb), both the non-feedback and radiative feedback recorded a strong wind strength that is easterlies. It was equally observed that the two winds are not in the same direction around the 850 mb – 750 mb and 400 mb – 300 mb, but the winds aligned together in the same direction at the upper level of 250 mb.

For Dakar (figure 4.64), unlike the other two (2) stations under this category that had one or two of their wind taking its source from the negative axis (easterlies) of the zonal wind component, both

the non-feedback and the radiative feedback impacted winds took their sources from the positive axis of the zonal wind component. This implies that there is the possibility of less convective systems over Dakar at this period since the positive zonal wind blows from the west while the negative blows from the east; and studies have identified the convective systems with the motion of trains of vortices that move from east to west over West Africa (Adefolalu, 1974; Obasi, 1974; Fasheun, 1979). Studies have also shown that in the northern storm track (i.e. north of 15^{o}N), convection tends to be suppressed west of the AEW trough, but is enhanced to the east of the trough where there is enhanced southerly flow of moist air into the arid region (Burpee, 1972; Duvel, 1990; Mathon *et al.*, 2002, Fink and Reiner, 2003). The westerly flow of the wind acts as suppression to the mid-tropospheric horizontal shear associated with the AEJ as it can be observed that none of the wind between the surface to 700mb satisfies the -20 to -5ms^{-1} condition for thunderstorms development (Omotosho, 1987).

Figure 4.65 (Praia) showed both winds being easterlies at the surface and thus meeting the criteria for thunderstorm development tendency as discussed above, with only the non-feedback vertical wind profile meeting both criteria for thunderstorm development. Though, the AEJ for radiative feedback only and TEJ for both feedbacks seem to be strong but present at 700 mb and 250 mb respectively. The strength of the wind may have been stronger than the wind component range defined for the mid-troposphere. But these areas of ascending motion (700 mb and 400 mb) are not favorable to trigger and intensify convection.

4.8 Impact of the non-local plume on radiative feedback outputs of simulated cloud cover, relative humidity, and temperature.

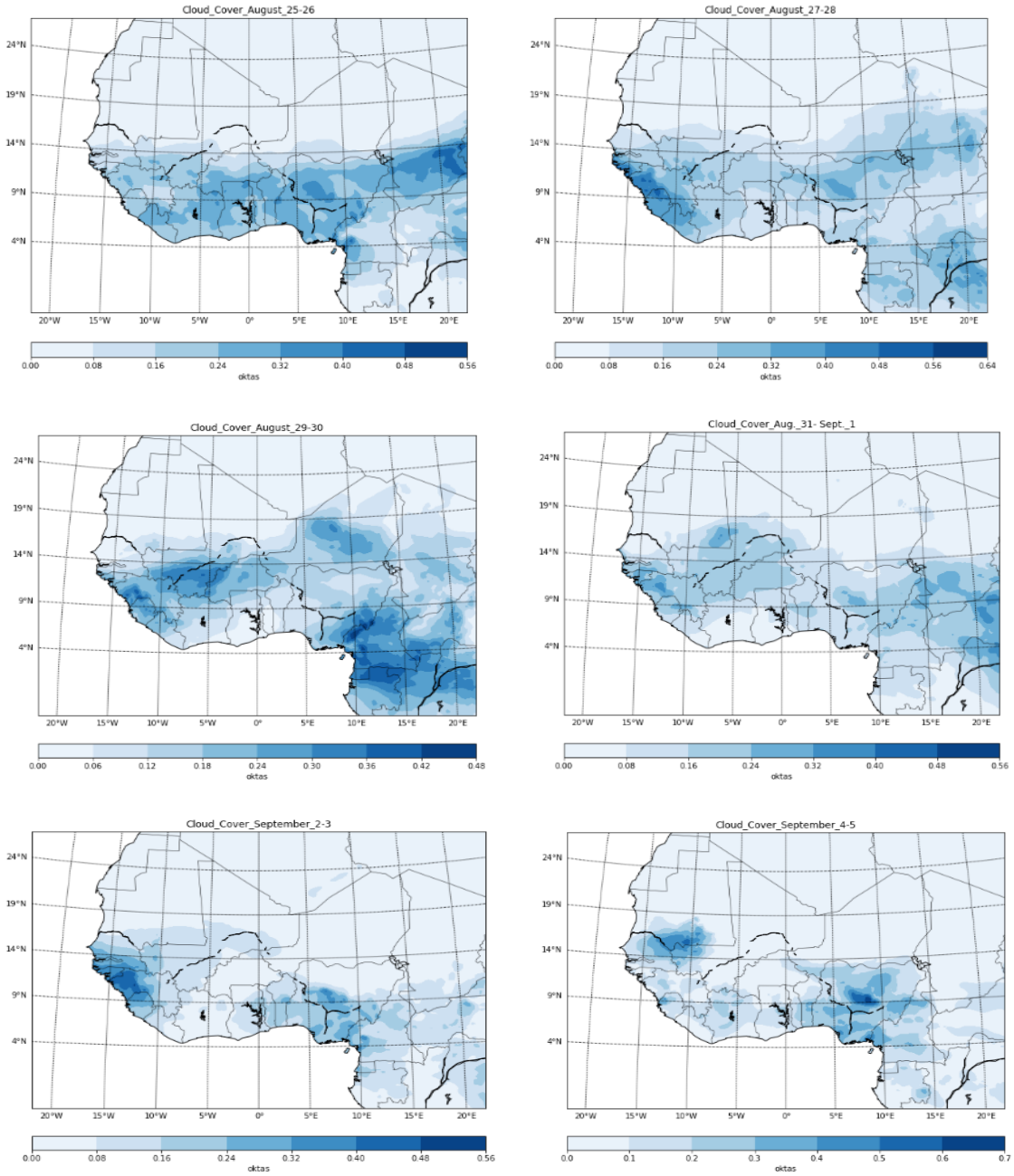

Figure 4.66: Cloud cover response to aerosol radiative feedback of 25th Aug. – 5th Sept. 2009 over West Africa.

In this section, the objective was to examine the impact of non-local plumes on simulated cloud properties, precipitation, and temperature. Based on the preceding statement, the cloud and other variables (both at the surface and upper level) were considered under feedback and non-feedback conditions. It should be noted that low clouds give heavy precipitation and are observed as a darker blue color. The period of the month considered was August to capture the cloud very well since inter-Tropical Discontinuity (ITD) would have been at the northernmost position of 22^{o}N (Ilesanmi, 1971; Omotosho, 1985) at this time of the year. For cloud cover of 25th – 26th August as seen in figure 4.66, the whole West Africa region was under a well-developed cloud situation, which had the propensity to give heavy precipitation. These clouds covered areas from the coast to about 14^{o}N, while some patches can be seen up to 18^{o}N. These clouds also extended to the central African countries of Chad Republic, Cameroun, Central Africa Republic, and the Democratic Republic of Congo. Despite the cloudy nature of most areas south of 14^{o}N, most coastal areas spanning from Benin Republic through Togo, Ghana, and Côte D'Ivoire to Liberia were devoid of low cloud which carries heavy precipitation. The figure for the 27th – 28th of August showed the clustering of heavy precipitation-laden clouds in areas around the Gulf guinea. Though other parts of West Africa have clouds, the middle clouds are sparsely distributed with low clouds recorded in the central states of Nigeria. The cloud has exceeded the 19^{o}N mark as seen in the previous figure. Hence, it can be deduced that the smaller the area covered by the cloud, the tendency to Upper-level-intensity precipitation. Some parts of central Africa also recorded a high-intensity cloud. It was also observed that most parts of Ghana were cloudless. Though, studies have shown that Accra, a coastal region, rainfall pattern that differs from other coastal regions of West Africa. Could this cloudless situation over the country at this month of the year be the reason why the coastal region record less annual rainfall compared to others? The figure for 29th – 30th August showed heavy

precipitation-laden clouds over areas around the Gu of Guinea, Mali, Niger Republic, and central Africa of Cameroun, Gabon, Central Africa Republic, and Sudan. The eastern axis of Nigeria from the Mambilla plateau in Taraba state down to the Cross River state boundary to Cameroun. But the central states of Nigeria through the western axis of the region to Côte D'Ivoire are devoid of intense clouds. Some patches of cloud can also be observed around the southern part of the North African countries of Algeria and Libya. The figure for 31st August – 1st September showed the spanning of the clouds across the region with the heavy precipitation-laden cloud sparsely distributed around Guinea Bissau, southern Mauritania, and the central and northeastern region of Nigeria. Areas south of 19°N are devoid of any heavy clouds. Figure 4.66 for 2nd – 3rd September showed the core of the clouds spotted over countries around the Gulf of Guinea. The clouds covered Sierra Leone, Guinea Bissau, Guinea, Senegal, and The Gambia. The other heavy clouds are spotted over Nigeria, around the north-central states, and some parts of the south-south region. Côte D'Ivoire and Burkina Faso recorded a clear sky, as well as the Savannah region of Nigeria. The figure for 4th – 5th September saw the heavy clouds around the Gulf of Guinea move up to the boundary of Mauritania, Mali, and Senegal. All parts of Nigeria were also covered by heavy clouds, albeit some areas had shallow clouds. The other parts of West Africa recorded shallow clouds, which may likely not be able to produce rain but can be effective in reducing the amount of radiation to earth and thus modulates the evaporation of water from the land surface.

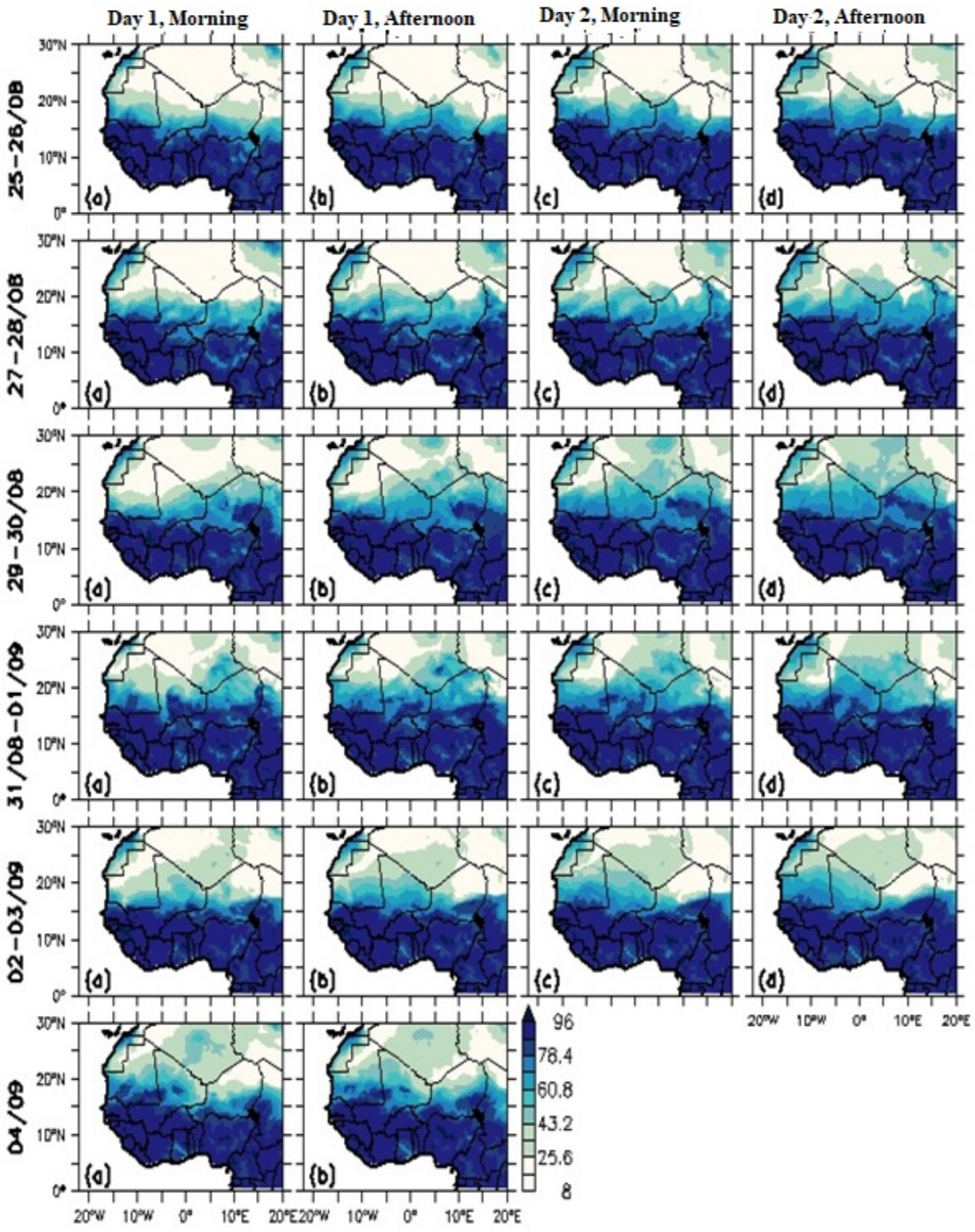

Figure 4.67: Surface relative humidity response to aerosol feedback of 25th Aug. – 5th Sept. 2009 over West Africa.

The relative humidity at the surface was observed for morning and afternoon hours, with each row of four (4) panels having 48-hour (2 days) plots. It is an undeniable fact that there are increased dynamics of the atmosphere during the day as a result of radiation and other factors. This can lead to turbulence and mixing in the atmosphere and thus alter the state of the atmosphere from a stable to an unstable situation (Holtslag, 2003). Results from figure 4.67 above showed that all the simulated days recorded a high relative humidity presence of about 96% over areas south of 15^{o}N, and about 60% over areas between 15^{o}N and 20^{o}N covering Niger, Mali, and Mauritania. The North African countries of Morocco and Libya also recorded relative humidity of about 44%, while Algeria recorded a relative humidity of about 8%. The latitudinal distribution of relative humidity as stated earlier conforms with earlier studies of (Ilesanmi, 1971), which attributed the northernmost position of inter-Tropical Discontinuity (ITD) to the high relative humidity present in the atmosphere. The graphs for 29th – 30th August showed a further build-up of the relative humidity from the preceding days. While the Niger Republic and Chad Republic's high relative humidity of above 96% exceeded latitude 15^{o}N, other parts of West Africa retained the same values below 15^{o}N. The 44% relative humidity record was observed in the southern part of Algeria on the morning of 29th August but had completely covered the country by the afternoon of 30th August. The figures for 31st August – 1st September revealed that the relative humidity value of above 96% was as high as about latitude 20^{o}N. The figures also showed the North African countries under 44% relative humidity while there sparsely distributed humidity value of about 8% in some parts of the same North Africa. The figures for 2nd – 3rd September saw a decline in the high relative humidity values of above 96% strictly limited to south of latitude 15^{o}N. These also led to the decline of the 40% - 60% range of relative humidity over areas north of latitude 15^{o}N, and more areas also

recorded a humidity value of about 8% when compared to the previous days. The figure for 4th September recorded an improvement from the preceding day's value as the high relative humidity of over 96% exceeded latitude 15°N, and almost all parts of Northern Africa were under the influence of the 40% - 60% range of relative humidity value.

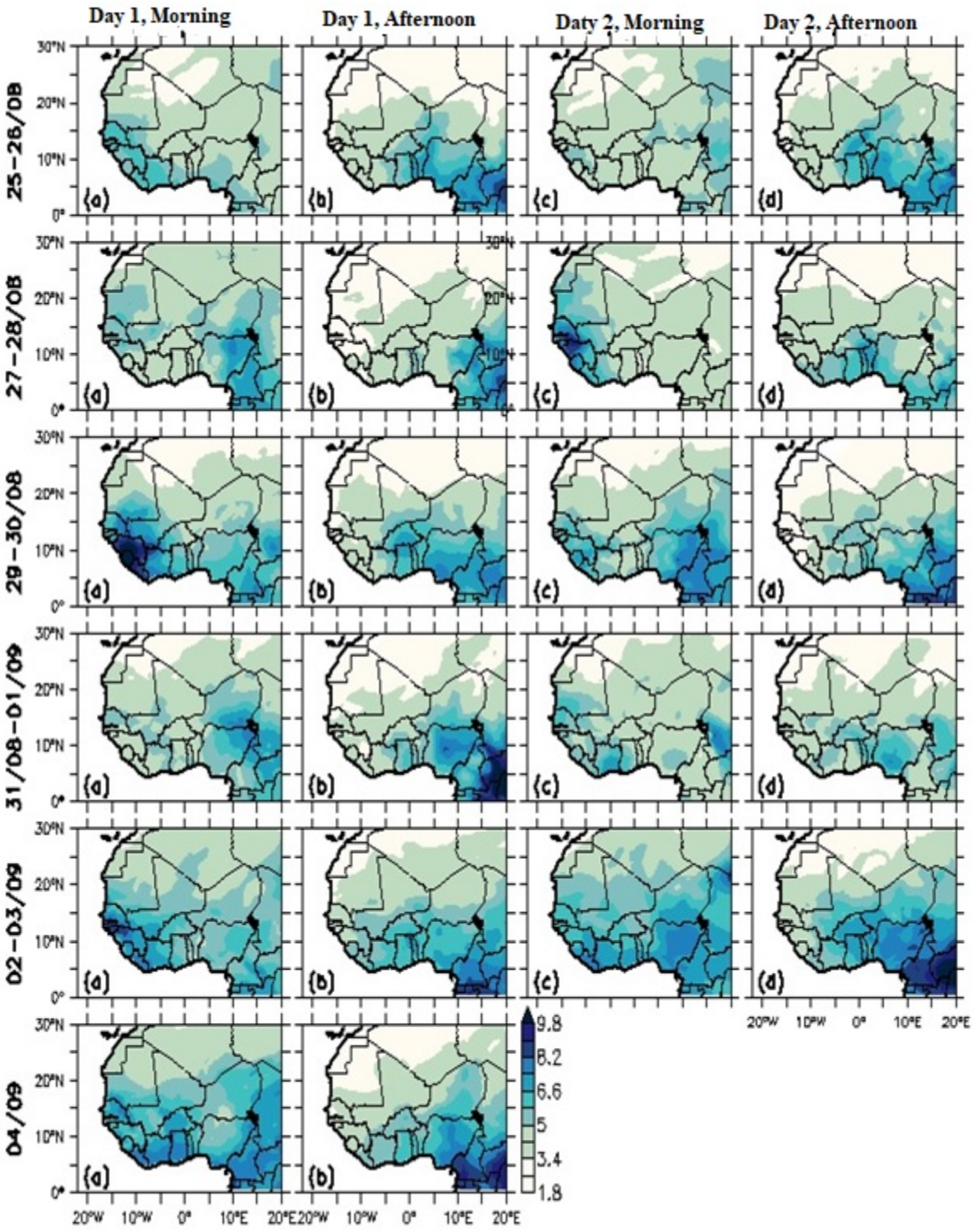

Figure 4.68: Upper level relative humidity response to aerosol feedback of 25th Aug. – 5th Sept. 2009 over West Africa.

Going by the general observation, the morning periods record more moisture content in the atmosphere than the afternoon periods. From the figure 4.68 above, the morning period for 25th August showed areas bounded by the Gulf of Guinea recording high relative humidity of about 8.2% while the other coastal areas of the West African region recorded about 6.6%. The inland areas of West Africa, as well as northern Africa, recorded about < 5% of relative humidity amount. Though, northern Mauritania and western Algeria had no record of relative humidity (i.e. 0%). The same zero relative humidity can be across all North African countries in the afternoon period of the same day. The high relative humidity amount was recorded over Ghana, Togo, Benin Republic, and Nigeria. This same high relative humidity was recorded over the central counties of Cameroun, Central Africa Republic, and southern Chad. Areas around the Gulf of Guinea and the inland areas of West African countries recorded relative humidity of < 5%. The morning figure for 26th August showed an entire area of low relative humidity of less than 6.6%, while the same axis as that of the morning of the preceding day showed zero relative humidity. Though, some areas actually recorded some scanty high relative humidity of > 6.6%. Looking across the remaining graphs spanning through the 27th of August – the 4th of September at the upper level, the figures are more or less the same scenario of high relative humidity content around the coastlines, areas of the Gulf of Guinea, and around some central African countries. The northern part of Africa sometimes records relative humidity of less than 5% or no humidity of zero. Aside from the 29th – 30th August and the 31st August – 1st September figures where most parts of northern Africa recorded zero relative humidity amount throughout the days, other figures showed some content of moisture in the atmosphere either in the morning or afternoon periods. In summary, the results showed that a similar scenario at the surface was also applicable at the upper level in which areas closer to the coast recorded more relative humidity content that the further inland area, albeit the difference was the level of the

moisture content present. Hence, the results, therefore, showed that the higher you go, the fewer moisture contents are recorded in the atmosphere. And this is in support of (Noh *et al.*, 2016) study.

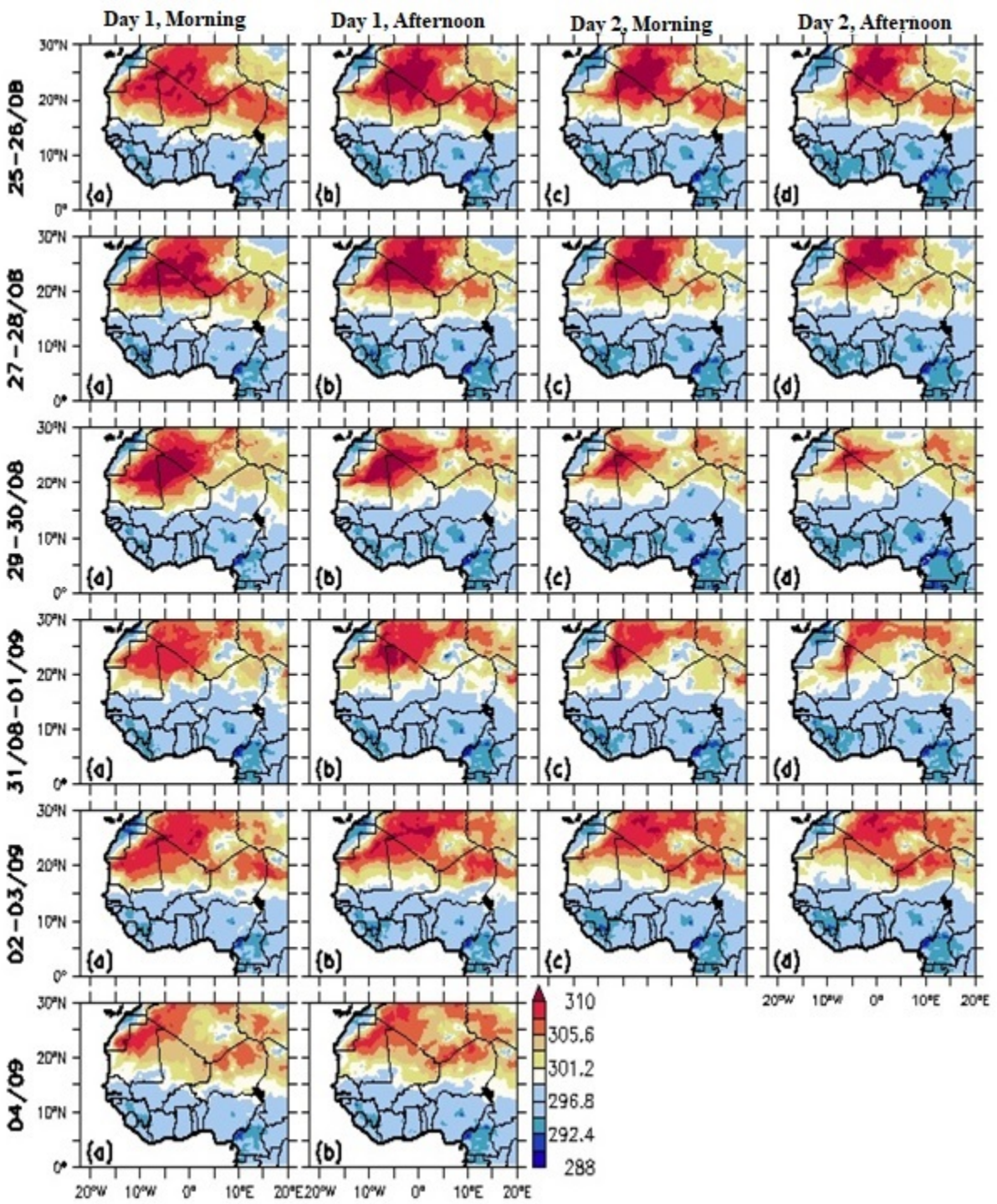

Figure 4.69: Surface temperature response to aerosol feedback of 25th Aug. – 5th Sept. 2009 over West Africa.

Based on the surface distribution of the relative humidity as indicated in figure 4.67, the surface temperatures (in kelvin) as shown in figure 4.69 were observed to be highest across areas where relative humidity was very low. Specifically, the northern part of Mali and the southwestern region of Algeria showed a temperature range of about 305 K (31.85^{o}C) to 310 K (36.85^{o}C) all through the figures from 25th August – 4th September, while some parts of the northern region of the continent recorded temperature range of 300 K (26.85^{o}C) to 305 K (31.85^{o}C). Other parts with high-temperature records include Chad Republic, Mauritania, and Niger Republic. All through the period of the study, areas south of 14^{o}N recorded less temperature which ranges from 288 K (14.85^{o}C) to 297 K (23.85^{o}C). The slight changes in temperature between day-time and night-time, especially over Chad regions, are supported by (Tegen and Kohfeld, 2006) study which concluded that the observed changes over the Chad region can be attributed to the enhancement of the wind speed over the dust cloud when analyzing the vertical temperature structure of the region. Central Africa region of Cameroun, the Gulf of Guinea region of Sierra Leone, Guinea, and Liberia, and the central state of Nigeria recorded the coldest temperature of between 288 K (14.85^{o}C) and 293 K (19.85^{o}C). The Western Sahara region of Morocco was also cold throughout despite being positioned around the North African region. This is because of the location of the country between the Atlantic Ocean, the Mediterranean Sea, and the Atlas Mountain in the northwest of Africa. Hence, the weather is formed by cold Atlantic currents and the impact of the Sahara Desert and mountains (Knippertz *et al.*, 2003; Driouech *et al.*, 2009; Schilling *et al.*, 2020).

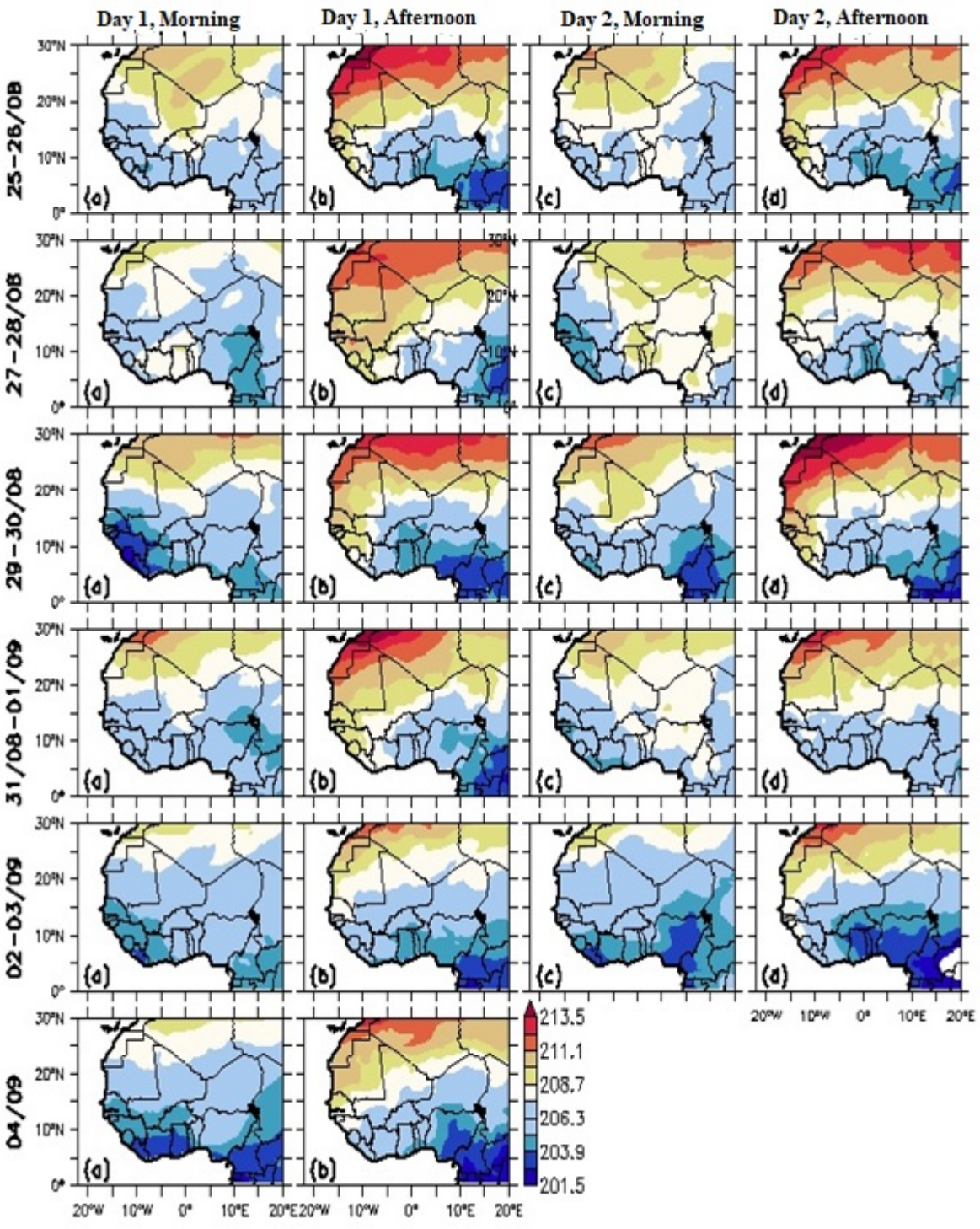

Figure 4.70: Upper-level temperature response to aerosol feedback of 25th Aug. – 5th Sept. 2009 over West Africa.

The temperatures at the upper level are mostly cold. This is not surprising as it is widely known that the higher one goes, the cooler it becomes. The highest temperature at the upper level during the period of the simulation was about 214 K (-59.15^{o}C), compared to the surface's highest temperature value of about 311 K (37.85^{o}C). Unlike the surface temperature where all areas south of 14^{o}N were under the influence of low temperature, most afternoons from figure 4.70 dated 25th August – 4th September had high-temperature encroached below that threshold of surface temperature, with some high-temperature values getting to the areas of the Gulf of Guinea. The colder temperatures were spotted around countries like the Gulf of Guinea area, the central African countries, and the coastal countries of Ghana, Togo, Benin Republic, and Nigeria. It can also be noted that the transition zone between the high and low temperatures is wider at the upper level compared to the surface temperature scenario where it looked more like an ITD path. The morning hours equally recorded low temperatures across the period of study, with the values ranging between 209 K and 211 K. But the morning period of 30th and 31st August recorded above 211 K around Morocco and northern Algeria. The temperatures were stronger between the afternoon periods of 25th August and 1st September.

4.9 Impact of the non-local plume on non-feedback outputs of simulated cloud cover, relative humidity, and temperature.

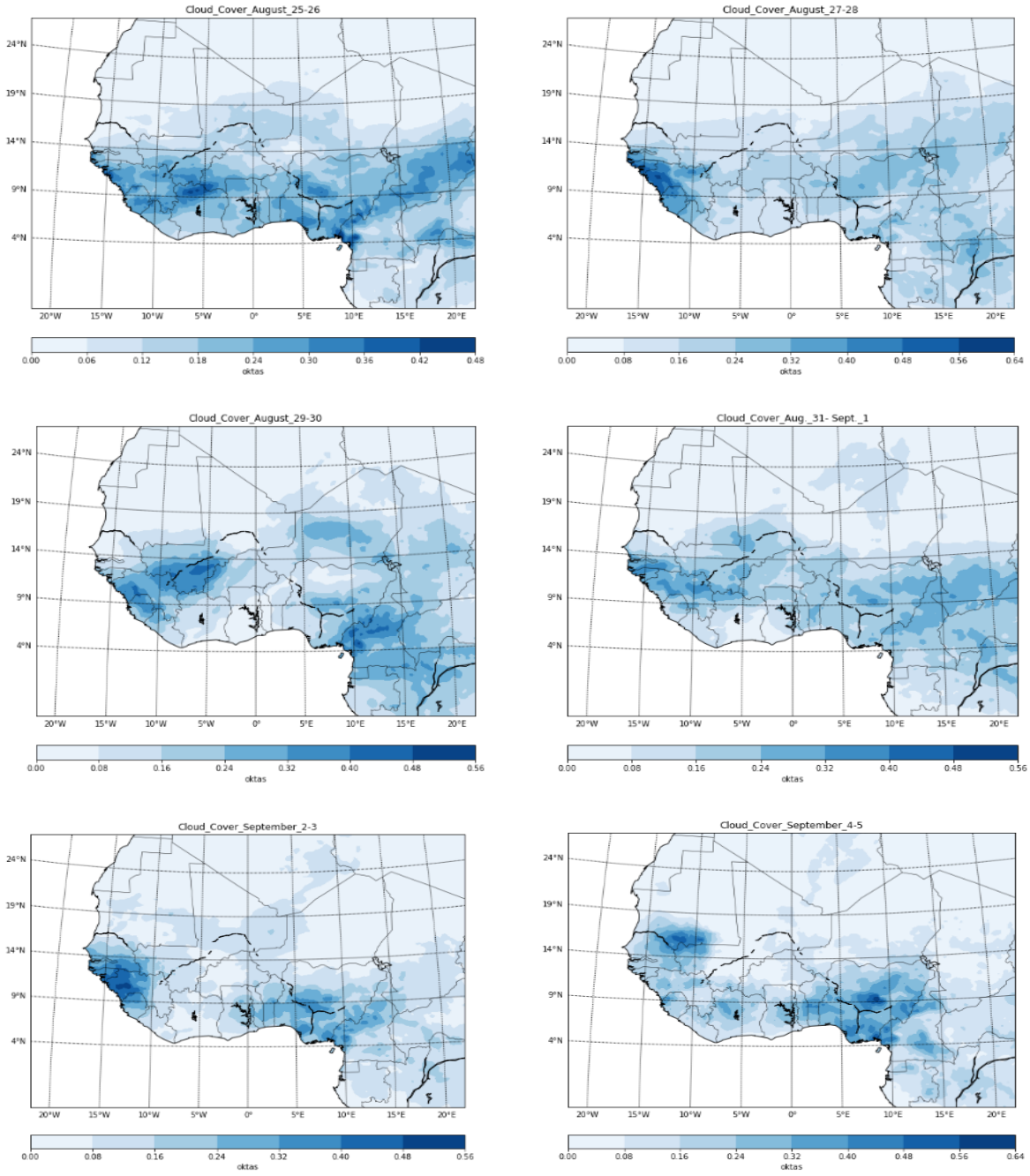

Figure 4.71: Non-feedback cloud cover of 25th Aug. – 5th Sept. 2009 over West Africa.

Considering the cloud cover of non-feedback mechanisms, figure 4.71 of 25th – 26th August showed a strong cloud at the border of Mali, Cote d'Ivoire, and Senegal. This low cloud extended to areas around the Gulf of Guinea. The same scenario can be found around the eastern part of Nigeria, which also extended to western Cameroun. The Chad Republic also had strong clouds, which span from the eastern part to the southwestern part of the country. There are signs of high cloud which extend up to 20°N compared to the feedback scenario. Observations from the figure for the 27th – 28th of August revealed an almost similar scenario with the figure and that of the feedback scenario of the same date. The countries around the Gulf of Guinea, Sierra Leone, Guinea Liberia, and Guinea Bissau were under the influence of strong clouds. Other parts of West Africa are covered with light clouds up to about 22°N. Also covered with light clouds are the central African countries of Chad Republic, Cameroun, Central Africa Republic, and Gabon. The figure for the 29th – 30th of August showed a developing and propagating cloud around the eastern part of Nigeria, close to the Mambilla plateau and the border of Cameroun. Comparing the initial figure with this, it can be deduced that the clouds started it developing process in the initial figure but have developed into some precipitation-laden clouds here. Mali and the areas of the Gulf of Guinea also possessed strong clouds. Comparing the figures from the two different outputs, feedback and non-feedback, it was obvious that the figure from the feedback mechanism possesses more clouds, both light and thick clouds, with a high probability of heavy precipitation outcome. The clouds in this figure of the 29th – 30th of August exceeded 24°N latitude. The figure for the 31st of August – the 1st of September showed scattered strong clouds over the inland areas of the central areas of the region. Some of the coastline countries of the region were devoid of any strong clouds but have the presence of light clouds, but Cote d'Ivoire and southern Ghana had no sign of clouds at all. There was an isolated light cloud over the northern Niger Republic and the border of Algeria and Libya.

The isolated light cloud exceeded the 24°N latitudinal position. Aside from the areas around the Gulf of Guinea and southern Nigeria, the figure for the 2nd – 3rd September showed most of the West Africa region devoid of strong clouds. Though, there were patches of light clouds scattered all over the region, as well as central and northern Africa. Some of the light clouds exceeded 25°N, extending from western Algeria to a small part of Libya. The figure for the 4th – 5th of September showed more parts of Nigeria, especially the northern part which was not covered by the cloud in the preceding day, having an almost overcast. This thick cloud was observed to be present over the Republic of Benin and parts of Togo and Ghana. The border of Senegal and Mauritania also recorded a strong cloud, while there is a developing cloud over Cote d'Ivoire. Based on the comparison between the feedback and non-feedback mechanism, it can be deduced from the simulated results that the latter had more light clouds but towering to a high latitudinal position when compared with the former, but the feedback outputs showed thicker clouds around central Africa.

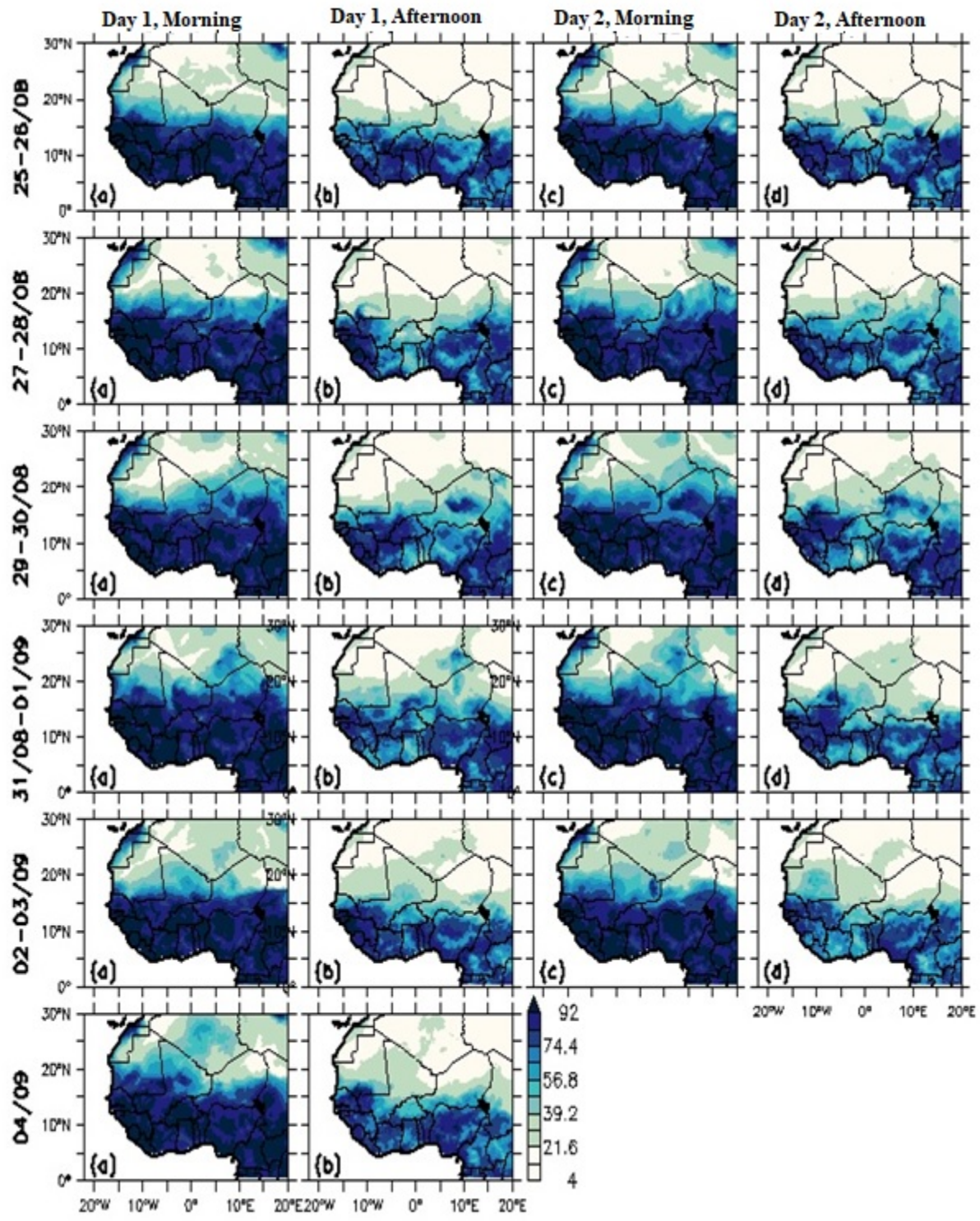

Figure 4.72: Non-feedback surface relative humidity of 25th Aug. – 5th Sept. 2009 over West Africa.

The relative humidity of the surface and upper level was also considered under the non-feedback situation, as they were under the radiative feedback mechanism. The 25th – 26th day of August in figure 4.72 showed a high relative humidity of above 92% in the morning period of both days, exceeding 15^{o}N. The relative humidity values over the West African countries of Mauritania, Niger, and Mali, which are closer to the North African region, were between 40% and 75%. There was variability in the relative humidity distribution across the North African region. While most parts of Algeria recorded relative humidity of about 4% - 20%, Libya recorded about 40% within its central regions, while the northern axis of the country recorded well over 70% in moisture content in the atmosphere. This high moisture content in the northern axis of Libya can be attributed to the presence of its closeness to the Mediterranean Sea (Knippertz *et al.*, 2003; Schilling *et al.*, 2020). The Moroccan axis also recorded high relative humidity of over 80%. This can also be attributed to its closeness to the canary sea. The afternoon period over Northern Africa was low on relative humidity amount, with most parts of the regions recording less than 20% in moisture content in the atmosphere. Gulf of Guinea areas of the West African region recorded high relative humidity of about 85%, while the inland areas recorded moisture content in the atmosphere of less than 70%. The coastal city of Accra (Ghana) also recorded less relative humidity amount when compared to other coastal cities in the neighboring countries of Togo, Benin, and Nigeria. This is in support of the earlier studies (Acheampong, 1982; and Amekudzi *et al.*, 2015) which affirmed the abnormality in the Accra weather situation when compared to other locations across the same zone. Cameroun and the Central Africa Republic also recorded relative humidity of less than 70% while the northern and southern Chad Republic recorded low relative humidity of less than 20% and high relative humidity above 80% respectively. From the observation of the remaining figures from the 27th of August – the 4th of September, the morning periods showed high relative humidity that ranges

between 80% and above 90% from the coast to about 15^{o}N over the West African region, while the inland areas over the Sahara region of West Africa to some North African countries recorded moisture content in the atmosphere between less than 20% and about 50%. The afternoon hours of the same days showed almost a general view of both high and low relative humidity over some coastal countries, while the countries close to the North Africa region upward, that is areas north of 15^{o}N, were under a very low relative humidity of between 40% and less than 20%. In summary, the feedback outputs tend to have higher relative humidity amounts both during the morning and especially in the afternoon hours compared to the non-feedback outputs. Thus, it can be concluded from the outputs of the simulations that the radiative interaction of the aerosol with the relative humidity at the surface helps to increase and also retained the number of moisture contents in the atmosphere, especially during the afternoon periods.

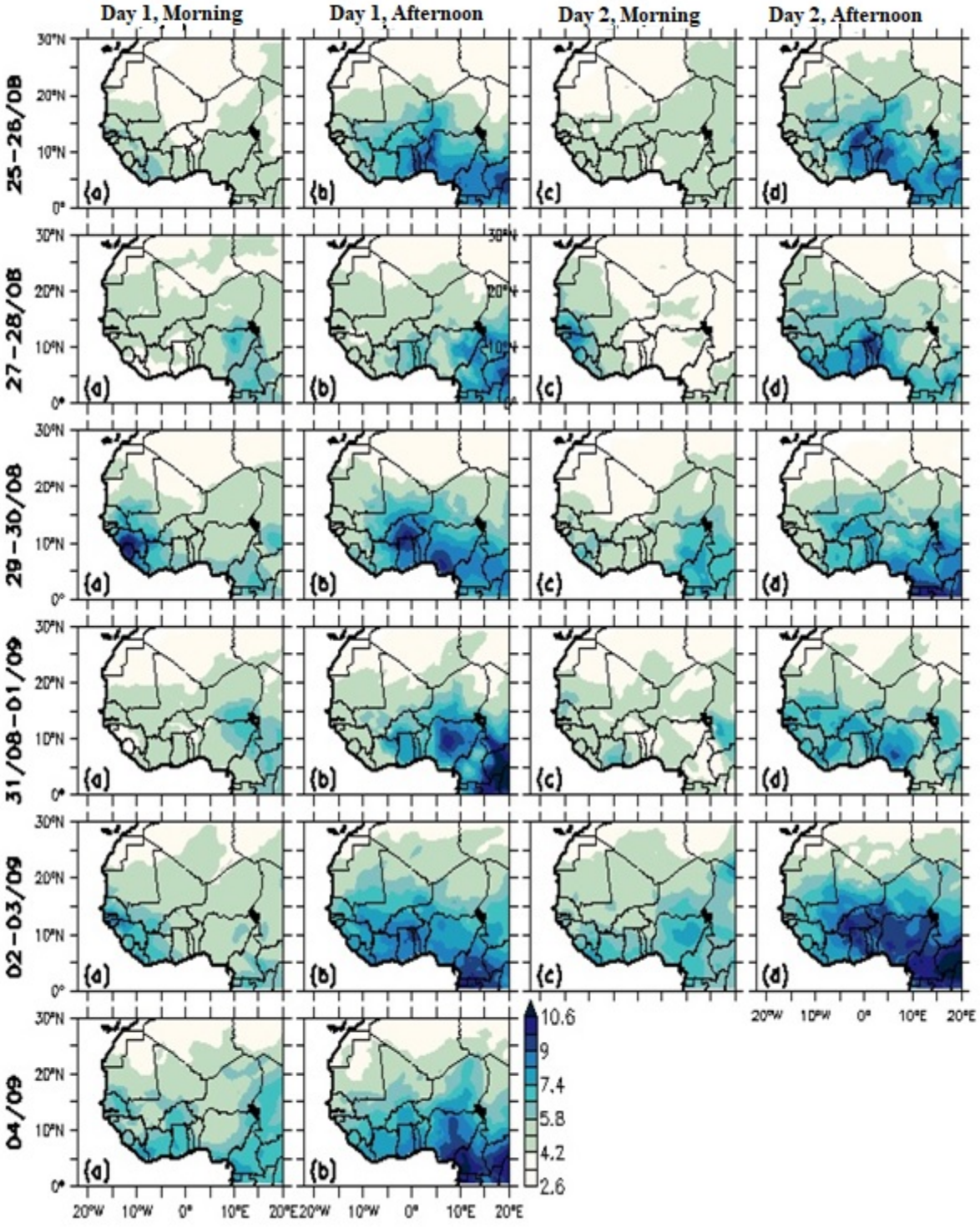

Figure 4.73: Non-feedback upper-level relative humidity of 25th Aug. – 5th Sept. 2009 over West Africa.

Moisture content in the upper layer of the atmosphere (as seen in figure 4.73) exhibited the presence of low moisture content when compared to the surface under the two (2) conditions. But feedback conditions seem to contain more moisture in the atmosphere than non-feedback conditions under the upper-level scenario for both mechanisms. The figure for the 25th – 26th of August showed the morning hours having less relative humidity amount over the coastal countries and some inland areas compared to the afternoon period. The North Africa and Sahara axes of West Africa's relative humidity amount range between 2% and 4%. The afternoon periods of the same days had more moisture content in the atmosphere around the coastline areas of West Africa and the Central African countries of Cameroun and the Central Africa Republic which ranges between 9% and 10%. The Sahara area of West Africa to the southern part of Algeria also had a moisture content of about 5%, while Libya recorded a low moisture content of 3% - 4%. The figures for the 2nd – 3rd of September showed that the relative humidity is high throughout the days. There were higher moisture contents around the coastal and central African areas compared to the other days. Relative humidity was not less than 6% even over the North African countries of Algeria and Libya. The afternoon of the 3rd of September recorded a relative humidity of about 10% from the central African region to the West African countries of Nigeria Benin Republic, Togo, and Burkina Faso. From general observations, the afternoon periods seem to have more moisture content availability in the atmosphere compared to the morning periods. Though the morning of 29th August had a relative humidity record of about 10% over Sierra Leone and Guinea Bissau, the build-up of that moisture started the morning of the preceding day. The relative humidity distribution in the feedback situation was evenly distributed between the morning and afternoon hours but the non-feedback condition showed a contrasting situation between the morning and afternoon periods.

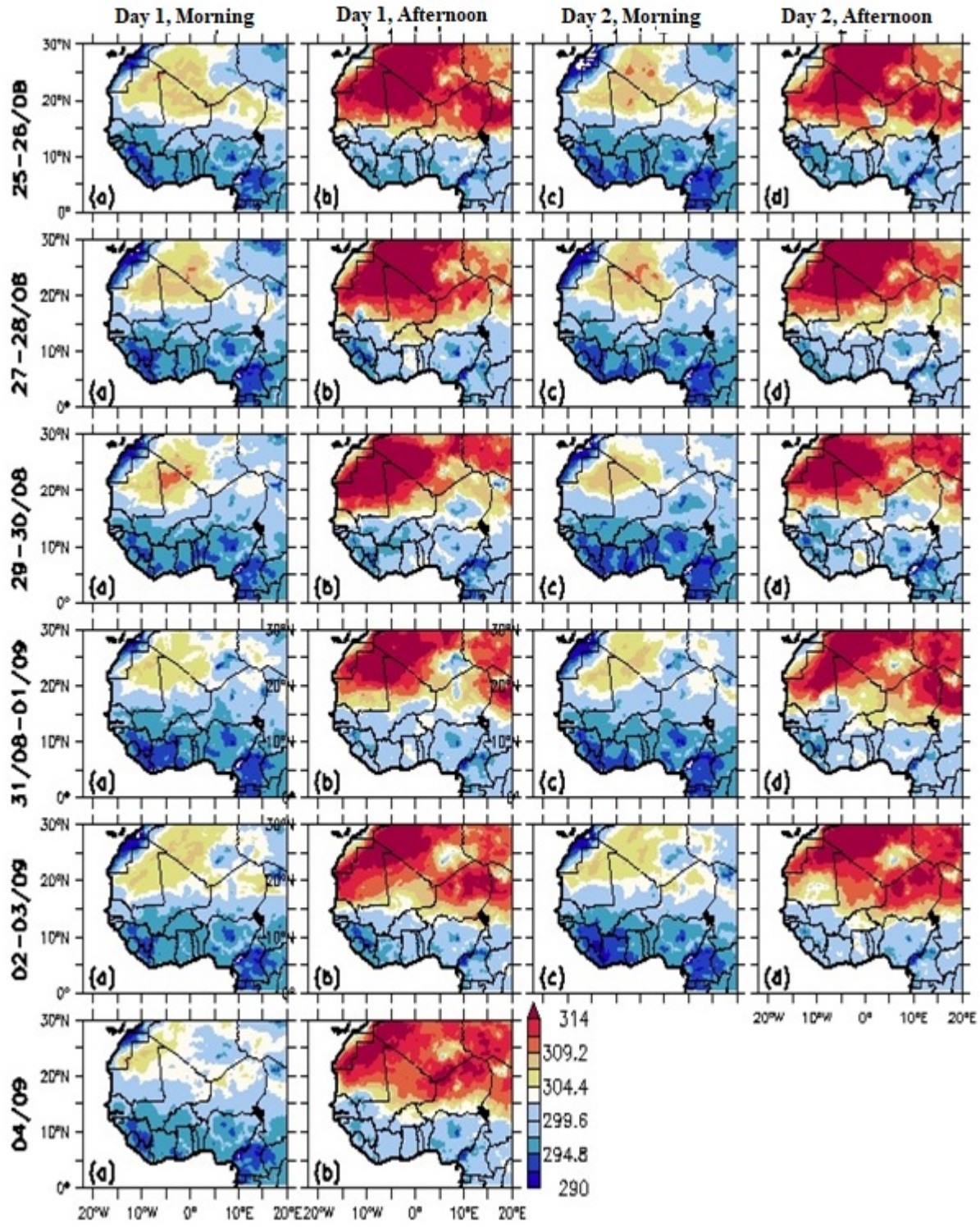

Figure 4.74: Non-feedback surface temperature of 25th Aug. – 5th Sept. 2009 over West Africa.

Going by the information from the surface non-feedback temperature outputs as shown in figure 4.74 above, and comparing the same to the feedback scenario in figure 4.68 showed a vast difference between the two (2) outputs, especially in the morning hours. The figures here, under the non-feedback scenario, showed a cool scenario during the morning hours all through the days of simulation, with the highest temperature values ranging between 304 K and 309 K. In comparison to the feedback scenario where the morning hours recorded high values of above 310 K which was the highest value in the figure. The areas south of 15^{o}N and up to 10^{o}N showed a cool temperature situation of about 295 K – 300 K over most countries such as Senegal, The Gambia, southern Mali, Niger, and Chad Republic, while it was cooler over Central Africa country of Cameroun, some parts of Nigeria and the Gulf of Guinea countries of Liberia, Sierra Leone, Guinea, and Guinea Bissau. The afternoon scenario showed high temperatures over areas north of 15^{o}N, which span across the North African countries of Morocco, Mauritania, Algeria, Mali, Chad Republic, and some parts of Libya. Summarily, the figures from the morning period of feedback output when compared to non-feedback suggest that aerosols, in their direct effects, help in reflecting solar radiation into space and make the atmosphere warmer. This conforms to the studies (Twomey, 1977; Seinfeld *et al.*, 2016).

The distribution of the temperature around this time of the year (wet season) as a result of the latitudinal position of the ITD, causing the coastal areas and areas south of ITD to be under the influence of monsoon flows (Oluleye and Okogbue, 2013), resulted to areas north of the latitude to be under the influence of dust. These absorbing aerosols heat the atmosphere (comparing the figure below) and cool the surface which leads to the stabilization of the boundary layers (BL) and the reduction in sensible and latent heat fluxes (Chung and Seinfeld, 2002).

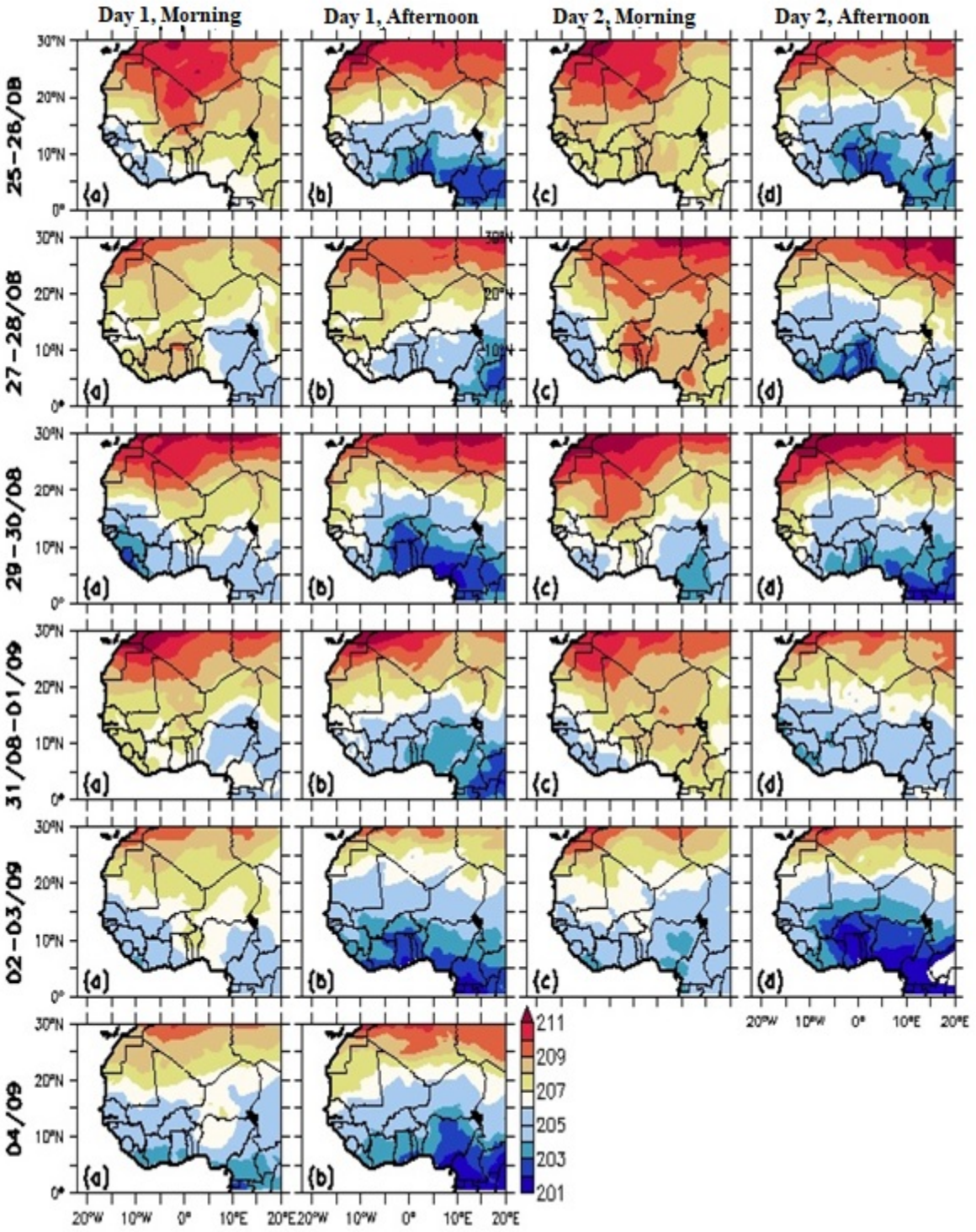

Figure 4.75: Non-feedback upper-level temperature of 25th Aug. – 5th Sept. 2009 over West Africa.

The figures for the upper-level temperature (figure 4.75) showed a high value over the morning hours. The high-temperature values spanned across the North African countries of Morocco, Algeria, and Libya and to the West African region of Mauritania, Mali, and part of Niger Republic as shown in the first figure of the 25th – 26th August. The coastal axis recorded temperature values that range between 205 K over the Gulf of Guinea areas of Liberia, Sierra Leone, and Guinea and 207 K over southern Nigeria, Ghana, and Togo through to Senegal, southern Mauritania, and Mali. The figure depicting the afternoon of the 25th of August showed a cooler temperature of about 200 K over the Central Africa Republic, Cameroun through to eastern Nigeria and the western part of Nigeria through to southern Benin, Togo, and Accra axis of Ghana. The hot temperature was limited to only the North African region, leaving the West African region warmer and cooler with a temperature range of 201 K – 211 K. On a general observation, the cool (low) temperature was experienced over the West African region in the afternoon period of 29th August and 3rd of September. The cool temperature covers the Central African countries of Cameroun and the Central Africa Republic to the West African coastlines of Nigeria to Ghana, up to 15^{o}N. The hot temperature seems to cover more areas during the morning period than the afternoon period. Comparing the results from both feedback and non-feedback conditions at the upper level, the results showed that the non-feedback at the upper level seems to be warmer in temperature values compared to the feedback mechanism. The scenario in a feedback mechanism can be attributed to the aerosol, e.g., water vapor, in the upper level served as a coolant to reduce the temperature value.

CHAPTER FIVE

5.0 CONCLUSION AND RECOMMENDATION

The research has provided valuable insights into aerosol distribution, its relationship with climatic parameters, and the impact of its radiative effects on convection initiation and propagation, cloud properties, temperature, and relative humidity. The selected aerosol types for this study showed that all pollutants were more pronounced in the dry months of December, January, and February (DJF), excluding dust which was present almost throughout the year over and around Bodélé depression. The findings also showed that most of the monthly trends and spatial distribution of biomass-burning and carbonaceous, as well as dust and $PM_{2.5}$, exhibited the same pattern. This shows that dust and $PM_{2.5}$ may not necessarily be separable by ordinary eyes while some studies have shown the possibility of both biomass and carbon happening simultaneously especially when biomass burning takes place. The daily heavy traffic situation and continuous emission of CO by industries in Ikeja may be responsible for the high carbon pronouncement over the location in the months of March/April/May (MAM). The presence of carbonaceous all through the months of the year over Ikeja cannot be unrelated to anthropogenic factors as it is seen as the commercial hub of West African states. The correlation between the climatic parameters and selected aerosol types showed that there exists some level of relationship between the variables. The findings from the correlation analyses between the aerosol types and climatic parameters at various locations showed a statistically significant relationship in probability value that ranges between 60% - 90% except for the correlation between biomass burning and wind speed which recorded about 40%. Over Praia, there was no existing relationship between all the climatic parameters and biomass-burning and carbonaceous. Results from the correlation also showed that particulate matter exhibits the highest

percentage of a strong relationship with all climatic parameters across all locations, but the savannah regions exhibited a high relationship between climatic variables and aerosol types.

The surface output for the modeled analysis of 21st – 30th December 2015 showed that aerosol (mineral dust) is ever present over the Bodélé depression, but this same feature cannot be seen over the upper-level analysed output. Validating the model output with EUMETSAT images, it can be deduced that model performed well. This assertion was made because the satellite images showed an influx of moisture around the Gulf of Guinea axis of Freetown up to Dakar in Senegal, and this can be said to be responsible for the confined spreading of the dust aerosols to as far as Accra and the eastern part of Cote D'Ivoire. The mixing level height analysis was mostly experienced to be high during the day (afternoon hours) which showed the importance of radiation to atmospheric turbulence. This occurs when the shortwave radiation heats the surface and the longwave radiation is reradiated back into the atmosphere and thus altered the stable atmosphere. The impact of the aerosol on convective initiation and propagation was also obvious in the analysis of the wind profile, as AEJ or TEJ were either altered or the two (2) wind formats (radiative feedback and non-feedback) does not flow in the same direction and not have same speed or strength. Thus, the impact of the radiative feedback on the wind profile for the rainforest region was more pronounced over Abidjan than in other locations within the same region. Also, the continuous vertical wind shear can be said to be responsible for the increasing intensity of convective systems during this period of the year.

The impact on non-local plumes showed that, whereas the non-feedback recorded light but a high latitudinal towering cloud, the radiative feedback output recorded thicker clouds that can be categorized as low clouds (clouds with strong convective activity). The presence of aerosols close to the surface may have been responsible for the retention of a water molecule in the atmosphere,

thus leading to the high relative humidity recorded even during the afternoon hours. The impact of radiative feedback on temperature resulted in high temperatures even during the early morning hours, but the information showed a relatively cool scenario under the non-feedback scenario. Hence, it can be deduced that the aerosols in the atmosphere may have acted as a shield that traps the heat from escaping into the upper atmosphere.

5.2 RECOMMENDATION

The result of this research work certain types of aerosols are available in the atmosphere all throughout the year, especially mineral dust at the point source - *Bodélé depression*. This is against the belief in some quarters that dust is an atmospheric phenomenon associated with dry season. Though, some other aerosol types only occur seasonally. But the monthly trend showed that most aerosol types are more prevalent during the dry seasons, while the aerosol types can be said to be negligible or insignificant during the rainy season. The presence of these aerosol types also showed that there exists certain level of relationship between the aerosols and some climatic parameters. And from the outputs of the COSMO-MUSCAT coupling modelling, the results showed that the model is good enough to capture episodes of these atmospheric-related events (aerosols and heavy precipitation) despite been used over West Africa for the first time, though there is room for improvement of the model. Also, the difference between aerosol radiative feedback and non-feedback mechanism on other meteorological (climatic) variables also showed that there is a relationship and impacts/effects of aerosols on these parameters. Hence, these aerosols' presence in the atmosphere should be put into consideration when making forecasts for heavy precipitation in terms of its characteristics.

CONTRIBUTION TO KNOWLEDGE

1.) The research work has produced two (2) publications, thereby adding or contributing to existing knowledge in literatures.

2.) The results from the research will help to inform meteorological agencies' decisions in their seasonal weather forecast by considering aerosols' presence during the forecast process.

3.) Policy makers on health related matters can make plans for air-pollution related diseases and can also help make adequate preparation for any eventuality.

REFERENCES

Abass, K. (2009): Regional Geography of Ghana for Senior High Schools and Undergraduates. Accra: Pictish Publications.

Abiodun, B. J., and Omotosho, J. B. (2007): A Numerical Study of Moisture Build-up and Rainfall over West Africa. *Meteorological Applications: A Journal of Forecasting, Practical Applications, Training Techniques and Modelling*, 14(3), 209-225.

Acheampong, P.K. (1982): Rainfall Anomaly along the Coast of Ghana – Its Nature and Causes. *Geogr. Ann.* 64(A) (3-4): 199-211.

Ackerman, A. S., Toon, O. B., Stevens, D. E., Heymsfield, A. J., Ramanathan, V., and Welton, E. J. (2000): Reduction of Tropical Cloudiness by Soot. *Science*, 288, 1042– 1047, doi:10.1126/science.288.5468.1042.

Adefolalu, D.O. (1972): On the Mean Troposphere and Lower Tropospheric Features of the Troposphere over West Africa. *M.Sc. thesis,* 321*pp, Dept. of Meteor.FSU, USA.*

Adefolalu, D.O. (1974): On the Scale Interactions and the Lower Tropospheric Summer Easterly Perturbation in Tropical West Africa. *Ph.D thesis. The Florida State University,* 276 *pp.*

Adefolalu, D.O. (1983): Monsoon onset in West Africa Application of Satellite Imagery. *Archives for Met. Geophy. and Brok*1. *Ser. B.* **32,** 219-239

Adefolalu, D. O. (1984): Weather Hazards in Calabar—Nigeria. *Geo. Journal*, *9*, 359-368.

Adekoya, J. O. (1979): The Little Dry Season in West Africa. *(Doctoral dissertation, M. Sc. Thesis. Dept. of Meteorology, Florida State University, USA).*

Amekudzi, L. K., Yamba, E. I., Preko, K., Asare, E. O., Aryee, J., Baidu, M., and Codjoe, S. N. (2015): Variability in Rainfall Onset, Cessation and Length of Rainy Season for the Various Agro-ecological Zones of Ghana. *Climate*, *3*(2), 416-434.

Ancellet, G., Pelon, J., Totems, J., Chazette, P., Bazureau, A., Sicard, M., Di lorio, T., Dulac, F., and Mallet, M. (2016): Long-range Transport and Mixing of Aerosol Sources during the 2013 North American Biomass Burning Episode: Analysis of Multiple Lidar Observations in the Western Mediterranean Basin. *Atmospheric Chemistry and Physics*, *16*(7), 4725-4742.

Anderson, C.J. and Arritt, R.W. (1998): Mesoscale Convective Complexes and Persistent Elongated Convective Systems over the United States during 1992 and 1993. *Mon. Wea. Rev.,* **126,** 578-599.

Andreae, M. O. (2019): Emission of Trace Gases and Aerosols from Biomass Burning: An Updated Assessment. *Atmospheric Chemistry and Physics*, *19*(13), 8523-8546.

Arevalo, J., Puentes, Y., and Pitkanen, S. (2016): Bio-Carbon and Rural Development in West Africa (BIODEV) – Assessment of Solid Woodfuel Situation in Sierra Leone and Burkina Faso. *Unpublished manuscript.*

Aron, R. (1983): Mixing Height — An Inconsistent Indicator of Potential Air Pollution Concentrations. *Atmospheric Environment (1967)*, *17*(11), 2193-2197.

Assamoi, E. M., and Liousse, C. (2010): A New Inventory for Two-wheel Vehicle Emissions in West Africa for 2002. *Atmospheric Environment*, *44*(32), 3985-3996.

Baldauf, M., Seifert, A., Förstner, J., Majewski, D., Raschendorfer, M., and Reinhardt, T. (2011): Operational Convective-Scale Numerical Weather Prediction with the COSMO Model: Description and Sensitivities. *Monthly Weather Review*, *139*(12), 3887-3905, doi:10.1175/MWR-D-10-05013.1.

Balogun, E.E. (1974): The Origin of Some Weather Disturbances over West Africa. *WASA Conf. Dakar* 1974.

Balogun, E.E. (1984): Seasonal and Spatial Variations in Thunderstorm Activity over Nigeria. *Weather* **36,** 192-196.

Barbosa, P., Stroppiana, D., Grégoire, J. M., and Pereira, J. C. (1999): An Assessment of Vegetation Fire in Africa (1981-1991): Burned Areas, Burned Biomass, and Atmospheric Emissions. *Global Biogeochem. Cycles,* **108,** 10.1029/1999GB900042.

Barefors, B. (1964): Disturbances in West Africa as Gravity Waves in the Inter-Tropical Discontinuity Surface. *Proc. Symp. on Trop. Met., Tech. Note No.* **29,** *Nig. Met. Dept., Lagos, Nigeria.*10 pp.

Barnes, G. and Sieckman, K. (1984): The Environment of Fast and Slow moving Tropical Mesoscale Convective Cloud Lines. *Mon. Wea. Rev.,* **112,** p 1782-1794.

Bello, N. J. (1989): On the Reliability of the Methods of Predicting the Onset and Cessation of the Rains in a Tropical Wet and Dry Climate, Ondo Nigeria as a case study. *Nigerian Meteorological Journal,* **1,** 41-54.

Ben-Ami, Y., Koren, I., and Altaratz, O. (2009): Patterns of North African Dust Transport over the Atlantic: Winter vs Summer, based on CALIPSO first year data. *Atmos. Chem. Phy.,* **9,** 10.5194/acp-9-7867-2009.

Bergeron, T. (1935): On the Physics of Cloud and Precipitation. *Proceedings of the Fifth Assembly of the International Union of Geodesy and Geophysics,* 2, 156-178.

Beucher, F., Lafore, J.-P., and Chapelon, N. (2019): Simulation and Analysis of the Moist Vortex Associated with the Extreme Rain Event of Ouagadougou in 2009. *Quart. Journ. of Roy. Met. Soc.* DOI:10.1002/qj.3645.

Bluestein, H.B. and Jain, M.H. (1985): Formation of Mesoscale Lines of Propagation; Severe Squall Lines in Oklahoma during Spring. *J. of Atmos. Science,* pg. 1711-1732

Bond, T. C., Doherty, S. J., Fahey, D. W., Forster, P. M., Berntsen, T., DeAngelo, B. J., Flanner, M. G., Ghan, S., Kärcher, B., Koch, D., Kinne, S., Kondo, Y., Quinn, P. K., Sarofim, M. C., Schultz, M. G., Schulz, M., Venkataraman, C., Zhang, H., Zhang, S., Bellouin, N., Guttikunda, S. K., Hopke, P. K., Jacobson, M. Z., Kaiser, J. W., Kilmont, Z., Lohmann, U., Schwarz, J. P., Shindell, D., Storelvmo, T., Warren, S. G., and Zender, C. S. (2013): Bounding the Role of Black Carbon in the Climate System: A Scientific Assessment. *Journal of geophysical research: Atmospheres*, *118*(11), 5380-5552.

Bou Karam, D., Flamant, C., Knippertz, P., Reitebuch, O., Pelon, P., Chong, M., and Dabas, A. (2008): Dust Emissions over the Sahel Associated with the West African Monsoon Inter-Tropical Discontinuity Region: A Representative Case-study. *Q. J. R. Meteorol. Soc.* 134: 621–634.

Boulon, J., Sellegri, K., Hervo, M., and Laj, P. (2011): Observations of Nucleation of New Particles in a Volcanic Plume. *Proceedings of the National Academy of sciences*, *108*(30), 12223-12226.

Bounoua, L. (1980): Relation enre Champ de Vent, Gene´seet Propagation Deslignes de Grains oust Africaines. *Me´moire de fin d'e´tude pour le Diplomed'ingenieurd'eta de la Meteorologie,* **108** pp. [Available from IHFR, BP7019, Seddikia, Oran, Algeria].

Bovallius, A. K. E., Bucht, B., Roffey, R., and Anäs, P. (1978): Three-year Investigation of the Natural Airborne Bacterial Flora at Four Localities in Sweden. *Applied and Environmental Microbiology*, *35*(5), 847-852.

Brown, S., Gillespie, A. J. R. and Lugo, A. E. (1989): Biomass Estimation Methods for Tropical Forests with Applications to Forest Inventory Data. *Forest Sci.* 35, 881–902.

Brunsell, N. A., Mechem, D. B., and Anderson, M. C. (2011): Surface Heterogeneity Impacts on Boundary Layer Dynamics via Energy Balance Partitioning. *Atmospheric Chemistry and Physics*, *11*(7), 3403-3416.

Burpee, R. W. (1972): The Origin and Structure of Easterly Waves in the Lower Troposphere of North Africa. *Journal of the Atmospheric Sciences*, *29*(1), 77-90.

Capes, G., Johnson, B., McFiggans, G., Williams, P. I., Haywood, J., and Coe, H. (2008): Aging of Biomass Burning Aerosols over West Africa: Aircraft Measurements of Chemical Composition, Microphysical Properties, and Emission Ratios. *Journal of Geophysical Research: Atmospheres*, *113*(D23). doi:10.1029/2008JD009845.

Capes, G., Murphy. J. G., Reeves, C. E., McQuaid, J. B., Hamilton, J. F., Hopkins, J. R., Crosier, J., Williams, P. I., and Coe, H. (2009): Secondary Organic Aerosol from Biogenic VOCs over West Africa during AMMA. *Atmos. Chem. Phys*., 9, 3841–3850.

Carbone, R.E., Tuttle, J.D., Ahijevich, D.A., and Trier, S. B. (2002): Inferences of Predictability Associated with Warm Season Precipitation Episodes. *J. Atmos. Sci.,* **59,** 2033-2056.

Cavalieri, D. J., Markus, T., Hall, D. K., Ivanoff, A., and Glick, E. (2010): Assessment of AMSRE Antarctic Winter Sea-ice Concentrations using Aqua MODIS. *IEEE Transactions on Geoscience and Remote Sensing*, *48*(9), 3331-3339.

Chancellor, J. (1946): West African Weather Patterns. *M.Sc. thesis, University of Chicago,* 150pp.

Changnon, S. A. (1957): Thunderstorm-Precipitation Relations in Illinois. *Illinois State Water Survey Rep. of Investigation* 34*, Champaign, IL,* 24 *pp. [Available from Illinois Water Survey. Champaign,* **11,** 61820-1.

Changnon, S. A. (2001a): Damaging Thunderstorm Activity in the United States. B*ull. Amer. Meteor. Soc.,* **82,** 597-608.

Changnon, S. A. (2001b): A National Index of Losses Caused by Weather and Climate Extremes. *Phys. Geogr.,* **18,** 1-29.

Charlson, R. J., Schwartz, S. E., Hales, J. M., Cess, R. D., Coakley Jr, J. A., Hansen, J. E., and Hofmann, D. J. (1992): Climate Forcing by Anthropogenic Aerosols. *Science*, *255*(5043), 423-430.

Chen, S., Houze, R., and Mapes, B. (1996): Multi-scale Variability of Deep Convection in Relation to Large-Scale Circulation in TOGO-COARE. *J. Atmos. Sci., vol.* **53,** no 10, p 1380-1409.

Chiapello, I., Bergametti, G., Gomes, L., Chatenet, B., Dulac, F., Pimenta, J., and Suares, E. S. (1995): An Additional Low-Layer Transport of Sahelian and Saharan Dust over the North-Eastern Tropical Atlantic. *Geophys. Res. Lett.,* **22,** 10.1029/95GL03313.

Chou, C., Formenti, P., Maille, M., Ausset, P., Helas, G., Osborne, S., and Harrison, M. (2008): Size Distribution, Shape and Composition of Dust Aerosols Collected during the AMMA SOP0 Field Campaign in the northeast of Niger, January 2006. *J. Geophys. Res*, *113*, D00C10.

Chung, S. H., and Seinfeld, J. H. (2002): Global Distribution and Climate Forcing of Carbonaceous Aerosols. *Journal of Geophysical Research: Atmospheres*, *107*(D19), AAC-14.

Cooper, O. R., Langford, A. O., Parrish, D. D., and Fahey, D. W. (2015): Challenges of a Lowered U.S. Ozone Standard. *Science* 348: 1096-1097.

Crippa, M., Guizzardi, D., Muntean, M., Schaaf, E., Dentener, F., van Aardenne, J. A., Monni, S., Doering, U., Olivier, J. G. J., Pagliari, V., and Janssens-Maenhout, G. (2018): Gridded Emissions of Air Pollutants for the Period 1970–2012 within EDGAR v4.3.2. *Earth Syst. Sci. Data*, 10, 1987–2013. doi.org/10.5194/essd-10-1987-2018.

Crumeyrolle, S., Gomes, L., Tulet, P., Matsuki, A., Schwarzenboeck, A., & Crahan, K. (2008): Increase of the Aerosol Hygroscopicity by Aqueous mixing in a Mesoscale Convective System: A Case Study from the AMMA Campaign. *Atmospheric Chemistry and Physics Discussions*, *8*(3), 10057-10103.

Cuesta, J., Marsham, J. H., Parker, D. J., & Flamant, C. (2009): Dynamical Mechanisms Controlling the Vertical Redistribution of Dust and the Thermodynamic Structure of the West Saharan Atmospheric Boundary Layer during summer. *Atmospheric Science Letters*, *10*(1), 34-42.

Czarnecka, M., Nidzgorska-Lencewicz, J., and Rawicki, K. (2019): Temporal Structure of Thermal Inversions in Łeba (Poland). *Theor. Appl. Climatol.* 136, 1-13.

Danjuma, A., Silué, S., Ogunjobi, K. O., Vogel, H., N'Datchoh, E. T., Yoboué, V., Diedhiou, A., and Vogel, B. (2021): Biomass Burning Effects on the Climate over Southern West Africa during the Summer Monsoon. In: Oguge, N., Ayal, D., Adeleke, L., da Silva, I. (eds) African Handbook of Climate Change Adaptation. Springer, Cham. https://doi.org/10.1007/978-3-030-45106-6_86.

Darfour, B., and Rosentrater, K.A. (2016): Agriculture and Food Security in Ghana. Agricultural and Biosystems Engineering Conference Proceedings and Presentations, 478, 1–16.

De Longueville, F., Hountondji, Y.C., Henry, S., and Ozer, P. (2010): What do we know about the Effects of Desert Dust on Air Quality and Human Health in West Africa compared to other Regions? *Sci. Tot. Environ*., 409:1–8.

Derimian, Y., Léon, J. F., Dubovik, O., Chiapello, I., Tanré, D., Sinyuk, A., Auriol, F., Podvin, T., Brogniez, G., and Holben, B. N. (2008): Radiative Properties of Aerosol Mixture Observed during the Dry Season 2006 over M'Bour, Senegal (African Monsoon Multidisciplinary Analysis campaign). *Journal of Geophysical Research: Atmospheres*, *113*(D23).

Dhonneur, G. (1970): Structure Continue de L'e´quateurme´te´orologiquesurl'Afrique Intertropicale. ASECNA, se´rie I 29:60

Ditas, J., Ma, N., Zhang, Y., Assmann, D., Neumaier, M., Riede, H., Karu, E., Williams, J., Scharffe, D., Wang, Q., Saturno, J., Schwarz, J. P., Katich, J. M., McMeeking, G. R., Zhan, A., Hermann, M., Brenninkmeijer, C. A. M., Andreae, M. O., Hang SU, U. P., and Cheng, Y. (2018): Strong Impact of Wildfires on the Abundance and Aging of Black Carbon in the Lowermost Stratosphere. *Proceedings of the National Academy of Sciences*, *115*(50), E11595-E11603.

Doms, G., Förstner, J., Heise, E., Herzog, H.-J., Mironov, D., Raschendorfer, M., Reinhardt, T., Ritter, B., Schrodin, R., Schulz, J.-P., and Vogel, G. (2011): A Description of the Non-hydrostatic Regional COSMO Model. *Deutscher Wetterdienst.*

Dong, B., Wilcox, L. J., Highwood, E. J., and Sutton, R. T. (2019): Impacts of Recent Decadal Changes in Asian Aerosols on the East Asian Summer Monsoon: Roles of Aerosol–Radiation, and Aerosol–Cloud interactions. *Climate Dynamics*, *53*, 3235-3256.

Dreher, K. L., and Costa, D. L. (2002): Systemic Health Effects of Ambient Air Particulate Matter Exposure. *Journal of Toxicology and Environmental Health, Part A*, *65*(20), 1491-1492.

Driouech, F., Déqué, M., and Mokssit, A. (2009): Numerical Simulation of the Probability Distribution Function of Precipitation over Morocco. *Climate Dynamics*, *32*, 1055-1063.

Duce, R. A., Liss, P. S., Merrill, J. T., Atlas, E. L., Buat-Menard, P., Hicks, B. B., Miller, J. M., Prospero, J. M., Arimoto, R., Church, T. M., Ellis, W., Galloway, J. N., Hansen, L., Jickells, T. D., Knap, A. H., Reinhardt, K. H., Schneider, B., Soudine, A., Tokos, J. J., Tsunogai, S., Wollast, R., and Zhou, M. (1991). The Atmospheric Input of Trace Species to the World Ocean. *Global biogeochemical cycles*, *5*(3), 193-259.

Duvel, J. P. (1990): Convection over Tropical Africa and the Atlantic Ocean during Northern Summer. Part II: Modulation by Easterly Waves. *Monthly Weather Review*, *118*(9), 1855-1868.

Echalar, F., Artaxo, P., Martins, J. V., Yamasoe, M., Gerab, F., Maenhaut, W., and Holben, B. (1998): Long-term Monitoring of Atmospheric Aerosols in the Amazon Basin: Source Identification and Apportionment. *Journal of Geophysical Research: Atmospheres*, *103*(D24), 31849-31864.

Elmore, K. L. (1982): Cell Structure and Evolution within a Squall Line as Revealed by the Doppler Radar. M. Sc. thesis, *School of Meteorology, University of Oklahoma,* 212 pp.

Eltahir, E. A., and Gong, C. (1996): Dynamics of Wet and Dry Years in West Africa. *Journal of Climate*, *9*(5), 1030-1042.

Eludoyin (2009): Monthly variation in the 1985-1994 and 1995-2004 Rainfall Distribution over Five Selected Synoptic Stations in Western Nigeria. *Journal of Meteorology and Climate Science.* 7:**11**-22

Engelstaedter, S. and Washington, R. (2007). Atmospheric Controls on the Annual Cycle of North African Dust. *J. Geophys. Res.*, 112, 10.1029/2006JD007195.

Ervens, B. T. B. W. R., Turpin, B. J., and Weber, R. J. (2011): Secondary Organic Aerosol Formation in Cloud Droplets and Aqueous Particles (aqSOA): A Review of Laboratory, Field and Model Studies. *Atmospheric Chemistry and Physics*, *11*(21), 11069-11102.

FAO, (2005): Fertilizer use by crops in Ghana. Rome: Food and Agriculture Organization of the United Nations.

Fasheun, A. (1979): Observation of a 3-5 day Periodicity and Diurnal Rhythms in Vertical Motion Field over GATE A/B Scale Array during Phase III of the GATE Experiment. *Pre-Wamex Symp. on Wamex Exp. Ibadan* **1,** 3 Nov., 1978.

Findeisen, W., Volken, E., Giesche, A. M., and Brönnimann, S. (2015): Colloidal Meteorological Processes in the Formation of Precipitation. *Meteorologische Zeitschrift,* 24(4), 443-454. doi: 10.1127/metz/2015/0675

Fink, A. H., and Reiner, A. (2003): Spatiotemporal Variability of the Relation between African Easterly Waves and West African Squall Lines in 1998 and 1999. *Journal of Geophysical Research: Atmospheres*, *108*(D11).

Flamant, C., Chaboureau, J. P., Parker, D. J., Taylor, C. M., Cammas, J. P., Bock, O., Timouk, J., and Pelon, J. (2007): Airborne Observations of the Impact of a Convective System on the Planetary Boundary Layer Thermodynamics and Aerosol Distribution in the Inter-Tropical Discontinuity Region of the West African Monsoon. *Quarterly Journal of the Royal Meteorological Society: A journal of the atmospheric sciences, applied meteorology and physical oceanography*, *133*(626), 1175-1189.

Flamant, P., Cuesta, J., Denneulin, M. L., Dabas, A., & Huber, D. (2008): ADM-Aeolus Retrieval Algorithms for Aerosol and Cloud Products. *Tellus A: Dynamic Meteorology and Oceanography*, **60**(2), 273-286.

Fomba, K. W., Müller, K., Van Pinxteren, D., Poulain, L., Van Pinxteren, M., & Herrmann, H. (2014): Long-term Chemical Characterization of Tropical and Marine Aerosols at the Cape Verde Atmospheric Observatory (CVAO) from 2007 to 2011. *Atmospheric Chemistry and Physics*, *14*(17), 8883-8904, https://doi.org/10.5194/acp-14-8883-2014.

Fontaine, B., Trzaska, S., and Janicot, S. (1998): Evolution of the Relationship between Near Global and Atlantic SST Modes and the Rainy Season in West Africa: Statistical Analyses and Sensitivity Experiments. *Climate Dynamics*, *14*(5), 353.

Formenti, P., Rajot, J. L., Desboeufs, K., Caquineau, S., Chevaillier, S., Nava, S., Gaudichet, A., Journet, E., Triquet, S., Alfaro, S., Chiari, M., Haywood, J., Coe, H., and Highwood, E. (2008): Regional Variability of the Composition of Mineral Dust from Western Africa: Results from the AMMA SOP0/DABEX and DODO Field Campaigns. *Journal of Geophysical Research: Atmospheres*, *113*(D23).

Fortune, M. (1977): The West African Squall Line - The Satellite Perspective of a Tropical Tempest. *M. Sc. dissertation, Department of Meteorology, University of Wisconsin, Madison, USA.* 100 pp.

Fovell, R. G. (2002): Upstream Influence of Numerical simulated Squall Linestorms. *Quart. J. Roy. Meteor. Soc.,* **128,** 893-912.

Fovell, R. G., Mullendore, G. L. and Kim, S. H. (2006): Discrete Propagation in Numerically Simulated Nocturnal Squall Lines. *Mon. Wea. Rev.,***134,** 3735-3752.

Gan, M. A., Kousky, V. E., and Ropelewski, C. F. (2004): The South America Monsoon Circulation and its Relationship to Rainfall over West-Central Brazil. *Journal of Climate*, *17*(1), 47-66.

Garnier, B.J. (1971): Weather Conditions in Nigeria. *Climatological Series #2, Dept. of Geog. McGill University,* **13,** 101-135.

Giglio, L., Randerson, J. T., and van der Werf, G. R. (2013): Analysis of Daily, Monthly, and Annual Burned Area using the Fourth-Generation Global Fire Emissions Database (GFED4), *J. Geophys. Res-Biogeo.*, 118, 317–328, https://doi.org/10.1002/jgrg.20042.

Goudie, A.S., (1996): Climate; Past and Present. *The Physical Geography of Africa,* W. M. Adams, A. S. Goudie and A. R. Orme, Eds., Oxford, 34-59.

Grieshop, A. P., Logue, J. M., Donahue, N. M., and Robinson, A. L. (2009): Laboratory Investigation of Photochemical Oxidation of Organic Aerosol from Wood Fires 1: Measurement and Simulation of Organic Aerosol Evolution. *Atmospheric Chemistry and Physics*, *9*(4), 1263-1277.

Grist and Nicholson, S.E. (2001): A Study of the Dynamic Factors Influencing the Variability of Rainfall in the West African Sahel. *J. Climate,* **14,** 1337-3171.

Gunn, R., & Phillips, B. B. (1957): An Experimental Investigation of the Effect of Air Pollution on the Initiation of Rain. *J. Meteorol.,* 14(3), 272-280, doi:10.1175/1520-0469(1957).

Hall, C. A. S., and Uhlig, J. (1991): Refining Estimates of Carbon Released from Tropical Land Use Change. *Can. J. Forest Res*. 21, 118–131.

Hamilton, R. A. and Archibold, J. W. (1945): Meteorology of Nigeria and Adjacent Territory. *Quart. Journ. Roy. Met. Soc.,* **3,** 213-265

Han, Q.Y., Rossow, W.B., Chou, J., and Welch, R.M. (1998): A global survey of the relationships of clouds albedo and liquid water path with droplet size using ISCCP. *J Clima* 11: 1516-1528.

Hand, J. L., Schichtel, B. A., Malm, W. C., and Pitchford, M. L. (2012): Particulate Sulfate Ion Concentration and SO_2 Emission Trends in the United States from the Early 1990s through 2010. *Atmospheric Chemistry and Physics*, *12*(21), 10353-10365.

Harrison, S.P., Kohfeld, K.E., Roelandt, C., and Claquin, T. (2001): The Role of Dust in Climate Changes Today, at the Last Glacial Maximum, and in the Future. *Earth-sci Rev* 54: 43-80.

Haywood, J., and Boucher, O. (2000): Estimates of the Direct and Indirect Radiative Forcing due to Tropospheric Aerosols: A Review. Rev *Geophy* 38: 513-543.

Haywood, J. M., Pelon, J., Formenti, P., Bharmal, N., Brooks, M., Capes, G., Chazette, P., Chou, C., Christopher, C., Coe, H., Cuesta, J., Derimian, Y., Desboeufs, K., Greed, G., Harrison, M., Heese, B., Highwood, J., Johnson, B., Mallet, M., Marticorena, B., Marsham, J., Milton, S., Myhre, G., Osborne, R., Parker, J., Rajot, J. L., Schulz, M., Slingo, A., Tanré, D., and Tulet, P. (2008): Overview of the Dust and Biomass-Burning Experiment and African Monsoon Multidisciplinary Analysis Special Observing Period-0. *Journal of Geophysical Research: Atmospheres*, *113*(D23).

Heinold, B., Tegen, I., Schepanski, K., Tesche, M., Esselborn, M., Freudenthaler, V., Gross, S., Kandler, K., Knippertz, P., Müller, D., Schladitz, A., Toledano, C., Weinzieri, B., Ansmann, A., Althausen, D., Müller, T., Petzold, A., and Wiedensohler, A. (2011): Regional Modelling of Saharan Dust and Biomass-Burning Smoke: Part I: Model Description and Evaluation. *Tellus B: Chemical and Physical Meteorology*, *63*(4), 781-799. doi:10.1111/j.1600-0889.2011.00570.x.

Herrmann, I., Stahr, K., and Jahn, R. (1999): The Importance of Source Region Identification and their Properties for Soil-derived Dust: The Case of Harmattan Dust for Eastern West Africa. *Contrib. Atmos. Phys.* 72: 141-150.

Hildebrand, P. H. (1998): Shear-Parallel Moist Convection over the Tropical Ocean: A Case Study from 18 February 1993 TOGA COARE. *Monthly weather review*, *126*(7), 1952-1976.

Hinneburg, D., Renner, E., and Wolke, R. (2009): Formation of Secondary Inorganic Aerosols by Power Plant Emissions Exhausted through Cooling Towers in Saxony. *Environmental Science and Pollution Research*, *16*, 25-35.

Hodges, K. I., and Thorncroft C. D. (1997): Distribution and Statistics of African Mesoscale Convective Weather Systems based on the ISCCP Meteosat imagery. *Mon. Weather Rev.,***125,** 2821–2837.

Holanda, B. A., Pöhlker, M. L., Walter, D., Saturno, J., Sörgel, A., Ditas, J., Ditas, F., Schulz, C., Franco, M. A., Wang, Q., Donth, T., Artaxo, P., Barbosa, H. M. J., Borrman, S., Braga, R., Brito, J., Cheng, Y., Dollner, M., Kaiser, J. W., Klimach, T., Knote, C., Krüger, O. O., Fütterer, D., Lavrič, J. V., Ma, N., Machado, L. A. T., Ming, J., Moraise, F. G., Paulsen, H., Sauer, D., Schlager, H., Schneider, J., Su, H., Weinzierl, B., Walser, A., Wendisch, M., Ziereis, H., Zöger, M., Pöschl, U., Andreae, M. O., and Pöhlker, C. (2020): Influx of African Biomass Burning Aerosol during the Amazonian Dry Season through Layered Transatlantic Transport of Black Carbon-rich Smoke. *Atmos. Chem. Phys.,* 20, 4757–4785, https://doi.org/10.5194/acp-20-4757-2020.

Holtslag, A. A. (2003): GABLS Initiates Inter-comparison for Stable Boundary Layer Case. *GEWEX news*, *13*(2), 7-8.

Houze, R. A., Geotis, S. G., Marks Jr., F. D. and West, A. K. (1981): Winter Monsoon Convection in the Vicinity of North Borneo. **Part I:** Structure and Time Variation of the Clouds and Precipitation. *Mon. Wea. Rev.,* **109,** 1595-1614.

Houze, R.A. (1977): Structure and Dynamics of a Tropical Squall Line System. *Mon. Wea. Rev.* **105,** 1540-1567.

Houze, R.A., Smull, B.F. and Dodge, P. (1990): Mesoscale Organization of Spring Time Rainstorms in Oklahoma. *Mon. Wea. Rev.* **118,** 613-654.

Houze, R. A., Jr. (1993): Cloud Dynamics. **573** pp., Academic, San Diego, Calif.

Houze, R. A., Jr., Chen, S. S., Kingsmill, D. E., Serra, Y. and Yuter, S. E. (2000): Convection over the Pacific Warm Pool in relation to the Atmospheric Kelvin-Rossby Wave, *J. Atmos. Sci., **57**, 3058–3089.*

Huang, J., Zhang, C., and Prospero, J. M. (2010): African Dust Outbreaks: A Satellite Perspective of Temporal and Spatial Variability over the Tropical Atlantic Ocean. *J. Geophys. Res.,* **115,** 10.1029/2009JD012516.

Ilesanmi O. O. (1968): The Inter-Tropical Discontinuity and Rainfall in Nigeria, 1956-57. *Seminar paper in climatology, Dept. of Geography, University of Wisconsin, Madison,* **24** *pp.*

Ilesanmi O. O. (1969): A study of Nigerian Rainfall Pattern from the view point of Precipitation Dynamics. *Ph.D. thesis, University of Wisconsin,* **170** *pp.*

Ilesanmi, O. O. (1971): An Empirical Formulation of an ITD Rainfall Model for the Tropics: A Case Study of Nigeria. *Journal of Applied Meteorology (1962-1982)*, 882-891.

Ireland, A. W. (1962): The Little Dry Season of Southern Nigeria. *Nigerian Geographical Journal*, *5*(1), 7-20.

Irving, D. B., Wijffels, S., and Church, J. A. (2019): Anthropogenic Aerosols, Greenhouse Gases, and the Uptake, Transport, and Storage of Excess Heat in the Climate System. *Geophysical Research Letters*, *46*(9), 4894-4903.

Janicot, S., Harzallah, A., Fontaine, B., and Moron, V. (1998): West African Monsoon Dynamics and Eastern Equatorial Atlantic and Pacific SST Anomalies (1970–88). *Journal of Climate*, *11*(8), 1874-1882.

Jirak, I. L. (2002): Satellite and Radar Survey of Mesoscale Convective System Development. *Atmos. Sci. paper No.* **727,** *Colorado State University,* 119 pp.

Jirak, I.L., Cotton, W.R. and McAnelly, R.L. (2003): Radar Survey of Mesoscale Convective System Development. *Mon. Wea. Rev.,* **131,** 2428-2449.

Johnson, R. H. (1986): The Development of Organized Mesoscale Circulations within Oklahoma-Kansas Pre-STORM Convective Systems. *Pre-prints, Inter. Conf. on Monsoon and Mesoscale Meteor., Taiwan.*100-104.

Johnson, B. T., Osborne, S. R., Haywood, J. M., and Harrison, M. A. J. (2008): Aircraft Measurements of Biomass Burning Aerosol over West Africa during DABEX. *Journal of Geophysical Research: Atmospheres*, *113*(D23).

Johnson, B. T., Heese, B., McFarlane, S. A., Chazette, P., Jones, A., and Belloiun, N. (2008b): Vertical Distribution and Radiative Effects of Mineral Dust and Biomass Burning Aerosol over West Africa during DABEX. *J. Geophys. Res.,* **113,** 10.1029/2008JD009848.

Johnston, E. C. (1981): Mesoscale Vorticity Centres Induced by Mesoscale Convective Complexes. *M.Sc. thesis, Dept. of Meteorology, University of Wisconsin,* **54** pp.

Kalu, A. E. (1979): The African Dust Plume: Its Characteristics and Propagation across West Africa in Winter. *SCOPE,* 14, 95-118.

Kamer, L. (2022): Largest Cities in Nigeria in 2021. *Statista Pub.*

Kaneyasu, N., Yamamoto, S., Sato, K., Takami, A., Hayashi, M., Hara, K., Kawamoto, K., Okuda, T., and Hatakeyama, S. (2014): Impact of Long-range Transport of Aerosols on the $PM_{2.5}$ Composition at a Major Metropolitan Area in the Northern Kyushu Area of Japan. *Atmospheric Environment*, *97*, 416-425.

Karaca, F., Anil, I., and Alagha, O. (2009): Long-range Potential Source Contributions of Episodic Aerosol Events to PM10 Profile of a Megacity. *Atmospheric Environment*, *43*(36), 5713-5722.

Karagulian, F., Belis, C. A., Dora, C. F. C., Prüss-Ustün, A. M., Bonjour, S., Adair-Rohani, H., and Amann, M. (2015): Contributions to Cities' Ambient Particulate Matter (PM): A Systematic Review of Local Source Contributions at the Global Level. *Atmospheric environment*, *120*, 475-483.

Karl, M., Dorn, H.-P., Holland, F., Koppmann, R., Poppe, D., Rupp, L., Schaub, A., Wahner, A. (2006): Product Study of the Reaction of OH Radicals with Isoprene in the Atmosphere Simulation Chamber, SAPHIR. *J. Atmos. Chem.,* 55, 167-187.

Karypis, G., Schloegel, K. and Kumar, V. (2003): ParMETIS: Parallel Graph Partitioning and Sparse Matrix Ordering Library (Version 3.1). University of Minnesota.

Kaufman, Y. J., Tanré, D., and Boucher, O. (2002): A Satellite view of Aerosols in the Climate System. *Nature*, **419**(6903), 215-223.

Kaufman, Y. J., Koren, I., Remer, L. A., Tanré, D., Ginoux, P., and Fan, S. (2005): Dust Transport and Deposition Observed from the Terra-Moderate Resolution Imaging Spectroradiometer (MODIS) Spacecraft over the Atlantic Ocean. *J. Geophys. Res.,* 110, D10S12, doi:10.1029/2003JD004436

Kaufman, Y. J., and Koren, I. (2006): Smoke and Pollution Aerosol Effect on Cloud Cover. *Science*, *313*(5787), 655-658.

Kelishadi, R., and Poursafa, P. (2010): Air Pollution and Non-respiratory Health Hazards for Children. *Archives of Medical Science*, *6*(4), 483-495.

Kessinger, C. J. (1983): An Oklahoma squall line; A Multi-Scale Observational and Numerical Study. M. Sc. thesis, *School of Meteorology, University of Oklahoma,* 211 pp.

Kesavanathan, J., and Swift, D. L. (1998): Human Nasal Passage Particle Deposition: The Effect of Particle Size, Flow Rate, and Anatomical Factors. *Aerosol Science and Technology*, *28*(5), 457-463.

Klein, C., Nkrumah, F., Taylor, C. M., and Adefisan, E. A. (2021): Seasonality and Trends of Drivers of Mesoscale Convective Systems in Southern West Africa. *Journal of Climate*, *34*(1), 71-87.

Knippertz, P., Christoph, M., and Speth, P. (2003): Long-term Precipitation Variability in Morocco and the Link to the Large-Scale Circulation in Recent and Future Climates. *Meteorology and Atmospheric Physics*, *83*(1), 67-88.

Knippertz, P. (2008): Dust Mobilization in the West African Heat Trough — The Role of the Diurnal Cycle and of Extra-tropical Synoptic Disturbances. *Meteorol. Zeitschr.*, 17, 553–563.

Knippertz, P., Ansmann, A., Althausen, D., Müller, D., Tesche, M., Bierwirth, E., Dinter, T., Müller, T., von Hoyningen-Huene, W., Schepanski, K., Wendisch, M., Heinold, B., Kandler, K., SchŮTZ, L., and Tegen, I. (2009): Dust Mobilization and Transport in the Northern Sahara during SAMUM 2006—A Meteorological Overview. *Tellus*, 61B, 10.1111/j.1600-0889.2008.00380.x.

Knoth, O. and Wolke, R. (1998b): Implicit-explicit Runge-Kutta Methods for Computing Atmospheric Reactive Flows, *Appl. Numer. Math*. 28, 327–341.

Kolusu, S., Marsham, J., Mulcahy, J., Johnson, B., Dunning, C., Bush, M., and Spracklen, D. (2015): Impacts of Amazonia Biomass Burning Aerosols Assessed from Short-Range Weather Forecasts. *Atmos. Chem. Phys.* 15, 12251-66.

Kommalapati, R. R., & Valsaraj, K. T. (2009): Atmospheric Aerosols and Their Importance. *Atmos. Aerosols.* Chapter 1, pp 1-10, doi:10.1021/bk-2009-1005.ch001

Koren, I., Remer, L. A., Altaratz, O., Martins, J. V., and Davidi, A. (2010): Aerosol-Induced Changes in Convective Cloud Anvils Produce Strong Climate Warming. *Atmospheric Chemistry and Physics*, *10*(10), 5001-5010.

Kuo, Y. H., Cheng, L. S. and Anthes, R. A. (1986): Mesoscale Analysis of Sichuan Flood Catastrophe, 11-15 July, 1981. *Mon. Wea. Rev.,* **114,** 1984-2003.

Lafore, J.-P. and Moncrieff, M.W. (1989): A Numerical Investigation of the Organization and Interaction of the Convective and Stratiform Regions of Tropical Squall Lines. *J. Atmos. Sci.,* **46,** 521-544.

Lafore, J.-P., Flamant, C., Guichard, F., Parker, D. J., Bouniol, D., Fink, A. H., Giraud, V., Gosset, M., Hall, N., Höller, H., Jones, S. C., Protat, A., Roca, R., Roux, F., Saïd, F., and Thorncroft, C. (2011): Progress in Understanding of Weather Systems in West Africa. *Atmospheric Science Letters*, *12*(1), 7-12.

Lafore, J.-P., Beucher, F., Peyrillé, P., Diongue-Niang, A., Chapelon, N., Boniol, D., Caniaux, G., Favot, F., Ferry, F., Guichard, F., Poan, E., Roehrig, R., and Vischel, T. (2009): A Multi-Scale Analysis of the Extreme Rain Event of Ouagadougou in 2009. *Quart. Journ. of Roy. Met. Soc.* DOI:10.1002/qj.3165.

Lang, *et al.* (2004): The Severe Thunderstorm Electrification and Precipitation Study, *Bull. Amer. Met. Soc.,* **85**, 1107.

Leary, C. A. and Rappaport, E. N. (1987): The Life Cycle and Internal Structure of a Mesoscale Convective Complex. *Mon. Wea. Rev.,***115,** 1503-1527.

Léon, J. F., Derimian, Y., Chiapello, I., Tanré, D., Podvin, T., Chatenet, B., Diallo, A., and Deroo, C. (2009): Aerosol Vertical Distribution and Optical Properties over M'Bour (16.96° W; 14.39° N), Senegal from 2006 to 2008. *Atmospheric Chemistry and Physics*, *9*(23), 9249-9261.

LeRoux, M. (1976): Processus de Information Etd'evolution des Lignes de Grainsde l'Afriquetropicaleseptentrionale. *Université de Dakar, Dept. Géograpie, Recherches de Climatologie Tropicale* **1,** *Dakar, Senegal.*

Levin, Z., Ganor, E., and Gladstein, V. (1996): The Effects of Desert Particles Coated with Sulfate on Rain Formation in the Eastern Mediterranean. *J App Meteorol* 35: 1511-1523.

Levitus, S., Antonov, J. I., Boyer, T. P., and Stephens, C. (2000): Warming of the World Ocean. *Science*, *287*(5461), 2225-2229.

Lieber, M. and Wolke, R. (2008): Optimizing the Coupling in Parallel Air Quality Model Systems. *Environ. Model. Softw.,* 23, 235-243.

Lin, M., Fiore, A. M., Cooper, O. R., Horowitz, L. W., Langford, A. O., Levy, H., Johnson, B. J., Naik, V., Oltmans, S. J., and Senff, C. J. (2012): Springtime High Surface Ozone Events over the western United States: Quantifying the Role of Stratospheric Intrusions. *Journal of Geophysical Research: Atmospheres*, *117*(D21).

Lindqvist, O., Johansson, K., Bringmark, L., Timm, B., Aastrup, M., Andersson, A., Hovsenius, G., Håkanson, L., Iverfeldt, Å., and Meili, M. (1991): Mercury in the Swedish Environment—Recent Research on Causes, Consequences and Corrective Methods. *Water, Air, and Soil Pollution*, *55*, xi-261.

Liousse, C., Guillaume, B., Grégoire, J. M., Mallet, M., Galy, C., Pont, V., Akpo, A., Bedou, M., Castéra, P., Dungall, L., Gardrat, E., Granier, C., Konaré, A., Malavelle, F., Mariscal, A., Mieville, A., Rosset, R., Serca, D., Solomon, F., Tummon, F., Assamoi, E., Yoboué, V., and Van Velthoven, P. (2010): Updated African Biomass Burning Emission Inventories in the Framework of the AMMA-IDAF Program, with an Evaluation of Combustion Aerosols. *Atmospheric Chemistry and Physics*, *10*(19), 9631-9646.

Long, M. S., Keene, W. C., Kieber, D. J., Erickson, D. J. and Maring, H. (2011): A Sea-state based Source Function for Size- and Composition-resolved Marine Aerosol Production. *Atmos. Chem. Phys.,* 11, 1203–1216. doi:10.5194/acp-11-1203-2011.

Ludlam, F. H. (1980): Clouds and Storms: *The Behavior and Effect of Water in the Atmosphere*. Pennsylvania State University Press.

Lyons, W. A., Dooley Jr, J. C., and Whitby, K. T. (1978): Satellite Detection of Long-Range Pollution Transport and Sulfate Aerosol Hazes. In *Sulfur in the Atmosphere* (pp. 621-631). Pergamon.

Maddox, R.A., (1980): Mesoscale convective complexes. *Bulletin of the American Meteorological Society, Vol.* **61,** 1374-1387.

Majewski, D., Liermann, D., Prohl, P., Ritter, B., Buchhold, M., Hanisch, T., Paul, G., Wergen, W., and Baumgardner, J. (2002): The Operational Global Icosahedral–Hexagonal Grid Point Model GME: Description and High-Resolution Tests. *Monthly Weather Review*, *130*(2), 319-338.

Maki, A., Carrico, A. R., Raimi, K. T., Truelove, H. B., Araujo, B., & Yeung, K. L. (2019). Meta-analysis of Pro-environmental Behaviour Spillover. *Nature Sustainability*, *2*(4), 307-315.

Mallet, M., Pont, V., Liousse, C., Gomes, L., Pelon, J., Osborne, S., Haywood, J., Roger, C., Dubuisson, P., Mariscal, A., Thouret, V., and Goloub, P. (2008): Aerosol Direct Radiative Forcing over Djougou (northern Benin) during the African Monsoon Multidisciplinary Analysis Dry Season Experiment (Special Observation Period-0). *Journal of Geophysical Research: Atmospheres*, *113*(D23).

Manucci, P. M., and Franchini, M. (2017): Health Effects of Ambient Air Pollution in Developing Countries. *Int. J. Environ. Res. Public Health.* 14:1048 10.3390/ijerph14091048

Mapes, B. and Houze, R. (1993): Cloud Clusters and Super-Clusters over the Oceanic Warm Pool. *Mon. Wea. Rev.,* **121,** p 1398-1415.

Mapes, B. and Houze, R. (1995): Diabatic Divergence Profiles in Western Pacific Mesoscale Convective systems. *J. Atmos. Sci.* **52,** 1807-1828.

Marsham, J. H., Parker, D. J., Grams, C. M., Taylor, C. M., and Haywood, J. M. (2008): Uplift of Saharan Dust south of the Inter-Tropical Discontinuity. *Journal of Geophysical Research: Atmospheres*, *113*(D21).

Marticorena, B., Chatenet, B., Rajot, J. L., Traoré, S., Coulibaly, M., Diallo, A., Koné, I., Maman, A., N'Diaye, T., and Zakou, A. (2010): Temporal Variability of Mineral Dust Concentrations over West Africa: Analyses of a Pluriannual Monitoring from the AMMA Sahelian Dust Transect. *Atmospheric Chemistry and Physics*, *10*(18), 8899-8915.

Marwitz, J.D., (1972a): The Structure and Motion of Severe Hailstorms. Part I: Super-cell Storms. *J. Appl. Meteor.* **11,** 166-179.

Marwitz, J.D., (1972b): The Structure and Motion of Severe Hailstorms. Part II: Multi-cell Storms. *J. Appl. Meteor.* **11,** 180-188.

Marwitz, J.D., (1972c): The Structure and Motion of Severe Hailstorms. Part III: Severely Sheared Storms. *J. Appl. Meteor.* **11,** 189-201.

Mass, C. F., Ovens, D., Westrick, K., and Colle, B. A. (2002): Does Increasing Horizontal Resolution Produce More Skillful Forecasts? The Results of Two Years of Real-Time Numerical Weather Prediction over the Pacific Northwest. *Bulletin of the American Meteorological Society*, *83*(3), 407-430.

Mathon, V. and Laurent, H. (2001): Life cycle of Sahelian Mesoscale Convective Cloud Systems. *Q. J. R. M. Soc.,* **127,** p 377-406.

Mathon, V., Laurent, H., and Lebel, T. (2002): Mesoscale Convective System Rainfall in the Sahel. *Journal of Applied Meteorology and Climatology*, *41*(11), 1081-1092.

Matsuki, A., Schwarzenboeck, A., Venzac, H., Laj, P., Crumeyrolle, S., and Gomes, L. (2010): Cloud Processing of Mineral Dust: Direct Comparison of Cloud Residual and Clear Sky Particles during AMMA Aircraft Campaign in Summer 2006. *Atmospheric Chemistry and Physics*, *10*(3), 1057-1069.

McConnell, C. L., Highwood, E. J., Coe, H., Formenti, P., Anderson, B., Osborne, S., Nava, S., Desboeufs, K., Chen, G., and Harrison, M. A. J. (2008): Seasonal Variations of the Physical and Optical Characteristics of Saharan Dust: Results from the Dust Outflow and Deposition to the Ocean (DODO) Experiment. *Journal of Geophysical Research: Atmospheres*, *113*(D14).

McConnell, C. L., Formenti, P., Highwood, E. J., and Harrison, M. A. J. (2010): Using Aircraft Measurements to Determine the Refractive Index of Saharan Dust during the DODO Experiments. *Atmospheric Chemistry and Physics*, *10*(6), 3081-3098.

Menard, J. H., Fritsch, J. M. and Hirschberg, P. A. (1986): Meso-Analysis of a Convectively Generated, Inertially Stable Meso-Vortex. *Pre-prints, 11th Conf. on Weather Forecasting and Analysis, Kansas City, Amer. Meteor. Soc.,* 149-199.

Menut, L. (2008): Sensitivity of hourly Saharan Dust Emissions to NCEP and ECMWF Modeled Wind Speed. *Journal of Geophysical Research: Atmospheres*, *113*(D16).

Middleton, N. J., and Goudie, A. S. (2001): Saharan Dust: Sources and Trajectories. *Transactions of the Institute of British Geographers*, *26*(2), 165-181.

Milton, S. F., Greed, G., Brooks, M. E., Haywood, J., Johnson, B., Allan, R. P., Slingo, A., and Grey, W. M. F. (2008): Modeled and Observed Atmospheric Radiation Balance during the West African Dry Season: Role of Mineral Dust, Biomass Burning Aerosol, and Surface Albedo. *Journal of Geophysical Research: Atmospheres*, *113*(D23).

Mohr, K. I., and Zipser, E. J. (1996a): Mesoscale Convective Systems defined by their 85-GHz ice Scattering Signature; Size and Intensity Comparison over Tropical Oceans and Continents. *Mon. Wea. Rev.,* **124**, 2417-2437.

Mohr, K. I., and Zipser,E. J. (1996b): Defining Mesoscale Convective Systems defined by the 85 GHz Ice-Scattering Signature. *Bull. Amer. Meteor. Soc*., **87,** 2417-2437.

Moncrieff, M. W., and Miller, M. J. (1976): The Dynamics and Simulation of Tropical Cumulonimbus and Squall Lines. *Quart. J. R. Met. Soc.* **102,** 373-394.

Morman, S. A., and Plumlee, G. S. (2014): Dust and Human Health. *Mineral Dust: A Key Player in the Earth system*, 385-409.

Nakazawa, T. (1988), Tropical Super Clusters within Intra-Seasonal Variations over the Western Pacific. *J. Meteorol. Soc. Jpn.,* **66,** 823–839.

Nenes, A., Pandis, S. N., and Pilinis, C. (1998): ISORROPIA: A New Thermodynamic Equilibrium Model for Multiphase Multicomponent Inorganic Aerosols. *Aquatic geochemistry*, *4*, 123-152.

Nesbitt, S. W. and Zipser,E. J. (2003): The Diurnal Cycle of Rainfall and Convective Intensity according to Three Years of TRMM Measurements. *J. Climate*, **16**, 1456-1475.

Nesbitt, S. W., Cipelli, R. and S. A. Rutledge, (2006): Storm Morphology and Rainfall Characteristics of TRMM Precipitation Features. *Mon. Wea. Rev.*, **134**, 2702-2721.

Newton, C. W. (1950): Structure and Mechanism of the Pre-frontal Squall Line. *J. Meteor.,* **7,** 210-222.

Nicholson, S. E., and Entekhabi, D. (1987): Rainfall Variability in Equatorial and Southern Africa: Relationships with Sea-Surface Temperatures along the South-western Coast of Africa. *J. Climate Appl. Meteor,* **26***,* 561-578.

Noh, Y. C., Sohn, B. J., Kim, Y., Joo, S., and Bell, W. (2016): Evaluation of Temperature and Humidity Profiles of Unified Model and ECMWF Analyses using GRUAN Radiosonde Observations. *Atmosphere*, *7*(7), 94.

Nymphas, E.F., Adeniyi, M.O., Ogolo, E.O. and Oladiran, E.O. (2004): Lightning Signature as an Index for the Determination of the Beginning of the Planting Season in Nigeria. *African Journal of Science and Technology (AJST); Science and Engineering series, vol.* **5,** no. 2, pp. 28-33

Obasi, G.O.P. (1974): Some Statistics Concerning the Disturbances Lines of West Africa. *Preprints Symp. Tropical Meteorology, Part II, Nairobi, Amer. Meteor. Soc.,* 52-66.

Ochei, M.C., Orisakwe, I.C., and Oluleye, A. (2015): Spatial, Seasonal and Inter-seasonal Variations of Thunderstorm Frequency over Nigeria. *Afr. Journ. Env. Sci. Tech.,* 9: 810-833.

Ochei, M.C. and Oluleye, A. (2017): Climate Variability Impact on the Frequency of Occurrence of Mesoscale Convective Systems in Northern Nigeria. *Journ. Climatol. Wea. Forecasting.* 5: 213.

Ochei, M.C., and Adenola, E. (2018): Variability of Harmattan Dust Haze over Northern Nigeria. *Int. Journ. of Pollu.* 1:107.

Ogura, Y. and Liou, M. T. (1980): The Structure of Mid-Latitude Squall Line. *J. Atmos. Sci.,* **37,** 553-567.

Okulaja, F.O. (1970): Synoptic flow perturbations over West Africa. *Tellus,* **22** pp. 663–680.

Oluleye, A., and Okogbue, E.C. (2013): Analysis of Temporal and Spatial Variability of Total Column Ozone over West Africa using Daily TOMS Measurements. *Atmos. Pollut Res.* 4: 387-397.

Oluleye, A., and Adeyewa, Z.D. (2016): Wind Energy Density in Nigeria as Estimated from ERA Interim Reanalyzed Dataset. *British J. App. Sci. Technol.* 17: 1-17.

Omotosho, J.B., (1981): A Theoretical and Observational Study of Cumulus Clouds and Mesoscale Environment. Ph.D. Thesis, *University of Reading,* 120*pp*

Omotosho, J. B., (1983): Prediction of Maximum Gusts in West African Line Squalls. *Nig. Met. Journ. Vol*. **1,** 94-100.

Omotosho, J. B., (1984): Spatial and Seasonal Variation of Line Squalls over West Africa. *Arch. of Met. Geoph. Biocl., Ser. A***33,** 143.

Omotosho, J.B., (1985): The Separate Contributions of Line Squalls, Thunderstorms and the Monsoon to the Total Rainfall in Nigeria. *Journ. of Climatology,* **5,**543-555.

Omotosho, J.B., (1987): Richardson Number, Vertical Wind Shear, and Storm Occurrences at Kano, Nigeria. *Atmos. Res., Elsevier* **21,** 123-137.

Omotosho, J. B. (1988): Spatial Variation of Rainfall in Nigeria during the 'Little Dry Season'. *Atmospheric Research*, *22*(2), 137-147.

Omotosho, J.B., Balogun, A.A. and Ogunjobi, K., (2000): Predicting Monthly and Seasonal Rainfall, Onset, and Cessation of the Rainy Season in West Africa using only Surface Data. *International Journal of Climatology* **20,** 865-880.

Omotosho, J. B. (2008): Pre-rainy Season Moisture Build-up and Storm Precipitation Delivery in the West African Sahel. *International Journal of Climatology: A Journal of the Royal Meteorological Society*, *28*(7), 937-946.

Orisakwe, I.C. (2015): Disaggregation and Quantification of Rainfall Associated with three Rainfall Producing Systems in Nigeria. *Unpublished M.Tech Thesis., FUTA, Nigeria.* Pg. 47

Osborn, H. B., and Reynolds, W. (1963): Convective Storm Patterns in the Southwestern U.S. Bull. *Int. Assoc. Sci. Hydrol.,* **8** (3), 71-83.

Osborne, S. R., Johnson, B. and Haywood, J. (2008): Physical and Optical Properties of Mineral Dust Aerosol during the Dust and Biomass Experiment (DABEX), *J. Geophys. Res.*, doi:10.1029/2007JD009551.

Palarz, A., Celiński-Mysław, D., and Ustrnul, Z. (2018): Temporal and Spatial Variability of Surface-based Inversions over Europe based on ERA-Interim Reanalysis. *International Journal of Climatology*, *38*(1), 158-168.

Palarz, A., Luterbacher, J., Ustrnul, Z., Xoplaki, E., & Celiński-Mysław, D. (2020): Representation of Low-Tropospheric Temperature Inversions in ECMWF Reanalysis over Europe. *Environmental Research Letters*, *15*(7), 074043.

Parker, M. D., (1999): May 1996 and May 1997 Linear Mesoscale Convective Systems of the Central Plains: Synoptic Meteorology and a Reflectivity-based Taxonomy. *Dept. of Atmospheric Science Paper No. 675, Colorado State University, Fort Collins, CO,* 185 pp. [Available from Dept. of Atmospheric Science, Colorado State University, Fort Collins, CO 80523].

Parker, M.D. and Johnson, R.H. (2000): Organizational Mode of Mid-Latitude Mesoscale Convective Systems. *Mon. Wea. Rev.,* **128,** 3413-3436.

Pastushkov, R. S. (1975): The Effects of Vertical Wind Shear on the Evolution of Convective Clouds. *Quarterly Journal of the Royal Meteorological Society*, *101*(428), 281-291.

Payne, S. W., and McGarry, M. M. (1977): The Relationship of Satellite-inferred Convective Activity to Easterly Waves over West Africa and the Adjacent Ocean during Phase III of GATE. *Mon. Weather Rev.,***105,** 413–420.

Pelon, J., Mallet, M., Mariscal, A., Goloub, P., Tanré, D., Bou Karam, D., Flamant, C., Haywood, J.,Posphical, B., and Victori, S. (2008): Microlidar Observations of Biomass Burning Aerosol over Djougou (Benin) during African Monsoon Multidisciplinary Analysis Special Observation Period 0: Dust and Biomass-Burning Experiment. *Journal of Geophysical Research: Atmospheres*, *113*(D23).

Peters, J. M., Nowotarski, C. J., and Morrison, H. (2019): The Role of Vertical Wind Shear in Modulating Maximum Super-cell Updraft Velocities. *Journal of the Atmospheric Sciences*, *76*(10), 3169-3189.

Petersen, W. A., and Rutledge, S. A. (2001): Regional Variability in Tropical Convection: Observations from TRMM. *J. Climate*, **14**, 3566-3586.

Pielke Sr, R. A., Adegoke, J., BeltraáN-Przekurat, A., Hiemstra, C. A., Lin, J., Nair, U. S., Niyogi,

D., and Nobis, T. E. (2007): An overview of Regional Land-Use and Land-Cover Impacts on Rainfall. *Tellus B: Chemical and Physical Meteorology*, *59*(3), 587-601.

Polcher, J., Parker, D. J., Gaye, A., Diedhiou, A., Eymard, L., Fierli, F., Genesio, L., Höller, H., Janicot, S., Lofore, J.-P., Karambiri, H., Lebel, T., Redelsperger, J.-L., Reeves, C. E., Ruti, P., Sandholt, I., and Thorncroft, C. (2011): AMMA's Contribution to the Evolution of Prediction and Decision-making Systems for West Africa. *Atmospheric Science Letters*, *12*(1), 2-6.

Pósfai, M., Anderson, J. R., Buseck, P. R., and Sievering, H. (1999): Soot and Sulfate Aerosol Particles in the Remote Marine Troposphere. *Journal of Geophysical Research: Atmospheres*, *104*(D17), 21685-21693.

Prospero, J. M. and Carlson, T. N. (1972): Vertical and Aerial Distribution of Saharan Dust over Western Equatorial North-Atlantic Ocean. *J. Geophys. Res.* **77:** 5255.

Prospero, J. M., and Carlson, T. N. (1980): Saharan Air Outbreaks over the Tropical North Atlantic. *Pure and Appl. Geophys.,* **119,** 677-691.

Prospero, J. M., Collard, F. X., Molinié, J., and Jeannot, A. (2014). Characterizing the annual cycle of African dust transport to the Caribbean Basin and South America and its Impact on the Environment and Air Quality. *Global Biogeochemical Cycles*, *28*(7), 757-773.

Rajot, J. L., Formenti, P., Alfaro, S., Desbouefs, K., Chevaillier, S., Chatenet, B., Gaudichet, A., Journet, E., Marticorena, B., Triquet, S., Maman, A., Mouget, N., and Zakou, A. (2008): AMMA Dust Experiment: An Overview of Measurements Performed during the Dry Season Special Observation Period (SOP0) at the Banizoumbou (Niger) supersite. *Journal of Geophysical Research–Atmospheres,* 113:D00C14, doi:10.1029/2008JD009906.

Ramanathan, V. C. P. J., Crutzen, P. J., Kiehl, J. T., and Rosenfeld, D. (2001): Aerosols, Climate, and the Hydrological Cycle. *science*, *294*(5549), 2119-2124.

Rasmusson, E. M., (1988): Global Climate Change and Variability: Effects on Drought and Desertification in Africa. Drought and Hunger in Africa: Denying Famine a Future. *M. H. Glantz, Ed., Cambridge,* 3-22.

Raut, J. C., and Chazette, P. (2008): Vertical Profiles of Urban Aerosol Complex Refractive Index in the Frame of ESQUIF Airborne Measurements. *Atmospheric Chemistry and Physics*, *8*(4), 901-919.

Reddington, C.L., Butt, E.W., Ridley, D.A., Artaxo, P., Morgan, W.T., Coe, H., and Spracklen, D.V. (2015): Air Quality and Human Health Improvements from Reductions in a Deforestation-related Fire in Brazil, *Nat. Geosci*., 8, 768–771.

Redelsperger, J. L., Thorncroft, C. D., Diedhiou, A., Lebel, T., Parker, D. J., and Polcher, J. (2006): African Monsoon Multidisciplinary Analysis: An International Research Project and Field Campaign. *Bulletin of the American Meteorological Society*, *87*(12), 1739-1746.

Renner, E., and Wolke, R. (2010): Modeling the Formation and Atmospheric Transport of Secondary Inorganic Aerosols with Special Attention to Regions with High Ammonia Emissions. *Atmospheric Environment*, *44*(15), 1904-1912.

Reeves, C. E., Formenti, P., Afif, C., Ancellet, G., Attié, J. L., Bechara, J., Borbon, A., Cairo, F., Coe, H., Crumeyrolle, S., Fierli, F., Flamant, C., Gomes, L., Hamburger, T., Jambert, C., Law, K. S., Mari, C., Jones, R. L., Matsuki, A., Mead, M. I., Methven, J., Mills, G. P, Minikin, A., Murphy, J. G., Nielsen, J. K., Oram, D. E., Parker, D. J., Ritcher, A., Schlager, H., Schwarzenboeck, A., and Thouret, V. (2010): Chemical and Aerosol Characterization of the Troposphere over West Africa during the Monsoon Period as Part of AMMA. *Atmospheric Chemistry and Physics*, *10*(16), 7575-7601.

Richardson, Y. P. (1999): The Influence of Horizontal Variations in Vertical Shear and Low-Level Moisture on Numerically Simulated Convective Storms. *The University of Oklahoma.*

Riehl, H., (1954): Tropical Meteorology. *NewYork, McGraw-Hill,* **392** pp.

Riemer, N., Ault, A. P., West, M., Craig, R. L., & Curtis, J. H. (2019): Aerosol Mixing State: Measurements, Modeling, and Impacts. *Reviews of Geophysics*, *57*(2), 187-249.

Ritter, B., and Geleyn, J. F. (1992): A Comprehensive Radiation Scheme for Numerical Weather Prediction Models with Potential Applications in Climate Simulations. *Monthly Weather Review*, *120*(2), 303-325.

Robe, F. R., and Emmanuel, K. A. (2001): The Effect of Vertical Wind Shear on Radiative Convective Equilibrium States. *J. Amos. Sci.,* 58, 1427-1445.

Rosenfeld, D., Lohmann, U., Raga, G. B., O'Dowd, C. D., Kulmala, M., Fuzzi, S., Reissell, A., and Andreae, M. O. (2008): Flood or Drought: How Do Aerosols Affect Precipitation? *Science*, *321*(5894), 1309-1313.

Rotunno, R., Klemp, J. B., and Weisman, M. L. (1998): A Theory for Strong, Long-lived Squall Line. *J. Amos. Sci.,* 45, 406-426.

Rutledge, S.A., Williams, E.R. and Keenan, T.D. (1992): The Down under Doppler and Electricity Experiment (DUNDEE) Overview and Preliminary Results. *Bulletin American Meteorological Society,* **73,** 3.

Rycroft, M.J., Odzimek, A., Arnold, N.F., Fullekrug, M., Kulak, A. and Neubert, T. (2007): New

Model Simulations of the Global Atmospheric Electric Circuit Driven by Thunderstorms and Electrified Shower Clouds: The Role of Lightning and Sprites. *J. Atmos. Solar-Terr. Phys.,* **69**, 445-456.

Saarikoski, S., Sillanpää, M., Sofiev, M., Timonen, H., Saarnio, K., Teinilä, K., Karppinen, A., Kukkonen, J., and Hillamo, R. (2007): Chemical Composition of Aerosols during a major Biomass Burning Episode over Northern Europe in Spring 2006: Experimental and Modeling Assessments. *Atmospheric Environment*, *41*(17), 3577-3589.

Salvador, R., Calbó, J., and Millán, M. M. (1999): Horizontal Grid Size Selection and its Influence on Mesoscale Model Simulations. *Journal of Applied Meteorology and Climatology*, *38*(9), 1311-1329.

Salvador, P., Almeida, S. M., Cardoso, J., Almeida-Silva, M., Nunes, T., Cerqueira, M. Alves, C., Reis, M. A., Chaves, P. C., Artíñano, B., and Pio, C. (2016): Composition and Origin of PM_{10} in Cape Verde: Characterization of Long Range Transport Episodes. *Atmos. Environ.* **127**: 326-339.

Sanders, F. and Emanuel, K. A. (1977): The Momentum Budget and Temporal Evolution of Mesoscale Convective System. *J. Amos. Sci.,* **34,** 322-330.

Sathiyamoorthy, V., Pal, P. K., and Joshi, P. C. (2004): Influence of the Upper-Tropospheric Wind Shear upon Cloud Radiative Forcing in the Asian Monsoon Region. *Journal of Climate*, *17*(14), 2725-2735.

Schättler, U., Doms, G. and Schraff, C. (2018): A Description of the Non-hydrostatic Regional COSMO-Model. Deutscher Wetterdienst, Offenbach. www.cosmo-model.org.

Schepanski, K., Tegen, I., and Macke, A. (2009): Saharan Dust Transport and Deposition towards the Tropical Northern Atlantic. *Atmos. Chem. Phys.,* **9,** 10.5194/acp-9-1173-2009.

Schilling, J., Hertig, E., Tramblay, Y., and Scheffran, J. (2020): Climate Change Vulnerability, Water Resources and Social Implications in North Africa. *Regional Environmental Change*, *20*, 1-12.

Schultz, M. G., Stadtler, S., Schröder, S., Taraborrelli, D., Franco, B., Krefting, J., Henrot, A., Ferrachat, S., Lohmann, U., Neubauer, D., Siegenthaler-Le Drian, C., Wahl, S., Kokkola, H., Kühn, T., Rast, S., Schmidt, H., Stier, P., Kinnison, D., Tyndall, G. S., Orlando, J. J., and Wespes, C. (2018): The Chemistry Climate Model ECHAM6.3-HAM2.3-MOZ1.0. *Geosci. Model Dev.*, 11, 1695–1723. doi:10.5194/gmd-11-1695-2018.

Seinfeld, J. H., and Pandis, S. N. (2006): Atmospheric Chemistry and Physics: From Air Pollution to Climate Change. 2nd edition, 600 (Wiley, 2006).

Seinfeld, J. H., Bretherton, C., Carslaw, K. S., Coe, H., DeMott, P. J., Dunlea, E. J., Feingold, G., Ghan, S., Guenther, A. B., Kahn, A. B., Kraucunas, I., Kreidenweis, S. M., Molina, M. J., Nenes, A, Penner, J. E, Prather, J. E., Ramanathan, K. A., Ramaswamy, V., Rasch, P. J., Ravishankara, A. R., Rosenfeld, D., Stephens, G., and Wood, R. (2016): Improving our Fundamental Understanding of the Role of Aerosol-Cloud Interactions in the Climate System. *Proceedings of National Academy of Sciences.* 113(21), 5781-5790. doi: 10.1073/pnas.1514043113.

Setzer, A. W., and Pereira, M. C. (1991): Amazonas Biomass Burnings in 1987 and an Estimate of their Tropospheric Emissions. *Ambio (Journal of the Human Environment, Research, and Management), Sweden*, 20(1).

Shinn, E. A., Smith, G. W., Prospero, J. M., Betzer, P., Hayes, M. L., Garrison, V., and Barber, R. T. (2000): African Dust and the Demise of Caribbean Coral Reefs. *Geophysical Research Letters*, *27*(19), 3029-3032.

Shrivastava, M., Cappa, C. D., Fan, J., Goldstein, A. H., Guenther, A. B., Jimenez, J. L., Kuang, C., Laskin, A., Martin, S. T., Ng, N. L., Petaja, T., Pierce, J. R., Rasch, P. J., Roldin, P., Seinfeld, J. H., Shilling, J., Smith, J. N., Thornton, J. A., Volkamer, R., Wang, J., Worsnop, D. R., Zaveri, R. A., Zelenyuk, A., and Zhang, Q. (2017): Recent Advances in Understanding Secondary Organic Aerosol: Implications for Global Climate Forcing. *Reviews of Geophysics*, *55*(2), 509-559.

Simpson, D., Benedictow, A., Berge, H., Bergström, R., Emberson, L. D., Fagerli, H., Flechard, C. R., Hayman, G. D., Gauss, M., Jonson, J. E., Jenkin, M. E., Nyiri, A., Semeena, V. S., Tsyro, S., Tuovinen, J.-P., Valdebenito, Á., and Wind, P. (2003): The EMEP MCS-W Chemical Transport Model. *Amos. Chem. Phys, 12, 7825-7865*

Simpson, R. M., Howell, S. G., Blomquist, B. W., Clarke, A. D., and Huebert, B. J. (2014): Dimethyl Sulfide: Less Important than Long-Range Transport as a Source of Sulfate to the Remote Tropical Pacific Marine Boundary Layer. *Journal of Geophysical Research: Atmospheres*, *119*(14), 9142-9167.

Slingo, A., Bharmal, N. A., Robinson, G. J., Settle, J. J., Allan, R. P., White, H. E., Lamb, P. J., Issa Lélé, M., Turner, D. D., McFarlene, S., Kassianov, E., Barnard, J., Flynn, C., and Miller, M. (2008). Overview of Observations from the RADAGAST Experiment in Niamey, Niger: Meteorology and Thermodynamic Variables. *Journal of Geophysical Research: Atmospheres*, *113*(D13).

Smull, B. F., and R. A. Houze, (1985): A Mid-Latitude Squall Line with a Trailing Region of Stratiform Rain: Radar and Satellite Observations. *Mon. Wea. Rev.,* **113,** 117-133.

Sow, M., Alfaro, S. C., Rajot, J. L., and Marticorena, B. (2009): Size Resolved Dust Emission Fluxes Measured in Niger during 3 Dust Storms of the AMMA Experiment. *Atmospheric Chemistry and Physics*, *9*(12), 3881-3891.

Steinbrecher, R., Smiatek, G., Köble, R., Seufert, G., Theloke, J., Hauff, K., Ciccioli, P., Vautard, R., and Curci, G. (2009): Intra-and Inter-annual Variability of VOC Emissions from Natural and Semi-natural Vegetation in Europe and Neighboring Countries. *Atmospheric Environment*, *43*(7), 1380-1391.

Steppeler, J., Hess, R., Schättler, U., and Bonaventura, L. (2003): Review of Numerical Methods for Non-Hydrostatic Weather Prediction Models. *Meteorology and Atmospheric Physics*, *82*, 287-301.

Stern, R., Builtjes, P., Schaap, M., Timmermans, R., Vautard, R., Hodzic, A., Memmesheimer, M., Feldmann, H., Renner, E., Wolke, R., and Kerschbaumer, A. (2008): A Model Inter-comparison Study Focusing on Episodes with Elevated PM_{10} Concentrations. *Atmospheric Environment*, *42*(19), 4567-4588.

Stier, P., Feichter, J., Kinne, S., Kloster, S., Vignati, E., Wilson, J., Ganzeveld, J., Tegen, I., Werner, M., Balkanski, Y., Schulz, M., Boucher, O., Minikin, A., and Petzold, A. (2005): The Aerosol-Climate model ECHAM5-HAM. *Atmospheric Chemistry and Physics*, 5(4), 1125-1156.

Stockwell, W. R., Kirchner, F., Kuhn, M., and Seefeld, S. (1997): A New Mechanism for Regional Atmospheric Chemistry Modeling. *J. Geophys. Res. Atmos.,* 102(D22), 25847–25879. doi.org/10.1029/97JD00849.

Stohl, A., Williams, E., Wotawa, G., and Kromp-Kolb, H. (1996): A European Inventory of Soil Nitric Oxide Emissions and the Effect of these Emissions on the Photochemical Formation of Ozone. *Atmospheric Environment*, *30*(22), 3741-3755.

Stryhal, J., Huth, R., and Sládek, I. (2017): Climatology of Low-Level Temperature Inversions at the Prague-Libuš Aerological Station. *Theor. Appl. Climatol.* 127, 409-420.

Stull, R. B. (1988): An Introduction to Boundary Layer Meteorology (Vol. 13). *Springer Science and Business Media.*

Taylor, C. M., Belušić, D., Guichard, F., Parker, D. J., Vischel, T., Bock, O., Harris, P. P., Janicot, S., Klein, C., and Panthou, G. (2017): Frequency of Extreme Sahelian Storms Tripled since 1982 in Satellite Observations. *Nature*, *544*(7651), 475-478.

Taylor, C. M., Fink, A. H., Klein, C., Parker, D. J., Guichard, F., Harris, P. P., and Knapp, K. R. (2018): Earlier Seasonal Onset of Intense Mesoscale Convective Systems in the Congo Basin since 1999. *Geophysical Research Letters*, *45*(24), 13-458.

Tegen, I. and Lacis, A. (1996): Modeling of Particle Size Distribution and its Influence on the Radiative Properties of Mineral Dust and Aerosol. *J. Geophys. Res.* **101:** 19237-19244.

Tegen, I., Harrison, S. P., Kohfeld, K., Prentice, I. C., Coe, M., and Heimann, M. (2002): Impact of Vegetation and Preferential Source Areas on Global Dust Aerosol: Results from a Model Study. *J. Geophys. Res.* 107(D21), 4576, doi:10.1029/2001JD000963.

Tegen, I., and Kohfeld, K. E. (2006): Atmospheric Transport of Silicon. *The Silicon Cycle: Human Perturbations and Impacts on Aquatic Systems*, 81-91.

Tesche, M., Ansmann, A., Müller, D., Althausen, D., Engelmann, R., Freudenthaler, V., and Groß, S. (2009b): Vertically Resolved Separation of Dust and Smoke over Cape Verde by using Multi-wavelength Raman and Polarization Lidars during Saharan Mineral Dust Experiment 2008. *J. Geophys. Res.,* **114,** 10.1029/2009JD011862.

Thompson, B.W. (1965): The Climate of Africa. *New York, Oxford Press,* **132** pp.

Thorpe, A. J., Miller, M. J., and Moncrieff, M. W. (1982): Two-Dimensional Convection in Non Constant Shear: A Model of Mid-Latitude Squall Lines. *Quarterly Journal of the Royal Meteorological Society*, *108*(458), 739-762.

Tiedtke, M. (1989): A Comprehensive Mass Flux Scheme for Cumulus Parameterization in Large Scale Models. *Monthly Weather Review*, *117*(8), 1779-1800.

Tilgner, A., Schaefer, T., Alexander, B., Barth, M., Collett Jr, J. L., Fahey, K. M., Nenes, A., Pye, H. O. T., Herrmann, H., and McNeill, V. F. (2021): Acidity and the Multiphase Chemistry of Atmospheric Aqueous Particles and Clouds. *Atmospheric Chemistry and Physics*, *21*(17), 13483-13536.

Tompkins, A. M. (2001): Organization of Tropical Convection in Low Vertical Wind Shear. The Role of Cold Pools. *J. Atmos. Sci.,* **58,** 1650-1672.

Toracinta, E. R., and E. J. Zipser, (2001): Lightning and SSM/I-Ice Scattering Mesoscale Convective Systems in the Global Tropics. *J. Appl. Meteor.,* **40**, 983-1002.

Tulet, P., Mallet, M., Pont, V., Pelon, J., and Boone, A. (2008). The 7–13 March 2006 Dust Storm over West Africa: Generation, Transport, and Vertical Stratification. *Journal of Geophysical Research: Atmospheres*, *113*(D23).

Tummon, F., Solmon, F., Liousse, C., and Tadross, M. (2010). Simulation of the Climatic Impacts of the Natural Aerosol Loading over Southern Africa during the Biomass Burning Season using $RegCM_3$. Accepted for publication in. *J Geophys Res*.

Twomey, S. (1977): Introduction to the Mathematics of Inversion in Remotes Sensing and Indirect Measurements, Elsevier Scientific, New York.

Walker S. Ashley, Thomas L. Mote, P. Grady Dixon, Sharon L. Trotter, Emily J. Powell, Joshua D. Durkee, and Andrew J. Grundstein (2003): Distribution of Mesoscale Convective Complex Rainfall in the United States. *Retrieved on* 2008-03-02.

United Nations, (2022): "World Population Prospects 2022". Population.un.org. *United Nations Department of Economic and Social Affairs, Population Division.* Retrieved 17 July 2022.

Van der Werf, G. R., Randerson, J. T., Giglio, L., Collatz, G. J., Mu, M., Kasibhatla, P. S., Morton, D. S., DeFries, R. S., Jin, Y., and van Leeuwen, T. T. (2010): Global Fire Emissions and the Contribution of Deforestation, Savanna, Forest, Agricultural, and Peat Fires (1997–2009). *Atmospheric Chemistry and Physics*, *10*(23), 11707-11735.

Velasco, I., and Fritsch, J. M. (1987): Mesoscale Convective Complexes in the America. *Journal of Geophysical Research: Atmospheres*, *92*(D8), 9591-9613.

Verstreten, W. W., Neu, J. L., Williams, J. E., Bowman, K. W., Worden, J. R., and Boersma, K. F. (2015): Rapid Increases in Tropospheric Ozone Production and Export from China. *Nat. Geosci.* **8:** 690-695

Vignati, E., Wilson, J., and Stier, P. (2004): M7: A Size Resolved Aerosols Moisture Module for the use in Global Aerosol Models. *J. Geophys. Res.,* 109, D22 202, doi:10.1029/2003JD004 485.

Vorkamp, K., and Rigét, F. F. (2014): A Review of New and Current-use Contaminants in the Arctic Environment: Evidence of Long-range Transport and Indications of Bioaccumulation. *Chemosphere*, *111*, 379-395.

Wegener, A. (1911): *Thermodynamik der Atmosphäre.* Leipzig: J.A. Barth.

Weisman, M. L., and Rotunno, R. (2004): "A Theory for Strong Long-Lived Squall Lines" Revisited. *Journal of the Atmospheric Sciences*, *61*(4), 361-382.

Wetzel, P. J., Cotton, W. R. and McAnelly, R. L. (1983): A Long-lived Mesoscale Convective Complex. Part II: Evolution and Structure of the Mature Complex. *Mon. Wea. Rev.,* **111,** 1919-1937.

Williams, E. J., Hutchinson, G. L., and Fehsenfeld, F. C. (1992): NO_x and N_2O Emissions from Soil. *Global Biogeochemical Cycles*, *6*(4), 351-388.

Wolke, R., and Knoth, O. (2000): Implicit-explicit Runge-Kutta Methods Applied to Atmospheric Chemistry-transport Modelling, *Environ. Model. Softw.,* 15, 711–719.

Wolke, R., and Knoth, O. (2002): Time-integration of Multiphase Chemistry in Size-resolved Cloud Models, *Appl. Numer. Math.,* 42(1-3), 473–487, doi:10.1016/S0168-9274(01)00169-6.

Wolke, R., Schröder, W., Schrödner, R., and Renner, E. (2012): Influence of Grid Resolution and Meteorological Forcing on Simulated European Air Quality: A Sensitivity Study with the Modeling System COSMO–MUSCAT. *Atmospheric environment*, *53*, 110-130. doi.org/10.1016/j.atmosenv.2012.02.085.

Wolke, R., Schroeder, W., Schroedner, R., and Renner, E. (2014): Influence of Grid Resolution and Biomass Burning Emissions on Air Quality Simulations: A Sensitivity Study with the Modelling System COSMO-MUSCAT. In *Air Pollution Modeling and its Application XXII* (pp. 559-563). Springer Netherlands.

Wu, L., Su, H., and Jiang, J. H. (2011): Regional Simulations of Deep Convections and Biomass Burning over South America: II. Biomass Burning Aerosol Effects on Clouds and Precipitation. *Journ. of Geophy. Res.: Atmosphere* 116

Yair, Y. (2008): Charge Generation and Separation Processes. *Space Sci. Rev.,* **137**, 119-131**.**

Zipser, E. J. (1977): Mesoscale and Convective-Scale Downdraughts as Distinct Components of Squall Line Circulation. *Mon. Weather Rev.,* **105,** 1568-1589

Zipser, E. J., Cecil, D. J., Liu, C., Nesbitt, S. W., and Yorty, D. P. (2007): Where are the most Intense Thunderstorms on Earth? *Bull. Amer. Meteor. Soc*., **87**, 1057-1071.